Peripheral Nerve Regeneration on Fibronectin Fibre Substrates

Thesis submitted for the Degree of
Doctor of Philosophy (PhD)

Zubair Ahmed
University College London
Division of Plastic and Reconstructive Surgery
September 1998

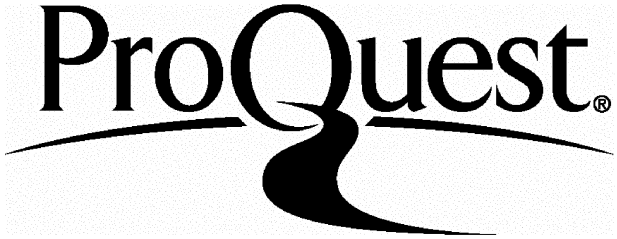

ABSTRACT

Peripheral nerve injuries commonly result in a surgically irreducible gap and represent a serious problem in surgery. Clinically, autologous nerve grafts are the most effective means of promoting axonal regeneration across the space, but normally produce donor site morbidity. Other variations of experimental models have been used with the aim of directing rapid nerve regeneration, including entubation, artery and vein grafts and Millipore. However, each of these have significant limitations which affect complete regrowth. Fibronectin (Fn), a large extracellular matrix cell adhesion glycoprotein has been made into three-dimensional mats with a predominant fibre direction and shown to successfully enhance peripheral nerve regeneration in a rat model. The aim of this study was to identify the main features of Fn-implants which are important for rapid nerve repair. This involved testing implanted versions of Fn-mat from rat and monkey models, assessment of cell-matrix interaction in vitro and modification of Fn-materials by chemical and growth factor addition. The results from this study show that new materials can be made from fibronectin which have a potential use in repair of long peripheral nerve lesions. These fibronectin-based materials may be stabilised with micromolar concentrations of copper and zinc which also support strong growth of Schwann cells within these materials in culture. Fibronectin mats may also be soaked with neurotrophins to enhance nerve cell survival and enhance nerve regeneration. The speed of Schwann cell migration and alignment (upto 50 μm away from the original fibre) was increased. Migration speed was further enhanced when the fibres were treated with micromolar concentrations of copper or made, with a substantial content of fibrinogen (optimum 50:50). Taken together, all these results suggest a first design for an ideal conduit material for peripheral nerve repair. This would be (a) dimensions (fibrous), (b) fibre orientation (c) 50:50 fibronectin: fibrinogen, (d) treated with micromolar concentrations of copper, (e) seeded with Schwann cells in culture, and (f) soaked with a 'cocktail' of neurotrophic growth factors including nerve growth factor and neurotrophin-3.

CONTENTS

LIST OF FIGURES

LIST OF TABLES

ABBREVIATIONS USED

ANOVA	Analysis of Variance
Ara-C	Arabinofuranosidase-C
BDNF	Brain-derived neurotrophic factor
BSA	Bovine serum albumin
CAF	Cell adhesion factor
CAM	Cellular adhesion molecule
CO_2	Carbon dioxide
CSP	Cell surface protein
Cu	Copper
CuFn-mats	Copper impregnated Fn-mats
$CuSO_4$	Copper sulphate
DEAE	Diethanolamine
DMEM	Dulbecco's Modified Eagles Medium
DMSO	Dimethyl sulphonic acid
ELISA	Enzyme-linked immunosorbant assay
F-actin	filamentous actin
FCS	Foetal calf serum
Fg	Fibrinogen
Fn	Fibronectin
FITC	Fluorescein isothiocyanate
Fn-mats	Fibronectin mats
HMDS	Hexamethyldisilazane
LETS	Large external transformation sensitive protein
LFn-cables	Large fibronectin cables
MHB	Modified Hank's Buffer
NGF	Nerve growth factor
NT-3	Neurotrophin-3
NT-4/5	Neurotrophin-4/5
PBS	Phosphate buffered saline
PEG	Poly-ethylene glycol
PFC	Plasma Fractionation Centre

PGP	Protein gene product
PNS	Peripheral nervous system
pNpp	para-nitrophenylphosphate
PVDF	Polyvinylidene fluoride
SEM	Scanning electron microscopy
sFn	Super fibronectin
SNBTS	Scottish National Blood Transfusion Service
SOD	Superoxide dismutase
TRITC	Tri-rhodamine isothiocyanate
trk	tyrosine kinase
Zn	Zinc

GLOSSARY OF Fn-based MATERIALS

Fn-mat	Fibronectin mats. Made from gelatine-Sepharose affinity purified Fn.
CuFn-mat	Fn-mats modified by copper ions.
ZnFn-mat	Fn-mats modified with zinc ions.
Cu/ZnFn-mat	Fn-mats modified with copper and zinc ions.
Fn-fibres/strands	Individual fibronectin fibres/strands measuring 7-14μm diameter aggregated from affinity purified Fn.
CuFn-fibres/strands	Fn-fibres/strands modified with copper ions.
LFn-cables	A 3:1 ratio of Fn:Fg (fibrinogen) aggregated to form large
cables	measuring 2-14 mm in diameter.
CuLFn-cable	LFn-cables modified by copper incorporation ions.
ZnLFn-cable	LFn-cable modified by incorporation of zinc ions.
Cu/ZnLFn-cable	LFn-cable modified by incorporation of copper and zinc ions.
Fn-cables	Individual cables measuring 200-250μm diameter made from 3:1 ratio of Fn:Fg.
Fn/Fg-cables	Individual fibres measuring 200-250μm diameter made from a 25-75% ratio of Fg:Fn.

ACKNOWLEDGEMENTS

I am forever indebted to my supervisor, Dr. Robert Brown for all his generous help throughout my PhD. He was a source of endless encouragement, support, wacky ideas, smart comments and jokes but above all "sensible, constructive" criticisms.

I would like to thank my wife for all her patience, perseverance and support throughout my PhD especially when my thesis took up most of the available space in the house.

I would also like to thank Kirsty Smith for all her help with Scanning/transmission electron microscopy and photography. Many thanks to Kanta Vellani for performing atomic absorption assays, Miss Charlotte Dean for teaching me to culture Schwann cells. I would also like to thank Dr. Giorgio Terenghi, Dr. Mikael Wiberg and Professor Susan Standring for their expert assistance. Finally, I would like to say a big thankyou to Dr. Vivek Mudera, Sarah Underwood (UCL_{be}), Sarah Harding (UCL_{be}), Dr. Rita Prajapati, Miss Kamaljit Sethi, Gyorgyi Talas, Rebecca Porter and everyone else whom I have not mentioned at the Department of Plastic and Reconstructive Surgery.

CHAPTER 1.0. INTRODUCTION

1.1. General Introduction

Nerve injury and repair presents a complex problem in repair biology. Trauma to the peripheral nerve may result in various levels of nerve fibre injury. The fate of the axon is critical for recovery after injury and usually determines the extent to which recovery of the severed nerve will occur. Functional recovery is usually complete, if axonal continuity following injury is preserved but the time taken for regeneration depends upon the pathophysiology of the lesion.

Following transection injuries to the peripheral nerve, a cascade of events occur. Phagocytic cells migrate to the site of injury and remove degenerating axons and myelin debris within the distal stump, termed Wallerian degeneration. Regenerating axonal sprouts extend from the proximal stump and migrate toward the distal stump while Schwann cells ensheathe and remyelinate the growing axons. Many axons elongate, reach their target and successfully reinnervate their original targets to form functional contacts. However, such reinnervates do not constitute a fully functional normal nerve.

For proper functional recovery all the different aspects of the peripheral nerve such as the axons, nonneuronal cells and the extracellular matrix (ECM) components must contribute fully to their normal functions. The parent cell body must firstly, survive axonal transection. Secondly, regenerating axons must grow across the site of transection and enter the distal stump as quickly as possible to minimise target site

morbidity and thirdly, regenerating axons seek out and connect to their respective end-organ targets.

1.2. Peripheral nerve injuries

Peripheral nerve injuries can be divided into several broad categories or classes, for example, neurapraxia, axonotmesis and neurotmesis (Lundborg et al, 1987, Sunderland, 1978, Seddon, 1972, Thomas, 1988) (Table 1). Trauma to the peripheral nerve may result in various extents of nerve fibre injury. The fate of the axon is critical for recovery after injury, as long as axonal continuity is preserved. When an axon is cut the distal part of the neuron induces changes in axoplasmic volume. The cell body is the major site of synthesis of proteins and other materials required for growth of the axon. The delivery of materials from the cell body to the axon by axonal transport is therefore an important factor in the regulation of axonal outgrowth.

Classification	Characteristics
Neurapraxia	Focal conduction block either transient due to ischemia or compression, etc, or more delayed but reversible, e.g. focal demyelination
Axonotmesis	Interruption of axonal continuity but preservation of Schwann cell basal lamina tubes
Neurotmesis	Interruption of axonal and Schwann cell basal lamina tubes

Table 1. *Classification of peripheral nerve injuries. (Taken from Madison et al, 1989).*

1.3. Anatomy of the peripheral nerve

Peripheral nerves are a complex structure composed of several tissue elements. The functional elements, the axons, are long cellular extensions from their respective nerve cell bodies in the anterior horn of the spinal cord (motor neurons) or in the dorsal root ganglion (sensory neurons). In the peripheral nerve, the nerve fibres are located in fascicles (Figure 1.1). The peripheral nerve trunk and its fascicle are held together by connective tissue layers, the epineurium, perineurium and the endoneurium. The epineurium is a loose connective tissue layer located superficially in the nerve and between the fascicles. Each fascicle is surrounded by a multilayered, condensed, mechanically strong membrane called the perineurium. The connective tissue in the intrafascicular space is called the endoneurium. This structural arrangement refers to the general anatomic principles of the peripheral nerves and the relative amounts of epineurial and endoneurial tissue may vary among and within nerves.

1.3.1. Connective tissue

The three main connective tissue sheaths of the peripheral nerve are the perineurium, epineurium and the endoneurium which vary in their function and makeup (Figure 1.2). The *epineurium* consists of areolar connective tissue (Sunderland 1965; Stolinski, 1995) that separates the fasciculi and holds them loosely together. This tissue becomes condensed on the surface of the nerve trunk to form a defined sheath surrounding the enclosed fasciculi. The collagen fibrils of the tissue are mostly arranged longitudinally, although some are arranged in a random criss-cross fashion (Thomas, 1963; Gamble and Eames, 1965; Osawa and Ide, 1986; Ushiki and Ide, 1990). Fibrils are typically 60-100nm in diameter and are generally thicker than those

of the perineurium or the endoneurium. The epineurium acts to protect the fasciculi from excessive extension and provides a loose matrix that dampen the effects deforming forces (Sunderland, 1978; Ushiki and Ide, 1990), similar to that of suspension springs on a motor vehicle. The epineurium and the perineurium serve as the principle sites at which sutures are placed during surgical repair of a transected peripheral nerve of a small gap (Sunderland, 1978; Mackinnon and Dellon, 1988; Terzis, 1987; Daniel and Terzis, 1977).

The *perineurium* is a dense and distinct sheath of connective tissue formed from concentric layers of connective tissue that surrounds the nerve fibres and the endoneurium of the fasciculus (Figure 1.2). The internal and the middle layers consist

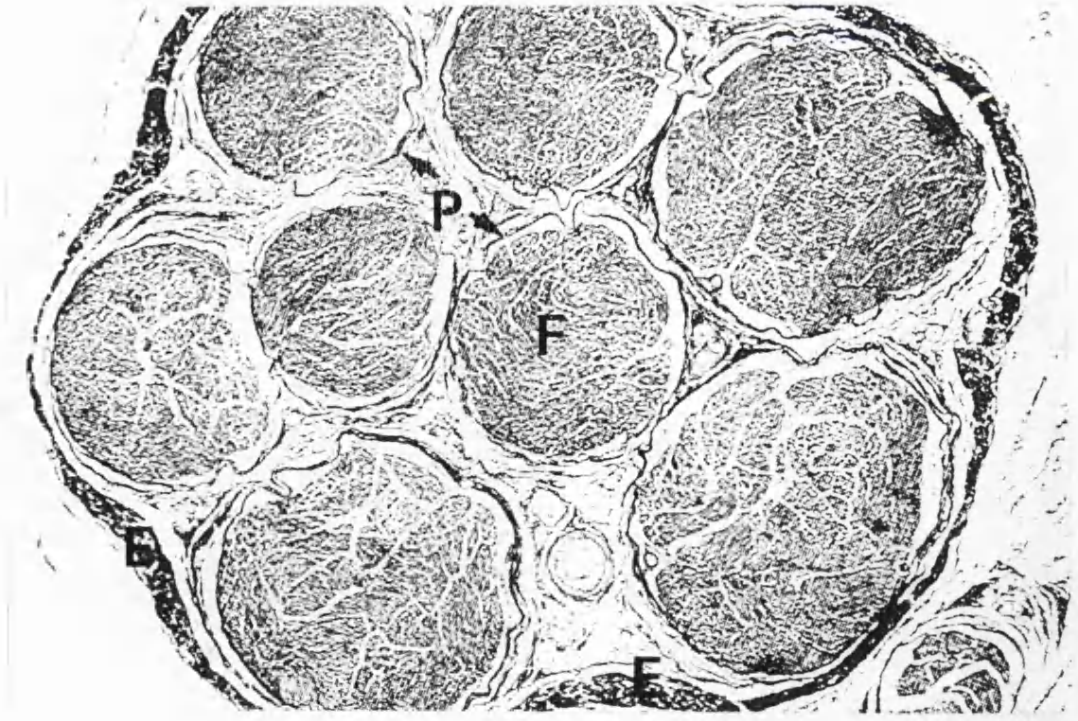

Figure 1.1. *Cross-sectional anatomy of the peripheral nerve. The micrograph illustrates the typical appearance of a medium sized nerve stained with van Gieson. This nerve consists of eight fascicles, F and each fascicle is surrounded by the perineurium, P while the whole nerve is surrounded by the epineurium, E.*

of flattened cells with long processes and a basement membrane (Shantha, 1968). The boundaries of the perineurial cells form tight junctions and their basement membranes fuse to form a single intervening membrane which acts as a diffusion barrier (Low, 1976; Thomas et al., 1993) and prevents free passage of proteins and other molecules and helps prevent the spread of infection and inflammation into the fasciculus (Thomas and Jones, 1967; Denny-Brown, 1946). The perineurium also provides physical strength to the nerve during extension (Sunderland and Bradley, 1952). The external layer forms a transitional zone from the perineurium to the epineurium where collagen fibres become disorderly and replaced by a more open arrangement and the perineurial cells are replaced by fibroblasts of the epineurium.

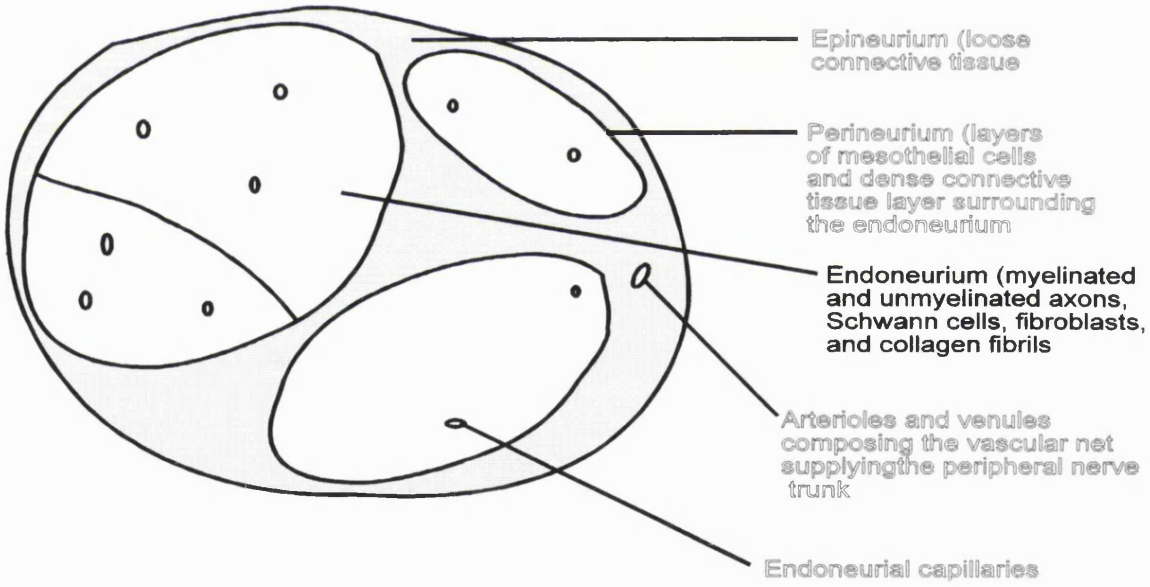

Figure 1.2. *Diagrammatic representation of the main connective tissues in cross-section of peripheral nerves.*

The *endoneurium* is the supporting connective tissue that fills the fasciculus and provides the packing material between nerve fibres (Figure 1.2). The endoneurium is mainly composed of fibroblasts and collagen fibrils which form tubes of loosely packed

fibrils around nerve fibres (Ushiki and Ide, 1990); the tubes contain Schwann cells and the axon (Thomas, 1963). The non-cellular components of these sheaths are mainly collagen fibrils, which presumably serve as scaffolds for nerve fibres (Ushiki and Ide, 1990). Fine intrafascicular septa partly divide the nerve fibres into smaller groupings. Spaces also exist in the endoneurium which are filled with extracellular fluid.

1.3.2. Fasciculi

Peripheral nerve trunks are composed of one or more fasciculi. The fasciculus is a bundle of nerve fibres surrounded by a thin but strong cellular layer, the perineurium (Sunderland, 1978). The pattern of fascicular formation in cross-section of nerves is often not constant down its entire length with the fasciculi branching, reforming and branching repeatedly. The diameter of human peripheral nerve fasciculi ranges from 0.04 mm to 2.0 mm with occasional fasciculus of 4.0 mm in diameter (Madison et al., 1989). Many fascicular patterns exist, including mono-, oligo- and polyfascicular.

1.3.3. Blood Vessels

Peripheral nerves are abundantly supplied by a vast system of vasculature throughout its entire length (Bell and Weddell, 1984a and 1984b; Lundborg, 1979 and 1975). 'Arteria nervorum' blood vessels enter and terminate within the nerve trunk and are derived from the main vessels of the limb or its branches and exclusively supply the nerve. Other vessels originate from muscular and cutaneous branches that predominantly supply the extraneural tissues. Macroscopic arterioles which have a longitudinal arrangement are usually visible on the surface of large peripheral nerves (Figure 1.3). The intraneural pattern of the venous network generally corresponds to

the arterial pattern, however, the number of intrafascicular venules appear to exceed the number of arterioles and drain into the principal vein, veins or venus plexus associated with the neighbouring artery. The endoneurial cells of the endoneurial capillaries have tight junctions which are normally impermeable to a wide range of substances and form the blood-nerve barrier.

1.3.4. The Schwann cell

One factor important in the regeneration of nerves is the Schwann cell, whose principle function is to provide myelin and unmyelinated ensheathment for peripheral

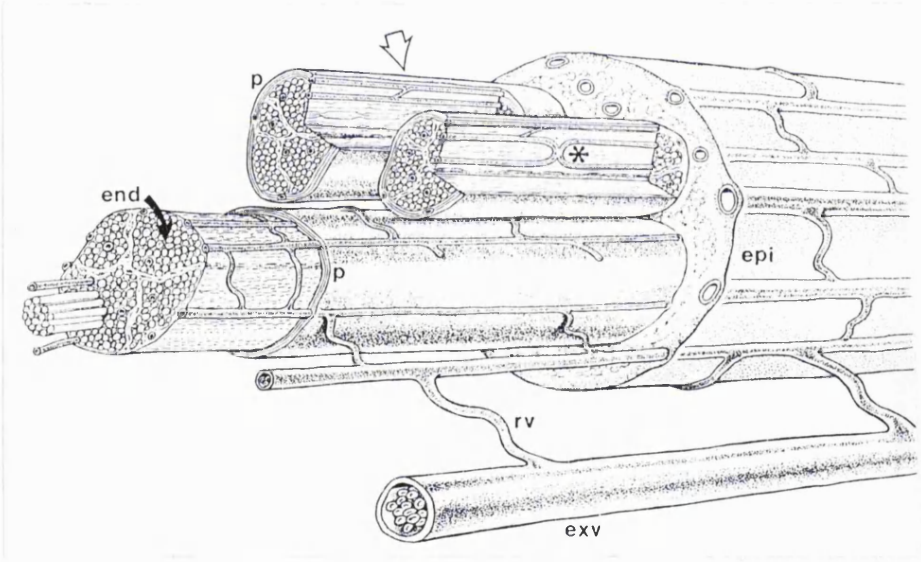

Figure 1.3. *Schematic diagram of intraneural microcirculation of peripheral nerves. Extrinsic vessels (exv) are linked by regional feeding vessels (rv) supporting vascular plexus in superficial and deep layers of the epineurium (epi), perineurium (p) and endoneurium (end). Vessels penetrate obliquely through the perineurium (arrows). Taken from Lundborg G. (1989). Nerve Injury and Repair. Churchill Livingstone, Edinburgh.*

nerve fibres (Figure 1.4.). In addition Schwann cells synthesise a portion of the peripheral nerve connective tissue matrix, including the basement membrane that

surrounds each cell-axon unit (Bunge et al, 1982). Schwann cells migrate extensively during the development and regeneration of peripheral nerves. To populate the PNS during development, Schwann cells first migrate along the axons at the outer surface of the developing nerve and then migrate perpendicular to the nerve axis into the axon bundles. Migrating Schwann cells may also play a role in axon growth and guidance during development (Keynes 1987; Noakes and Bennet, 1987).

When peripheral nerves are damaged Schwann cells have been shown to migrate together with macrophages, which reside in the nerve or are recruited as blood-borne monocytes from the surrounding damaged tissue into the affected site (Perry et al., 1987; Griffin et al., 1993) and are responsible to carry out Wallerian degeneration. Myelin sheaths are degraded into various forms of myelin balls within Schwann cells and subsequently phagocytosed by macrophages (Williams and Hall, 1971; Stoll et al., 1989). Schwann cells proliferate at the early phase of Wallerian degeneration, and later cease while extending slender cytoplasmic processes, which form cellular strands called the Schwann cells column (reviewed by Ide, 1996). Schwann cell columns serve as effective pathways for the growth of axons. Schwann cells in a damaged nerve serve a dual role in that they serve as scaffolds for regenerating axons by expressing adhesion molecules on the surface plasma membrane and produce various trophic factors for regenerating axons (Bunge, 1993).

Macrophages were originally thought to enter the site of tissue damage and phagocytose debris and clear the path of regenerating axons. There was also suggestion of the involvement of Schwann cells in Wallerian degeneration either alone

(Nathaniel and Pease., 1963; Satinsky et al., 1969) or co-operatively with histocytes or macrophages (Weinberg and Spencer, 1987; Stoll et al., 1989). Some studies however, have questioned whether Schwann cells have any role in myelin degradation at all

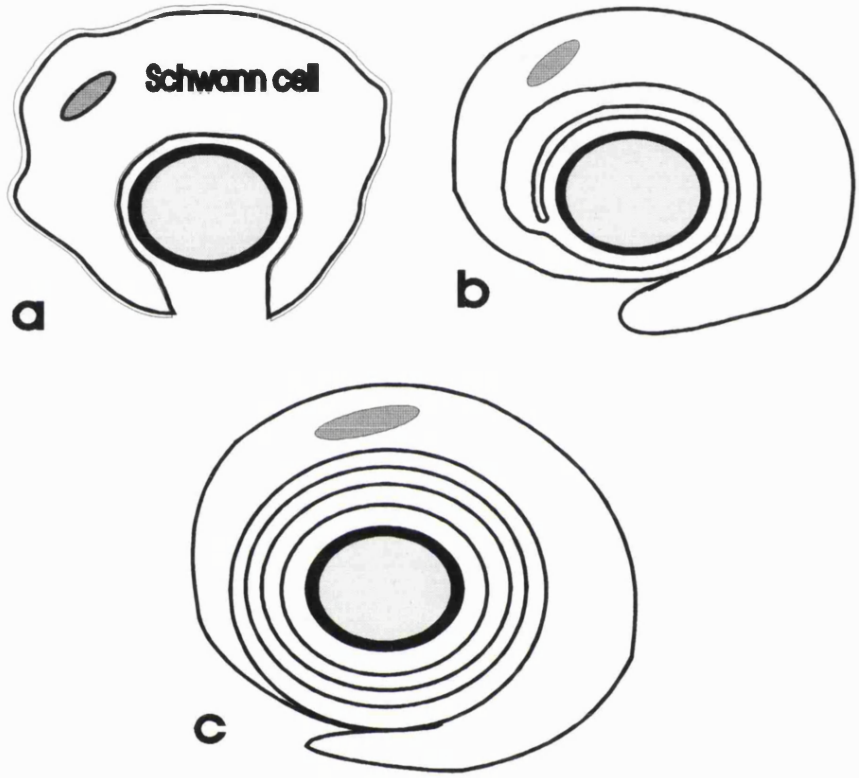

Figure 1.4. *Diagrammatic representation of Schwann cell myelination. (a) The Schwann cell invaginates a single nerve fibre forming mesaxons. (b) As myelination proceeds the mesaxon wraps around the axon enveloping the axon in a spiral layer of Schwann cell cytoplasm. (c) As the process continues, the cytoplasm is excluded; by maturity, the inner layers of plasma membrane fuse with each other so that the axon becomes surrounded by layers of modified membranes which together constitute the myelin sheath.*

(Crang and Blakemore, 1986; Beuche and Friede, 1984) and emphasise the role of macrophages in myelin phagocytosis, stimulation of Schwann cell proliferation (Beuche and Friede, 1984) and induction of gene expression in non-neuronal cells of

the sciatic nerve (Lindholm et al., 1987; Brown et al., 1991; Venezie et al., 1995). However, a recent study has shown that Schwann cells are able to degrade myelin and proliferate in the absence of macrophages in vitro (Fernandez-Valle et al., 1995).

1.4. Axon guidance

Axons actively navigate to their targets by reading chemical cues in their environment. This leads to the emergence of growth cones which continually extend and retract broad membranous sheets called lamellipodia, and slender, spikelike protrusions termed filopodia, for distances of tens of micrometers, as if sampling the substrate in every direction. Filopodia appear to be able to adhere to the substrate and pull the growth cone in their direction. The mechanism of this interaction is shown in Figure 1.5. Actin filaments are propelled rearward by interactions with molecules of myosin anchored to the membrane. Actin monomers are added to filaments at the leading edge, and filament depolymerization occurs in the central region of the growth cone. Extension of the leading edge may be powered by the polymerisation of actin, or by the movement of myosin molecules in the region of the leading edge along actin filaments whose rearward movement has temporarily been halted by the inactivity of more centrally located myosin molecules (Smith, 1988; Sheetz et al., 1992). Using immunocytochemistry it has been shown that actin filaments align with filopodia in the periphery of the growth cone, randomly orientated filaments are often concentrated near the central domain. However, microtubules are concentrated in the axon; some also extend to the growth cone margins.

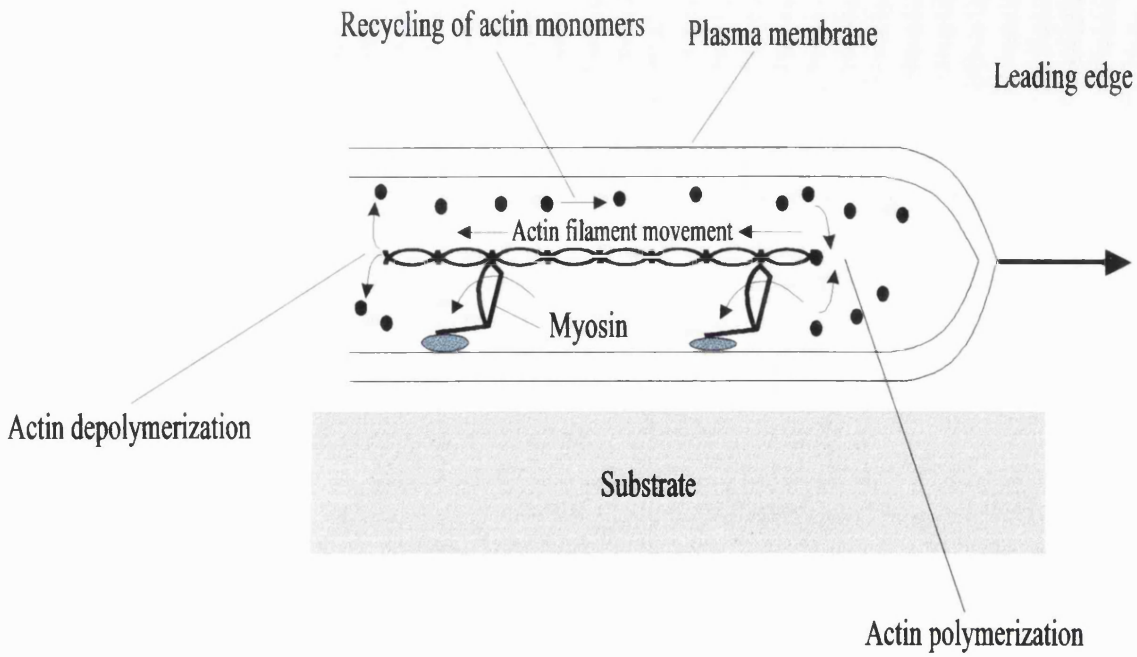

Figure 1.5. *Model for actin-based motility of growth cones. Actin filaments are propelled rearward by interactions with molecules of myosin anchored to the membrane. Actin monomers are added to filaments at the leading edge, and filament depolymerization occurs in the central region of the growth cone. Extension of the leading edge maybe powered by the polymerisation of actin, or by the movement of myosin molecules in the region of the leading edge along actin filaments whose reward movement has temporarily been halted by inactivity of more centrally located myosin molecules. (After Smith, 1988; Wayne et al., 1992).*

Recent reports have accumulated evidence that the growth cone translates extracellular signals into directed growth cone motility, which relies upon a rise in intracellular calcium levels. A variety of molecules such as adhesion molecules and neurotransmitters, increased intracellular calcium, and artificial manipulations of growth cone calcium levels affect growth cone morphology and neurite outgrowth (Chang et al, 1995). In this interaction it is apparent that calcineurin, a protein phosphatase enriched in growth cones that is dependent on calcium ions and calmodulin, functions in neurite outgrowth and directed filopodial motility in cultured

chick dorsal root ganglia neurons (Chang et al, 1995). However, Cyclosporin A and FK506, which are potent inhibitors of calcineurin, delayed neuritogenesis and inhibited neurite extension (Chang et al, 1995). Chromophore-assisted laser (micro-CALI) inactivation of calcineurin in regions of growth cones causes localised filopodial and lamellipodial retraction and influences the direction of subsequent outgrowth (Chang et al, 1995). This study suggests that a spatial distribution of calcineurin activity within the growth plate regulate growth cone motility and directed outgrowth.

Schwann cells play a role in axon growth during development. This has been elucidated by Bixby and co-workers, who have used antibodies against Ca^{2+} independent CAM, L1/Ng CAM, Ca^{2+} dependent CAM and N-cadherin. It was observed that growth cones use integrin class extracellular matrix receptors and at least two CAMs-N-cadherin and Ll/NgCAM- for growth on Schwann cells in vitro (Bixby et al, 1988). The mechanism of this interaction with the growth cone is show in Figure 1.6.

1.5. Primary and secondary repair of peripheral nerves

Following a nerve transection injury an immediate primary repair of a sharply cut nerve is desirable. In this early phase it is possible to achieve an exact orientation of the cut nerve end because of well-preserved landmarks such as the fascicular pattern in the transected surfaces and the longitudinal epineurial vessels. The ends are usually coapted without tension. The epineurial suture technique (Figure 1.7.) represents a simple procedure for nerve repair however, this does not achieve the correct matching of internal fascicular structures (reviewed by Lundborg et al., 1989). The 'group

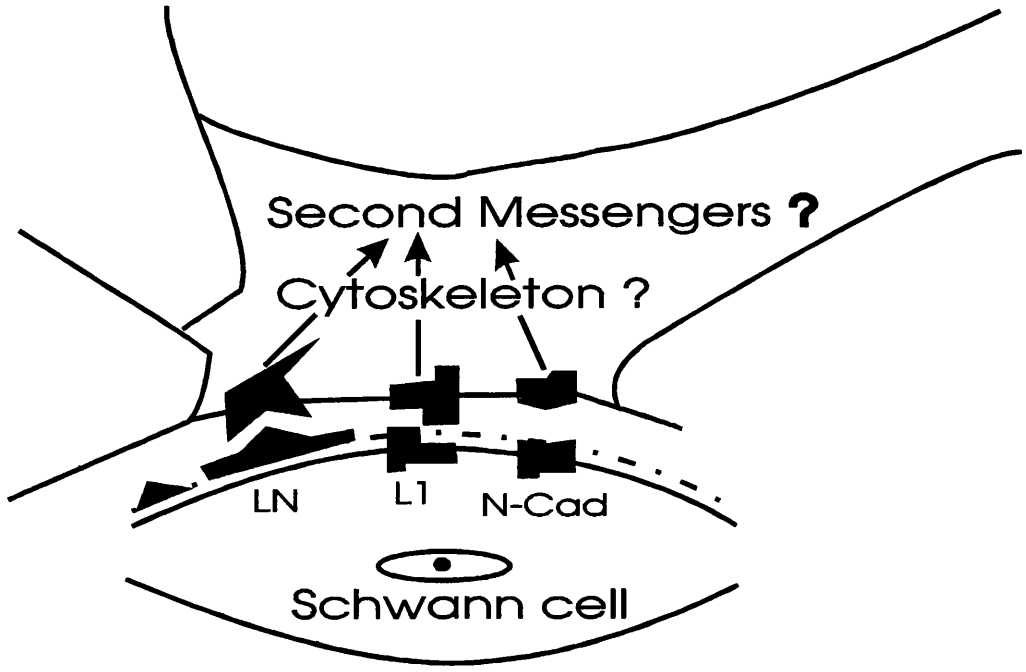

Figure 1.6. *Model of surface interactions mediating neuronal process outgrowth on Schwann cells. The model illustrates a neuronal growth cone interacting with a Schwann cell. The model shows Ll/NgCAM (Ll) and N-cadherin (N-Cad) in the Schwann cell membrane interacting by homophilic binding with the same molecules in the growth cone membrane. Similarly, ECM proteins secreted by Schwann cell including laminin (LN) are shown interacting with ECM receptors of the integrin family (Int) in the growth cone membrane. These binding events cause intracellular changes in the growth cone through cytoskeletal events to release second messengers (eg. intracellular free Ca2+). This in turn is postulated to lead to axonal elongation. (Taken from Bixby et al, 1995).*

fascicular' repair technique (Figure 1.8.) is a better technique to obtain optimal orientation and adaptation of groups of fascicles (reviewed by Lundborg et al., 1989). With this technique, epinurial tissue is resected over a short distance, fascicular groups are dissected and corresponding fascicular structures in both nerve ends are sutured individually. This technique carries a greater risk however, of microhemorrhage, edema and scarring.

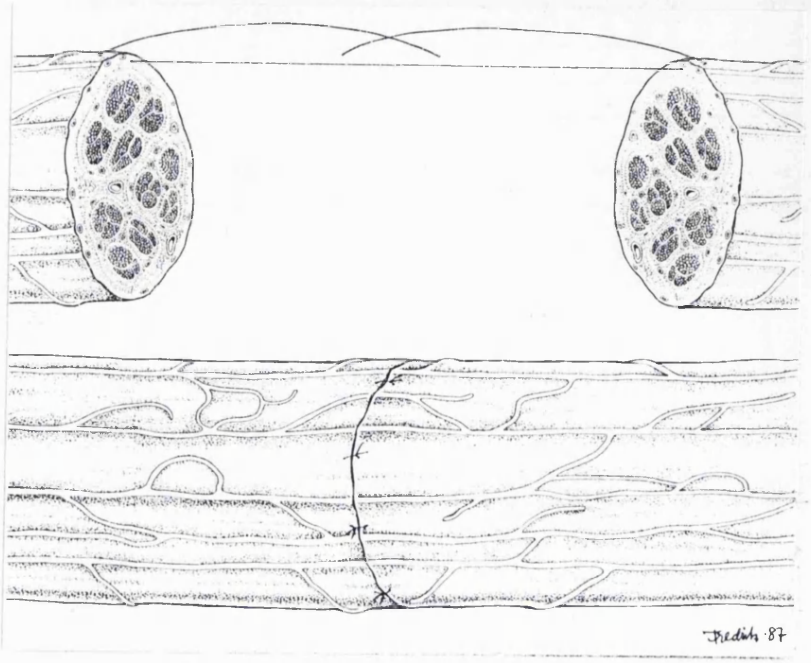

Figure 1.7. *Epineurial suture technique to repair transected peripheral nerves. Taken from Lundborg, G. (1989). Nerve Injury and Repair. Churchill Livingstone, Edinburgh.*

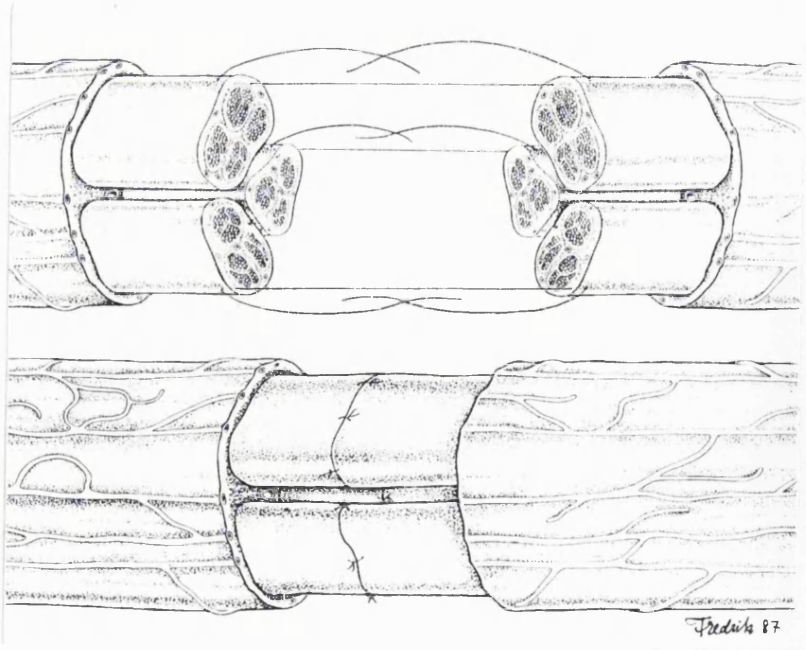

Figure 1.8. *Group fascicular technique to repair transected peripheral nerve. Taken from Lundborg, G. (1989). Nerve Injury and Repair. Churchill Livingstone, Edinburgh.*

Many attempts by investigators have been made to decipher which is the better technique but no consistent advantage of one technique over the other has been demonstrated (Lundborg et al., 1989). However, reports suggest that there is improved specificity of muscle reinnervation after fascicular suture in the rat sciatic nerve (Lundborg et al., 1989). These techniques are restricted to primary repair i.e. where the gaps are very short. Commonly though, nerve injuries produce a surgically irreducible gap which must be repaired with the use of a suitable conduit material.

1.6. Entubation repair of peripheral nerves

Entubation repair has been used extensively to enhance or study the mechanisms of peripheral nerve repair. The effects of gap length, distal stump components and initial ingrowth have been studied previously by Lundborg et al, 1982 and Longo et al, 1983 by bridging transected rat sciatic nerves with silicone tubes. There are several characteristics of a successful nerve guide conduit. These include control over the rate of resorption and change in mechanical properties with time in vivo, the permeability properties of the conduit membrane, the surgical techniques used to stabilise the nerve stumps within the conduit and flexibility in terms of manufacturing various sizes of conduits.

Many biodegradable and non-biodegradable materials have been used to regenerate peripheral nerves. These include polylactate/polyglycolate copolymers (Reid et al., 1978; Dellon and Mackinnon, 1988); acrylic copolymers (Uzman and Villegas, 1983; Hurtado et al., 1987); polyvinylidene fluoride (PVDF) (Aebischer et al., 1987; Aebischer and Guenard et al., 1988); polyglactin mesh (Molander et al., 1982)

Millipore filter material (Noback et al., 1958); silicone (Longo et al., 1983; Lundborg et al., 1982a; Lundborg et al., 1982b); Gore tex (Young, 1984); arterial cuffs (Zachery and Holmes, 1946; Weiss and Davis, 1943; Weiss and Taylor, 1946); preformed mesothelial tubes (Lundborg et al., 1981); collagen (Braun, 1964; Kline and Hayes, 1964; Archibald et al., 1988; Archibald et al., 1989; Archibald and Madison, 1991; MacKinnon et al., 1984); polylactates (Madison et al., 1985; Madison et al., 1984) and various other synthetic polyesters (Nyilas et al., 1983; Henry et al., 1985).

1.7. Fibronectin

Fibronectin (Fn) has been used extensively in this thesis due to its cell adhesion property and the fact that it promotes neurite outgrowth. Fn-mats were shown to enhance peripheral nerve regeneration in a rat model by providing a surface guidance structure for Schwann cell infiltration and axonal outgrowth (Whitworth et al., 1995a, 1995b, 1996). After peripheral nerve injury, the normal nerve undergoes degeneration leaving Schwann cell basal lamina which acts as a surface for migration of regenerating components of nerves. Fn-mats as a conduit provides a network of fibrils which allows outgrowth of regenerating components similar to that provided by the basal lamina in a normal nerve or a nerve graft. For this reason Fn-mats were used as support materials with a potential to grow cultured Schwann cells within mats such that these may then be implanted into the injured gap.

Fn is a glycoprotein which was initially isolated, independently, by a number of different researchers (Morrison and Edsall, 1948). At first called cold-insoluble globulin because coprecipitation with fibrinogen was a characteristic of the protein,

plasma Fn did not appear to have any discernible function, nor did it attract much attention. With the identification of its in vivo properties Fn became known as a large, external, transformation sensitive protein (LETS), cell surface protein (CSP) or cell adhesion factor (CAF) referring to its cell adhesion properties (Yamada and Olden, 1978) of the cellular form of Fn. Fn is a large 500 kD glycoprotein found on the surface of several cell types such as fibroblasts, large quantities in plasma (~0.3 g/L) and in the extracellular matrix. It is a dimer composed of two nearly identical polypeptide chains which contains distinct and specific binding sites for cell surface receptors, extracellular matrix materials such as collagen, glycosaminoglycans and Fn itself (Figure 1.9.). Fibronectin has several functions including adhesive and ligand binding characteristics. Fibronectin can also affect cell morphology, influence intracellular mechanisms, promote phagocytic activities and stimulate cell movement (Yamada, 1983).

During wound repair fibroblasts synthesise Fn (Carsons, 1989; Mosher, 1989) and use the endogenously produced Fn to facilitate reactive processes, such as migration (Ali and Hynes, 1987) and phagocytosis (Carsons, 1989). Fibronectin can act as a chemotactic factor for peripheral blood monocytes and as a non-specific opsonin of debris during the inflammatory phase of wound repair. During granulation tissue formation, Fn provides a substrate for cell movement. The fibroblasts that migrate into the wound region rapidly secrete an extensive Fn-matrix and shortly thereafter large amounts of type III collagen are deposited onto this matrix, acting as a provisional scaffold (Grinnell, 1984; Clark et al., 1982).

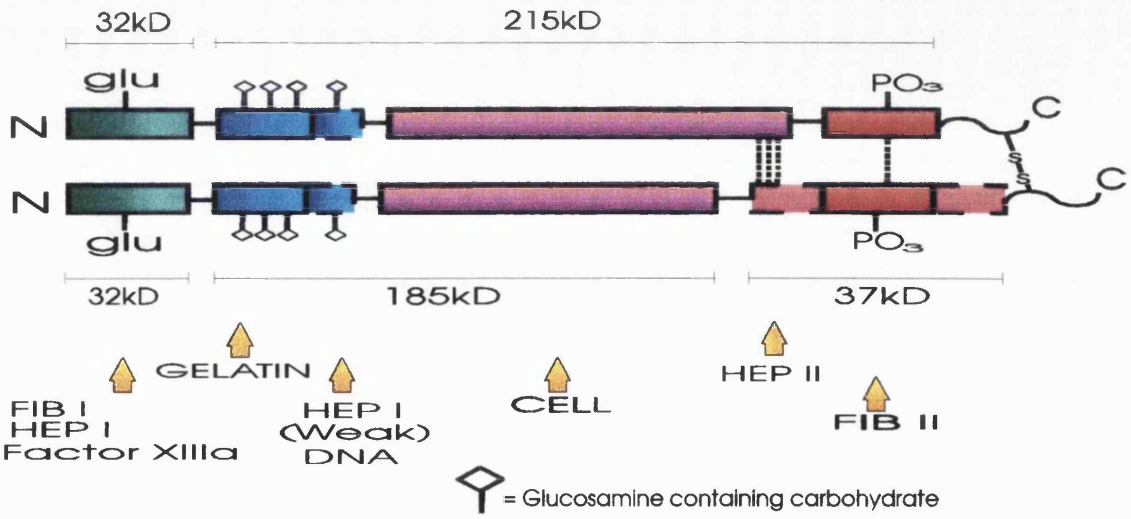

Figure 1.9. *The structure of Fn. FIB= fibronectin and HEP = heparin binding sites. Courtesy of Mrs. G. Talas, UCL.*

Fn adsorbs rapidly to culture surfaces, producing a substratum amenable to the attachment and growth of a variety of anchorage-dependent cell types (reviewed by Mosher, 1980). Plasma Fn bound to a particular substrata (untreated plastic, glass or collagen) have been shown to enhance their capacity to support retinal neurite outgrowth (Akers et al, 1981). This promotion of neurite outgrowth was found over a range of Fn concentrations with as little as 2.5μg/mL Fn on plastic culture dishes producing a four-fold increase in the percentage of aggregates extending neurites compared with untreated dishes (Akers et al, 1981). Fn has also been reported not only to promote rat Schwann cell growth and motility (Evercooren et al, 1982) but also acted as a chemoattractant for Schwann cells. This mitogenic effect was shown to be dose- and time-dependant.

Models for the assembly of fibronectin into a fibrillar matrix propose a stepwise process initiated by binding to cell surface receptors followed by assembly and

reorganisation into fibrils (McDonald, 1988; Mosher et al., 1991; Mosher et al., 1992; Mosher, 1993; Akiyama et al., 1991; Chernousov et al., 1991; Nagai et al., 1991; Schwarzbauer, 1991; Morla and Ruoslahti, 1992; Hynes 1990). The first step involves the capture of fibronectin dimers from the surrounding environment and is likely to involve the $\alpha 5\beta 1$ integrin and the molecules which bind to the amino-terminal 70 kDa region. The second step is the translocation of these captured dimers to the growing end of the Fn fibre. The third step is thought to involve the regions of Fn self-association which cause Fn-Fn alignment and finally, the fourth step involves covalent stabilisation of the aligned Fn fibril molecules by disulfide cross-links.

There are two distinct groups of fibronectin molecules in the human body- plasma and tissue or cellular fibronectin. Circulating plasma fibronectin is synthesised and secreted by liver cells (hepatocytes) (Owens and Cimino, 1982). The steady-state plasma concentration is about 0.3 g/L. Cellular fibronectin is produced by fibroblasts and remains localised on the cell surface. Plasma fibronectin contains two nearly identical polypeptide chains (Mr= 220,000-250,000), which are held together near the carboxyl terminus by two disulfide bonds.

1.7.1. Plasma Fibronectin

Fibronectin has increasing solubility with temperature and thus at body temperature the molecule is soluble in the plasma (Yamada and Olden, 1978). Plasma fibronectin is produced by vascular endothelial and liver cells, allowing secretion of the molecule into the blood. Many cell types, including macrophages are thought to have a pool of plasma Fn which is produced by hepatocytes of the liver (Saba, 1989). Hepatocytes in

culture produce Fn which co-migrates with human plasma Fn on electrophoresis (Mosher, 1984).

1.8. Fibrinogen

The source material used to make Fn-cables and LFn-cables normally contains 25% fibrinogen (Fg) and 75% Fn. However, as a result of a mistake during production the composition altered to 25% Fn and 75% Fg. Cells were unable to adhere to cables made from this composition of Fn/Fg on many attempts. It was proposed that high concentrations of Fg were detrimental to cell adhesion and therefore tested by reducing the concentration of Fg within cables. An additional hypothesis drawn from this result was that cell migration on cables may be increased by increasing the concentration of Fg within cables.

Fibrinogen (Fg) is a glycoprotein which is synthesised in the microsomes of liver parenchymal cells (Barnhart and Anderson, 1962) and in the platelets (Rosiek et al., 1969). Liver fibrinogen is stored in the soluble fraction of the parenchymal cells until released into the blood. Release of Fg occurs as a response to many conditions such as physiological (age, pregnancy) and pathological (infection, inflammation) in addition to normal homeostatic requirements. Fg is also classified as an acute phase reactant since its plasma level may rise in response to various pathologies (reviewed by Marsh, 1981). Besides these functions Fg takes part in the inflammatory response, in defence against infection and in wound healing (reviewed by Marsh, 1981).

Fg has a molecular weight of 340 kDa and is mainly polymerised to form fibrin. The conformational shapes and dimensions of the molecule are summarised in Figure 1.10.

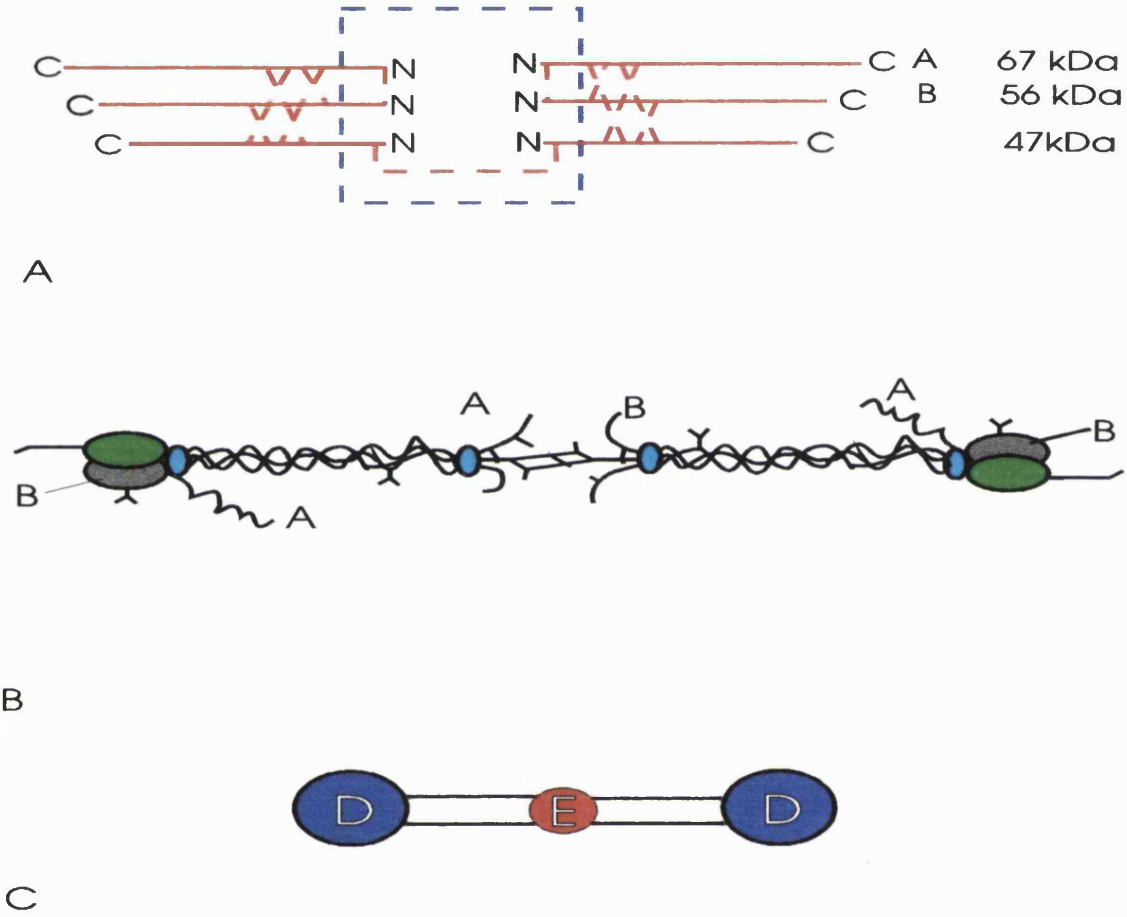

Figure 1.10. *Schematic representation of the fibrinogen structure. (A) Pairs of Aα, Bβ and γ chains are linked by inter-chain disulphide bonds (represented by broken lines) to form a fibrinogen molecule. (B) The N-terminal domain containing the disulphide bridges is connected to the carboxyl terminal domains by the coiled-coil regions. (C) Schematic of the trinodular structure of fibrinogen. The E domain corresponds to the N-termini of the three pairs of chains, while each D domain contains the C-terminus of one Bβ and γ chain and the random coil region near the C-terminus of the Aα chain. The latter has a flexible C-terminus extending away from the D domain region.*

The molecule appears as a trinodular rod, 7 × 48 nm and contains three pairs of non-identical chains Aα (67 kDa), Bβ (56 kDa) and γ (47 kDa). Assembly of Fg occurs through complex interchain disulphide bonding involving the N-terminal regions of the three polypeptides; together, these form the central modular E domain. The globular ends of the D domain, containing the C-termini of Bβ and γ chains. D and E domains are connected by the coiled-coil regions of the three chains while the Aα C-terminus appears as a flexible appendix of the oblong molecule. One N-linked carbohydrate chain exists on each of the Bβ and γ chains (Townsend et al., 1982).

Fibrin together with plasma Fn form the main components of thrombus (Furie and Furie, 1988; Clark et al., 1982; Gailit and Clark, 1994). Clot formation occurs when soluble Fg is converted by thrombin to fibrin, the structural protein that spontaneously assembles into fibrin polymer. After this assembly, the transglutaminase, coagulation factor XIII (also to Fn N-terminal domain), stabilises the structure by cross-linking covalently the α and γ chains. Fg has been shown to induce adhesion, cell spreading and microfilament organisation in endothelial cells in vitro (Dejane et al., 1987).

1.9. Fibronectin Mats and Peripheral Nerve Regeneration

In our laboratory we have been able to make orientated mats of fibronectin developed by Ejim et al., 1993. The crude starting material obtained from BPL (BPL Bio Products Ltd, Elstree, Middlesex, England), is initially purified by gelatine Sepharose affinity chromatography. The solution of purified fibronectin is then introduced into an

ultrafiltration cell where a unidirectional shear force is applied. During the final stages of concentration, a mat of fibronectin forms around the shaft, which is rinsed in a large volume of distilled water and freeze dried (Figure 1.11.a and b). The overall unidirectional orientation of the fibres is apparent from Figure (1.11.b). Orientation can also be seen clearly with scanning electron micrographs of mats (Figure 1.11.c). Scanning electron micrographs also show 'pockets' (indicated by the arrow in Figure 1.11.c) where cells can enter, invade and remodel the mat.

Fn-mats have been used in a number of experimental models to assess its uses as a potential implantable material in peripheral nerves. The experimental model used for these studies has been the sciatic nerve of male Wister rats in which a 1cm gap is created by incision (Figure 1.12.). Fn-mats were formed into a conduit by suturing each end of the nerve onto the flat Fn sheet which was then rolled over and sutured to the epineurium to form a cylindrical conduit. The fibronectin is hydroscopic and expands rapidly so that by the end of the procedure the cylinders had expanded to form a solid conduit without a hollow centre (Porter et al., submitted).

Whitworth et al have been able to show that Fn-mats are capable of supporting the regeneration of peripheral nerves (Whitworth et al, 1995a). They found that by day 15, regenerating axons had extended to the distal end forming a thin bridge which had a volume of regenerated axons and Schwann cells that were comparable to nerve grafts. In a further study Whitworth et al showed that Fn-mats impregnated with NGF released NGF slowly over a period of 7 days in a bioactive form (Whitworth et al, 1996). The delivery of NGF to the site of injury in rats produced an increase in the

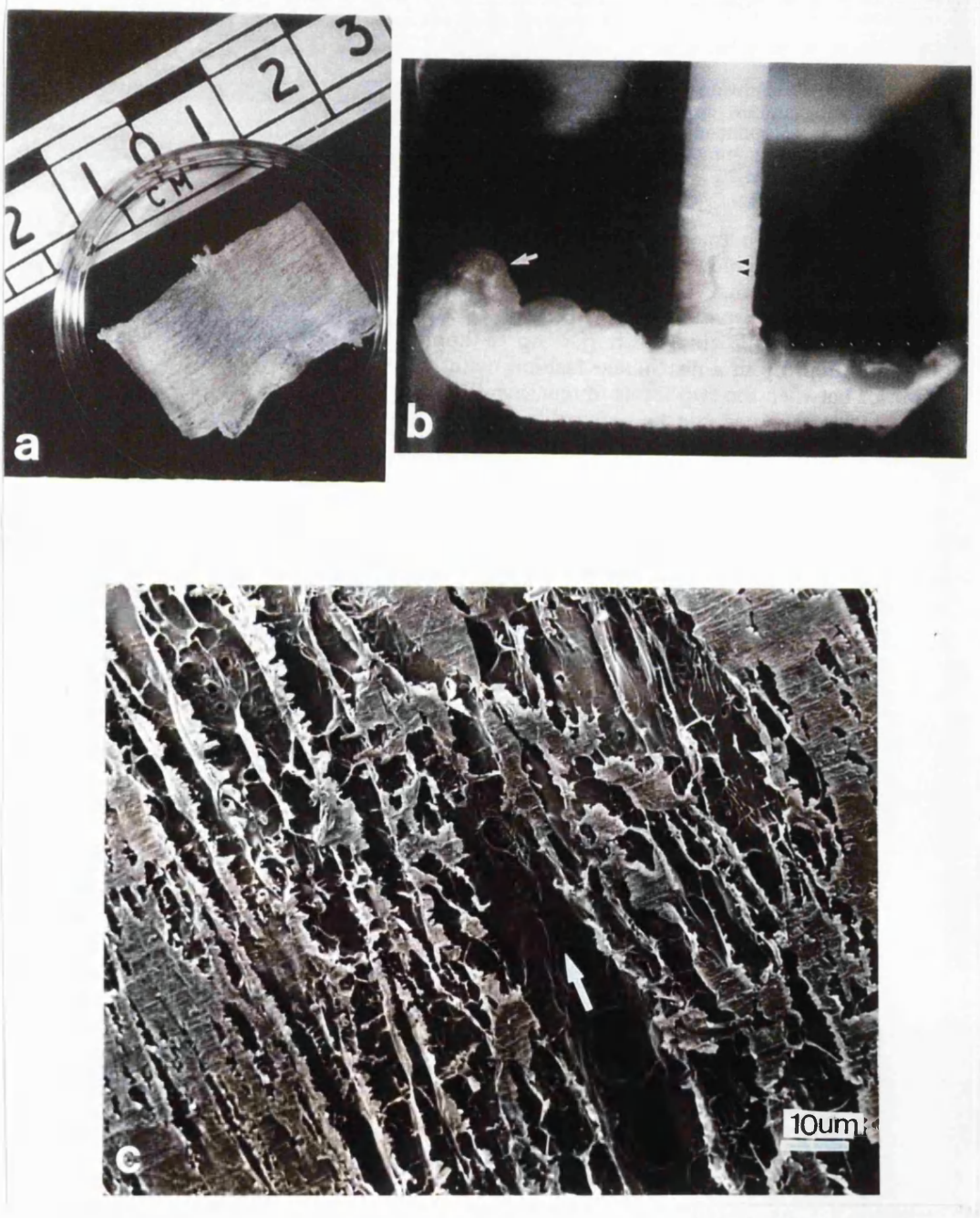

Figure 1.11. *The stirred cell with a mat formed around the shaft (a). (b) Appearance of the mat after freeze drying in which the fibrillar nature of the mat can be seen. (c) Scanning electron micrograph of Fn-mat indicating fibrillar structure with pockets for cell infiltration (arrow).*

volume of axonal and Schwann cell regeneration when compared to conduits of plain Fn (Whitworth et, 1996). Further, NGF impregnated mats used for targeted delivery of nerve growth factor in both control and diabetic rats, increased the distance and amount of regenerating immunoreactivity to CGRP and GAP-43 in both control and diabetic rats (Whitworth et al, 1995b).

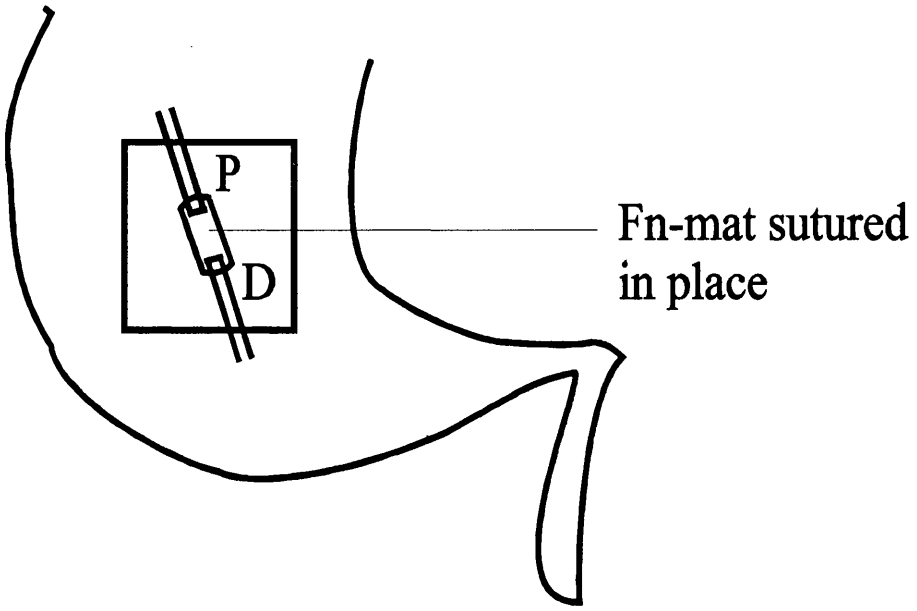

Figure 1.12. *Diagram to show the experimental model of peripheral nerve regeneration in rats with Fn-mat conduits. The Fn-mat is joined to the proximal and distal stumps by the epineurial sutures. P= proximal and D= distal stumps of sciatic nerve*

Fn-mats impregnated with NT-3 has also been shown to improve sciatic nerve regeneration in a similar way to that of NGF (Sterne et al., 1997a) but much higher concentrations of NT-3 must be used compared to NGF. NT-3 impregnated Fn-mats were further shown to improve selective recovery of muscle fibre expressing myosin heavy chains 2b with an overall beneficial effect on motor target organs (Sterne et al.,

1997b). Studies using Fn-mats to show the inter-relationship of angiogenesis and nerve regeneration showed that graft vascularisation initially proceeded from the adjacent muscle bed and that a neovascularisation front preceded axonal regeneration (Hobson et al., 1996). Further, Schwann cells and axons extended together but never exceeded the area of vascularisation and appeared most numerous in well vascularised areas. The vessels within the mat were longitudinally orientated in the original axis of the fibrils within Fn-mats (Hobson et al., 1996).

Porter et al., submitted, studying ultrastructural features of Fn-mats grafted in a 1cm lesion of the rat sciatic nerve showed that invading axons and Schwann cells were orientated along the fibres of the Fn-mat. Light microscopy revealed a cone of axon sprouts emerging from the proximal stump which had entered into the mat by day 4. By day 15 a thin regenerate had formed bridging the lesion. Electron microscopy showed the mat was able to orientate collagen within the nerve and fibroblasts were also orientated in the epineurium. However, the interaction of macrophages with Fn-mats caused the complete degradation of the mats by day 15 (Figure 1.13.).

1.10. Fibronectin strands

Strands of Fn can be made by drawing out single fibres from a small pool of purified Fn solution (1mg/mL in PBS), (as described by Ejim et al, 1993). This method can be used to draw a strand of aggregated protein which can extend for several millimetres from the surface of the liquid. The microscopic strands of the same protein as Fn-mats were used as a model for the matting process. Fn-mats are composed of many of these fibres and thus isolation of a single strand of Fn provides a simpler two dimensional

surface for the study of cell adhesion and migration as well as the effects of topography on cultured cells compared to Fn-mats. Cell behaviour in vitro can easily monitored on this system by time-lapse video-microscopy and other immunostaining and histological methods. We hypothesised that Fn-strands will speed up cellular migration, particularly of Schwann cells, as a response to topographical cues as well as the cell adhesion property of Fn. We further hypothesised that Fn-strands will cause the alignment of cells and their cytoskeleton to the direction of fibre axis.

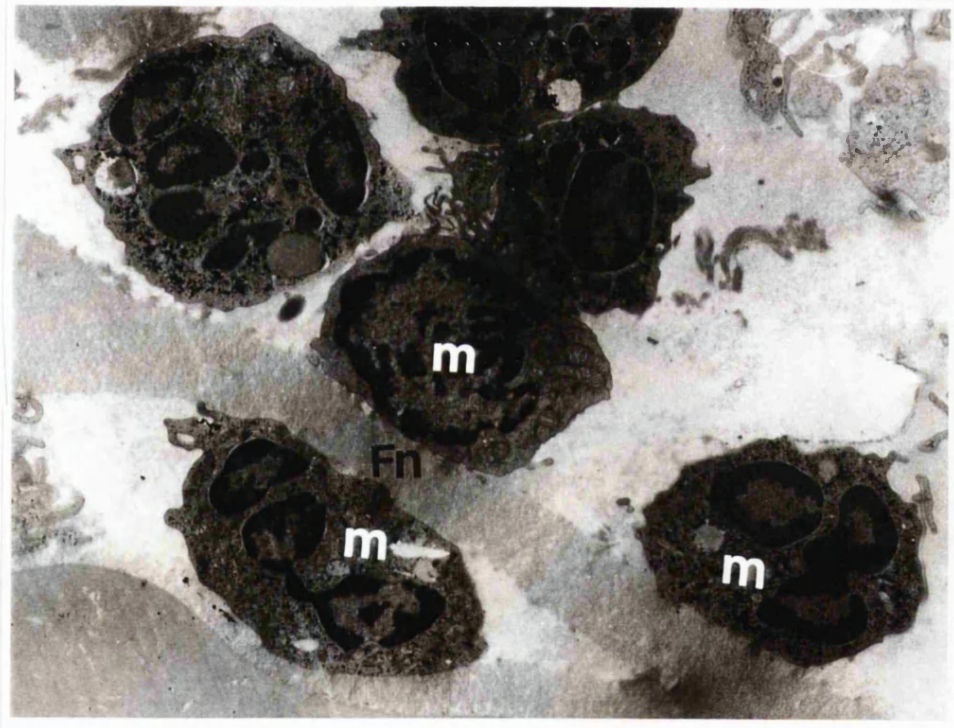

Figure 1.13. *Transmission electron micrograph of macrophage (m) interaction with Fn-mats (Fn). Macrophages degrade the Fn-mat by day 15 in vivo. Courtesy of Porter et al. submitted.*

Human dermal fibroblasts cultured with such strands attached to one side and became aligned along the axis of the strands (Ejim et al, 1993). Similar fibres were also used to investigate the behaviour of different populations of fibroblasts, macrophage-like

P388D1 cells and neurones cultured from rat dorsal root ganglia (Wojciak-Stothard et al, 1997). The fibres significantly promoted cell spreading and caused a marked alignment of actin filaments in fibroblasts and focal contacts in fibroblasts and macrophages while increasing polymerisation of F-actin in cells (Wojciak-Stothard et al, 1997). Fn fibres also increased the speed and persistence of cell movement and the rate of neurite outgrowth (Wojciak-Stothard et al, 1997).

A variant form of the Fn strands (known as Fn-cables) can be prepared from an enriched Fn preparation containing Fg. These Fn-cables are pulled out and precipitated into strands by a similar method though involving treatment with low pH solution. (Sarah Underwood, PhD Thesis, UCLMS; Underwood et al. submitted) (Figure 1.14.). These cables are easy to produce and can be made to a larger scale than that allowed by Fn-strands. The diameter of these fibres can also be altered from 100-200μm thereby allowing cells to adhere onto the surface which can then be used as transplant of cells if required. Here it is proposed that Fg is less adhesive than Fn and therefore a small concentration of Fg may block some of the highly adhesive sites on the Fn molecule thus causing increased cell migration. This will be beneficial in that peripheral nerve regeneration would occur quicker thus reducing the effects of donor site morbidity (a significant complication in nerve repair). Additionally, Fn-cables are larger in diameter (200-250μm) and therefore allow a greater number of aligned cells to populate its surface which can then be transplanted to a nerve defect on a suitable backing material. Human dermal fibroblasts cultured over the surface of such cables were shown to align along the long axis with propagation of cell alignment up to 500 μM away from the original cable (Harding et al., in prep).

In further experiments we postulated that treatment of Fn-strands and cables with copper ions cause an increase in cell migration speed. The basis for this experiment arose from Fn-mat and LFn-cable modification experiments where copper ions caused cross linking of Fn-fibres leading to increased stability of these materials. We hypothesised that if copper causes cross-linking between Fn-molecules then some of the highly adhesive sites on the Fn-molecule may be blocked-off, as we have done with Fg, such that cells will migrate faster on these Fn-strands/cables while material stabilisation was also accomplished. We used Fn-strands composed of gelatine-Sepharose purified Fn and Fn-cables composed of 75% Fn and 25% Fg, as two test systems for this hypothesis.

1.11. Superfibronectin

Chernousov et al., 1991 and Mosher et al., 1992 have shown that the first type-III repeat in Fn is known to play a key role Fn matrix assembly and Fn-Fn binding. Morla et al., 1994 produced a recombinant fragment of the type III domain (III_1-C), which was modelled after the C-terminal two-thirds of the III_1 repeat. Treatment of the type III_1-C fragment with purified Fn in solution resulted in the appearance of multimers of Fn with high relative molecular masses. Morla et al., 1994 further showed that the multimers were only held together by disulphide bonds which are similar to the Fn in the matrix in vivo (Hynes and Destree, 1977; Keski-Oja et al., 1977; Ali and Hynes, 1978). Although cell adhesion is vastly enhanced when purified Fn is treated with this fragment (hence the name superfibronectin), cell migration however, is suppressed (Morla et al., 1994). This led to the work of Pasqualini et al., 1996 who preincubated human tumorigenic cells (human osteosarcoma, melanoma and carcinoma) with

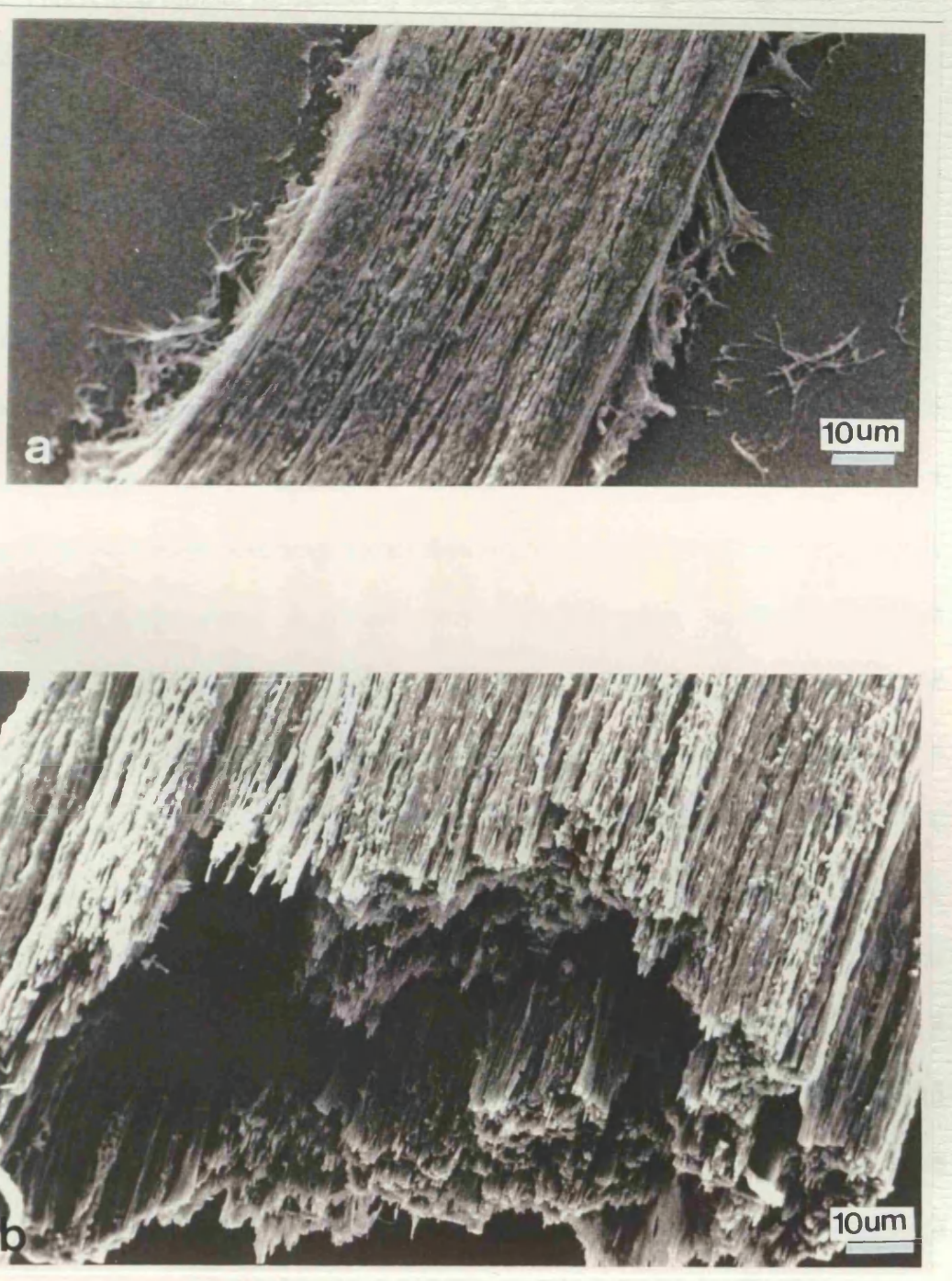

Figure 1.14. *(a) Scanning electron micrograph to show an Fn/Fg strand and (b) high power to show microfibres within Fn/Fg strands. Fibrillar orientation is quite apparent in these micrographs. Courtesy of Underwood et al submitted.*

superfibronectin (sFn) and injected them subcutaneously to look at tumour formation in a nude mouse model. The study showed that the cells were viable but treatment with sFn prevented tumour formation by blocking cell spreading and migration in vivo. In our Fn-mat system however, the preferred aim is not to suppress cell spreading and migration but to promote these in order to ensure a quick reconnection of damaged axons to prevent target organ atrophy.

1.12. Other ways of enhancing peripheral nerve regeneration

Nerve regeneration can be enhanced by electric fields. Electromagnetic fields have been used to induce electric currents. These time-varying currents have been reported to significantly enhance sciatic nerve regeneration in rats (Rusoven and Kanje, 1991, Rusoven and Kanje, 1992). A second method of generating an altered electrical environment is to allow regeneration through tubes made from polymer electret or piezoelectric tubes. These implanted tubes produce a time-varying electric field in response to mechanical deformation. This technique increased the number of regenerating myelinated axons (Aebischer et al, 1987; Fine et al, 1991; Pollock, 1995). Finally, galvanic currents have been used to create constant and relatively uniform fields about injured nerves. Using this technique, an increased rate of functional recovery after delayed treatment of sciatic lesions has been reported (Beveridge and Politis, 1988). Other important reported features of growth cones and Schwann cells in nerve regeneration include: antibodies to CD9, a cell surface glycoprotein involved in intercellular signalling and found to be expressed by neurons and glial cells of the PNS promotes adhesion and induces Schwann cell proliferation and migration in vitro (Hadjiargyrou and Patterson, 1995; Anton et al, 1995); overexpression of GAP-43

induces nerve sprouting and acts as an intrinsic potentiator of neurite outgrowth (Algner et al, 1995).

1.13. Neurotrophins in nerve regeneration

Fn-mats are inherently hygroscopic and have been used to deliver neurotrophins (NGF and NT-3) to the site of the lesion in rats. These neurotrophins have been shown to be released over a period of 7 days in a bioactive form. Continuous delivery of neurotrophic growth factors to a local site may provide a better quality of regenerate. Neurotrophins are a family of structurally and functionally related growth factors that exert a major influence on the survival and development of sensory and sympathetic neurons. These factors are mainly produced by glial cells and cells in the target organ and influence the survival and gene expression of various nerve cells. Cells which produce these factors include fibroblasts and muscle cells (Brewester et al., 1994; Lindsay et al., 1994; Maness et al., 1994; Bandtlow et al., 1987; Ernfors et al., 1990). Members of this family include nerve growth factor (NGF) (Levi-Montalcini, 1987), neurotrophin-3 (NT-3) (Hohn et al., 1990; Maisonpierre et al., 1990; Rosenthal et al., 1990; Ernfors et al., 1990), brain-derived neurotrophic factor (BDNF) (Leibrock et al., 1991; Hallbrook et al., 1991; Ip et al., 1992) and neurotrophin-4/5 (NT4/5) (Lewin and Barde, 1996); Lindsay, 1996; Berkemeier et al., 1991).

Nerve growth factor (NGF), the most extensively characterised neurotrophic factor, is necessary for normal function of many dorsal root ganglia sensory neurons and sympathetic neurons, supports neurones in vitro, prevents developmental neuronal death in vivo, stimulates direct neurite outgrowth and influence neuronal phenotype

(Levi-Montalcini, 1987; Liu et al., 1995; Lindsay and Harmer, 1989). NGF is characterised as a protein composed of two identical 118-amino acid chains (Angelitti and Bradshaw, 1971). The gene that encodes NGF was cloned and sequenced in 1983 (Scott et al., 1983; Ulrich et al., 1983). NGF is synthesised in the targets of NGF-dependent sensory and sympathetic neurons in proportion to their final innervation density (Davies, 1994; Davies and Wright, 1995). Exogenous NGF has been shown to rescue neurones (Rich et al., 1987). It also protects adult sensory neurones from cell death and atrophy following nerve damage (Rich et al, 1987). The levels of NGF protein and mRNA are increased in the injured peripheral nerve (Richardson and Ebendal, 1982; Heuman et al., 1987) which supports its involvement in nerve regeneration (Raivich and Kreutzberg, 1993). In certain classes of fibre in primary afferent and sympathetic nerves, regeneration is stimulated by NGF (Aloe et al., 1985; Heumann et al., 1997; Lindsay et al., 1988). Interestingly, NGF injected into a silicone chamber has been shown to enhance motoneuron regeneration (Chongliang et al., 1992). Administration of NGF either locally in a silicone chamber (Derby et al., 1993) or systemically (Diemel et al., 1994; Fernyhough et al., 1995) has been shown to improve axonal regeneration in normal animals.

The expression of NGF gene is thought to be controlled by microtubule networks (Baudet et al, 1995). This was shown by adding microtuble disrupting drugs such as colchicine, nocadazole and vinblastine, which caused an increase in NGF mRNA and cell secreted NGF proteins in mouse fibroblasts and primary astrocytes in vitro (Baudet et al, 1995). Recent studies have shown that when nerve grafts are pre-degenerated for as little as 1 day, nerve regeneration is improved. The regenerating

axons enter the nerve graft more rapidly by decreasing the initial delay in regeneration (Danielson et al, 1994). This may be attributed to NGF which reaches a maximum 24hrs after nerve injury and remains elevated for 14 days (Heumann et al, 1987). The initial elevation of NGF is due to the transportation of retrogradely accumulated NGF from the periphery, whereas later on, NGF is synthesised by non-neuronal cells eg. keratinocytes (Pincelli et al., 1994), Schwann cells and fibroblasts (Heumann et al., 1997; Brown et al., 1991; Ide, 1996; Barde, 1989; Taniuchi et al., 1988; Raivich et al., 1991), in the distal nerve segment. Thus newly cut axons, entering a pre-degenerated graft, face an environment already enriched with NGF.

Receptor studies have revealed that NGF acts on functionally distinct populations of adult sensory neurons (McMahon et al., 1994). Cellular responses to neurotrophins are mediated by two functionally interacting classes of receptors. The first neurotrophin receptor to be biochemically characterised and cloned is a 75-kDa protein called p75 (Grob et al., 1985; Chao et al., 1986; Johnson et al., 1986; Marano et al., 1987; Radeke et al., 1987). Several structurally related receptors have been identified including two tumour necrosis factors (TNFR-I and TNFR-II), Fas, and CD40 (Bothwell, 1996). Although p75 was initially described as an NGF receptor, it binds all of the neurotrophins (Rodriguez-Tebar et al., 1990; Dechant et al., 1994). Subsequently a further distinct class of neurotrophin receptors were identified (Kaplan et al., 1991). TrkA is primarily the receptor for NGF, trkB is a primary receptor for BDNF and NT/4-5 and trkC, primarily a receptor for NT-3. The trk receptors are capable of mediating many important functional responses without participation of p75 (Barbacid, 1995).

Trk receptors are so named because they are tyrosine receptor kinases. Their signal transduction resembles those of other tyrosine receptor kinases. Neurotrophin binding to receptors induces receptor dimerization, which leads to receptor autophosphorylation by an intrinsic tyrosine-specific kinase activity. Phosphorylation of tyrosyl residues within SH2 domains leads to association with the receptor of specific cytoplasmic signalling proteins, including SHC, PI3-kinase, and phospholipase C (Kaplan and Stevens, 1994).

1.14. Contact guidance

Contact guidance is the phenomena by which the physical shape of the substratum induces alignment or directional growth of cells. Contact guidance of cells by physical contours was recognised in the infancy of tissue culture (Harrison, 1914) and at later stages where cells aligned to topographical features of their substrata (Weiss, 1945; Curtis and Varde, 1964). Although little is known about the cellular events of contact sensing and their transduction into directional growth, many examples of this process do exist. These include fibroblasts (Elsdale and Bard, 1972) and neurones (Ebendal, 1976; Rajnicek et al., 1997; Rajnicek and McCaig, 1997) guided by parallel arrays of aligned collagen fibrils or on grooves manufactured in artificial substrata (Hirono et al., 1988; Clark et al., 1990; Oakley and Brunette, 1993).

Cells exhibiting contact guidance, align parallel to the groove/ridge axis and move in a 'bi-directional' way having maximum probability of migrating in opposite directions. These preferred directions are associated with chemical, structural and/or mechanical anisotropies of the substratum (Dunn, 1982). Contact guidance is thought to be

important in morphogenetic mechanisms, where traction forces exerted by cells may create the fibre orientation that serves to guide their migration (Stopak and Harris, 1982). During wound healing, retraction of the fibrin clot by platelets and contraction of the wound site by fibroblasts could cause radial orientation of the extracellular matrix fibres and thereby guide cells to the wound (Lackie, 1986). Contact guidance is also important in the growth of cells in normal embryonic pattern formation (Newgreen, 1989).

Early experiments using smooth glass fibres as topographical cues, indicated that fibre diameters of less than 100 μm were necessary to orientate cells parallel with the fibre axis (Dunn and Heath, 1976). Recent experiments have shown that topographical cues on microgrooved or patterned substrata such as silicone (den Braber et al., 1995; Green et al., 1994), titanium (Chehroudi et al., 1991) and silica (Clark et al., 1991; Wojciak-Stothard et al., 1995) having groove dimensions between 2-30 μm were sufficient to cause cellular alignment of eg. epithelial cells, fibroblasts and neurites. Further, neurons extended fourfold faster as a result of grooved rather than smooth substrata (Curtis et al., 1995).

1.15. Cell adhesion and migration

Cell adhesion i.e. attachment to the ECM proteins, such as Fn, collagen and laminin, play a crucial role in cellular morphology by anchoring cells and providing signals that direct cellular proliferation and differentiation (Ruoslahti and Pierschbacher, 1987; reviewed by Hynes, 1992). Numerous physiological and pathological processes rely on cell adhesion, including development and differentiation, tumor growth and metastasis,

leukocyte homing and activation, hemostasis, wound healing and cellular responses to mechanical stress (Shattil et al., 1994; DeSimone, 1994; Schwartz and Ingber, 1994; Juliano and Varner, 1993). Cell-ECM attachment is mediated mainly via integrins, a widely expressed family of divalent cation-dependent transmembrane glycoprotein cell surface receptors (Hynes, 1987; Hynes, 1992; Ruoslahti and Pierschbacher, 1987; Yamada, 1989; Albelda and Buck, 1990; Hemler, 1990). Integrins exist on the cell surface as heterodimers of noncovalently associated α and β subunits (Figure 1.15.). In many instances, the binding between receptor and ligand occurs through an arginine-glycine-aspartic acid (RGD) recognition sequence, which is present in many proteins, including fibronectin, vitronectin and fibrinogen (Ruoslahti and Pierschbacher, 1987).

Cell migration is critical during embryonic development, wound healing and many pathological processes (Humphries et al., 1991). In embryogenesis, cellular migration is important in morphogenetic processes ranging from gastrulation to development of the nervous system (reviewed by Lauffenburger and Horwitz, 1996). Migration remains an inherent capacity in the adult organism, in normal physiology as well as pathology (reviewed by Lauffenburger and Horwitz, 1996). Cell migration is also crucial to technological applications such as tissue engineering, playing an essential role in colonisation of biomaterial scaffoldings (reviewed by Lauffenburger and Horwitz, 1996).

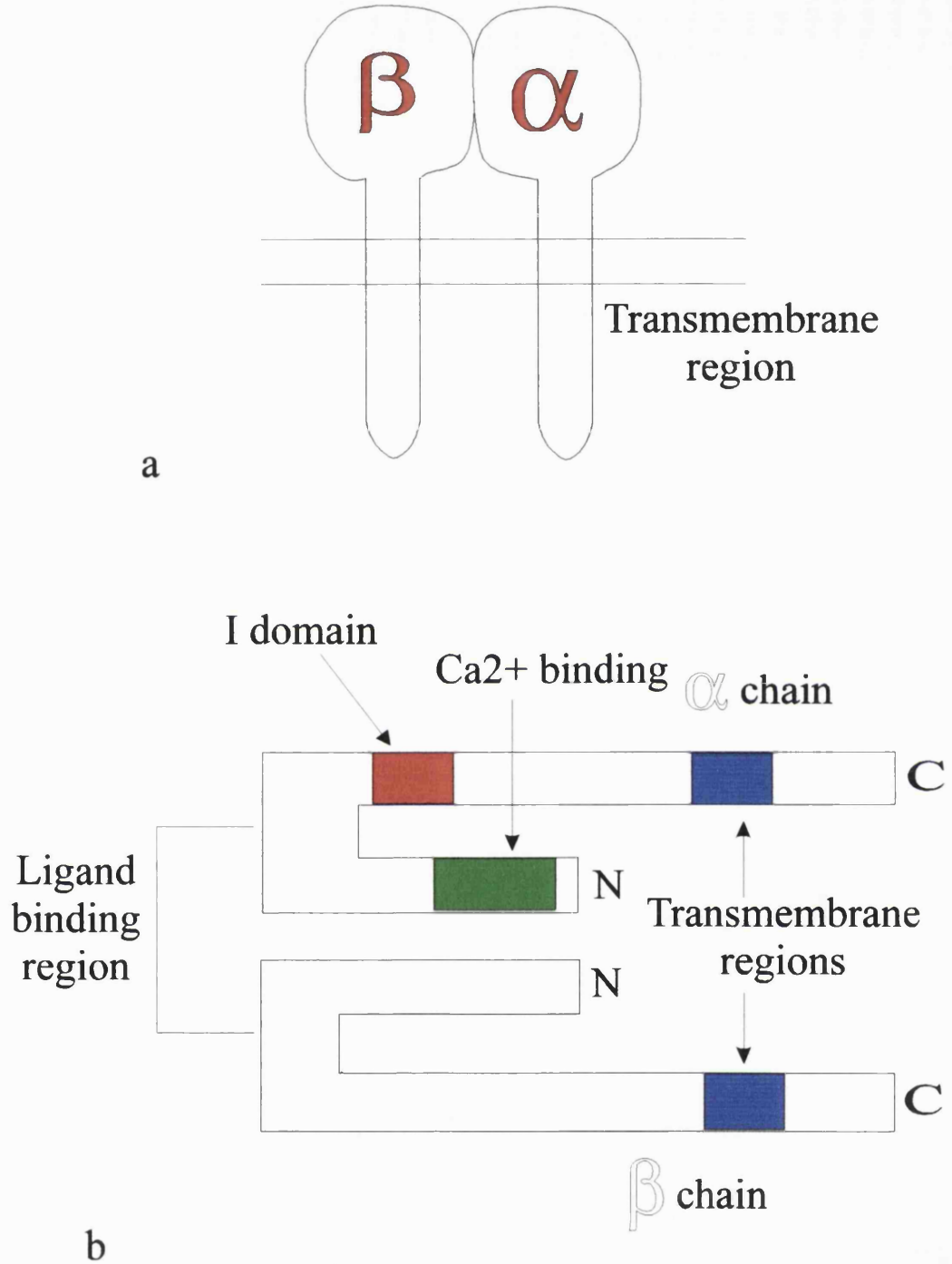

Figure 1.15. *Integrin structure. (a) shows a model of the alpha and beta chains of integrins and (b) shows a schematic diagram of human basic integrin structure indicating the transmembrane and the ligand binding regions.*

Cell-ECM attachment during migration in many cells is mediated by specific reversible interactions between integrins. Cell migration as well as morphology may depend on transient cell-substratum attachments (Stein and Bronner, 1989). Weakly adhesive surfaces cell-substratum interactions cannot provide traction for the cell to move and the cells spread poorly. Highly adhesive surfaces cause the cell to spread well but become immobilised so regular dynamic disruption of the cell-substratum attachment becomes difficult hindering cells migration. However, an intermediate cell to substratum adhesiveness allows cells to spread moderately while allowing maximum migration potential (Figure 1.16). Mathematical models have been developed to predict that maximum cell migration occurs at an intermediate ratio of cell-substratum adhesiveness to intracellular contractile mechanisms (Figure 1.17.), at which the cell is able to form new attachments at the front while being able to break attachments at the rear (DiMilla et a., 1991; DiMilla et al., 1993).

1.16. The Biology of Copper

Fn-mats when implanted into a 1 cm gap in the rat sciatic nerve model were shown to be degraded over a 15 days while there was a thin regenerate formed between the gap. Electron microscopy revealed macrophage infiltration and subsequent degradation of the mat as a natural process in nerves. Furthermore, Fn used to make Fn-mats was derived from human plasma Fn which may add to the inflammatory process by presenting mats as foreign material to the immune system of rats. All these factors contribute to the rapid degradation of the mat. The hypothesis here is that micromolar concentrations of copper will stabilise Fn-mats for longer survival in vivo and therefore support outgrowth of a greater volume of regenerating axons leading to an

Figure 1.16. *Schematic of the relationship between surface concentration of ECM protein, strength of cell-substratum attachment, and cell speed. (a) The strength of cell-substratum attachment, measured as the critical force necessary for detachment, increases linearly with surface concentration of ECM protein. The slope of the line is predicted to increase (within limits) with increasing adhesion-receptor/ECM protein affinity or receptor number. (b) An optimal surface concentration of ECM protein exists for cell movement speed. The specific surface concentration of ECM protein for maximum speed is predicted to increase with decreasing receptor number and adhesion-receptor/ECM protein affinity. The range of surface concentration of ECM protein allowing movement is predicted to depend on the magnitude of the asymmetry in the cell-substratum interaction between front and rear of the cell. (c) An optimal strength of cell-substratum attachment exists for cell movement speed. The strength of attachment for maximum speed is predicted to increase with decreasing receptor number. Both increasing cell-surface asymmetry and receptor number increase the range of attachment strength allowing significant movement. Taken from DiMilla et al., 1993.*

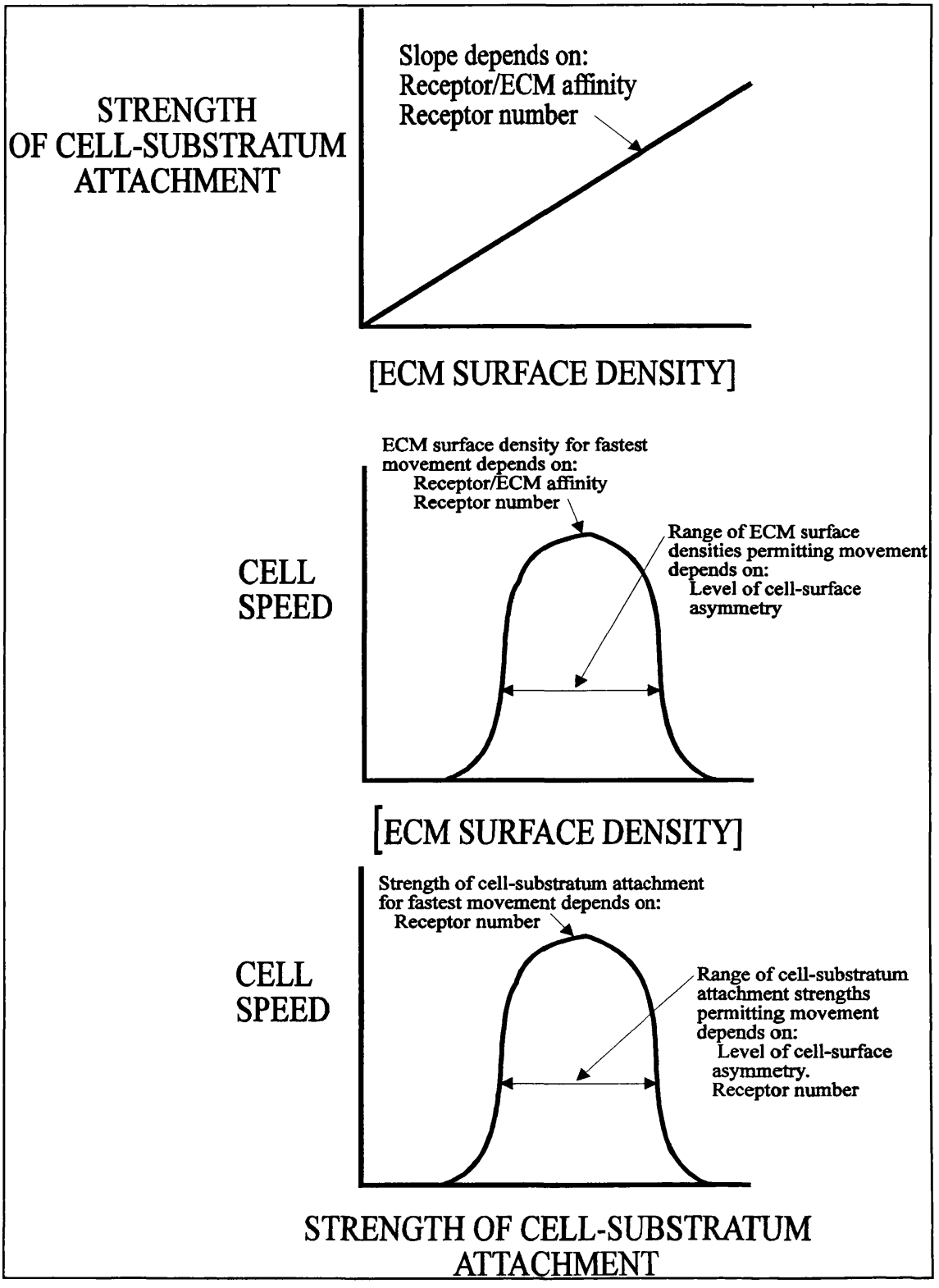
STRENGTH OF CELL-SUBSTRATUM ATTACHMENT
Slope depends on:
Receptor/ECM affinity
Receptor number
[ECM SURFACE DENSITY]
CELL SPEED
ECM surface density for fastest movement depends on:
Receptor/ECM affinity
Receptor number
Range of ECM surface densities permitting movement depends on:
Level of cell-surface asymmetry
[ECM SURFACE DENSITY]
CELL SPEED
Strength of cell-substratum attachment for fastest movement depends on:
Receptor number
Range of cell-substratum attachment strengths permitting movement depends on:
Level of cell-surface asymmetry.
Receptor number
STRENGTH OF CELL-SUBSTRATUM ATTACHMENT

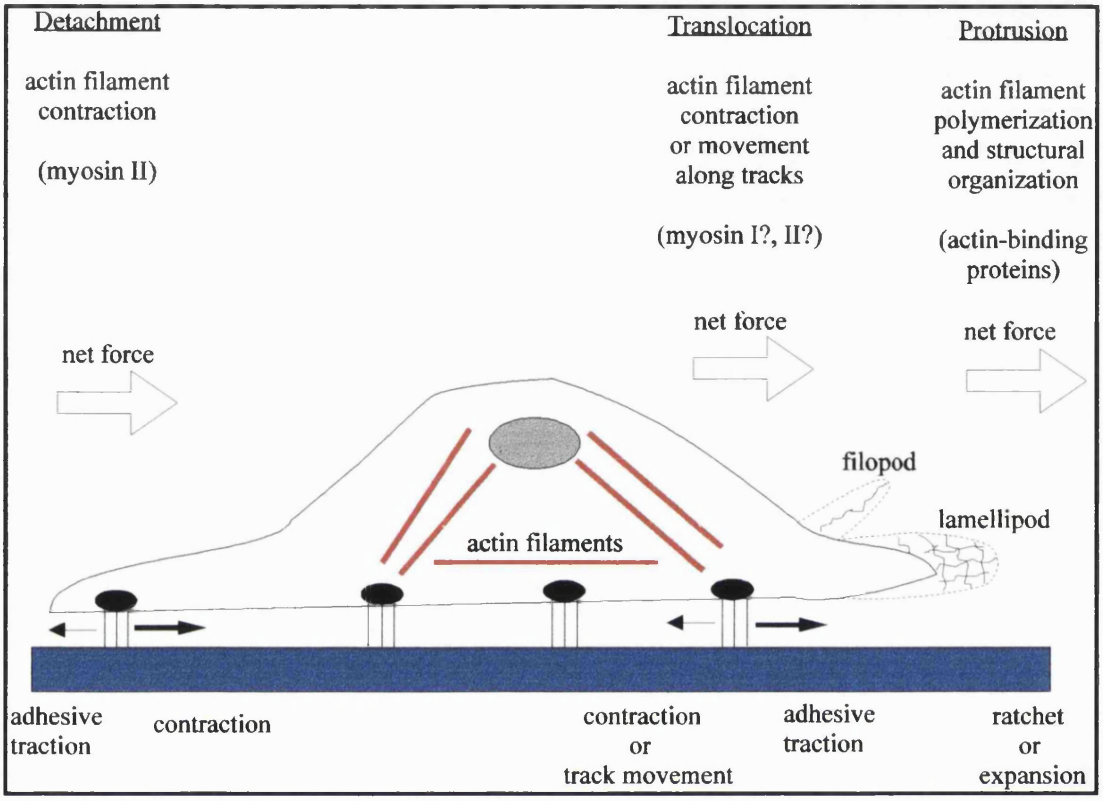

Figure 1.17. *Diagrammatic representation of the different forces involved in cell migration. Protrusion of membrane lamellipodia and filipodia requires force generated by actin polymerization, by the Brownian ratchet mechanism, the cortical expansion mechanism, or a combination of these. Translocation of the cell body forward, once the membrane protrusion has become adherent to the substratum, may occur by myosin interactions with actin filaments; possible mechanism for this include contraction of filaments connecting cell-substratum adhesion complexes with intracellular structures, or relative movement of adhesion complexes across cortical actin filament 'tracks'. In either case, the magnitude of traction is greater than the rearward pull on the adhesion complexes. Detachment of the cell rear involves disruption of cell-substratum attachments, perhaps accelerated by myosin-mediated actin filament contraction pulling on adhesion complexes. Here, the magnitude of traction is less than the contraction force.* ADAPTED FROM LAUFFENBURGER AND HORWITZ, 1996.

improved quality of regenerate than plain mats currently allow. In addition to material stabilisation, it is possible that local delivery of Cu^{2+} would assist some aspects of tissue repair as it is an essential component of the enzymes lysosome oxidases and superoxide dismutase (Sorenson, 1987) and in ascorbate transport into the cell (Sorenson, 1987). These are central to collagen production and inflammatory mediation. In attempting to stabilise Fn-mats with copper, it is important to maintain the fibrillar nature of the mats as contact guidance of cells on this material is a key feature of this conduit but also cell binding sites to the Fn-substrata must not be completely blocked as this would hinder cell attachment and subsequent migration.

The biological significance of copper has only recently been realised (Kies, 1987; Kutsky, 1987). Copper has been recognised as an essential metalloelement like sodium, potassium and iron (Sorenson, 1987). Copper ions are actively involved in the biological oxidation of organic substrates by molecular O_2 (Sorenson, 1987). Copper dependant enzymes include: Cytochrome c Oxidase, Superoxide Dismutase (SOD), Tyrosinase, Lysyl Oxidase and Amine Oxidase (Sorenson, 1987). Copper has also been recognised as an essential metalloelement in many proteins and enzymes exhibiting diverse functions (Ochiai, 1993).

The adult body contains between 1.4 and 2.1 mg of copper per kilogram of body weight. All tissues of the body need copper for normal metabolism and levels of copper vary depending on metabolic activity. The highest levels of copper are in the liver, brain and heart (680, 370 and 350 μg/g of tissue, respectively) (Sorenson, 1987). In normal individuals, copper homeostasis is controlled by the balance between

intestinal absorption of dietary copper and hepatic secretion of excess copper in bile (Cuthbert, 1995). In Wilson's disease (Cuthbert, 1995), hepatic copper is neither secreted in bile nor incorporated into ceruloplasmin and copper accumulates to toxic levels. Ceruloplasmin is thought to be the principal copper-containing component of blood, estimated in humans to be 90-95% of the total copper in serum (Sorenson, 1987). It is thought that copper attached to ceruloplasmin is in transit, destined for uptake by cells and incorporation into cellular enzymes.

Levels of copper are thought to decrease in healing wounds. A study in burn patients showed that copper levels increased significantly only in urine samples and was reduced in the burn tissue (Selmanpakoglu, 1994). Lysyl oxidase which catalyses the formation of aldehyde cross-links, and acts primarily on collagen and elastin, is known to be increased during wound healing and fibrotic disorders (Kobyashi et al., 1994). In this study lysyl oxide was localised intracellularly and extracellularly in skin. Lysyl oxide was also immunolocalized along collagen and elastic fibres (Kobyashi et al., 1994). In severe burn trauma patients, the response of ceruloplasmin as an acute-phase reactive protein was absent. The reduction of ceruloplasmin was correlated with burn severity (Cunningham et al., 1993). Supplying copper in protein bound form locally to a wound site would give a slow but continued release of copper to the surrounding area.

1.17. The biology of zinc

Again, the hypothesis here was that zinc may be used similarly to copper ions inorder to stabilise Fn-mats and prevent rapid degradation. The incorporation of zinc into Fn-

mats would prove to be an added benefit since zinc is present in filamentous structures in connective tissues as a component of all MMP's (Williams, 1989). Zinc is the most common heavy metal ion in the cytoplasm of cells and has many diverse functions. It is present in all organs, tissues, fluids and secretions of the body with the highest estimated concentrations being present in bone (100 μg/g wet wt) and hair (150 μg/g wet wt) (reviewed by Jackson, 1989). Zinc dependent proteins include insulin, S-100, carbonic anhydrase, SOD, carboxypeptidase, alcohol dehydrogenase, metallothionein and σ-Factor IIIA (reviewed by Williams, 1989).

A deficiency in zinc has been shown to cause decreased sciatic nerve conduction velocity in chicks and guinea pigs while guinea pigs developed hypersensitivity to touch and pain during movement (O'Dell, 1993). Peripheral neuropathy was readily reversed by zinc replacement therapy (O'Dell, 1993). Furthermore, overexpresssing the Cu/Zn superoxide dismutase was shown to enhance the survival of transplanted dopamine neurones in a rat model of Parkinson's disease (Nakao et al., 1995) suggesting that a combination of copper and zinc within Fn-mats may be a beneficial strategy in such cases.

1.18. Chemical modification of proteins

Cross-linking of proteins by imidoesters has been used extensively to study subunit structures of polymeric proteins and derivation of proximity relationships in more complex assemblies such as ribosomes and membranes. These chemicals such as dimethylsuberimidate, either cause intramolecular (David and Stark, 1970) or intermolecular (Bickle et al., 1972; Clegg and Hayes, 1974) cross-linking. Methyl 4-

mercaptobutyrimidate has also been used as a reversible cross-linking agent of proteins where disulfide-cross links form between protein molecules (Traunt et al., 1973). Gluteraldehyde has long been used as a cross-linking agent, especially in fixation of samples for electron microscopy. Reactions of gluteraldehyde with proteins have been shown to involve lysinyl (and hydroxlysinyl) residues (Korn et al., 1972) while protein structure is perturbed in a minor way (Reeke et a., 1967; Quiocho and Richards, 1964). Formaldehyde has also been used to form cross-links in proteins and shown to cross-link asparagine and serine residues of neighbouring molecules (Myers and Hardman, 1971). It is envisaged that copper being a divalent cation will react with negative residues with the Fn-molecule causing cross-links to form thus leading to material stabilisation.

1.19. AIMS OF THE STUDY

Currently there are 4-5000 people a year in the UK who require nerve grafts to repair peripheral nerve lesions. Surgical operative results are frequently very poor. Peripheral nerve injury (eg. hands, shoulder, and face) often leaves gaps between the cut nerve ends which are too long to repair using sutures. Where the stumps can be joined by a graft or a tube, some regrowth and regeneration will occur, though the rate of regeneration is too slow to be clinically useful. Currently, nerve autografts are the most effective conduit materials to date but lead to loss of donor site function. Longer gaps (>15 mm) present even more of a problem since regeneration is slower with worse results.

The aims of the current study are to:

1. Increase the life of Fn-mats (currently 15 days in vivo) without disrupting fibrillar arrangement by chemical modification using copper ions. This will allow Fn-mats to support greater numbers of axons thus improving the quality of the regenerate.

2. Assess the effectiveness of Fn-mats supplemented with NGF in a monkey nerve model. So far, Fn-mats have only been tested in rats and it is thought that monkeys are closely related to humans which will reduce the inflammatory response and may provide different results to that seen with rats. This will be used as a basis for clinical trials.

3. To construct new forms of Fn-materials capable of being used for the repair of long peripheral nerve lesions. These will provide guidance and support cues for regenerating components of peripheral nerves.

4. To study individual strands of Fn with peripheral nerve cells in vitro in order to understand the mechanism of contact guided repair of peripheral nerves using Fn-mats in vivo.

5. To increase the migration of nerve cells on Fn-materials with a view to speeding up the repair process to minimise target organ atrophy and dysfunction (the ultimate aim of any peripheral nerve conduit material).

6. To develop an in vitro method for delivering grafted Schwann cells (and perineurial fibroblasts) pre-aligned within Fn-materials to augment the repair of peripheral nerves.

CHAPTER 2.0. MATERIALS AND METHODS

2.1. General Methods

2.1.1. Preparation of fibronectin mats

Fibronectin was purified from the crude, plasma fractionation product, glycine saline supernatant (Bio-Products Limited, Elstree, Middlesex), by gelatin-Sepharose (Sigma, Poole, Dorset, England) affinity chromatography. The adsorbed Fn was washed with three bed volumes of 0.05M Tris-buffer containing 0.5M NaCl, pH 7.6 and eluted with 4M Urea buffer containing 0.05M Tris-HCl and 0.5M NaCl. The concentration of protein was determined by measuring the absorbance at OD_{280} and then supplemented into the equation below (1) to determine protein concentration per mL:

$$\textit{Protein concentration in } mg/mL = E_{icm\ (280nm)} / \varepsilon \quad \text{where } \varepsilon = \text{extinction coefficient of fibronectin } (\varepsilon \text{Fn} = 1.2) \qquad (1)$$

Orientated mats of fibronectin were produced by self-association of and continuous aggregation of plasma fibronectin, concentrated from a solution under continuous unidirectional stirring. The mats were produced according to the method of Ejim et al, (1993). A 200mL fibronectin solution (0.9-1 mg/mL) with 4M urea, 0.05M Tris-HCl and 0.5M NaCl, pH 7.6, was diluted with an equal volume of buffer containing 0.05M Tris-HCl, 0.1M NaCl, pH 7.6 (final concentration of 2M urea). This was introduced into an ultrafiltration-stirred cell (Amicon, Stonehouse, UK) fitted with a 75 mm Diaflo, PM10 (10,000 molecular weight cut-off) ultrafiltration membrane (Amicon) at 4°C. The solution was stirred at around 300 revolutions per minute in a cell pressurised using compressed N_2 to 0.2 Pa. The liquid was never allowed to foam and the stirring speed was lowered to 100 revolutions per minute as the volume reduced. A fibronectin mat formed on the shaft of the rotor during the final stages of concentration; this was

removed, rinsed in a large volume of distilled water and freeze dried overnight, still attached to the stirrer. Once prepared the mats were stable when stored under vacuum desiccation. Before use the mats were sterilised by gamma irradiation (2 megaRads for 24 hours) (*Courtesy of Dr. Giorgio Terenghi, Blond McIndoe Research Centre, QVH*).

2.1.2. Preparation of Ultrathin Fibronectin Fibres

Ultrathin fibronectin fibres (0.2-10 μm) were made by using the method of Ejim et al, 1993. Plasma fibronectin was purified by affinity-chromatography from a crude blood fraction obtained (BPL, Elstree, Middlesex, England) as described above in Chapter 2.1.1. A thin glass rod (BDH, Dorset, England) was dipped into a concentrated solution of fibronectin (5 mg/mL) and individual fibres were pulled out and attached to alcohol washed round coverslips (BDH), which were coated with poly-L-lysine. The attached fibres were air dried for 24 hours before gamma irradiation as described in Chapter 2.1.1.

2.1.3. Polyethylene Glycol Precipitation of Fibrinogen/Fibronectin

Polyethylene glycol (PEG) can be used to fractionally purify fibrinogen (Fg) from fibronectin (Fn). Initially PEG is added to precipitate a large proportion of Fg from solution. The concentration of PEG is then increased to bring the remaining Fg and Fn out of solution. 1 g of a cryoprecipitate of Fn/Fg (Scottish National Blood Transfusion Service (SNBTS), Protein Fractionation Centre (PFC), Edinburgh, Scotland) was dissolved in 6 mL of PBS (Oxoid) before adding 4% v/v PEG to remove Fg, stirred and left for 1 hour at room temperature. The resulting suspension was centrifuged at

4500 rpm at 4°C in a rotor centrifuge for 15 minutes. The Fg precipitate was discarded leaving the supernatant behind. The concentration of PEG was raised to 10% v/v and added to the supernatant, stirred and left for 1 hour at room temperature before being centrifuged as described above. The remaining precipitate contains the Fn/Fg which is then redissolved as required and assayed for content of Fg using the method described below.

2.1.4. Assay for fibrinogen

The assay measures the amount of Fg present by measuring the turbidity of the solution when Fg is heated to 56°C in the presence of tri-sodium citrate. It can be described as a heat denaturation assay. Fg standards were made up from commercially available fibrin glue kit (SNBTS, PFC, Scotland). Each sample of Fg was diluted in PBS (Oxoid) to give concentrations between 0-1 mg/mL. To a 96 well plate (Falcon City) 125 μL of the test sample and 125 μL of the assay buffer (20mM Tris and 40mM Tri-sodium citrate dihydrate, pH 7.5) were added. The plate was heated for 15 minutes at 56°C with the plate covered to prevent evaporation. The plate was then allowed to cool and the turbidity of the resulting solution measured at 410 nm on a plate reader (Dynatec Labs, Billinghurst, UK). A calibration curve was constructed and from this the concentration of fibrinogen in a test sample was calculated.

2.1.5. Two-antibody non-competitive fibronectin ELISA

200 μL of different concentrations of fibronectin diluted in 0.01M PBS (Oxoid) (ranging from 10 μg/mL double diluting to 0.1 ng/mL) were added to a 96 well ELISA plate (Falcon) and left to incubate overnight at 4°C. The plate was wrapped with foil to

prevent evaporation. The incubation step was terminated with the addition of 150 µL of 0.01M PBS, pH 7.4 with 0.02% Tween 20 for 10 minutes at room temperature followed by rinsing the plate twice with distilled water. The remaining binding sites were blocked with 100 µL of blocking buffer containing 150 mM NaCl, 100 mM Tris, pH 7.6 and 1% (w/v) bovine serum albumin (BSA) and incubated for 30 minutes at room temperature. The plates were washed with 150 µL of 0.01M PBS, pH 7.4 containing 0.02% Tween 20 followed by rinsing twice with distilled water. 100 µL of the primary antibody rabbit anti-human fibronectin (Sigma, Poole, Dorset, England) diluted 1:10,000 with 0.01M PBS, pH 7.4 and 1% w/v BSA (Sigma) was added to the plate and incubated for 1 hour at room temperature before terminating the reaction and washing the plate as described above. This was followed by addition of the secondary antibody, goat anti-rabbit IgG alkaline-phosphatase, diluted 1:8000 with 0.01M PBS and 1% w/v BSA and allowed to incubate for 1 hour at room temperature. Repeat terminations and washings were performed as described earlier followed by addition of 100 µL of enzyme substrate disodium paranitrophenyl phosphate (pNpp) in diethanolamine (DEAE) buffer (2 mg/mL pNpp, 10% DEAE, pH 9.8 and 0.5 mM $MgCl_2$) and incubated for 1 hour at room temperature in the dark. The intensity of the resultant colour was then measured at wavelength 490 nm using an ELISA plate reader.

2.1.6. Preparation of Fn-strands

Fn-cables (100-200 µm in diameter) were made from a cryoprecipitate obtained from SNBTS, PFC, Scotland by the method developed by Underwood et al., submitted, in these lab. The cryoprecipitate contains 25-34 % Fg mixed in with Fn. 1 g of the

cryoprecipitate was cut into small pieces to aid dissolution and dissolved in 3 mL of 6M Urea (BDH) to give an approximate final concentration of protein of 20 mg/mL. The concentrated solution of Fn/Fg was diluted in 6M Urea to give a final protein concentration of 5 mg/mL. Fn-cables were pulled out from a solution with a 3:1 ratio of Fn/Fg : 0.25M HCl and 2% calcium chloride, pH 0.9. The cables were pulled and adhered to round glass coverslips (Merck, Dorset, England) and left to air dry overnight. All cables were gamma irradiated before use in culture or protein dissolution experiments as described in Chapter 2.1.1.

2.1.7. Preparation of large Fn-cables (LFn-cables)

1 g of cryoprecipitate obtained from SNBTS was dissolved in 3 mL of 6M Urea (BDH) as described earlier. More cryoprecipitate was added as required and concentrated by introducing the solution into an ultrafiltration-stirred cell (Amicon, Stonehouse, UK) fitted with a 75 mm Diaflo, PM10 (10,000 molecular weight cut-off) ultrafiltration membrane (Amicon) at 4°C. The solution was stirred at around 50 revolutions per minute in a cell pressurised using compressed N_2 to 0.2 Pa. The final desired concentration of protein required to make LFn-cables was >70 mg/mL as determined by Underwood et al., submitted.

Large Fn-cables (LFn-cables) were made by a modified method of Underwood et al., submitted. A 1 mL syringe was used to pick up the concentrated solution of Fn/Fg (approx. 78 mg/mL) in Urea and squeezed into small beaker containing a solution of 0.25M hydrochloric acid and 2% calcium chloride, pH 0.9. Fn/Fg-fibres precipitated immediately and these were scooped together to form large Fn-cables. The cables were

washed for a total of 1 hour in two changes of PBS followed by rinsing in a large volume of distilled water (200 mL) to remove acidity and then freeze dried on Teflon discs. LFn-cables were gamma irradiated as described above in Chapter 2.1.1., before use in culture.

2.1.8. Fibroblast cultures

Human dermal fibroblasts were obtained from explants grown from skin taken directly from the operating theatre (Burt and McGrouther, 1992). Cubes of tissue (2-4 mm) were plated into 25 cm^2 culture flasks (Bibby-Sterelin), with 5 mL of Dulbecco's Modified Eagles Medium (DMEM) (Gibco, Paisley, U.K.), supplemented with 10% foetal calf serum (FCS) and streptomycin/penicillin (Gibco) and gassed with 5% CO_2 prior to incubation at 37°C.

Rat Achilles tendon, rat tail and skin fibroblasts were also cultured in a similar way.

2.1.9. Schwann cell culture

Rat Schwann cells were prepared from a modified method of Brockes et al., (1979). The sciatic and the brachial plexus nerves from 3 day rat pups (Sprague-Dawley, UCL Biological Services) were dissected out under sterile conditions and placed in DMEM-HEPES buffer (Gibco). The epineurial sheath was manually removed using a dissecting microscope (Zeiss) and the nerves were then cut into 2 mm segments and digested with 0.25% trypsin (Sigma) and 0.4% collagenase (Sigma) dissolved in DMEM-HEPES (Gibco) for 35 minutes at 37°C and 5% CO_2. The enzyme reaction was then stopped by adding an equal volume of DMEM-HEPES containing 10% FCS (Gibco) and gently triturated three times through 19 and 23G needles, respectively. Cells were

centrifuged for 10 minutes at 1000 rpm and the cell pellet resuspended in DMEM (Gibco) containing 10% FCS and Penicillin/Streptomycin (Gibco). Cells from 1 rat were plated onto a 35mm petri-dish coated with 1 mg/mL poly-L-lysine (Sigma) dissolved in PBS and laminin (Sigma) dissolved in DMEM (Gibco-BRL). After cells had adhered to the bottom of the dish, Ara-C (Sigma), which is a metabolic poison to stop proliferation of contaminating fibroblasts, was added at a final concentration of 10^{-5} M dissolved in DMSO (Sigma). Ara-C was removed by washing with PBS after 3 days and replaced with DMEM containing 10 % FCS, Penicillin/Streptomycin, L-Glutamine, 50 μg/mL bovine pituitary extracts dissolved in PBS (Sigma) and 5 μM forskolin (Novabiochem-Calbiochem, Nottingham, U.K.). Cells were incubated at 37°C and 5% CO_2 until confluent. Contaminating fibroblasts were removed by treatment with monoclonal mouse anti-rat Thy 1.1 (Diluted 1:100 in PBS/BSA) (Harlan Sera-Lab, Sussex, UK) followed by incubation with low toxicity rabbit complement (Sigma) for 10 minutes at 37°C and 5% CO_2, to allow antibody-complement mediated cell lysis. The reaction was stopped by adding an equal volume of DMEM and centrifuged at 1000 rpms for 3 minutes. The cell pellet was then resuspended in DMEM containing 10% FCS and Penicillin/streptomycin. Some cells were plated onto sterile round coverslips for 24 hours to assess the purity of Schwann cells. Purity was assessed by immunofluroescence using monoclonal mouse anti-S-100 (Sigma) (protein on surface of Schwann cells) diluted 1:100 in PBS for 45 minutes at 37°C followed by incubation with FITC-labelled anti mouse IgG diluted 1:50 in PBS for 1 hour at room temperature. Coverslips were washed with PBS and counterstained with 1% propidium iodide. Coverslips were then washed, mounted using Citifluor (UKC, Canterbury, England) and viewed under a fluorescence microscope. The

number of stained nuclei compared to the number of S-100 positive cells was calculated. Cultures of Schwann cells used for all experiments was estimated at 98% by this method.

2.2. SPECIFIC METHODS

2.2.1. Stabilisation of Fibronectin Mats with Micromolar Concentrations of Copper

2.2.1.1. Preparation and impregnation of copper into fibronectin mats

Fibronectin mats were prepared using the method of Ejim et al., 1993 as described in Chapter 2.1.1. 1, 10, 100 and 200 μM concentrations of copper II sulphate solutions were either in distilled water or PBS and filter sterilised using a 0.2 μm Acrodisc membranes (Sartorius, Gottingen, Germany). Under sterile conditions orientated mats of similar size, dimensions and weight were aseptically cut into small pieces and impregnated with copper in 10 mL of $CuSO_4$ solution for 10 minutes at room temperature with continuous agitation. The copper impregnated mats (CuFn-mats) were then rinsed in distilled water with three changes of 5 minutes each. CuFn-mats were then placed in 5 mL of sterile distilled water or PBS and left at either room temperature or at 37°C. The dissolution of protein was assessed by either taking out aliquots from each sample and measuring the absorbance at 280nm using a Phillips model spectrophotometer, making sure to replace the volume removed with the same solution, or by taking out 10 μL from each and performing a protein assay using the Bio-Rad BRADFORD chromogenic protein assay kit (Bio-Rad, UK) (Bradford, 1976). After 8 (at 37°C) or 15 days (at room temp.) the remaining mat was digested

with 800 μg/mL of trypsin (Sigma) and total protein concentration was measured. It was noted that mats treated with copper took 2-4 times longer.

The same methods were used to impregnate zinc and equimolar copper and zinc into Fn-mats and subsequent dissolution of protein was measured in the same way.

2.2.1.2. Copper assay

Dried Fn-mats were treated in a single concentration (1.56 mM) of reagents of Cu including copper (I) chloride, copper (II) acetate monohydrate, copper (II) hydroxide and copper (II) sulphate for 3 hours at 37°C and washed in PBS. The CuFn-mats were solubilised using trypsin (Sigma) for 1 hour before assaying for content of copper by routine atomic absorption spectrophotometry.

Fn-mats were also treated with 1, 10, 100 and 200μM copper sulphate for 10 minutes at room temperature before being washed in PBS on a mechanical roller and digested with 800 μg/mL trypsin for 24 hours at room temperature and assayed for copper content in a similar way as above.

2.2.1.3. Scanning electron microscopy (SEM)

Samples of orientated mats were placed in copper sulphate solution at the above concentrations for 10 minutes. Control mats were placed in distilled water for the same period of time. The control and CuFn-mats were freeze dried overnight and sputter coated with gold in an EM Scope sputter coater (EM Scope Labs, Ashford, Kent, England,). CuFn-mats were then viewed in a scanning electron microscope at 10kV.

2.2.1.4. Cell culture on copper stabilised Fn-mats

Rat tendon, skin and tail fibroblasts and Schwann cells were cultured as described in Chapter 2.1.8 and 2.1.9.

Orientated mats (n=8 in each group) were soaked in copper sulphate solution for 10 minutes as described above in Chapter 2.2.1.1. When placed onto tissue culture plastic for 1 hour at 37°C, these moistened mats would adhere to the plastic. 50,000 cells of each population were plated with CuFn-mats in 4 well plates to assess the toxicity of copper released from the mat. Cells were also plated onto untreated Fn-mats and cells onto plastic, without Fn-mats to determine the baseline growth response of cells without copper treatment.

2.2.1.5. Estimation of cell numbers after 3 weeks

After 3 weeks in culture, the remaining mats were removed from the bottom of the culture wells using sterile forceps and digested using 1 mL of 0.2% collagenase (Sigma) and 0.25% trypsin (Sigma) in PBS (BDH) and incubated for 20 minutes at 37°C in a humidified chamber. After digestion was complete an equal volume of DMEM containing 10% FCS was added and the cells were recovered by centrifugation at 1500 revs/min for 3 minutes. The cell pellets were resuspended in 1 mL DMEM-HEPES (Gibco) and counted using a heamocytometer.

Cells attached to tissue culture plastics were removed by addition of 0.25% trypsin (Sigma) in PBS (BDH) and incubated under continuous shaking for 5 minutes. An equal volume of DMEM containing 10% FCS was added and cells were recovered

from a pellet as described above. The number of cells were again counted using a heamocytometer.

2.2.1.6. Histology

Copper was impregnated into Fn-mats as described above in Chapter 2.1.1.1. and left in culture for 21 days. Schwann cells were only cultured on 1 μM CuFn-mats. The mats (n=8) were removed from the bottom of the 4-well plate and mounted into blocks for frozen sectioning in OCT mounting medium (Tissue Tek, Miles Inc, USA), bearing in mind the orientation of the mat in relation to the culture vessel. 10 μm thick sections were cut using a cryostat (Brights Instrument), stained with heamotoxylin and eosin, dehydrated in a series of alcohols and mounted in DPX mountant (BDH), before examining under light microscopy.

2.2.2. Nerve Growth Factor Delivered Locally Via Fibronectin Mats Enhances Peripheral Nerve Regeneration in The Non-Human Primate

2.2.2.1. Preparation and impregnation of fibronectin mats with NGF

Orientated mats of fibronectin were produced according to the method of Ejim et al, (1993), and as described earlier in Chapter 2.1.1.

The method for impregnation of Fn-mats with NGF has been reported earlier (Whitworth et al, 1995b). Briefly purified NGF-β (Sigma, UK) was reconstituted in a solution of Dulbecco's Modified Eagle Medium (DMEM; Gibco) containing FCS, glutamine, penicillin and streptomycin. Fibronectin mats were impregnated by incubating the mat in the solution of NGF (3 ng/mL) for 24 h at 37°C. The release

profile and bioactivity of the NGF has been shown previously (Whitworth et al, 1995a).

2.2.2.2 Surgical Procedure

(All surgical procedures were carried out by Dr. Mikael Wiberg, Cristina Ljungberg; University of UMEA, Sweden and Dr. Giorgio Terenghi (Blond McIndoe Centre, East Grinstead, UK).

Fifteen adult male monkeys *(Macaca fascicularis)* weighing between 3.4-7.0 kg were used for the experiments. The experiments were approved by the Animal Ethics Committee of the Swedish University of Agricultural Sciences. The monkeys were premedicated and anaesthetised with Ketamine hydrochloride intramuscularly (initial dose 10 mg/kg i.m.) and pentobarbitone (5-15 mg/kg intra-peritonelly); to maintain anaesthesia ketamine was given i.m. as required. Using an operating microscope the superficial branch of the radial nerve of one forearm was isolated and transected just proximal to the wrist. A gap of 4-5 mm between the nerve-ends was in one group of 5 animals replaced with a sural nerve-graft harvested from the lower leg. The nerve graft was secured by two or four epineurial sutures (9-0, monofilament polyamide; Ethilon) in each end. In a second group of 5 animals the gap was replaced by a fibronectin mat which was wrapped around the two nerve-ends, leaving the gap within the formed fibronectin tube. The tube was secured to the proximal and distal part of the nerve by one epineurial suture (9-0 Ethilon) in each end. In the third group of 5 animals the gap was replaced by the use of fibronectin mats, in the same way as the former group, but in this latter group the fibronectin was impregnated with 3 ng/mL NGF. In all animals the contralateral side served as the control.

After 4 months animals were reanaesthetised again and fixed by transcardial perfusion with 5 litres of 4% paraformaldehyde in 0.1M phosphate buffer (pH 7.4, 37°C), following a rinse with 3 litres of buffer to which 4000 IU (international units) of sodium heparin had been added. After fixation nerve specimens were removed for further fixation and analysis as described below.

2.2.2.3. Fixation, light and transmission electron microscopy of nerves

The graft area, with proximal and distal nerves attached, was fixed in 2.5% gluteraldehyde (Agar Scientific, Stansted, Essex, UK) for 6 hours at room temperature and then washed in 0.1M phosphate buffer, pH7.4. Nerve samples were then post-fixed in 1% osmium tetroxide (Agar), dehydrated in ethanol and embedded in Spurrs resin (Agar). Semi-thin (1-2μm) and ultrathin sections were cut, both longitudinally and transversely to the nerve axis. Sections were stained with toluidine blue or haemotoxylin and eosin for light microscopy, and with lead nitrate and uranyl acetate for electron microscopy (using a Philips CM12 and a Jeol JEM 100S transmission electron microscope). Collagen fibril diameter (in transverse sections) was calculated from photomicrographs which were scanned into an image analysis system using a high resolution UMAX SuperVista S-12 (Umax Data Systems Inc, Hsinchu, Taiwan) scanner and Openlab computer software package (Improvision, Coventry, England). The image was calibrated and the diameter of collagen fibrils measured in all experimental groups. Students t-test was used to compare the mean regenerated collagen fibril diameter using the MINITAB software (MINITAB Inc. P.A., USA).

2.2.2.4. Myelinated fibre analysis

Semi-thin (1μm) transverse sections of the nerve 5 mm distal to the grafts were stained with thionin blue and acridine orange to enhance myelinated fibres and examined by light microscopy.

A dedicated software programme run on a computerised image analysis system (Seescan Analytical Services, Cambridge, UK) was used to count the number of myelinated axons in three randomly chosen fields under a 40X objective magnification lens (representing about 10% of the total fascicular area of each nerve). Total fascicular area of each nerve was measured and an indication of the total number of myelinated axons within each distal nerve was calculated by multiplying these two measured parameters. Axonal diameter, axonal size distribution, myelin thickness and g-ratio (axonal diameter/myelinated fibre diameter) were calculated for all counted axons in each experimental group. Normal un-operated contralateral control nerves were also collected and myelinated fibre analysis was carried out as described above and used as controls. Statistical analysis of the degree of regeneration in the grafted area was carried out using the MINITAB software package (Minitab Inc. P.A. USA). Myelinated fibre counts and fascicular area measurements were compared by a Kruskal-Wallis one-way ANOVA on ranks. Differences between individual groups were then isolated by the use of an appropriate all pairwise multiple comparison procedure. The G-ratio's were corrected for diameter by performing a mixed model ANOVA. The relationship between G-ratio and diameter was not linear and was therefore modelled as cubic.

2.2.3. Production of Large Cables of Fibronectin as a Potential Conduit for Repair of Long Peripheral Nerve Lesions

2.2.3.1. Preparation of Fn-mats and LFn-cables

Fn-mats were prepared by the method of Ejim et al., 1993, as described earlier in Chapter 2.1.1. Large Fn-cables (LFn-cables) were prepared from a modified method of Underwood et al. (submitted), as described in Chapter 2.1.7.

2.2.3.2. Structural analysis: Scanning electron microscopy and histology

Samples of LFn-cables were made and washed quickly in a series of distilled water. Samples were critically point dried and gold sputter coated in an EMSCOPE gold sputter coater (EMSCOPE Labs, Ashford, Kent, England). Cross sectional and longitudinal surface structures were looked at using a scanning electron microscope at 10kV for comparisons with Fn-mats.

Scanning electron microscopy of Fn-mats have been published earlier (Ejim et al., 1993).

Specimens of LFn-cables were examined histologically in comparison with Fn-mats after hydration. The structure of LFn-cables after hydration was critical as implanting the cables in vivo will result in their hydration from exudates of the nerve and the surrounding area. LFn-cables and Fn-mats were re-hydrated in 0.1M PBS at 37°C for 30 minutes before being fixed in 4% paraformaldehyde and embedded in OCT mounting medium (Tissue Tek, Miles Inc, USA). Re-hydrated Fn-mats were first rolled into a tight tube (so that the fibres within the mat run in a longitudinal orientation) for comparison with the cross section of LFn-cables. 10 μm thick cryostat

sections were cut and stained with 1% Toluidine Blue and examined by routine light microscopy.

2.2.3.3. Fibril orientation analysis

Histological sections stained with haemotoxylin and eosin were viewed under an inverted microscope (Nikon, Surrey, England) and images recorded by using a CCD high performance camera (Sony CCDXC-77CE, Sony UK) and an Openlab Image analysis software package (Improvison, Coventry, England). After initial thresholding and background subtraction, a constant line was drawn corresponding to the central longitudinal axis (reference line) of the cable (this represents parallel orientation). A modified orientation index originally devised by Herman for measuring orientation of polarised cells in relation to a groove or fibre (ref from Dunn and Brown, 1986), was used to reflect the orientation of fibrils within the cable and is given by the equation: $S = 2 (\cos^2 a)-1$, where 'a' is equal to the angle between the axis of an individual fibril in relation to the axis of the reference line. The term $(\cos^2 a)$ denotes the square cosine of (a) averaged over all measured fibrils. An S value of 1 would indicate parallel alignment and a value of 0 would indicate total random alignment of fibrils. Values of S were calculated for 100 fibrils in 10 random fields in each of 12 cables of equal dimensions (5 mm wide × 10 mm long).

2.2.3.4. Re-hydration properties of LFn-cables compared to Fn-mats

Previously freeze dried LFn-cables and Fn-mats rolled into tubes measuring 4 mm (±1 mm) diameter, 5 mm (± 1 mm) length and 9 mg (±2 mg) in weight (n=14 in each group) were re-hydrated in 5 mL of 0.1M PBS at 37°C and the change in dimensions

and mass were monitored at 5 minute intervals over a period of 40 minutes, as a measure of re-hydration.

2.2.3.5. Cell culture with LFn-cables

Fibroblasts were cultured as described by Burt and McGrouther, 1994 from skin explants taken directly from the operating theatre and in Chapter 2.1.8.

Schwann cells were cultured using a modified method of Brockes et al., 1979 as described earlier by Ahmed et al, 1998, in press, and in Chapter 2.1.9. LFn-cables measuring 5 mm length × 3mm diameter were soaked in DMEM containing 10 % FCS and adhered to the bottom of tissue culture plastics by incubation at 37°C for 1 hour. 50,000 Schwann cells and human dermal fibroblasts were plated onto these cables and left to incubate at 37°C and 5% CO_2 for 2 weeks. The cells were then fixed with 2.5% Gluteraldehyde (Agar Scientific, UK) and blocked up in OCT (Miles Inc). 10 μm thick longitudinal sections were cut on a cryostat (Brights Instruments) and stained with Haemotoxylin and Eosin before mounting in DPX mountant (BDH) and viewing under a light microscope (Zeiss).

Cells were difficult to distinguish from the LFn-cable, therefore immunostaining for surface proteins on Schwann cells (S-100) and fibroblasts (Thy 1.1) was used to elucidate the orientation of the cells in comparison to the fibres. LFn-cables left in culture for 3 weeks were fixed in 2.5% gluteraldehyde in 0.1M Phosphate buffer (PB) overnight at 4°C. The cables were then washed with 0.1M PB and mounted for frozen sectioning in OCT mounting medium (Miles Inc). 30 μm thick sections were cut and adhered onto vectabond (Merc) coated slides. Background immunofluorescence was

blocked using 20mM sodium borohydride in PBS for 1 hour at room temperature. The sections were then stained with monoclonal mouse anti S-100 (Sigma) (Schwann cells) or monoclonal mouse anti rat Thy1.1 (Fibroblasts- cross reacts with human fibroblasts) diluted 1:100 in PBS containing 0.5% BSA for 45 minutes at 37°C. Sections were then washed three times in PBS followed by incubation with FITC-labelled goat anti mouse IgG diluted 1:50 in PBS containing 0.5% BSA for 45 minutes at 37°C. Sections were then washed in PBS containing 1% GOC solution (0.18 mg/mL catalase; 0.5 mg/mL glucose oxidase and 0.1 mg/mL glucose in Modified Hanks Buffer (MHB)) to enhance staining (Methodology courtesy of Dr. Werner Baschong, Switzerland). Sections were then mounted in Mowiol-4-88 (Hoechst, Frankfurt, Germany) and examined under a Bio-Rad MRC-600 confocal laser scanning microscope, equipped with an Argon-ion laser working with the Bio-Rad Image System (COMOS 7.0, Bio-Rad, UK). Cells stained for FITC were viewed under 490nm excitation wavelength with a 60× objective. Using the Bio-Rad Image System, serial optical sections at 5μm intervals from the surface of the section were taken and the computer software was then used to combine all the sections to produce an image of the whole section.

2.2.4. Copper Stabilisation of Large Fibronectin Cables: Cell Substrate Properties

2.2.4.1. Preparation, copper (and zinc) impregnation and protein dissolution of LFn-cables

Free-dried LFn-cables were prepared as described in Chapter 2.1.7. Impregnation of copper sulphate and subsequent dissolution of protein measurements were achieved by using the methods described earlier in Chapter 2.1.1.1. Cables were impregnated with

zinc sulphate and equimolar concentration of copper sulphate and zinc sulphate in exactly the same way and subsequent protein dissolution was measured as in Chapter 2.1.1.1.

2.2.4.2. Scanning electron microscopy

Copper impregnated LFn-cables were treated in a series of alcohols followed by two 5 minute washes in 100% hexamethyldisilazane (HMDS), Sigma), the second of which was allowed to evaporate at room temperature (Chissoe et al., 1994). Samples were then sputter coated and viewed under a scanning electron microscope at 10kV.

2.2.4.3. Cell culture on copper stabilised LFn-cables

Copper treated LFn-cables were cultured with 50,000 Schwann cells, rat tendon, skin and tail fibroblasts in the same way as described earlier in Chapter 2.1.1.4. The same method was employed for cells cultured on zinc and copper/zinc LFn-cables.

2.2.4.4. Estimation of cell numbers after 3 weeks

After 3 weeks in culture, the CuLFn-cables were removed from the bottom of the well plates using sterile forceps and digested using 0.2% collagenase (Sigma) and 0.25% trypsin (Sigma) in PBS as described in Chapter 2.1.1.5. Cells were recovered and counted as described in Chapter 2.1.1.5.

The same methods were used to count the number of cells in zinc and copper/zinc LFn-cables.

2.2.4.5. Immunohistochemistry

Schwann cells were immunostained for S-100 protein to locate their position within LFn-cables by the method already described in Section 2.2.3.5.

2.2.5. Large Cables and Mats from Fibronectin: Effect of Freeze Drying on Fibrillar Structure

2.2.5.1. Freeze-fracture of LFn-cables

Following LFn-cable production and testing, cables were immersed in liquid nitrogen between forceps. Once the sample had frozen a second force was used to snap the cables longitudinally. Cables were fixed in 2.5% Gluteraldehyde (BDH, Poole, UK) in phosphate buffer, pH 7.4 and prepared for scanning electron microscopy as below.

2.2.5.2. Effect of hydration on Fn-mats

Fn-mats were formed as described above and either fixed in 2.5% gluteraldehyde (Agar Scientific) followed by processing for scanning electron microscopy as described later or treated with distilled water for 30 minutes, 4 hours or overnight followed by processing for scanning electron microscopy as described later. These mats were compared with control unprocessed freeze dried (i.e. dried once) mats for variations in fibrillar structure.

2.2.5.3. Scanning electron microscopy (SEM)

Samples of LFn-cables and Fn-mats were dehydrated in a series of alcohols before being washed in 2 changes of 100% hexamethyldisilzane, the last of which was allowed

to air dry. Samples were then sputter coated and viewed under a scanning electron microscope at 10kV.

2.2.6. A study of Adhesion, Alignment and Migration of Cultured Schwann cells on Ultrathin Fibronectin Fibres

2.2.6.1. Preparation of fibronectin fibres

Ultrathin fibronectin fibres were made by using the method of Ejim et al, 1993 as described in Section 2.1.2. Individual fibres were pulled out and attached to sterilised round coverslips (BDH), which were coated with 1 mg/mL poly-L-lysine. The attached fibres were air dried for 24 hours before gamma irradiation.

2.2.6.2. Schwann cell culture on fibronectin strands

Rat Schwann cells were cultured from a modified method of Brockes et al, 1979 as described in Chapter 2.1.8. Schwann cells at passage 4-5 were plated at a density of 5 x 10^4 cells/coverslip in 4-well plates for culture onto fibronectin fibres and left for 24 hours.

2.2.6.3. Measurement of the speed of Schwann cell movement on fibronectin fibres

Cell cultures were placed on the stage of the inverted phase-contrast microscope and incubated at 37°C. The movement of Schwann cells along Fn-fibres was viewed under an inverted microscope (Nikon, Surrey, England) and recorded by time-lapse video using a CCD high performance camera (Sony CCDXC-77CE, Sony UK) and an Openlab Image analysis software package (Improvision, Coventry, England). The

position of each individual cell, defined as the position of the cell nucleus, was recorded every hour for 10 hours and then all the distances between the subsequent positions were summed to give the length of the cell path (S).

Parameters measured:

The methodology for measuring various parameters of the behaviour of cells have been described earlier by Wojciak et al., 1996. Briefly:

a. The mean speed of cell movement ($V_{effective}$) was calculated using the following equation:

$$V_{effective} = S / t$$

Where S = the length of the total cell path

t = the duration of the recording

b. The real speed of cell movement (V_{real}) :

$$V_{real} = S / t\text{-}N$$

Where N = the number of time intervals when the cell did not move (hours).

For calculation of V_{real} we took into account only the time intervals when Schwann cells were seen to be moving.

c. The total cell translocation which is defined as the distance between the first and the last point of the cell path was calculated.

d. Persistence parameter (Pr):

Pr = total cell translocation/ total length of cell path (S).

Pr would equal 1 for the cell moving persistently along one straight line in one direction.

2.2.6.4. Light microscopy and orientation analysis

Binary images of Schwann cells on strands captured from the Image analysis system, as described above, were used to calculate the orientation of cells in relation to the strand. An orientation index devised by Herman (ref; Guido and Tranquillo, 1993) was used to reflect the orientation of cells. As Schwann cells display a polarised appearance, the angle of alignment can be measured directly in relation to the strand axis and is given by the equation: $S = 2 (\cos^2 a)-1$, where a is equal to the angle between the central plane of individual cells to the axis of the strand. The term $(\cos^2 a)$ denotes the square cosine of (a) averaged over all measured cells. An S value of 1 would indicate perfect alignment and a value of 0 would indicate total random orientation of cells. Values of S were calculated for 100 cells along each fibre.

Cultured cells grown on fibres for 24 hours were fixed in 2.5% gluteraldehyde and attached to microscope slides using DPX and left to dry at room temperature. Samples were stained with haemotoxylin and eosin for routine histology. Images of cultures were scanned into a computer to give Schwann cells orientation after 24 hours as described above.

2.2.6.5. Measurement of cell area and cell extension

Binary image captured from the various time points were used to calculate the area of cells (i.e. cell spreading) and cell extension on the different substrata using the same technology as described earlier. Calculations of cell area and cell extension was performed by the published methods of Dunn and Brown, 1986. Binary images captured from the various time points were used to calculate the area of cells (i.e. cell

spreading) and cell extension on the different substrata using the same technology as described earlier. Calculations of cell area and cell extension was performed by the published methods of Dunn and Brown, 1986 in which moments of a shape are used to calculate cell spreading parameters as follows:

1. Calculation of moments

Moments of a shape. For each cell, the zero-order, the two first-order and the three second-order moments of its shape were calculated. The zero order moment is calculated as the number (n) of pixels in the digitized image of the cell, and the remaining five moments (m) were calculated by obtaining the following sums from the x and y pixel co-ordinates of all n pixels:

$$m_{00} = n \quad m_{10} = \Sigma x \quad m_{01} = \Sigma y \quad m_{20} = \Sigma x^2 \quad m_{11} = \Sigma xy \quad m_{02} = \Sigma y^2$$

Central moments. Central moments, defined as moments referred to the centroid of the shape as the origin of the co-ordinate system. These moments are invariant to translation i.e. they do not change with changes in the position of the object. The second order central moments were calculated for each cell as:

$$\mu_{20} = m_{20} - (m^2_{10}/m_{00}) \quad \mu_{11} = m_{11} - (m_{10}m_{01}/m_{00}) \quad \mu_{02} = m_{02} - (m^2_{01}/m_{00})$$

Normalised central moments. Normalised central moments are invariant to changes in size of the shape. For the second order, these were calculated as follows:

$$\eta_{20} = \mu_{20}/m^2_{00} \quad \eta_{11} = \mu_{11}/m^2_{00} \quad \eta_{02} = \mu_{02}/m^2_{00}$$

These three moments are the basis for the following measures.

2. Calculation of the measures of cell shape

The measures of cell shape was calculated from two second order measures of cell shape defined by Hu, 1962, which are invariant to rotation:

$$\phi_1 = \eta_{02} + \eta_{20} \qquad \phi_2 = (\eta_{02} - \eta_{20})^2 + 4\,\eta^2_{11}$$

From these, the following two rotational invariants were calculated:

$$\lambda_1 = 2\pi(\phi_1 + (\phi_2)) \qquad \lambda_2 = 2\pi(\phi_1 - (\phi_2))$$

These were used to calculate, for each cell, the cellular extension:

Extension = $\log_2(\lambda_1)$

This is a measure of how much the cell shape differs from a circle and takes the value of zero if the shape is circular and increases without limit as the shape becomes more compact.

Cellular area was pre-calculated and displayed by the image analysis system.

2.2.6.6. Scanning electron microscopy (SEM)

Coverslips containing Fn-fibres and cultured cells grown for 24 hours were fixed in 2.5% gluteraldehyde (Agar Scientific) for 10 minutes, then in 1% osmium tetroxide in PBS for 15 minutes. The cultures were then hydrated in a series of alcohols (10 minutes per wash) and two 5 minute washes in 100% hexamethyldisilazane (HMDS, Sigma), the second of which was allowed to evaporate at room temperature (Chissoe et al., 1994). The samples were then sputter coated and examined under a scanning electron microscope at 10kV.

2.2.6.7. Immunostaining of F-actin

Cultured cells on strands were rinsed in PBS and fixed in 1% gluteraldehyde for 15 minutes. Background staining was reduced by using 20mM sodium borohydride in PBS for 1 hour at 37°C. Coverslips were washed three times in PBS and permeabilized

in 0.5% Triton X-100 (Sigma) for 15 minutes. After washing three times in PBS cells were incubated in 1μg/mL TRITC-phalloidin solution in PBS for 45 minutes at 37°C and washed three times in PBS containing 1% GOC solution (0.18 mg/ml catalase; 0.5 mg/ml glucose oxidase and 0.1 mg/ml glucose in MHB) to enhance staining (*Methodology courtesy of Dr. Werner Baschong*). Labelled samples were then mounted in Mowiol-4-88 (Hoechst) and examined under a Bio-Rad MRC-600 confocal laser scanning microscope, equipped with an Argon-ion laser working with the Bio-Rad Image System (COMOS 7.0, Bio-Rad UK). Cells stained for actin were examined under 529nm excitation wavelength with a 60x objective.

2.2.6.8. Immunostaining of vinculin

Cells cultured with Fn-fibres were washed with PBS, fixed in 4% paraformaldehyde and background staining was reduced by incubation in 20mM sodium borohydride in PBS for 1 hour at room temperature. Coverslips were washed three times in PBS for 5 minutes each and permeabilised in 0.5% Triton X-100 for 15 minutes. Coverslips were then washed three times in PBS for 5 minutes and incubated with 200μL of mouse monoclonal anti-human vinculin antibody (Sigma) diluted 1:100 in PBS containing 0.5% BSA and 0.5% Tween 20 (PBST-BSA) for 1 hour at 37°C. The cells were then washed three times in PBS and incubated with 200 μL of FITC-labelled anti-mouse antibody diluted 1:50 for 1 hour at 37°C. The coverslips were then washed three times in PBS containing GOC solution (as for F-actin) and viewed under the Bio-Rad MRC-600 confocal scanning laser microscope (Bio-Rad) equipped with an Argon-ion laser. Cells stained for vinculin were examined under 490nm excitation wavelength with a 60x objective.

2.2.6.9. Statistical analysis

Unless otherwise stated 100 Schwann cells were analysed for each variation of substrata and treatment. Means and standard deviations were calculated for cell spreading area orientation and cell velocities. Student's t-test was used to compare groups of results.

2.2.7. High Concentrations of Fibrinogen Inhibit Cell Adhesion and Migration on Fibronectin/Fibrinogen Composite Cables

2.2.7.1 Preparation of Microthin Fn/Fg-cables with varying concentrations of Fg

A solution of Fn/Fg containing 75% Fg, determined by assay of Fg (Courtesy of Sarah Underwood, UCLbe) as described in Section 2.1.4., was prepared from a cryoprecipitate (SNBTS) as described in Section 2.1.5. Fg was partially removed by polyethylene glycol (PEG) precipitation in a stepwise manner starting from a 1% rising to 10% PEG solution to precipitate out Fg. The process was monitored by assaying Fg content using the method described in Chapter 2.1.4. Fn/Fg-cables from these solutions containing different concentrations of Fg were made as described earlier in Chapter 2.1.5. Percentage concentrations of Fg were determined as: 25, 35, 49, 64 and 75 %. The cables were adhered onto poly-L-lysine coated glass coverslips (BDH) and dried overnight at room temperature. The coverslips were then gamma irradiated before use. To determine the total protein concentration in each cable on a coverslip, the strand was digested with 0.25% trypsin (v:v) and a protein assay was performed using the Bio-Rad protein assay kit (Bio-Rad UK). Total protein concentration of each individual cable ranged between 34-50 μg.

Pure Fn-fibres were made as described in Section 2.1.2.

2.2.7.2. Cell Culture

Schwann cells were cultured as described in Chapter 2.1.8. using a modified method of Brockes et al., 1979. Human dermal, rat tendon and rat skin fibroblasts were cultured from explants of tissue as described in Chapter 2.1.7. (Burt and McGrouther, 1992). 200,000 cells/well (13mm diameter) were cultured for 10 and 24 hours on Fn/Fg-cables in a humidified incubator at 37°C and 5% CO_2. The cells were then washed with PBS and fixed in 2.5% gluteraldehyde (Taab Laboratories Equipment Ltd., Reading, Berkshire, UK) in 0.1M phosphate buffer overnight. The cells still attached to the coverslips were then washed with distilled water and stained with haemotoxylin and eosin and viewed using a light microscope.

2.2.7.3. Cell adhesion assay

200,000 cells were plated onto the different ratios of Fn/Fg-cables (n= 8 (4 strands on each coverslip)) in 4-well plates (Falcon) and left for 10 hours before fixing in 2.5% gluteraldehyde. The cultured cells were then placed under an inverted phase contrast microscope and the number of cells attached to the strands were counted using the Openlab Software package (Improvision) (described in Section 2.2.6). This was difficult due to the fact that the strands occupied very little surface area of the culture vessel and therefore few cells adhered to them. To try to improve on this a monolayer system was also used as described below.

1 mL of the different ratios of Fn/Fg (0.5 mg/mL) were used to coat a monolayer of Fn/Fg on glass coverslips in 4-well plates (Falcon, UK) and left for 48 hours at 37°C in a humidified incubator. To check the concentrations of Fn adsorbed on the coverslips a

double antibody ELISA technique for Fn was performed as described in Chapter 2.1.5. An equal volume of suspension containing 200,000 cells from each population was plated onto the coated substrata, 1 mL of DMEM-complete was added and incubated at 37°C and 5% CO_2 for 10 hours. Non adhered cells were washed off carefully with sterile PBS while adhered cells were removed by trypsinization (0.25% w:v Trypsin-EDTA (Gibco) for 5-10 mins) and recovered by centrifugation at 1500 rev/min for 3 minutes. The cells were suspended in 1 mL of DMEM and counted using a haemocytometer.

2.2.7.4. Measurement of the speed of Schwann cell movement on Fn/Fg cables

200,000 cells were cultured on the various ratios of Fn/Fg-cables and topped with 1 mL of DMEM containing 10% FCS, penicillin/streptomycin and 25 mM HEPES buffer. The cultures were placed on the stage of an inverted phase-contrast microscope equipped with a 37°C incubation chamber (Nikon, Surrey, England). The movement of Schwann cells along Fn/Fg-cables were recorded and $V_{effective}$, V_{real} , the total cell translocation and the persistence parameter (Pr) were calculated exactly the same way as described in Section 2.2.6.3.

2.2.7.5. Cell spreading

Binary images captured from the various time points were used to calculate the area of cells (i.e. cell spreading) and cell extension on the different substrata using the same technique as described earlier. Calculations of cell area and cell extension were performed by the published methods of Dunn and Brown, 1986, as described in 2.2.6.5.

2.2.7.6. Immunostaining of vinculin

Cells cultured with strands were washed with PBS, fixed in 4% paraformaldehyde, stained for vinculin and viewed under a confocal laser scanning microscope as described in Section 2.2.6.8.

Images from the confocal laser microscope were recorded onto hard drive via the Bio-Rad COMOS 7.0a image analysis software package (Bio-Rad, UK). The software package was used to draw round each cells and measure the integrated fluorescence of each individual cell. Integrated fluorescence for a total of 50 cells in each of 5 randomly selected fields along the Fn/Fg-strand was measured. The mean integrated fluorescence/cell ± s.d. was then plotted.

2.2.7.7. Statistical analysis

All statistical analysis was carried out using the MINITAB software package (MINITAB Inc, P.A., USA). Means and standard deviations were calculated for cell velocities, cell spreading area and integrated fluorescence. Student's t-test was used to compare groups of results. Unless otherwise stated 100 cells were analysed for each variation of fibrinogen.

2.2.8. Increased Cell Migration and Alignment on Two Forms of Fibronectin Strands/Cables After Stabilisation with Micromolar Concentrations of Copper

All methods used described previously.

3.0. METHODS DEVELOPMENT

3.1. Copper Stabilisation of Fibronectin Mats

Following copper stabilisation of Fn-mats, the mats became resistant to breakdown by the enzyme trypsin. The mats need to undergo complete digestion following protein dissolution tests inorder to measure the total protein content. The time required to cause the complete digestion varied depending on the concentration of copper used and varied in a dose dependent manner. Initial experiments were performed to determine the length of time and the concentration of trypsin needed for complete digestion of Fn-mats.

The first concentration of trypsin selected was 200 μg/mL. To a known weight of CuFn-mat 5 mL of trypsin was added into a universal tube and incubated at room temperature and at 37°C on mechanical rollers to aid diffusion. The tubes were monitored over time. As soon as the Fn-mats were visually seen to dissolve, aliquots were taken out and a protein assay was performed to determine the total amount of protein which had dissolved. Table 3.1. shows the length of time taken to digest copper stabilised mats. From the table it can be seen that untreated Fn-mats dissolve more rapidly than treated mats which took 6-96 hours depending on the dose of copper used. This indicates the stability of such treated mats. Mats treated with 200 μM copper were particularly difficult to digest, a waiting time of upto 4 days for the mats to dissolve would slow down the process and may even have time for bacterial growth which would complicate the protein assay procedure.

Test conditions	Time taken (hours) to dissolve mats with 200 μg/mL trypsin at:	
	Room temp.	37°C
Untreated Fn-mat	4-6	2-3
1 μM CuFn-mat	6-9	3.5-6
10 μM CuFn-mat	9-13	5-7
100 μM CuFn-mat	17-24	24-29
200 μM CuFn-mat	90-96	36-40

Table 3.1. *Time taken to digest copper treated Fn-mats with 200 μg/mL trypsin at room temperature and at 37°C.*

Digestion times were determined under the same conditions for 2 and 4 times the concentration of trypsin on copper treated Fn-mats. Table 3.2. shows that digestion times with 400 μg/mL of trypsin had reduced considerably and 200 μM treated CuFn-mats were taking 12-18 hours at 37°C and 30-36 at room temperature to dissolve completely. The results after treatment with 800 μg/mL trypsin showed that digestion times for all copper and non-copper treated mats were acceptable. Digestion times for 200 μM treated Fn-mats had reduced to 1-1.5 hours at 37°C. For subsequent protein digestion used throughout this thesis, 2 hour digestion time at 37°C in 800 μg/mL trypsin was used to ensure complete digestion after copper treatment.

Test conditions	Time taken (hours) to dissolve mats with 400 μg/mL trypsin at:	
	Room temp.	37°C
Untreated Fn-mat	2.5-4	1-2
1 μM CuFn-mat	3-4	2-2.5
10 μM CuFn-mat	4.5-7	3-4
100 μM CuFn-mat	10-15	5-8
200 μM CuFn-mat	30-36	12-18

Table 3.2. *Time taken to digest copper treated Fn-mats with 400 μg/mL trypsin at room temperature and at 37°C.*

Test conditions	Time taken (hours) to dissolve mats with 800 μg/mL trypsin at:	
	Room temp.	37°C
Untreated Fn-mat	2-2.5	0.2-0.3
1 μM CuFn-mat	3-4	0.3-0.4
10 μM CuFn-mat	4-5	0.5-0.6
100 μM CuFn-mat	5-6	0.7-1
200 μM CuFn-mat	8-10	1-1.5

Table 3.3. *Time taken to digest copper treated Fn-mats with 800 μg/mL trypsin at room temperature and at 37°C.*

3.2. Production of Large Cables of Fibronectin

3.2.1. Problems with keeping the circular structure of the LFn-cable

Once precipitated Fn-fibres were scooped together to make LFn-cables (Section 2.17.), the structures were freeze-dried for easier storage. Initially the cables were placed on Teflon discs and freeze-dried. However, due to the vast number of fibres within the LFn-cable, the structure flattened such that it did not retain its original circular appearance. When these cables viewed by scanning electron microscopy, they appeared flattened with Fn-fibres densely packed. Although the general orientation could be seen, fibrillar nature of the cable was less apparent (Figure 3.1a). Cables in cross-section also showed a densely packed nature with very few pores (Figure 3.1b).

The problem of the cable collapsing was remedied by using small diameter drinking straws (3-4 mm diameter). These straws were cut into 1 cm pieces and one surface was longitudinally slit such that once cables were made and washed they could be inserted in the middle and freeze-dried. This enabled the cables to retain their original circular appearance without damaging surface fibril orientation (see SEM's of cables in Chapter 4.3.).

3.2.2. Neutralisation of acidity from LFn-cables

LFn-cables made by extrusion into an acid bath remain acidic (<pH 4) in nature even after 2 hours of washing in PBS. Initially longer washes in PBS and DMEM were sufficient to cause a reduction of acidity to neutral pH. After 24 hour soaking in PBS or DMEM, the pH was around 7. However, the long soaking stage damaged the structure of LFn-cables such that after 24 hours the cables were no longer circular and

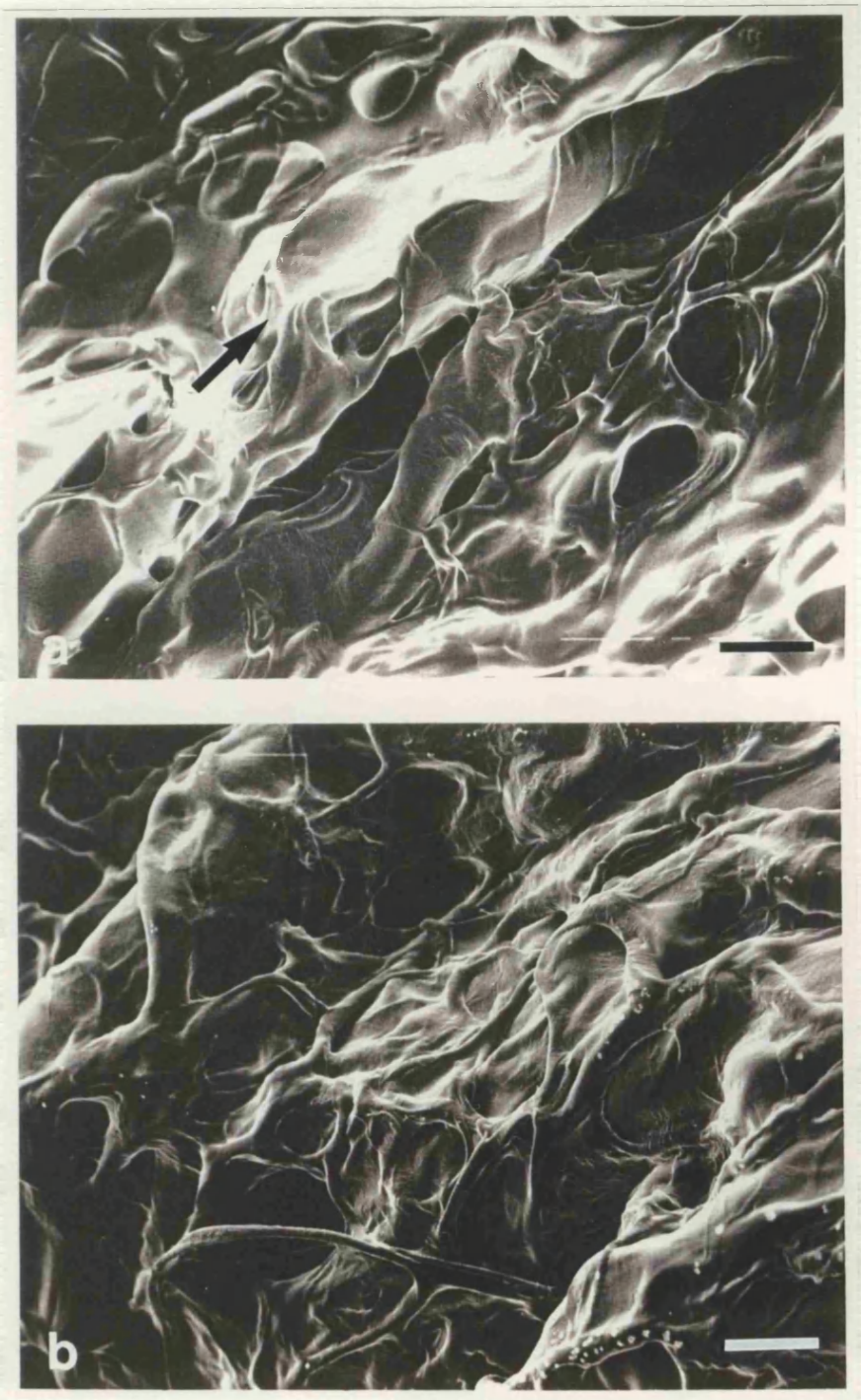

Figure 3.1. *Scanning electron micrographs of LFn-cables freeze-dried on Teflon discs. (a) longitudinal and (b) cross-sectional surfaces. Note the dense appearance of the fibrils in longitudinal sections. Arrow indicates fibre orientation. Scale bar = 100μm.*

easy to handle but flattened and gel-like in nature and very difficult to handle. Clearly, PBS and DMEM are very weak buffers and greater neutral buffering capacity was required. This was solved using a quick neutralisation stage using 200 mM Tris-HCl buffer (pH 7.6) which produced neutral LFn-cables (pH 7) after only 15 minute soak in a large volume with gentle rolling.

3.3. A study of Adhesion, Alignment and Migration of Cultured Schwann cells on Ultrathin Fn-fibres

Digitised images of Schwann cells cultured on Fn-fibres were used to calculate cell area, cell extension and orientation parameters. The image analysis system converted images captured by the attached CCD camera to digital images which the computer programme used to calculate these parameters. A major problem is the fact that when cells are in close contact with one another, the computer does not distinguish between them. This however, was overcome by using the drawing facilities of the software programme (Openlab) to separate such groups of cells, manually. The 'cleaned up' image was then used for subsequent calculations of these parameters. An example of this process is shown in Figure 3.2. where digital images were 'cleaned' for easier use of the software package. The cleaned up digital image however, is very close to the original real time captured image and therefore represents a good way of overcoming such problems.

Figure 3.2. *Example of real time image (a) and 'cleaned up' digital image (b) of Schwann cells cultured on Fn-fibres after 10 hours. Note that the 'cleaned up' image is very similar to the real image. Scale bar = 20μm.*

4.0. RESULTS

4.1. Stabilisation of Fibronectin Mats with Micromolar Concentrations of Copper

4.1.1. Fn-mats and strand stabilisation

Porter et al., submitted, showed that plain Fn-mats survived for 15 days in vivo in a rat sciatic nerve model, with the formation of a thin bridge of axons. The regeneration would be improved if Fn-mats would provide a surface for migration of regenerating components of axons for longer time periods. With this in mind the aim of this experiment was to stabilise Fn-mats so that they would have a longer survival time in vitro and in vivo. We have previously used copper at high concentrations (500μM) and shown that stability of Fn-mats could be improved. Clearly, such concentrations of copper would be detrimental to cell survival and therefore lower concentrations were used here. Additionally, the effect of copper on cross-linking of Fn-fibres was investigated by scanning electron microscopy. Finally cells were grown in vitro to determine the effect of copper on cell survival (toxicity) and proliferation. The effect of zinc ions on stability was also investigated.

Fibronectin mats, placed in copper sulphate solution, chelate copper almost immediately and became visibly blue after approximately 1 minute in 200μM solutions of copper. When these CuFn-mats were incubated at room temperature, in subsequent release of protein from the material over 24 hours, measured by either total protein assay or by extinction at 280nm, showed that dissolution of protein from control untreated Fn-mats was approximately 3 times higher than that of copper stabilised mats (Figure 4.1).

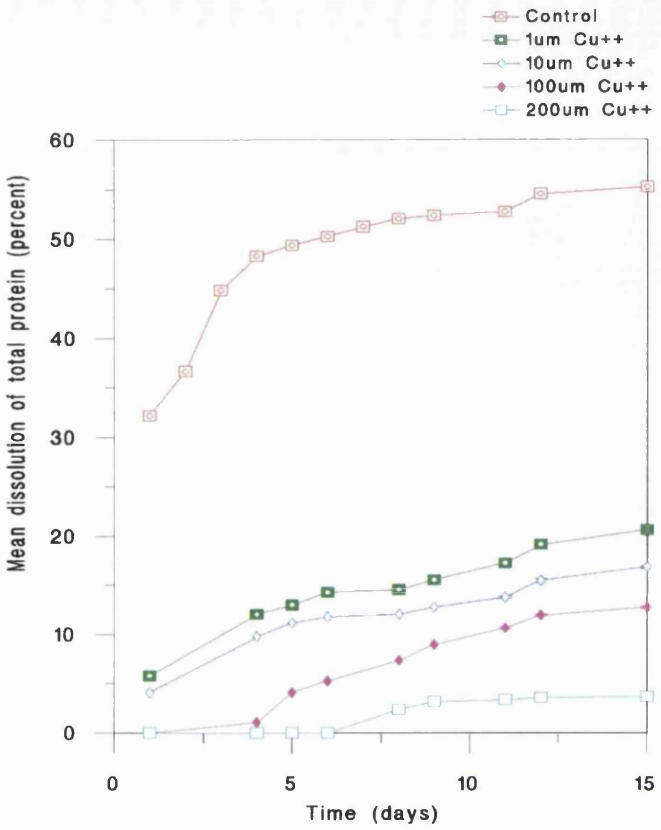

Figure 4.1. *Dissolution of Fn protein from control and CuFn-mats at room temperature.*

Overall loss of protein from control mats was 57% of total over 8 days whilst for Fn-mats treated with 200μM Cu^{2+}, total protein loss was only 5%. By the 8 day stage a plateau was reached and little additional loss was seen over the remaining 7 days. 1, 10 and 100 μM concentrations of copper gave a final protein dissolution of 22, 17 and 13% respectively.

Parallel assessment of stability at 37°C rather than room temperature indicated a similar response to treatment with copper. The greatest dissolution of protein occurred within 24 hours and by day 8 protein loss ranged from 35 to 5% (treatments with 1-200 μM)

in contrast to control mats which lost 61% (Figure 4.2). Similar stabilisation was seen with CuFn-mats incubated in PBS at all concentrations of copper used, although the stability of the mats were slightly higher (approximately 10% higher) than in distilled water (Figure 4.2). It was noted that trypsinization to assay for total protein took 3-4 times longer for Fn-mats treated with copper compared to untreated mats.

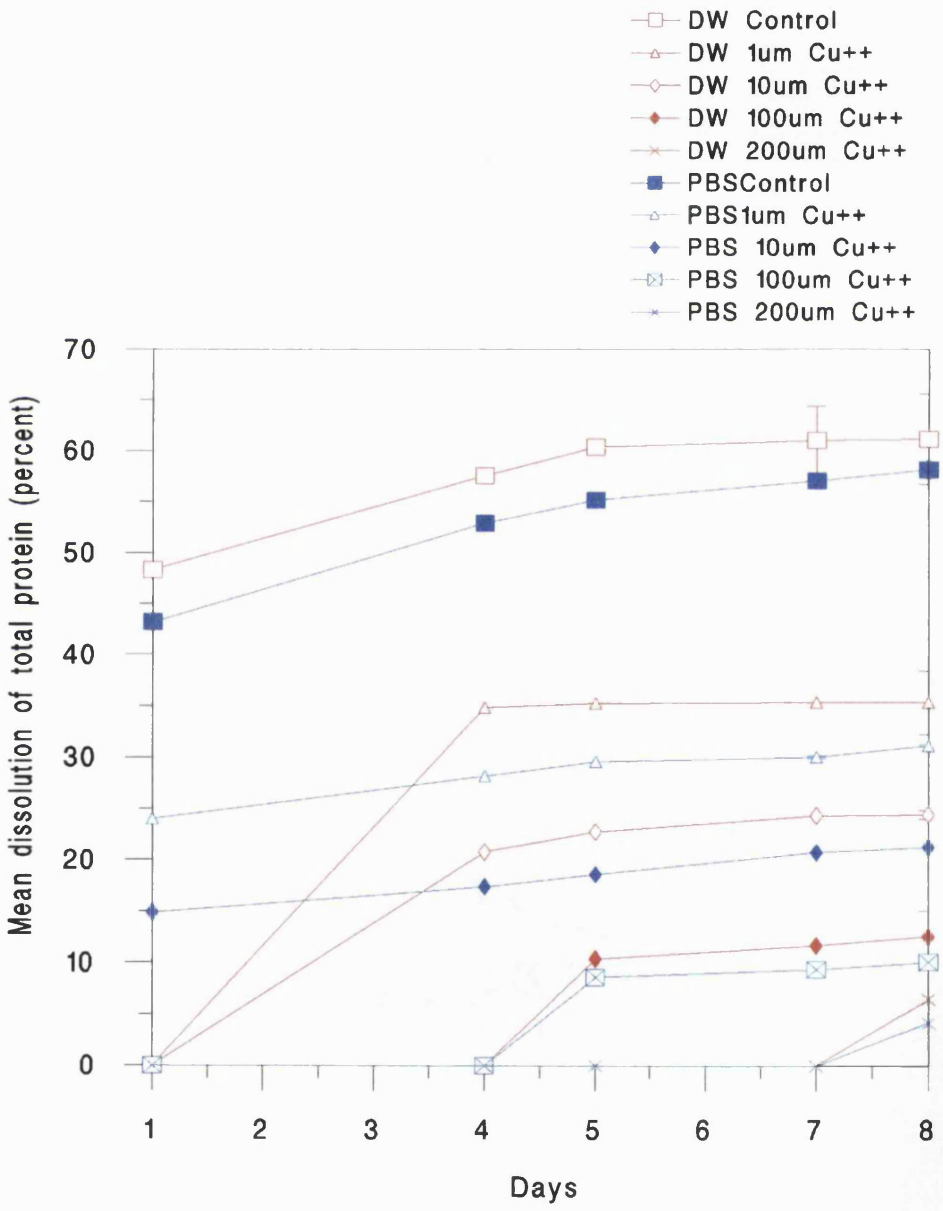

Figure 4.2. *Dissolution of Fn protein into distilled water (DW) and PBS (PBS) at 37°C. CuFn-mats were at least twice more stable than control mats.*

Assessment of protein dissolution after incorporation of zinc showed a slightly lower level of stabilisation of Fn-mats but followed a similar dose dependent response as copper alone (Figure 4.3). However, treatment of the mats with an equimolar concentration of copper and zinc ions caused a 6% greater stabilisation of Fn-mats than copper or zinc alone (Figure 4.3).

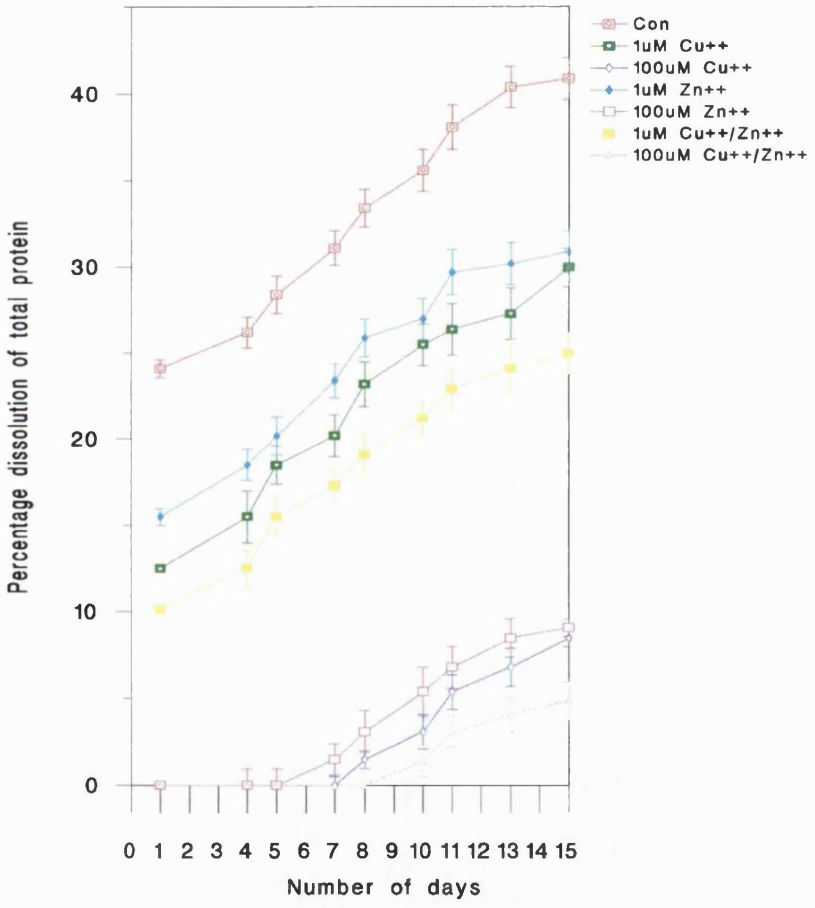

Figure 4.3. *Dissolution of Fn protein after incorporation of Zn, and Cu+Zn together compared to Cu alone, at 37°C in PBS.*

Figure 4.4 shows that using the same concentration of copper, the mean amount which bound to Fn-mats was not significantly different for a variety of copper salts. The

amount of copper ions chelated by mats at the micromolar range is shown in Figure 4.4. In mats treated with 200 and 100 μM copper, 26.5 and 13.5 nmoles of Cu^{2+}/mg Fn, respectively, was detected by atomic absorption. However, in mats treated with lower concentrations of copper, actual Cu^{2+} levels were too low to be detected. Assuming the molecular weight of Fn as 500,000, the molar ratio of Cu^{2+}: Fn is equal to 13.25: 1.

4.1.2. Scanning electron microscopy of CuFn-mats

Figure 4.5 compares the surface features of control and CuFn-mats. Control mats which were rehydrated in either distilled water or PBS for 10 minutes retained a predominant fibre orientation (Figure 4.5a). Small groups of individual fibres had fused under these conditions to form sheet-like structure (Figure 4.5a). It was apparent that 1 μM copper was not only able to cross-link the strands of fibronectin but also separated the fibres such that gaps remained between fibres measuring from 7-20 μm (Figure 4.5b). These fibres also exhibited an overall orientation as indicated in the inset in figure 4.5b. 10 μM copper caused further cross-linking such that in places strands were no longer seen, as indicated by the arrows in figure 4.5c, with the loss of overall orientation. With increasing concentrations of copper (100 and 200 μM) there was further cross-linking such that strands of fibronectin fused together forming sheets of protein with total loss of orientation, as indicated by the arrows in figure 4.5d and e, respectively.

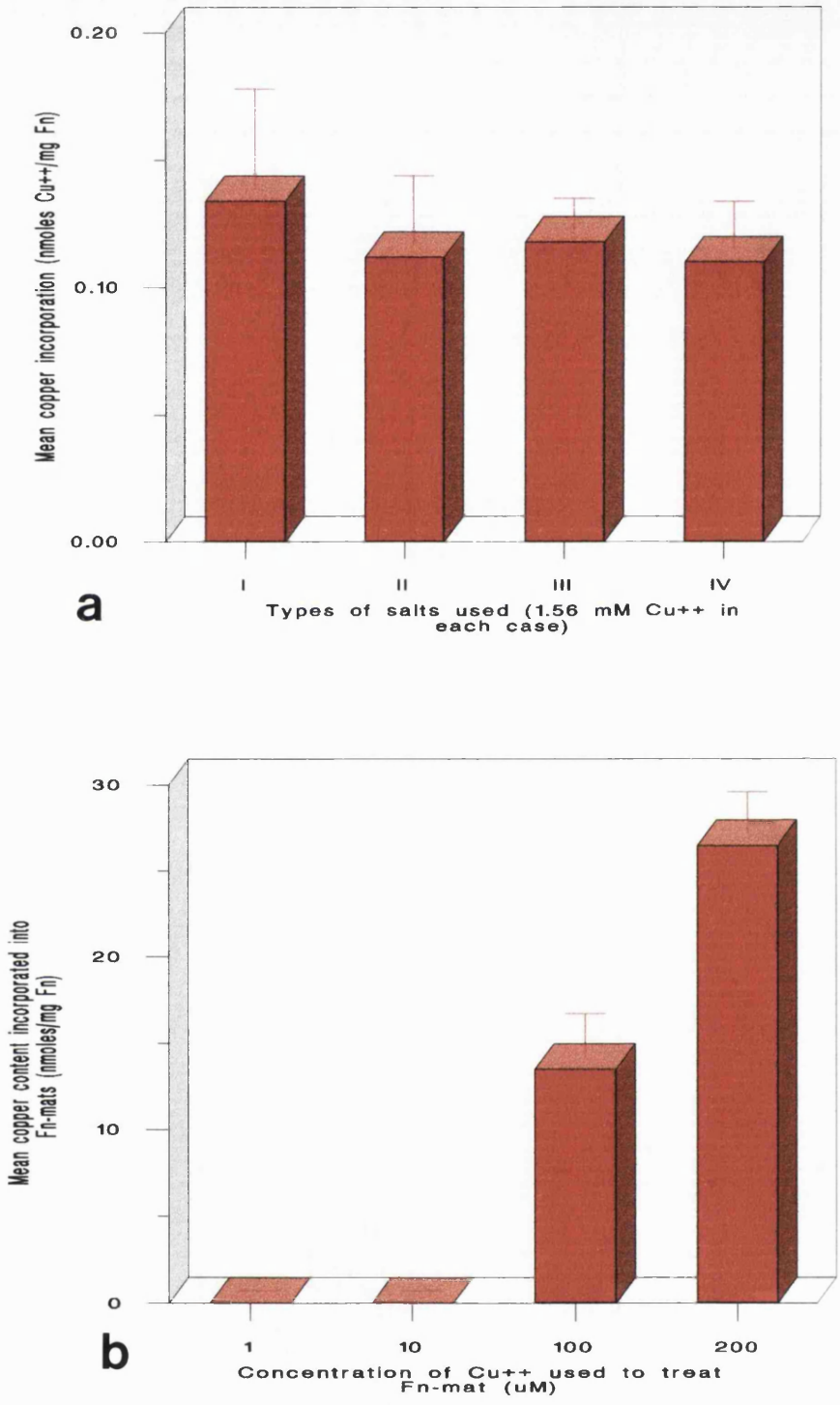

Figure 4.4. *Mean copper content bound to Fn. The graph indicates that the counterion is not important* ***(a)****. I = copper (I) chloride, II = copper (II) acetate monohydrate, III = copper (II) hydroxide and IV = copper (II) sulphate.* ***(b)*** *Mean copper content incorporated when mats were treated with 1, 10, 100 and 200 μM copper($CuSO_4$) (n=4). Copper levels at 1 and 10 μM treatments were not detectable.*

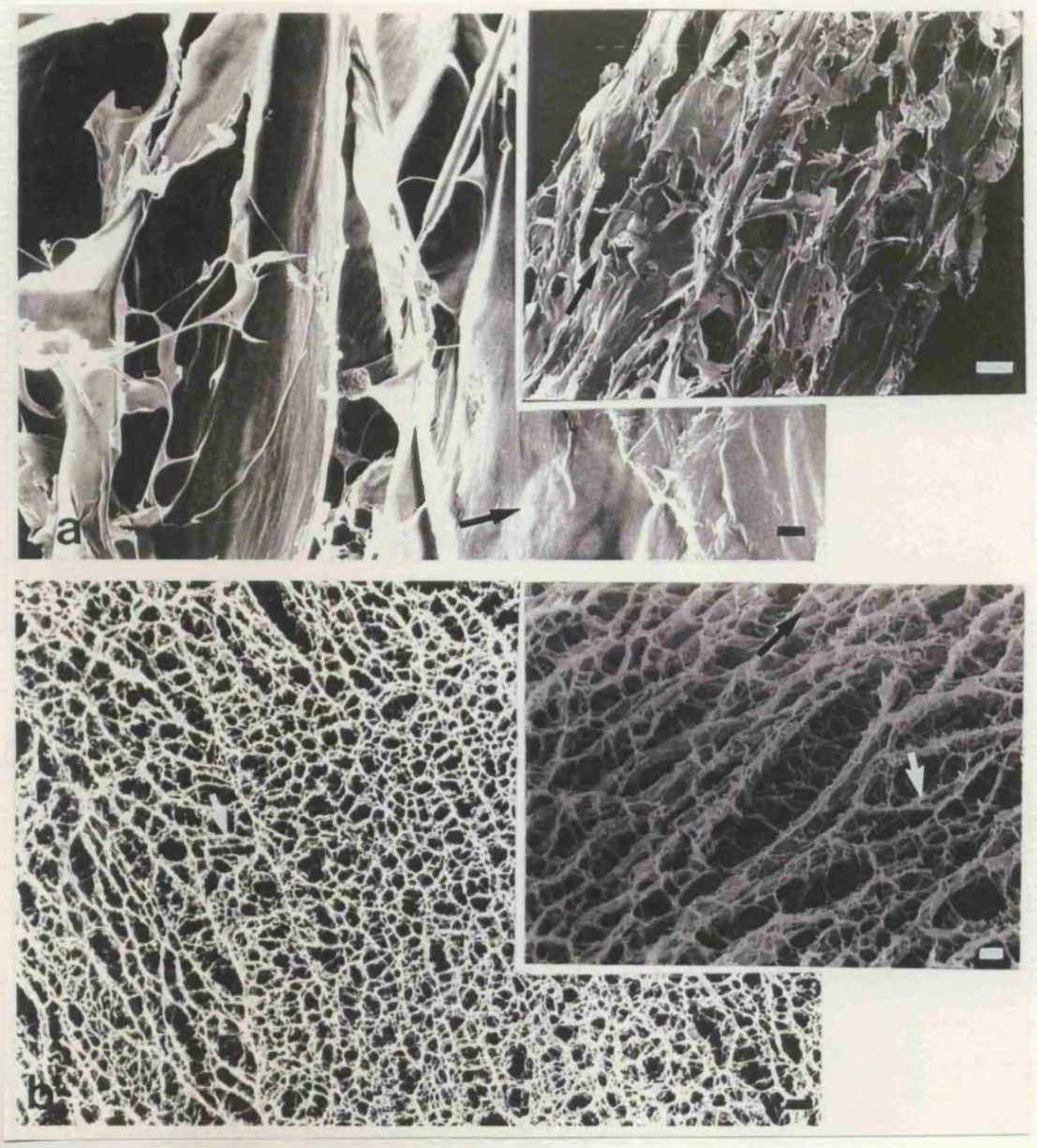

Figure 4.5. *Scanning electron micrographs to show the structure of the mat after copper incorporation.* ***(a)*** *Rehydrated control Fn-mats indicating the overall orientation of the fibres with some aggregation. The fibres had fused to each other by self aggregation as indicated by the arrow; Inset: shows low power scanning electron micrograph indicating overall orientation (arrow).* ***(b)*** *1 μM CuFn-mat showing overall orientation with some cross-linking between the individual fibres (arrow); Inset: shows detailed features of the mat indicating cross-links between fibres, orientation indicated by thick arrow.*

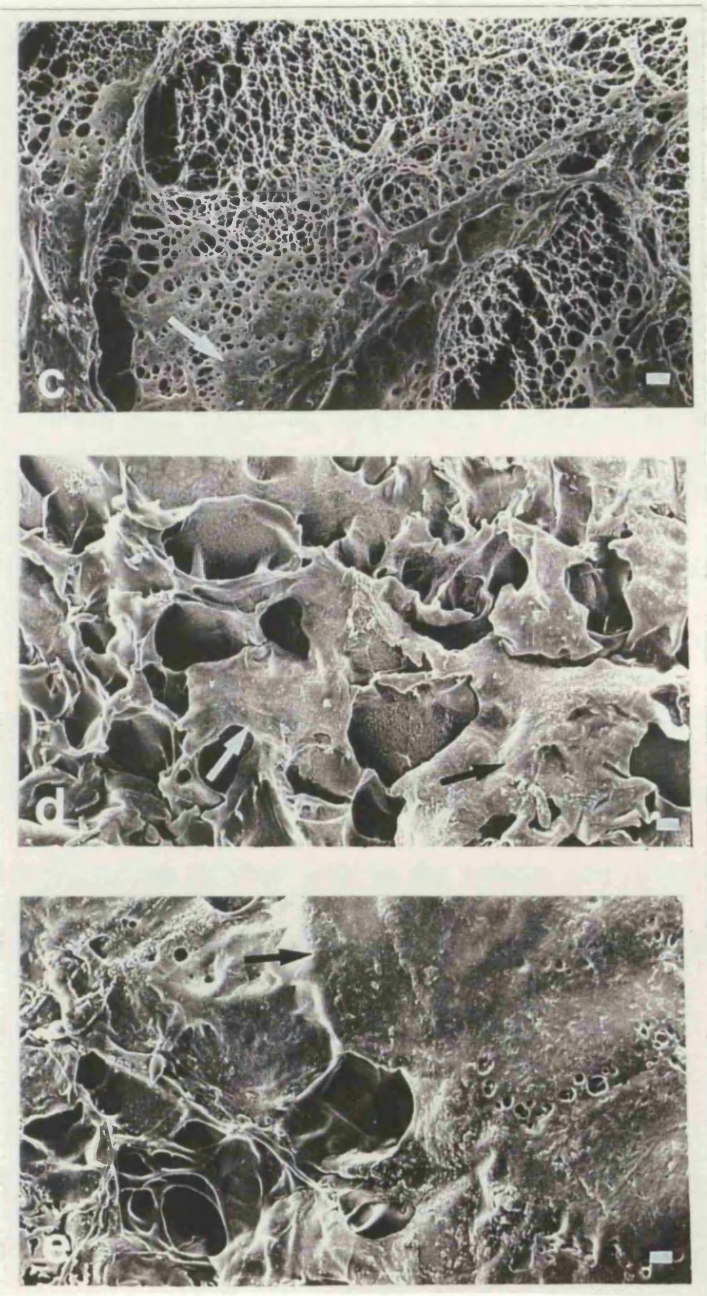

(c) *10 μM CuFn-mat showing sheet formation, loss of orientation of the fibres and clumped protein, as indicated by the arrow.* ***(d)*** *100 μM CuFn-mat showing extensive cross linking with total loss of orientation, as indicated by the arrow, and further clumping of fibres.* ***(e)*** *200 μM CuFn-mat showing further sheet formation and loss of fibre content (arrow). Scale bars in (a), (b), (c), (d) and (e) = 10μm. Scale bar in (a): inset = 100μm and scale bar in (b): inset = 1μm.*

4.1.3. Cell culture on CuFn-mats

Cell types such as human dermal, rat tail and rat Achilles tendon fibroblasts were used to assess toxicity to copper (50,000 cells in each group) (Figure 4.6b, c and d), respectively. Fibroblast derived cells were all able to grow with very little cell mortality (a little sensitivity shown by rat tendon fibroblasts but only after 19 days in culture) at all concentrations of copper ions used, upto the experimental time of 3 weeks. In contrast cultured Schwann cells were only able to grow normally for 3 weeks with mats treated with the lowest concentration of copper (1μM) (Figure 4.6a). Routine histology revealed viable Schwann cells within the fibrillar structure of the mat being guided by the fibres and had adopted a migratory bipolar phenotype (4.6a: inset). Schwann cells were also able to grow with 10 μM copper treated mats for three days but after 24 hours 60% of the total number of cells incubated had died (not shown). After 48 hours, the proportion of dead cells in the culture had risen to 85% with complete death of the culture day 3. No Schwann cells grew in cultures with mats treated at higher concentrations of copper (100 and 200 μM copper ions).

4.1.4. Cell numbers after 21 days in culture

Table 4.1 shows the number of cells that were recovered after 3 weeks in culture. The number of cells in all cultures had increased over time at non-toxic Cu^{2+} doses as expected. However, all cultures which were grown with CuFn-mats had significantly higher numbers of cells than those grown with cells on tissue culture plastic alone, cells plus Cu and Fn-mats. The number of cells recovered were greatest for Schwann cells for which the mean cell number was 68% over plain Fn-mats. However, most of this additional cell division was localised within CuFn-mats (rather than cells on the

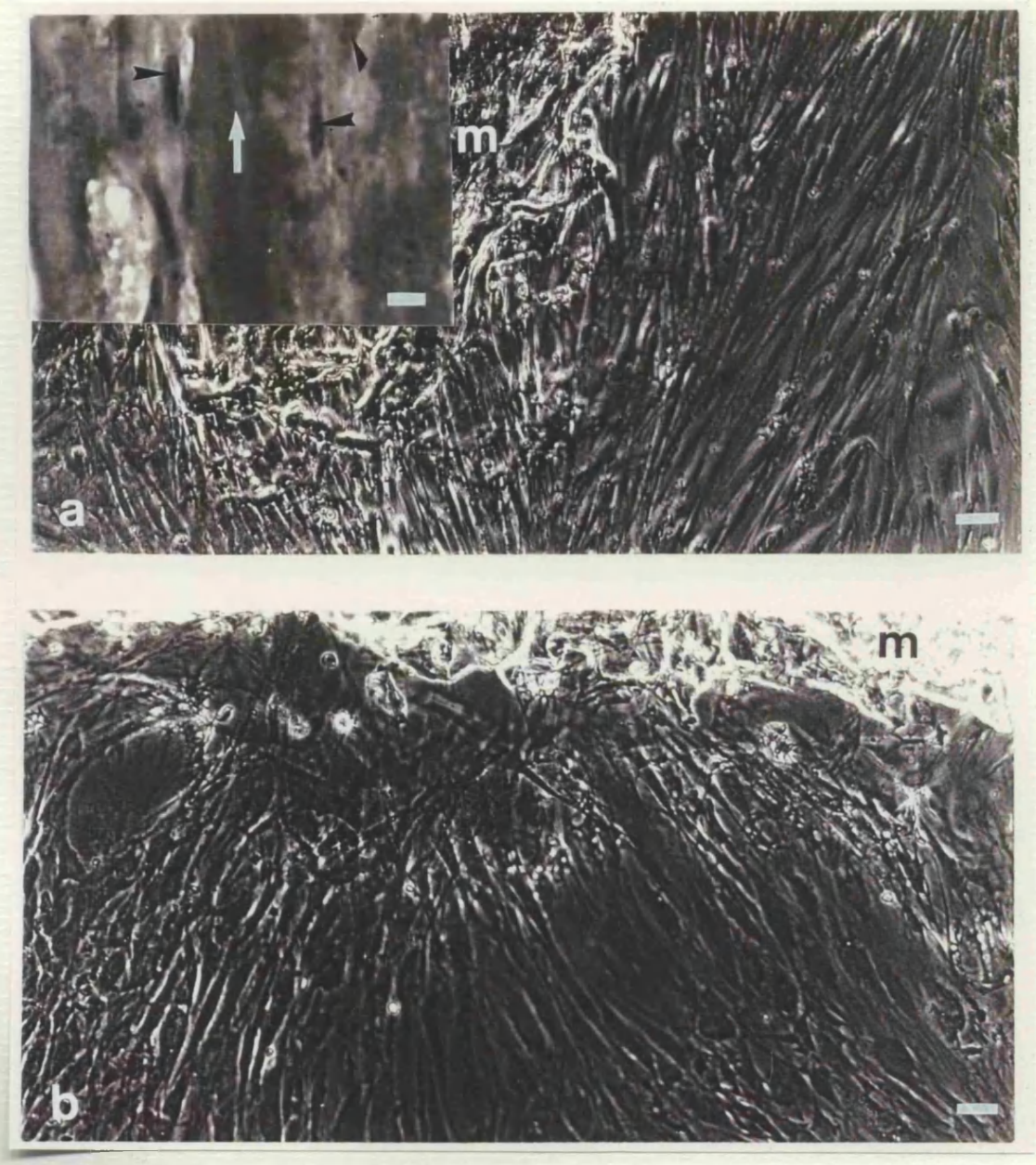

Figure 4.6. *Growth of cells in culture with CuFn-mats. Micrographs show strong growth of:* ***(a)*** *Schwann cells cultured with 1 μM CuFn-mat indicating survival of cells plated: inset shows histological cryo-section of Schwann cells cultured with 1 μM treated CuFn-mats and stained with haemotoxylin and eosin. This showed Schwann cells within CuFn-mats interacting with the fibres without any adverse effects (black arrowheads show Schwann cell nuclei and white arrow shows Fn-mat fibre orientation);* ***(b)*** *human dermal,*

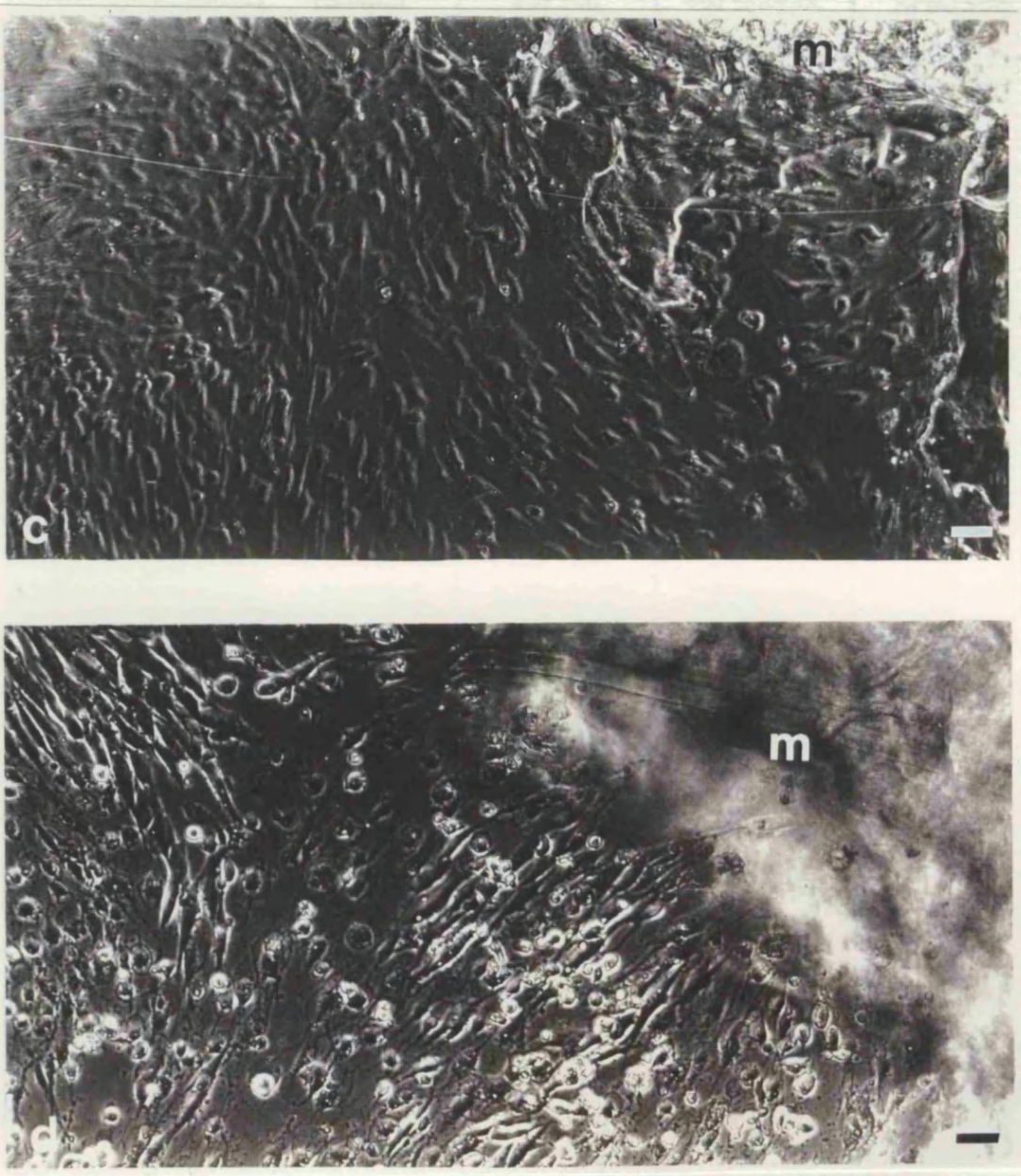

Figure 4.6. *(c) rat tail and* ***(d)*** *rat tendon fibroblasts cultured on 200μM CuFn-mats. Scale bars in (a), (b), (c) and (d) = 20μm; (a): inset = 10μm.* ***m*** *denotes Fn-mat.*

Test conditions	Mean total number of cells recovered for different types of cells			
	Dermal fibroblasts	rat tail fibroblasts	rat tendon fibroblasts	Schwann cells
Cells alone (total)	137,920 ± 4,201	130,127 ± 1,510	142,827 ± 2,522	159,000 ± 1,920
Fn-mat total	139,600 ± 2,207	132,000 ± 1,612	149,275 ± 2,262	176,000 ± 2,050
within mat	9,024±2,207	7,345±324	5,689±240	7,567±135
1μM CuFn-mat total	150,000 ± 5,000	149,500 ± 1,516	156,200 ± 2,102	*260,000 ± 2,100
within mat	7,890±235	7,356±231	6,985±120	*17,034±97
10μM CuFn-mat total	165,000 ± 2,500	161,500 ± 1,600	162,900 ± 1,905	no survival-toxic
within mat	6,760±345	8,021±140	7,894±102	
100μM CuFn-mat total	175,000 ± 2,615	169,600 ± 1,900	177,291 ± 1,705	no survival-toxic
within mat	7,678±320	7,567±98	7,439±94	
200μM CuFn-mat total	167,000 ± 2,007	165,720 ± 2,100	ϕ174,220 ± 987	no survival-toxic
within mat	7,569±125	7900±119	7,861±79	

Table 4.1. *Mean number of cells recovered after 21 days in culture with different concentrations of CuFn-mats. The initial number of cells cultured were 50,000 cells/133 mm^2 coverslip (n= 8 in each group).* $^{\phi}$*Some toxicity to copper shown after 21 days in culture.* *$p<0.0001$ *for cells grown on 1 μM CuFn-mats vs Fn-mat alone, Students t-test. Schwann cells were unable to grow on 10, 100 and 200 μM copper treated mats due to the toxicity of copper.*

surrounding plastic), for which there was an approximately 2.5 fold increase in cell number relative to plain Fn-mats. The number of fibroblasts recovered from within the mat did not differ significantly whether grown on Fn-mats or CuFn-mats. However, the

number of Schwann cells recovered from within 1 μM treated CuFn-mats increased nearly 3 fold over the number recovered from Fn-mats alone.

The results from the experiment showed that copper stabilised Fn-mats by 2-3 times that of control mats, in vitro, while forming cross-links between Fn fibres. The overall orientation of the Fn-mat was retained with low concentrations of copper. Schwann cells were only able to survive at the lowest concentration of copper used while the rate of cell proliferation within the Fn-mat increased by 3 times that of control mats.

4.2. Nerve Growth Factor Delivered Locally via Fibronectin Mats Enhances Peripheral Nerve Regeneration in The Non-Human Primate

4.2.1. Axonal regeneration

Fn-mats are particularly useful for the delivery of NGF locally to the regenerating site since they are highly hygroscopic and release NGF over a period of 7 days in a bioactive form (Whitworth et al., 1996). This system was shown to improve nerve regeneration in a rat sciatic nerve model. Here, the same approach was used to assess the effects of NGF on a purely sensory nerve in a primate model. This was used as step closer to clinical trials since primates are thought to be close relatives of humans and have very similar physiology. Initially a 1cm gap was to be created but reduced due concerns over animal welfare. Instead, a 5mm gap was created in the median nerve of the hand and the mat was sutured into the gap with or without NGF. All the animals were left for 4 months before being sacrificed due to costs. Semi-thin and ultrathin sections of the graft area and 5 mm distal to the graft were analysed by light and transmission electron microscopy to assess the extent of regeneration. Myelinated fibre counts were also performed.

By 4 months axons had formed a bridge between the proximal and distal nerve stumps in all experimental cases with no evidence of any remaining Fn-mat. The size of the regenerate in the centre of the graft, when it was sectioned transversely, was not significantly different between the experimental cases (Figure 4.7a-d). However, it was apparent that in animals grafted with Fn-mats alone there was a mass of regenerating axons which were not grouped into organised fascicles (Figure 4.7d). In contrast, animals grafted with Fn+NGF showed regenerating axons neatly arranged into fascicles surrounded by an organised perineurium and epineurium (Figure 4.7c). Animals grafted with autologous nerves and contralateral controls showed a similar clear organisation (Figure 4.7a and b).

Figure 4.8 shows a comparison of the centre of the regenerate between the experimental groups, based on semi-thin longitudinal sections. In the contralateral control and nerve graft groups (Figure 4.8a: control (and inset: high power), (b) nerve graft (inset: high power)), axons were clearly organised parallel to each other. These were myelinated continuously throughout the graft area. Fn+NGF grafted nerves had a similar appearance with myelinated axons which were clearly organised parallel with the original fibre orientation of the implanted Fn-fibres (Figure 4.8c (inset: high power)). However, repair sites grafted with plain Fn-mats showed fewer continuously myelinated loosely organised axons, although they were very clearly orientated throughout the graft, parallel with the original axis of Fn-mat implants (Figure 4.8d: (inset: high power)).

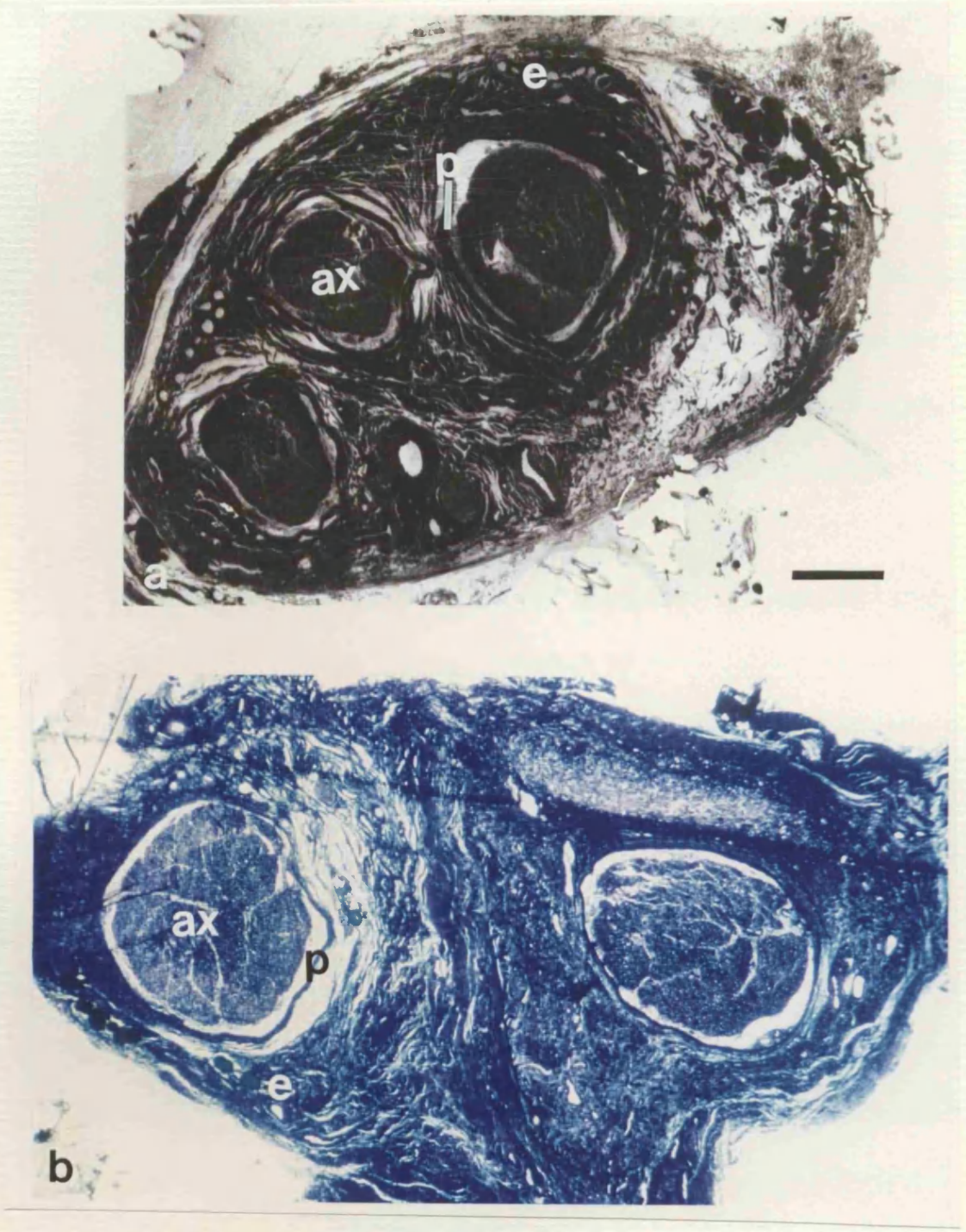

Figure 4.7. *Semi-thin transverse sections of the central region of conduits. From (a) non injured (contralateral control) (b) nerve graft.*

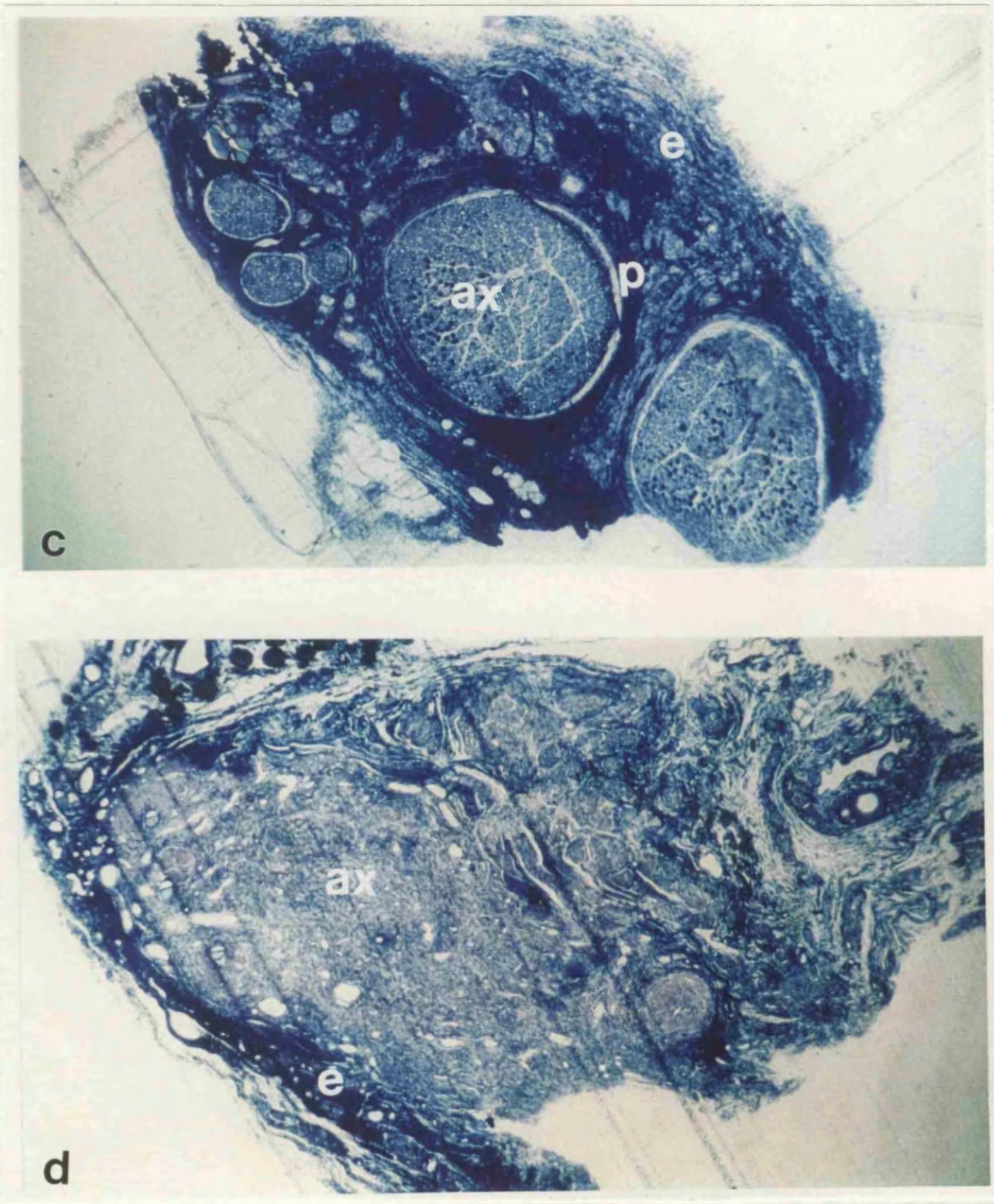

Figure 4.7. *(c) Fn+NGF and (d) Fn, stained with Toluidine Blue. Normal contralateral nerves appeared similar to that of nerve grafted injuries. Figures show axons organised into fascicles in animals grafted with nerve and Fn-NGF but little or no fascicular arrangement with plain Fn-mats. Scale bar in a = 50μm (same scale bar for b, c, and d).*

Figure 4.8. *Semi-thin longitudinal sections stained with toluidine blue of the centre of the graft. Micrographs show features of myelination from: (a) low and inset: high magnification of non injured (contralateral control); (b) low and inset: high magnification of nerve graft; (c) low and inset: high magnification of Fn+NGF; and (d) low and inset: high magnification of Fn-mat alone groups. Animals grafted with Fn+NGF had a similar regeneration pattern compared to animals grafted with nerves and Fn-mats alone. Scale bars in a, b, c and d = 100μm. Scale bars in inset to a, b, c and d = 40μm. Thick arrow shows original Fn-mat implant orientation. Arrowheads show myelinated axons.*

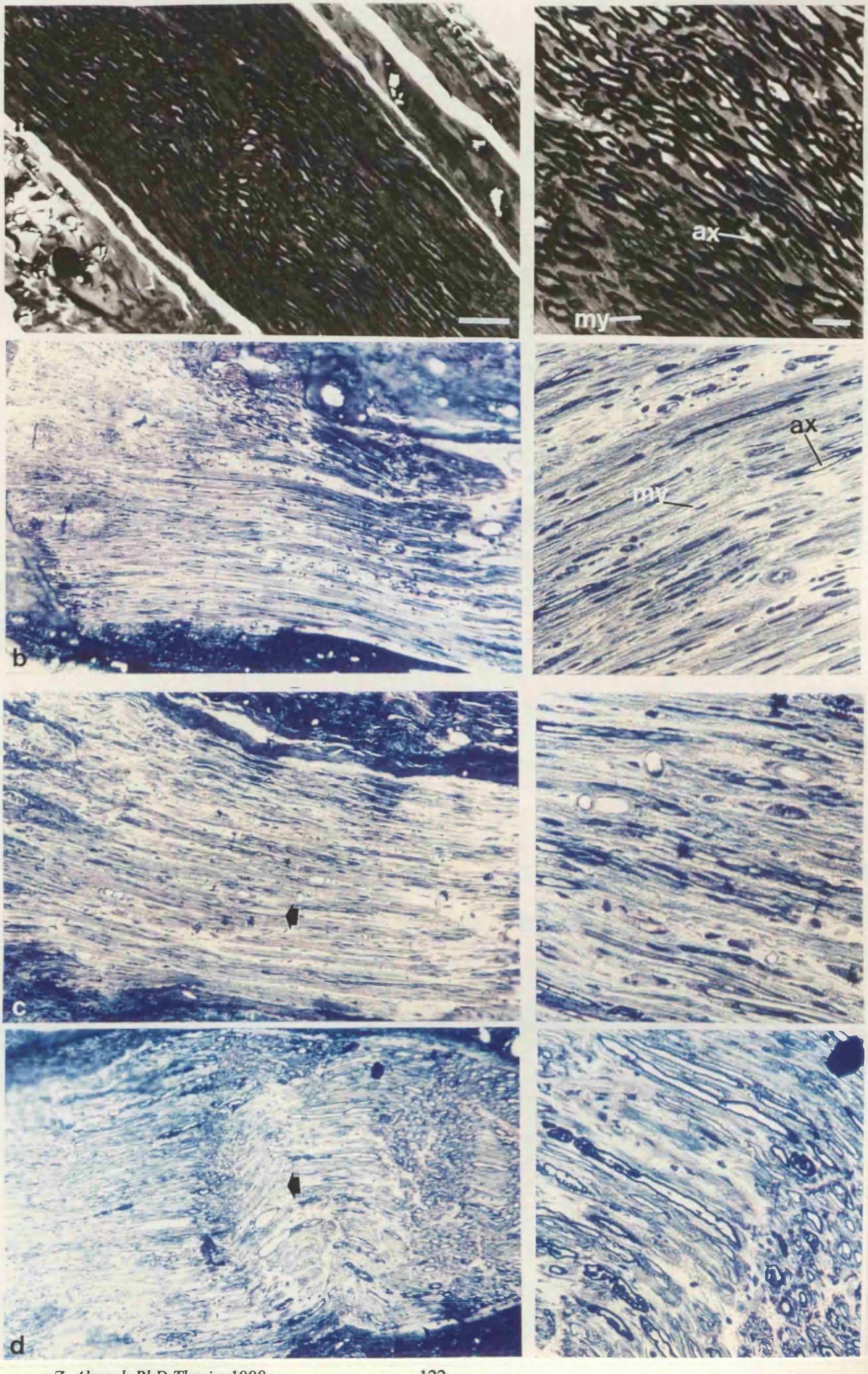
a
ax
my
b
ax
my
c
d

4.2.2. Myelinated fibre analysis

Semi-thin transverse sections showed that axons in animals grafted with Fn+NGF (Figure 4.9c) were larger in diameter and had thicker myelination than those grafted with Fn-mat alone (Figure 4.9d). Unoperated control nerves showed very similar axonal appearance to nerve grafted animals (Figure 4.9a and b). At the electron microscope level, transverse sections of contralateral controls (not shown) and nerve grafts (Figure 4.10a) showed thick myelinated axons surrounded by Schwann cells forming Schwann cell/axon units. Regenerates grafted with NGF impregnated Fn-mats were similar in appearance (Figure 4.10b) while plain Fn-mat grafts contained axons ensheathed by Schwann cells but myelination was thinner with more connective tissues (Figure 4.10c).

The results of myelinated fibre analysis 5mm distal to the graft site are shown in Table 4.2, Figure 4.11 and 4.12. Comparisons of myelinated fibre counts between grafts showed that animals grafted with Fn-mats alone had a significantly reduced number of axons when compared with Fn+NGF (ANOVA, Tukey test, $p<0.001$). There were no significant difference in the number of myelinated axons between control animals and animals grafted with nerve or Fn+NGF. The mean fascicular area of the distal radial nerve was significantly less in the nerve graft and Fn-mat alone groups compared to controls (ANOVA, Tukey test, $p<0.001$ control vs nerve graft and $p<0.001$ vs Fn alone), however there was no significant difference in mean fascicular area between un-operated control and the Fn+NGF group. In addition, the mean total fascicular area of

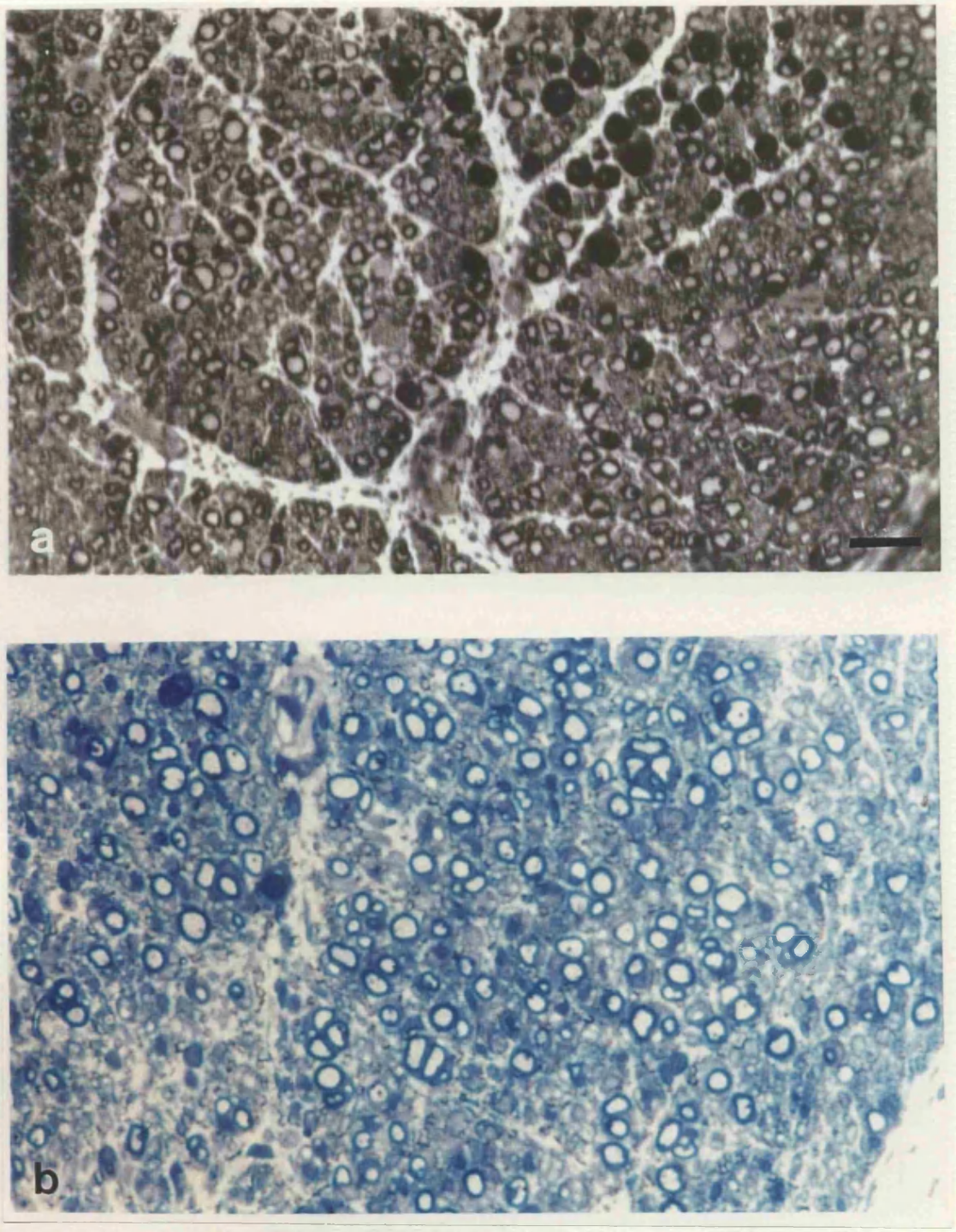

Figure 4.9. *Semi-thin transverse sections of nerves stained with toluidine blue. Sections from animals with (a) non injured (contralateral control) and grafted with (b) nerve graft.*

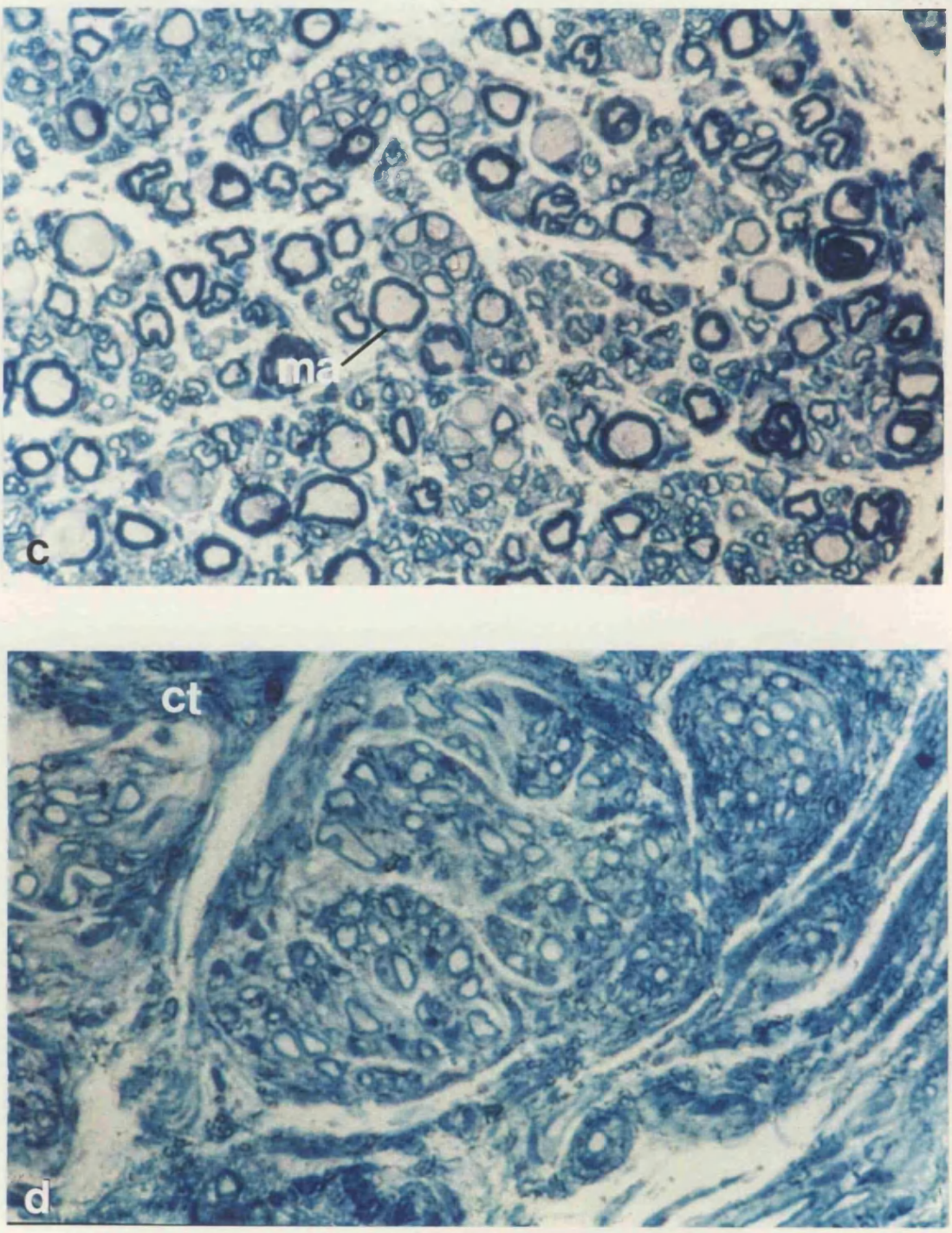

Figure 4.9. *(c) Fn+NGF and (d) Fn-mat alone. Animals grafted with Fn+NGF showed thicker myelination and larger axons when compared with nerve grafts or Fn-mat alone. Fn-mat alone had fewer axons in a similar field area. Scale bar in (a) = 20μm (same scale bar for b, c and d).*

Figure 4.10. *Transmission electron micrograph showing ultrastructure in the centre of the graft area in transverse sections. Micrographs show sections of (a) nerve grafts, (b) Fn+NGF and (c) Fn-mat only. Contralateral control was very similar in appearance to the nerve graft group (not shown). Evidence of some large axons in the Fn-mat+NGF group with thick myelination while neighbouring axons were less myelinated. Scale bars same in all micrographs = 5μm.*

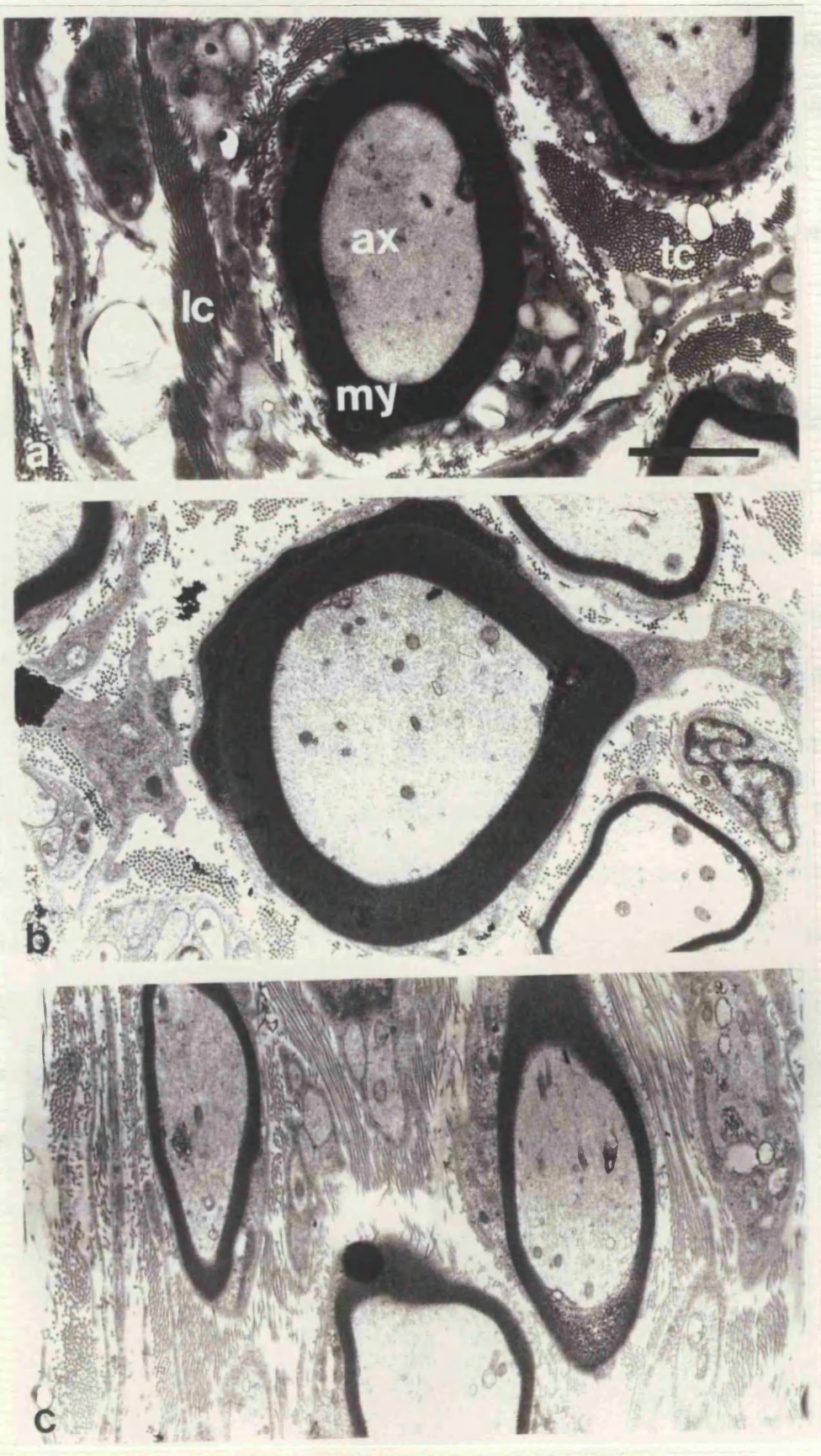
ax
lc
tc
my
a
b
c

the Fn+NGF group was significantly greater than that of the Fn-mat alone group (ANOVA, Tukey test, $p<0.001$). The estimated total number of myelinated fibres in the distal radial nerve was calculated from the above parameters and like count/field this showed a significant increase in Fn+NGF grafts compared to Fn-mat grafts (ANOVA, Tukey test, $p<0.001$). However, there was no significant difference between Fn+NGF, nerve grafts and control animal groups.

The frequency distribution of axonal diameters in the distal radial nerve is shown in Figure 4.11. The normal nerve exhibited a uni-modal, non-normal distribution over a range of 2-14μm with the major peak at 10μm. In nerves distal to the repair sites for all experimental groups axonal diameter was in a uni-modal, non normal distribution with the nerve graft and Fn groups having a comparable range of 2-12μm with peak frequency at 10μm (nerve graft) and 8μm (plain Fn-mat group). Plain Fn-mat group showed a significant shift towards smaller axons when compared to the un-operated control group (ANOVA, Dunnett's method, $p<0.05$), though the nerve graft group showed no significant difference when compared to uninjured controls. However, the NGF+Fn-mat group showed a distribution over an extended range (2-19μm) with a peak frequency of 17μm indicating a shift towards larger axons when compared to controls (ANOVA, Dunnett's method, $p<0.001$).

	Unoperated control	Nerve graft	Fn+NGF	Fn-mat
Mean axon counts/field	162 (7)	160 (10)	177* (12)	120 (6)
Mean total fascicular area in mm^2	1.892 (0.027)	1.800 (0.057)	1.896* (0.060)	1.803 (0.050)
Estimated total fibre count	14,050 (907)	13,000 (427)	13,015* (590)	6,100 (605)
Median axonal diameter in μm (25th-75th centiles)	10.15 (8.75-11.25)	9.40 (8.12-10.75)	16.57** (15.52-17.30)	7.65 (6.62-8.75)
Median myelin thickness in μm (25th-75th centiles)	2.75 (2.25-3.12)	2.68 (2.15-3.27)	4.28*** (3.75-4.78)	2.15 (1.75-2.47)
Median G-ratio (25th-75th centiles)	0.62 (0.43-0.72)	0.61 (0.47-0.67)	0.63* (0.49-0.71)	0.55 (0.41-0.61)

Table 4.2. *Myelinated fibre analysis-results at 4 months. Myelinated fibre counts and fascicular areas are given as the mean measurements and (± SEM) from 3 frames per nerve. Axonal diameter, myelin thickness and G-ratio were non-normally distributed and values are accordingly given as median (25^{th}-75^{th} centiles). * $p<0.001$ for Fn-NGF vs Fn, ANOVA. ** $p<0.001$ for Fn-NGF vs control. *** $p<0.001$ for Fn-NGF vs normal, ANOVA.*

Figure 4.11. *The size distribution of regenerated myelinated axons. Size distribution for: (a) contralateral control, following regeneration at four months with (b) nerve graft (c) NGF impregnated and (d) plain Fn-mat. The local delivery of NGF significantly increased the size of regenerated myelinated axons compared to contralateral controls ($p<0.001$, ANOVA).*

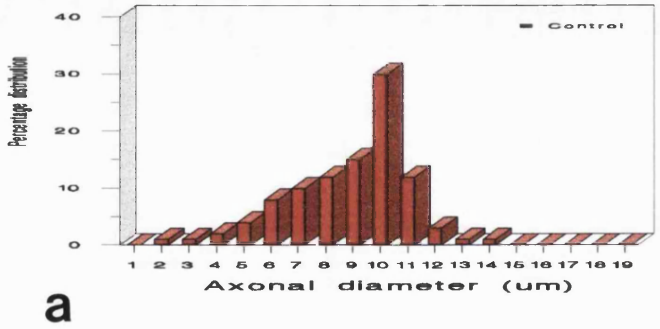
Control
Percentage distribution
0
10
20
30
40
1 2 3 4 5 6 7 8 9 10 11 12 13 14 15 16 17 18 19
Axonal diameter (um)

a

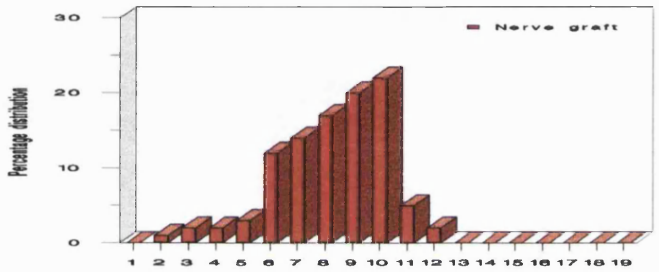
Nerve graft
Percentage distribution
0
10
20
30
1 2 3 4 5 6 7 8 9 10 11 12 13 14 15 16 17 18 19

b

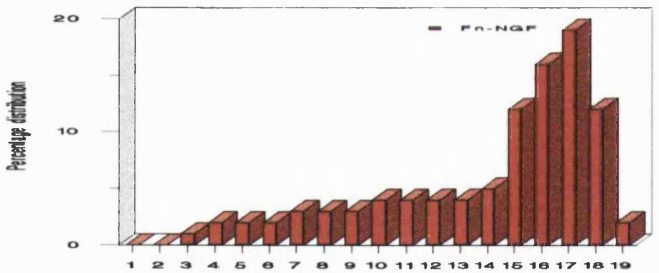
Fn-NGF
Percentage distribution
0
10
20
1 2 3 4 5 6 7 8 9 10 11 12 13 14 15 16 17 18 19

c

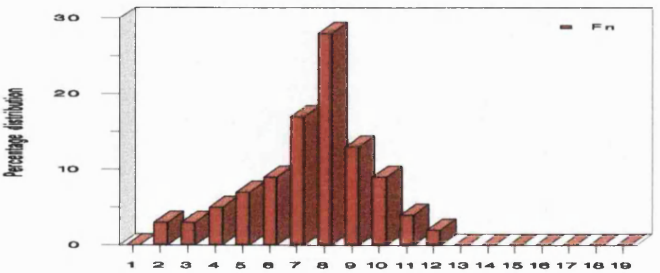
Fn
Percentage distribution
0
10
20
30
1 2 3 4 5 6 7 8 9 10 11 12 13 14 15 16 17 18 19

d

The myelin thickness of regenerated fibres for the Fn+NGF group was significantly greater than that of the Fn-mat, nerve graft and control groups (ANOVA, Dunnett's method, $p<0.001$ vs nerve graft and controls; $p<0.001$ vs Fn-mat alone) (Table 4.2). There was significantly greater thickness in myelin in animals grafted with nerve graft and controls when compared to plain Fn-mats (ANOVA, Dunnett's method, $p<0.001$). The G-ratio quotient, which described the relationship between axon calibre and myelinated fibre calibre for myelinated axons (G-ratio = axonal diameter/myelinated fibre diameter) was non-normally distributed in each group (Table 4.2). There was no significant difference in the median G-ratio between the control, nerve graft and Fn+NGF group however, the Fn-mat group had significantly smaller G-ratio compared to the other experimental groups (ANOVA, Dunnett's method, $p<0.001$). Graphical representation of axonal diameter vs G-ratio shows that for all experimental groups, G-ratio increased as axonal diameter increased (Figure 4.12). However, the Fn+NGF group extends to a greater G-ratio of 0.79 when axonal diameter was 19μm.

4.2.3. Connective tissue regeneration

Semi-thin sections stained with toluidine blue showed that in all experimental animal grafts, a new epineurial sheath had formed throughout the graft area which was visibly organised along the same axis as the regenerating axons (Figure 4.13a: typical epineurial organisation). The ultrastructural appearance of the epineurial sheath in all experimental groups showed a dense network of fibroblasts set in a matrix of collagen fibrils (Figure 4.13b), however in the Fn-mat alone group there was evidence of more connective tissue.

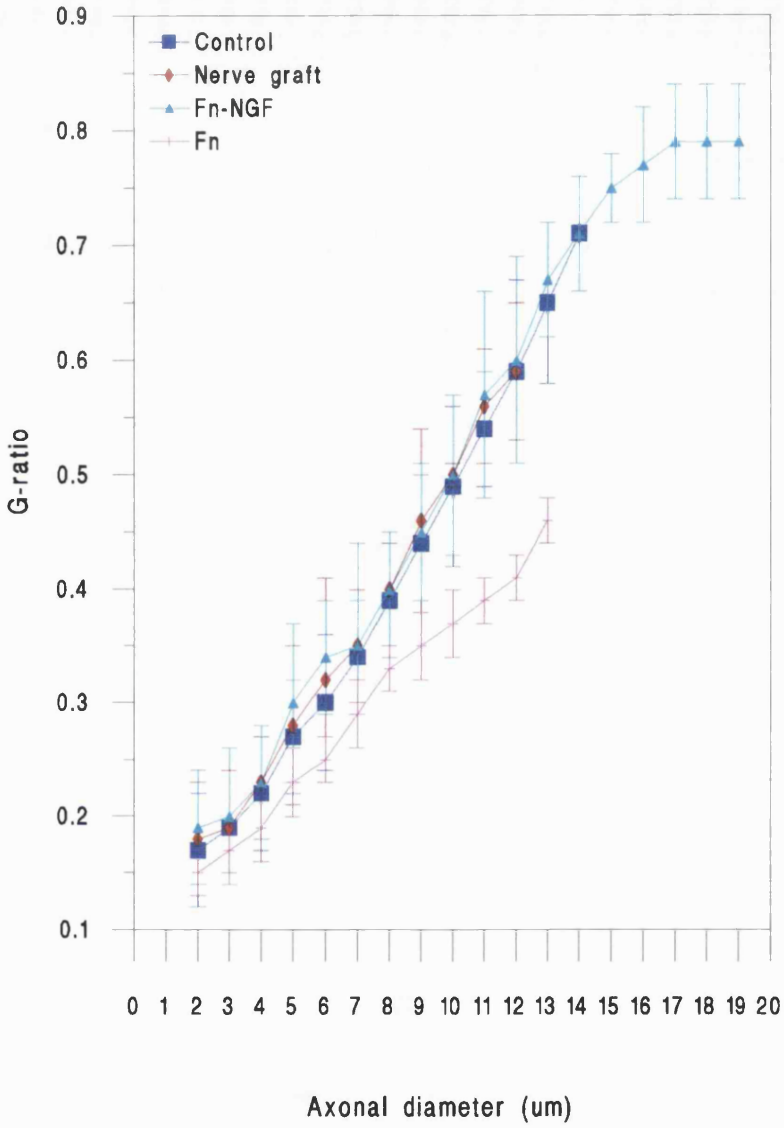

Figure 4.12. *G-ratio of normal and regenerated fibres in relation to axon diameter at 4 months post-operatively. The graph demonstrates a non-linear relationship of G-ratio and axonal diameter and shows that it is maintained throughout regeneration. Application of NGF significantly increased the G-ratio ($p<0.05$, ANOVA) of axons with a diameter above 10 μm, when compared to plain Fn-mat but there was no significant difference between control and animals grafted with nerve of Fn-NGF conduits.*

The collagen fibrils in all groups were clearly organised into bundles some of which were orientated parallel to the axis of the regenerating nerve and some circumferentially around the new tissue (Figure 4.13c). The fibrils were symmetrical and regularly arranged within the bundles. At higher magnification in cross-section, each fibril was composed of a large number of smaller, spherical cross-sectional elements which were linked by small interconnecting processes between individual fibrils (Figure 4.13d). The appearance and ultrastructure of the epineurial sheath and collagen fibrils were exactly the same in animals grafted with autologous nerves. Regenerated collagen fibril diameter in all experimental groups ranged from 40-80nm in diameter and the means from each experimental group was not significantly different. (Mean collagen fibril diameter in: unoperated control= 67 ± 7 nm, nerve graft= 65 ± 4 nm, Fn-mat+NGF= 68 ± 5 nm and Fn-mat alone= 64 ± 7 nm).

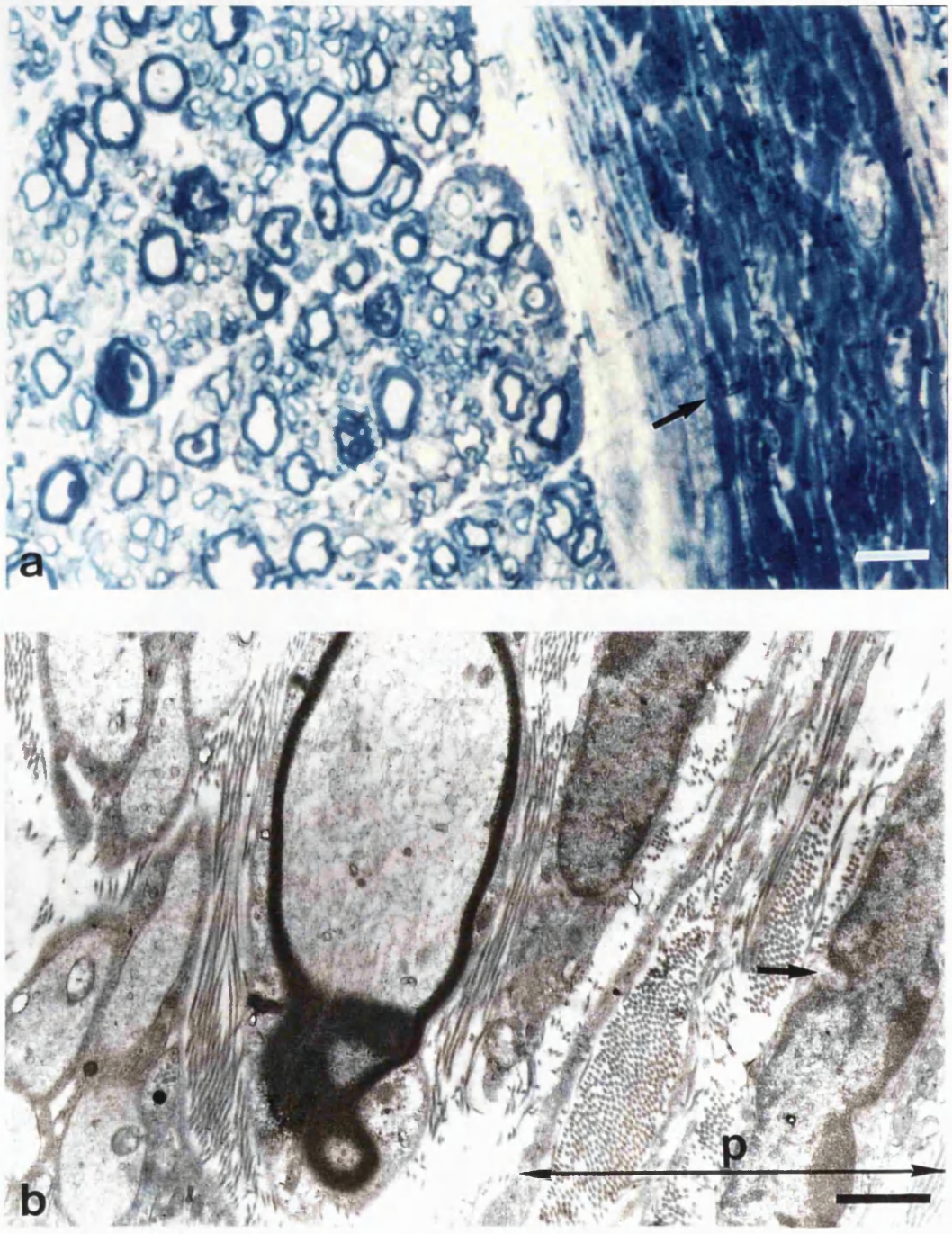

Figure 4.13. *Appearance of regenerated connective tissues. (a) Semi-thin transverse section of a typical epineurium stained with toluidine blue. The arrow shows the dense layers of fibroblasts orientated along the axis of the regenerating axons. (b) shows ultrastructure of the orientated epineurium and aligned fibroblasts within, as indicated by the arrow.*

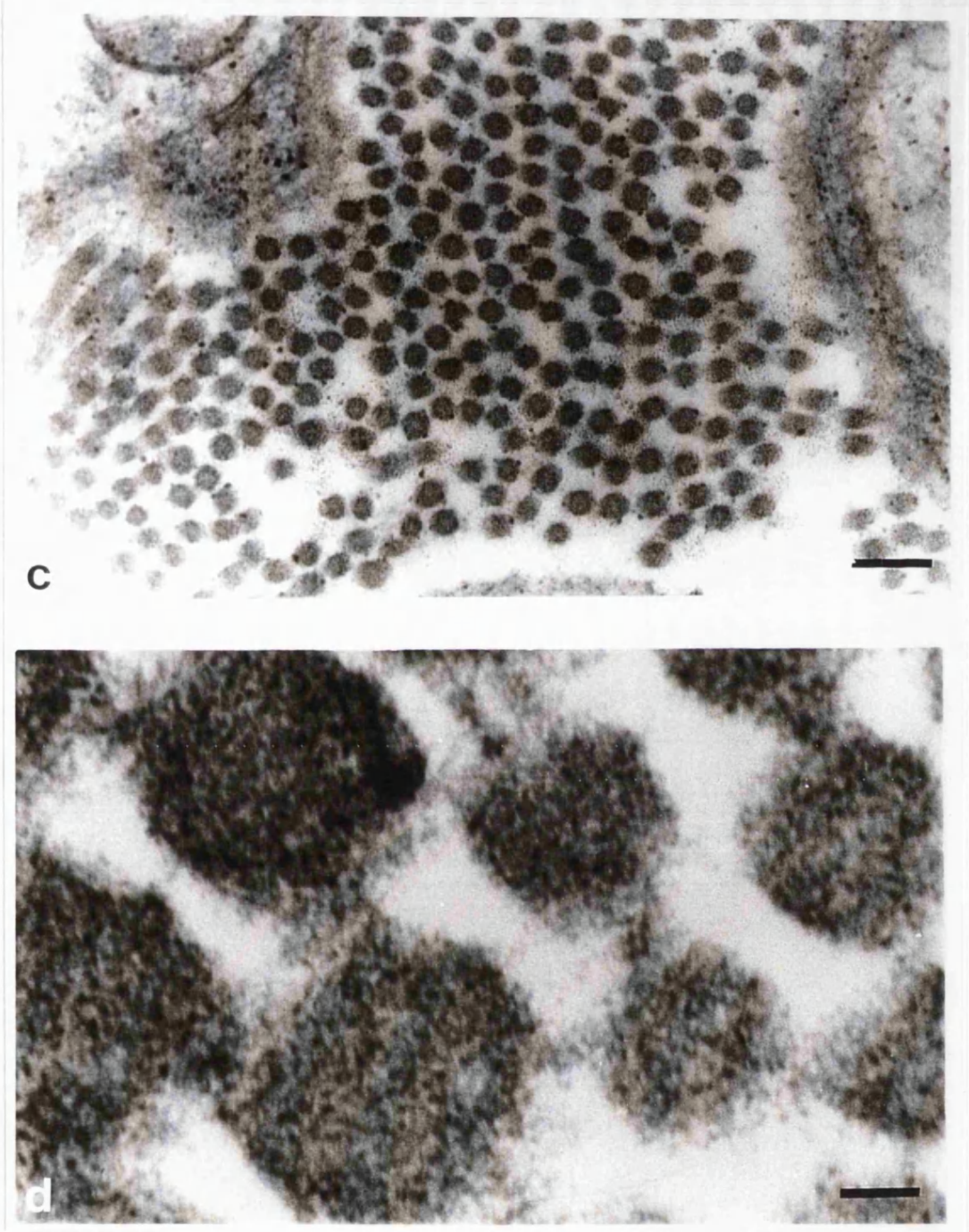

Figure 4.13. *(c) Collagen fibre ultrastructure cut in transverse sections and (d) high-power electron micrograph of collagen showing individual fibrils within the collagen fibre. Scale bars in: (a) = 20μm, (b) 2.5μm, (c) 160 nm and (d) 20 nm.*

These results showed that Fn-mats were suitable conduits to promote contact guided repair of axons since parallel, myelinated fibres were observed. Addition of NGF, improved the quality of the regenerate and increased the size of myelinated axons while improving the quality of the connective tissue regeneration within the graft area. These results support the use of Fn-mats in peripheral nerve regeneration.

4.3. Large Cables of Fibronectin Designed for Tissue Engineering and Implants for Long Peripheral Nerve Lesions

Currently, Fn-mat production is laborious, unpredictable and size limited in the sense that mats can be made with dimensions of 2 × 1 cm. The aim here was to devise a long nerve conduit from fibronectin which would contain all the benefits (contact guidance, fibrillar orientation, cell adhesion surface, hygroscopic and pockets for cell infiltration) of Fn-mats but not be limited to size. An additional benefit would be to grow Schwann cells already aligned within cable materials which can then be transplanted to the injured nerve thereby improving nerve repair and support regeneration of axons over a longer distance. The structure of cables was investigated by scanning electron microscopy and light microscopy. Hygroscopicity, fibrillar orientation and behaviour of cultured cells was also investigated.

4.3.1. Production of LFn-cables

Large cables of Fn (LFn-cables) were formed reproducibly, typically between 2-15 mm in diameter. Once formed, rinsed in distilled water and freeze-dried, LFn-cables retained their high length : diameter ratio, which would be required for use in nerve repair (Figure 4.14) although freeze dried samples were less than half the original

diameter. Samples which were air dried were more compact in structure with a macroscopic glassy appearance (not shown).

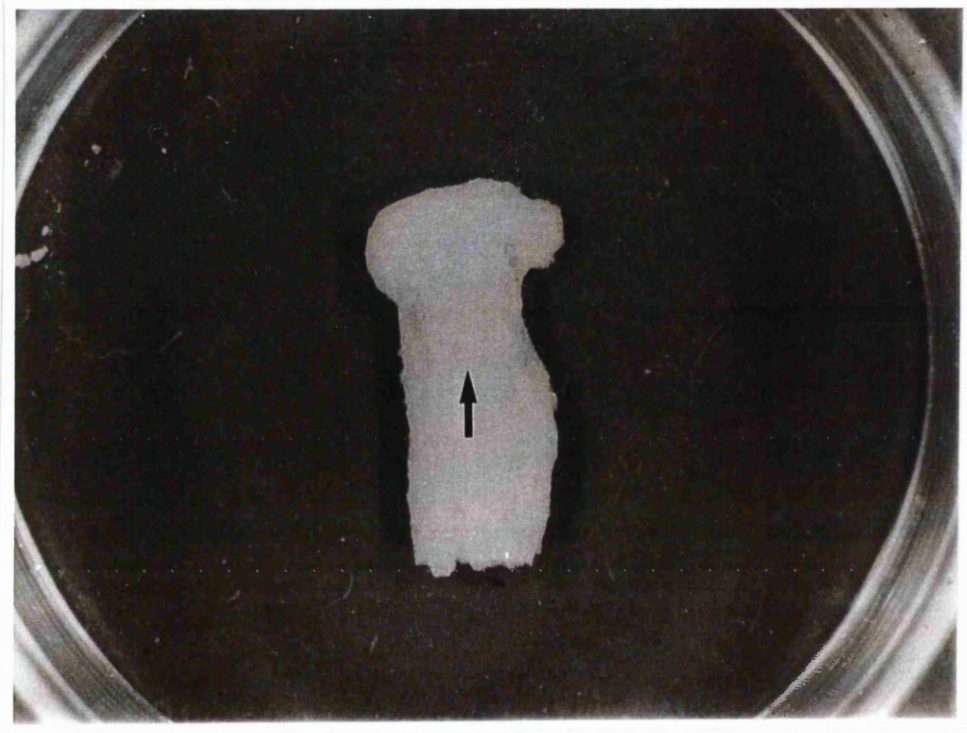

Figure 4.14. *Macroscopic features of freeze dried LFn-cable. The orientation of the fibrils is indicated by the arrow. Dish size = 10.4 cm.*

4.3.2. Scanning electron microscopy

Scanning electron microscopy of air dried specimens of LFn-cables (Figure 4.15a) revealed a non-fibrous dense surface structure dissimilar to the Fn-mats which are composed of many fibres which range from 2-7μm in diameter (Ejim et al, 1993), however, the overall orientation of the cable can be seen in figure 4.15a. The cross sectional surface had many small pores throughout the whole area which measured between 2-3 μm in diameter (Figure 4.15b). In contrast, surface structure of freeze-

dried samples showed a predominant orientation throughout the cable (Figure 4.15c), with a more porous structure comparable to that of freeze dried Fn-mats reported earlier (Ejim et al., 1993; Brown et al., 1994; Brown et al., 1997). Cross-sectional structure of these LFn-cables confirmed their porous nature with pore sizes between 50-100 μm in diameter (Figure 4.15d). However, density of fibre packing was variable across the cross sectional surface leading to local differences in porosity.

4.3.3. Histology of LFn-cables and Fn-mats

Longitudinal sections of freshly prepared LFn-cables revealed a predominant fibril orientation comparable to that of rolled Fn-mats. However, some areas of LFn-cables were more dense than others (Figure 4.16a). The Fn-mat however, showed a much more uniform structure with overall fibril orientation throughout (Figure 4.16b).

Cross sectional structure of Fn-mats (Figure 4.17b and d) showed a more uniform porosity of fibres compared to LFn-cables (Figure 4.17a and c). Within LFn-cables pore sizes ranged from 1-100μm in diameter due to variation in fibril density throughout LFn- cables. Samples of LFn-cables which were freeze dried and subsequently fully hydrated differed from the structure of freshly extruded fibres in that there was a much more uniform pore size throughout the cross (Figure 4.18a) and transverse (Figure 4.18b) sectional areas. Pore sizes in cross section were typically 50-100μm in diameter.

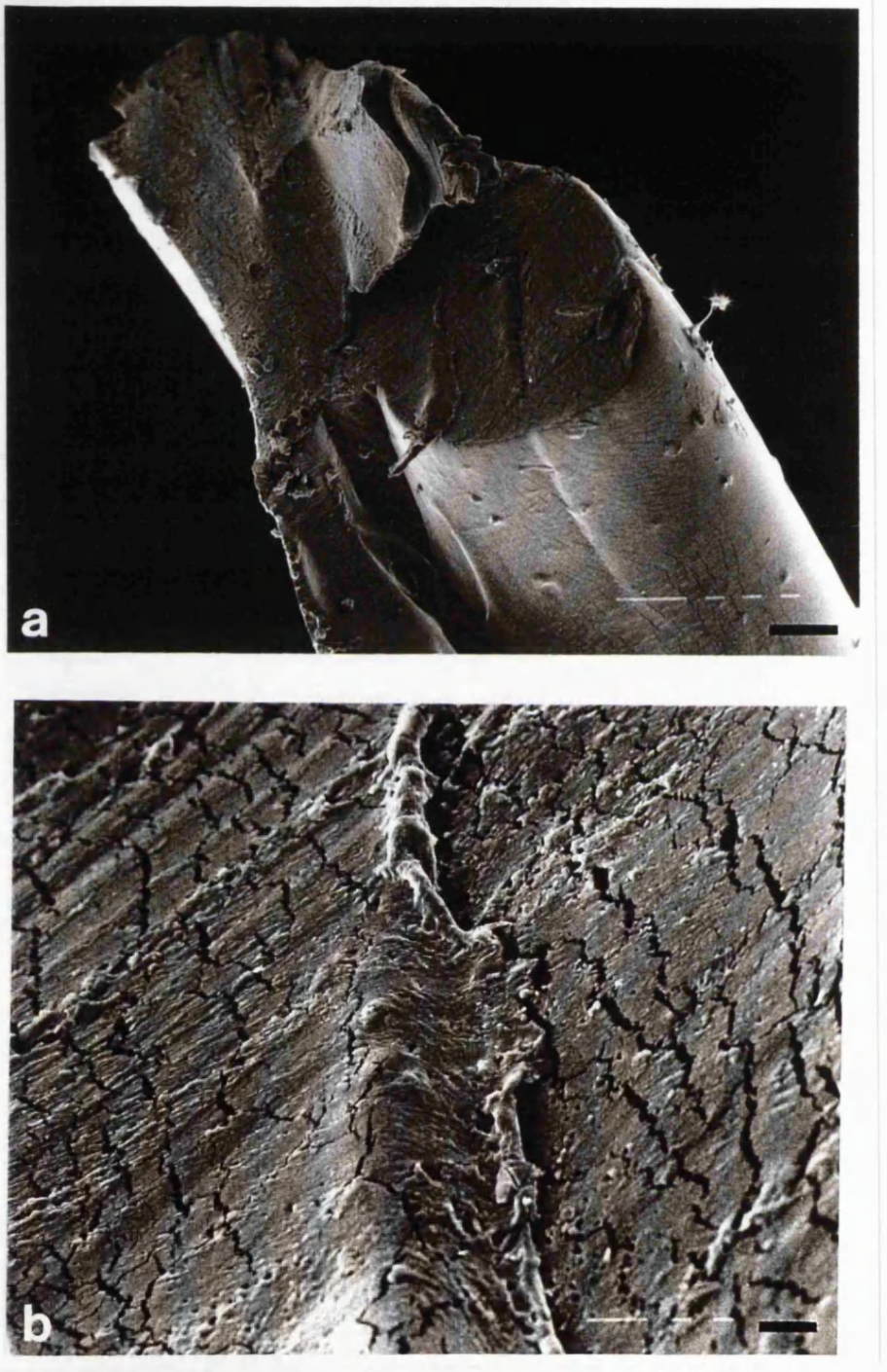

Figure 4.15. *Scanning electron microscopy of LFn-cables. SEM's of* ***(a)*** *longitudinal and* ***(b)*** *cross-sectional surfaces of air dried. Air dried samples appeared dense, with minimal porosity and non-fibrillar structure compared to freeze dried fibres which resemble the surface features of Fn-mats described earlier (Ejim et al., 1993).*

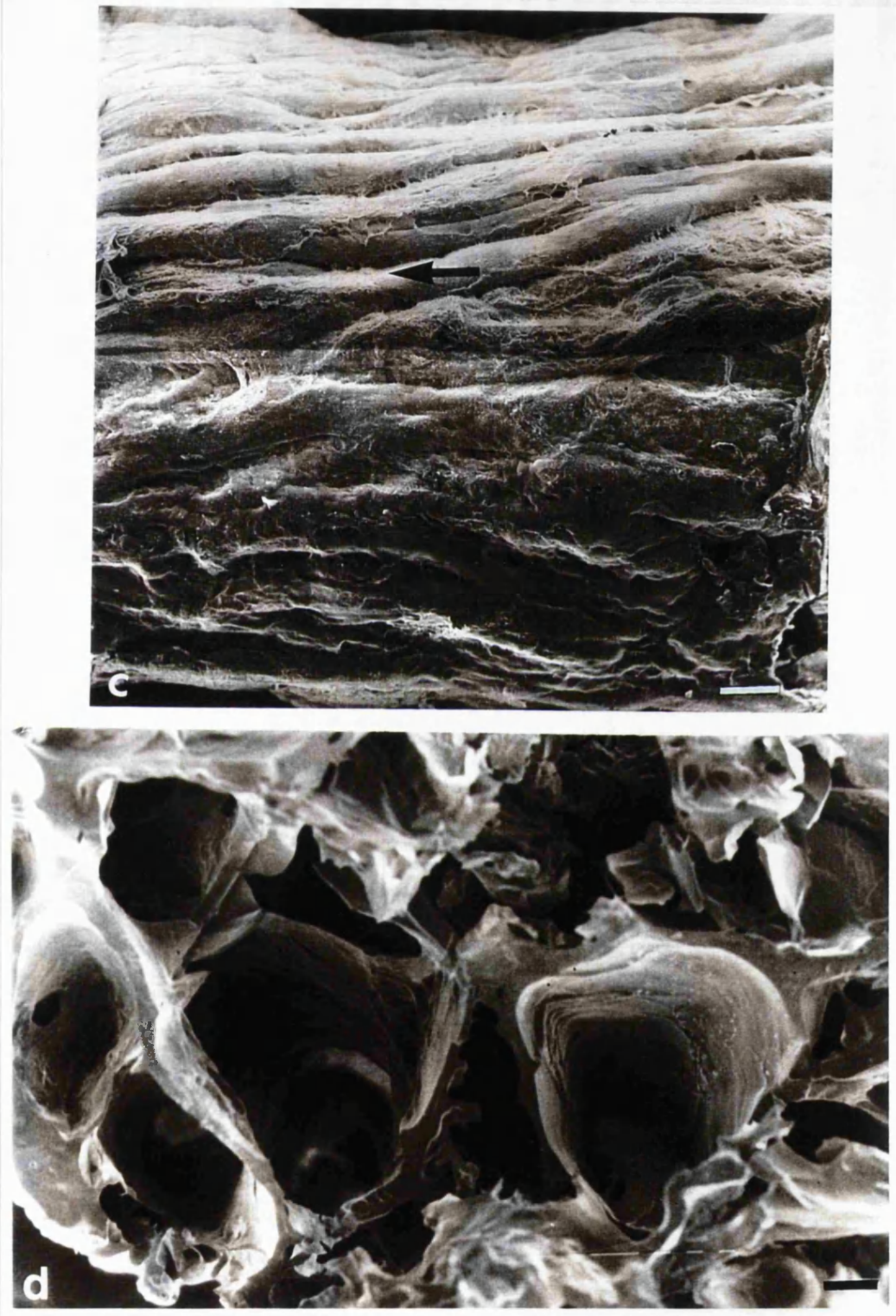

Figure 4.15. *SEM of* **(c)** *longitudinal and* **(d)** *cross sectional surfaces of freeze dried LFn-cables. Note the fibrous alignment indicated by the arrow in freeze dried specimens (c). Scale bars in (a) and (c) = 100 μm; (b) and (d) = 10 μm.*

Figure 4.16. *Histology of LFn-cables. Longitudinal histological section stained with H&E of* ***(a)*** *a freshly made (non freeze dried) LFn-cable showing a predominant fibre orientation parallel to the axis of the cable (arrow) with variable pore sizes compared with* ***(b)*** *Fn-mat, which has a more uniform structure (fibril axis shown by arrow). Scale bars in (a) and (b) = 50μm.*

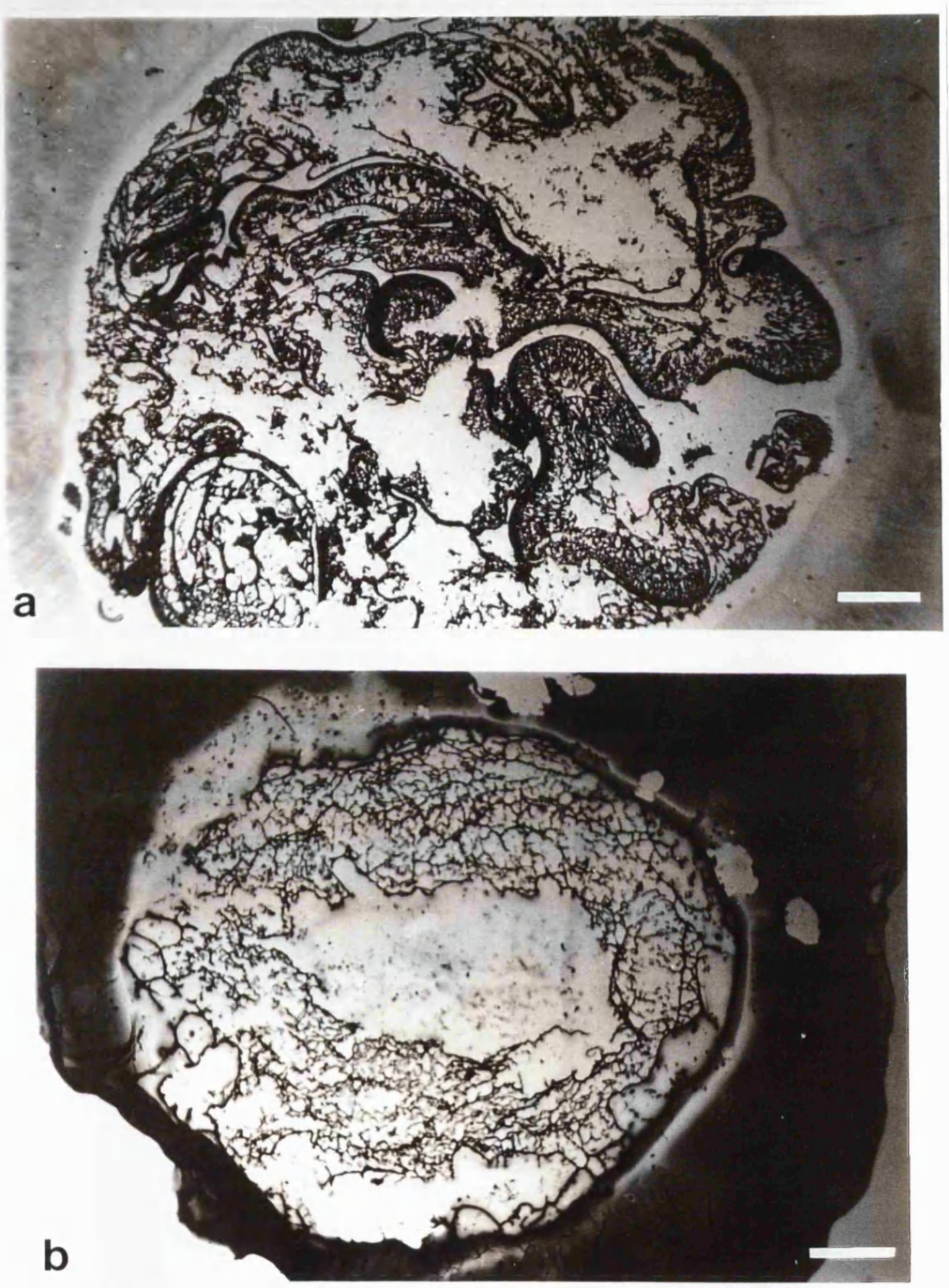

Figure 4.17. *Histology of LFn-cables. Transverse histological section of* ***(a)*** *freshly made LFn-cable and* ***(b)*** *rolled Fn-mat showing general structure, diameter and heterogeneity of cables when compared to rolled Fn-mats.*

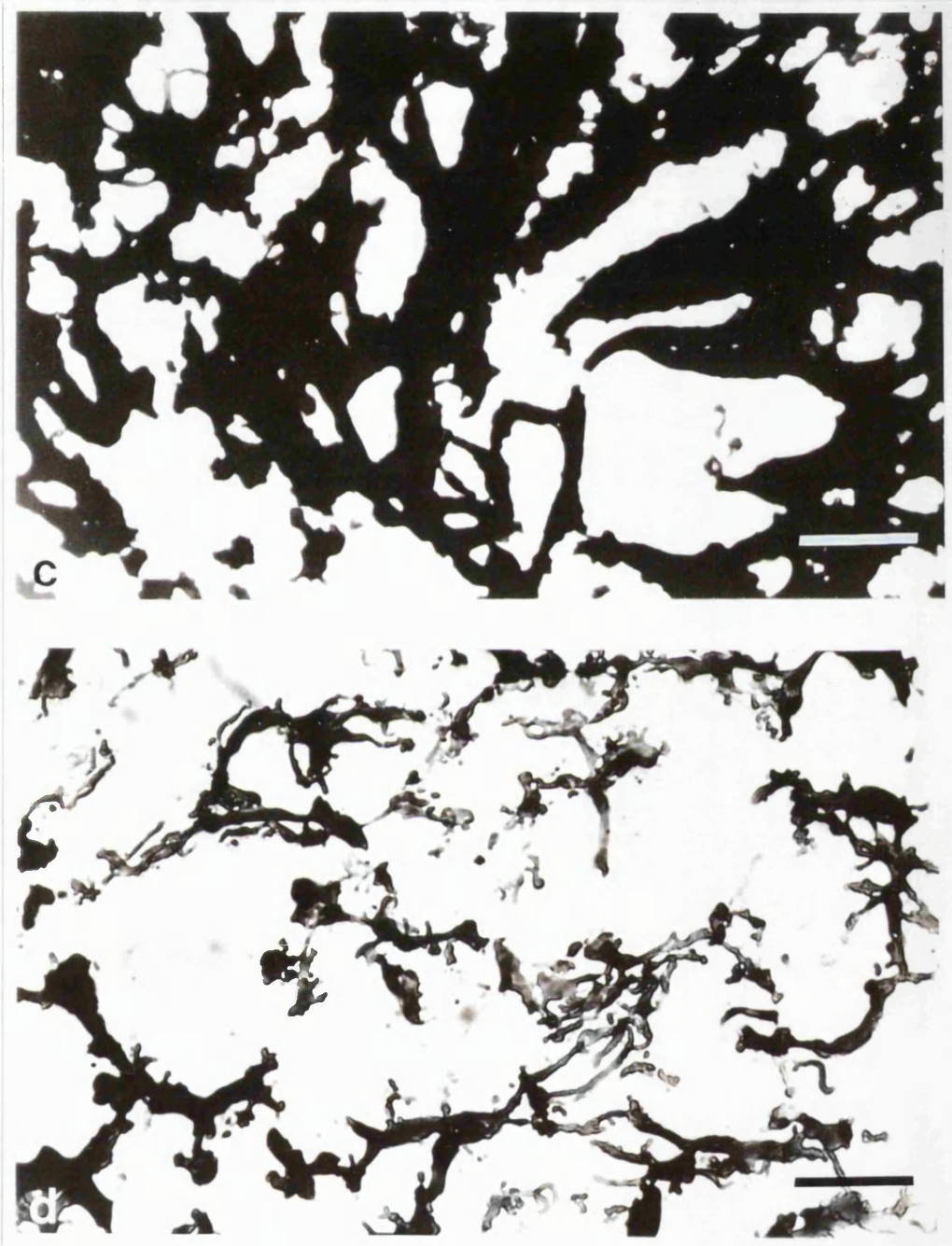

Figure 4.17. *(c) and* ***(d)*** *show detailed structures of LFn-cable and Fn-mat, respectively, revealing the difference in pore sizes. Pore sizes typically measure between 1-100μm (mean = 37μm) in diameter in LFn-cables and 40-120μm (mean = 64μm) in Fn-mat, however, LFn-cables generally have denser aggregates of fibres than Fn-mats. Scale bars in (a) and (b) = 0.5 mm; (c) and (d) = 50 μm.*

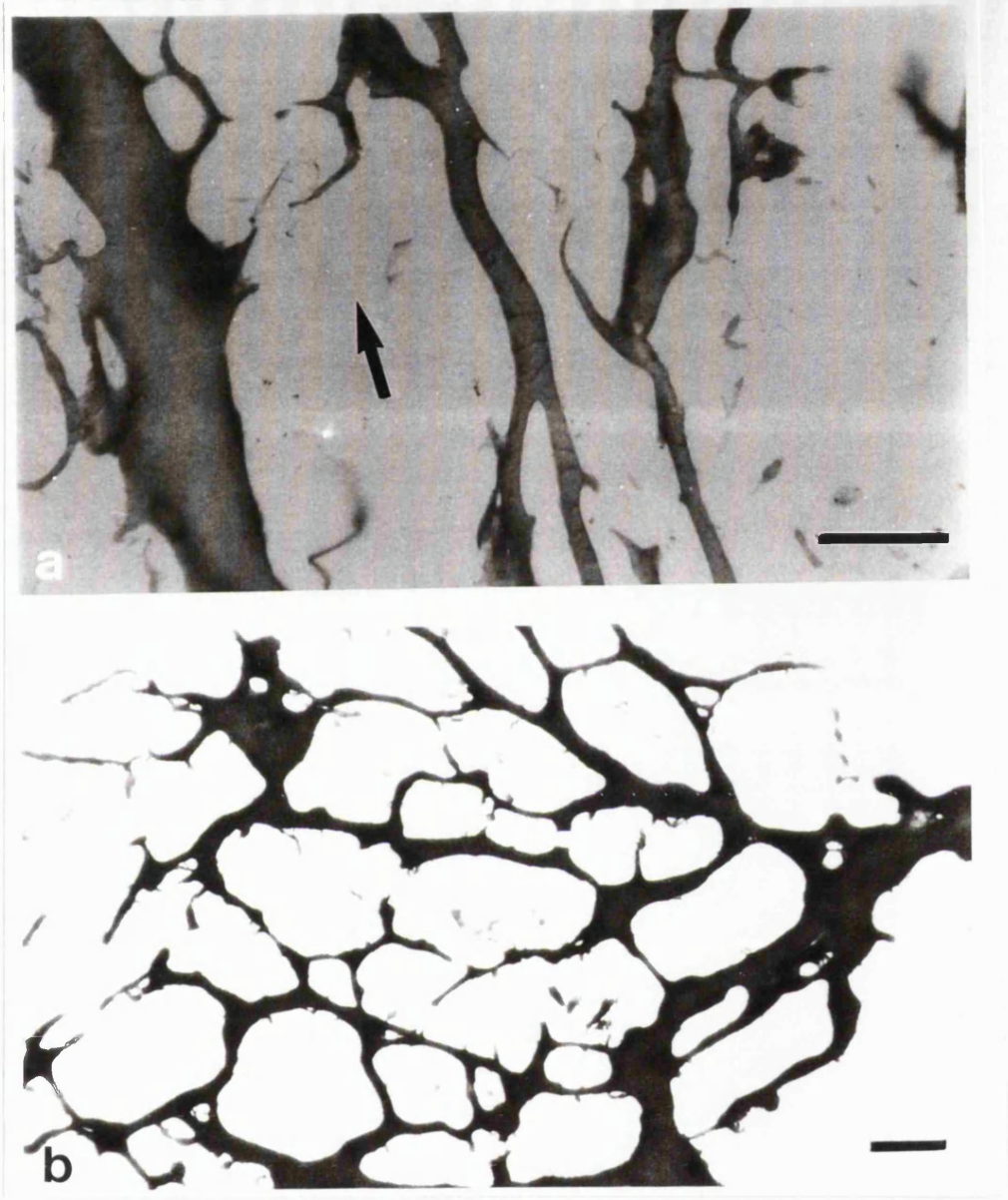

Figure 4.18. *Histology of freeze dried cable.* ***(a)*** *and* ***(b)*** *show longitudinal and transverse histological sections, stained with Haematoxylin and Eosin respectively, of a freshly made cable which has been freeze dried and then fully hydrated for 40 minutes in distilled water. Cables which have been freeze dried and hydrated show a reduction in densely packed regions such that they appear comparable to the cross-sectional appearance of Fn-mats (c.f. figure 4(d)) and retain an overall orientation (direction shown by arrow). Pore sizes now typically measure between 50-100μm in diameter. Scale bar in (a) and (b) = 25 μm.*

4.3.4. Fibre orientation analysis

The results of the distribution of fibre orientation analysis are shown in figure 4.19. 86% of the fibres had an orientation index of between 1 to 0.90. This equates to orientation in degrees as between 0 (i.e. parallel alignment) to 12.5 degrees from the reference line. Less orientation within the cable was exhibited by 14% of fibres with indexes ranging from 0.89 to a minimum of 0.75 (13.5 to 20.5 degrees from parallel). There were a relatively few cross fibres (<1%) which had orientation values between 30 and 120 degrees (disregarded in figure 4.19).

4.3.5. Re-hydration properties of LFn-cables

Both LFn-cables and rolled Fn-mats swelled rapidly increasing in diameter by 250 and 80%, respectively. Rolled Fn-mats swelled to a maximum surface area, weight and cross-sectional diameter after 20 minutes in PBS at 37°C, whereas LFn-cables reached maximum swelling after 35 minutes (Figure 4.20a-d). By the end of 40 minutes LFn-cables had swelled to 1.6, 4.8, 9 and 6.5 times their original length, cross-sectional diameter, total surface area and weight, respectively, compared to rolled Fn-mats which swelled to 1, 1.7, 5.4 and 1.8 times their original dimensions.

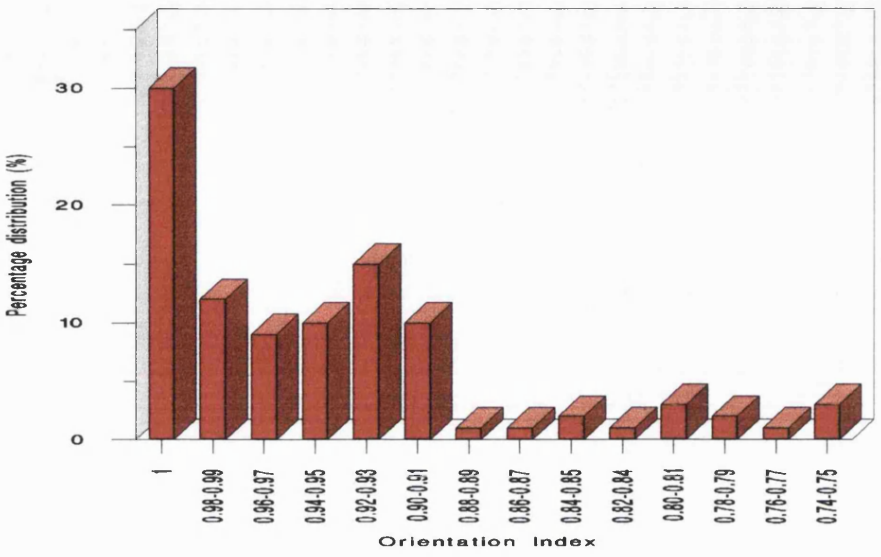

Figure 4.19. *Percentage distribution of fibril orientation within LFn-cables. An S value of 1 indicates parallel fibril orientation whereas an S value of 0 indicates random fibril orientation.*

4.3.6. Cell Culture with LFn-cables

When human dermal fibroblasts and SC's were cultured for 2 weeks on LFn-cables, cells which were attached to the plastic culture dish were orientated parallel to the axis of the LFn-cable at each of its cut ends and were apparently migrating into the ends of the fibres (Figure 4.21a, human dermal fibroblasts and 4.21b, Schwann cells). Cells also docked along side the fibrils and became oriented parallel with the axis of the fibre presumably by contact guidance (not shown). Longitudinal sections of dermal fibroblasts cultured with LFn-cables showed that cells interacted with the Fn-fibre to take on an elongated bipolar morphology (Figure 4.21c and inset). Similarly Schwann cells were being guided by the Fn-fibre and cells adopted a migratory bipolar phenotype (Figure 4.21d and inset).

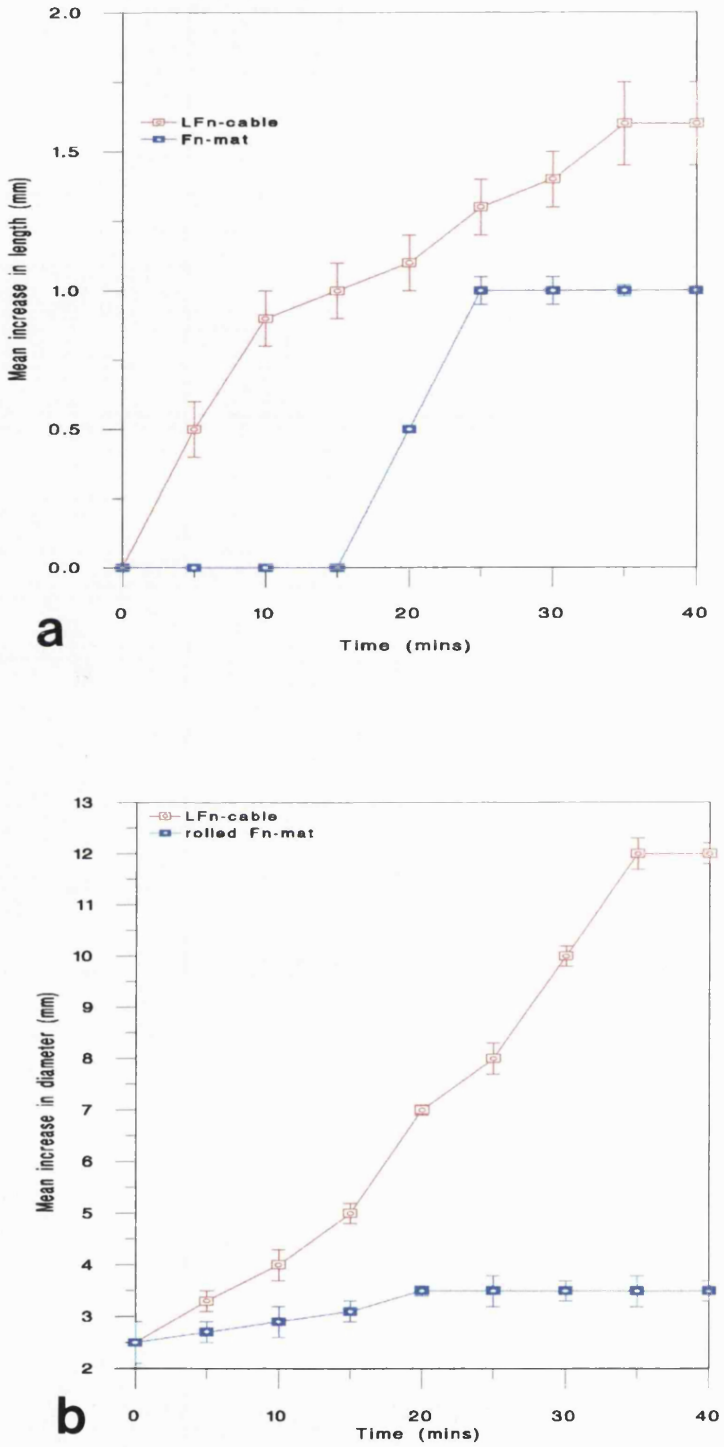

Figure 4.20. *Changes in dimensions following rehydration. Graphs showing the mean increase (+SD) in* ***(a)*** *length,* ***(b)*** *diameter.*

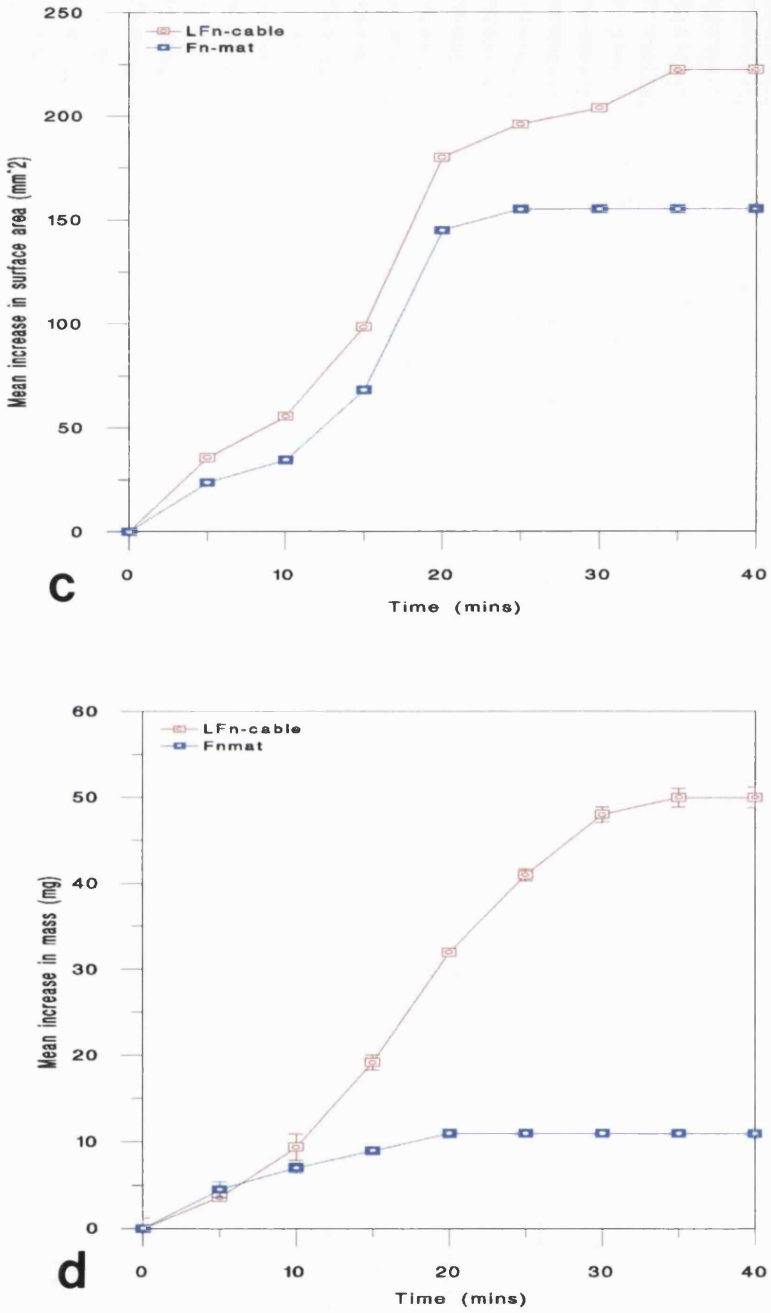

Figure 4.20. *Graphs showing mean increase in (±SD)* ***(c)*** *surface area and* ***(d)*** *weight upon rehydration of LFn-cables in PBS over time. (Initial dimensions of both rolled Fn-mats and LFn-cables were: length = 5 mm; diameter = 2.5 mm; surface area = 28.2 mm^2 and weight = 9 mg, n=10).*

Figure 4.21. *Cell culture on LFn-cables.* ***(a)*** *Human dermal fibroblasts and* ***(b)*** *Schwann cells became aligned in culture with the axis of the fibrils within the cable (axis of fibre indicated by the arrow) at one end of the cut cable. Human dermal fibroblasts and Schwann cells appeared to line up in the culture dish with the axis of the fibrils and migrate into the cable. Longitudinal histological sections of cells grown on LFn-cables stained with H&E showed fibroblasts* ***(c)*** *and Schwann cells* ***(d)****, within these cables. Cells were aligned parallel with the axis (arrows) and attached to the fibrils within cables (aligned nucleus indicated with arrowheads). Scale bars in (a) and (b) = 250 μm; (c) and (d) = 25 μm.*

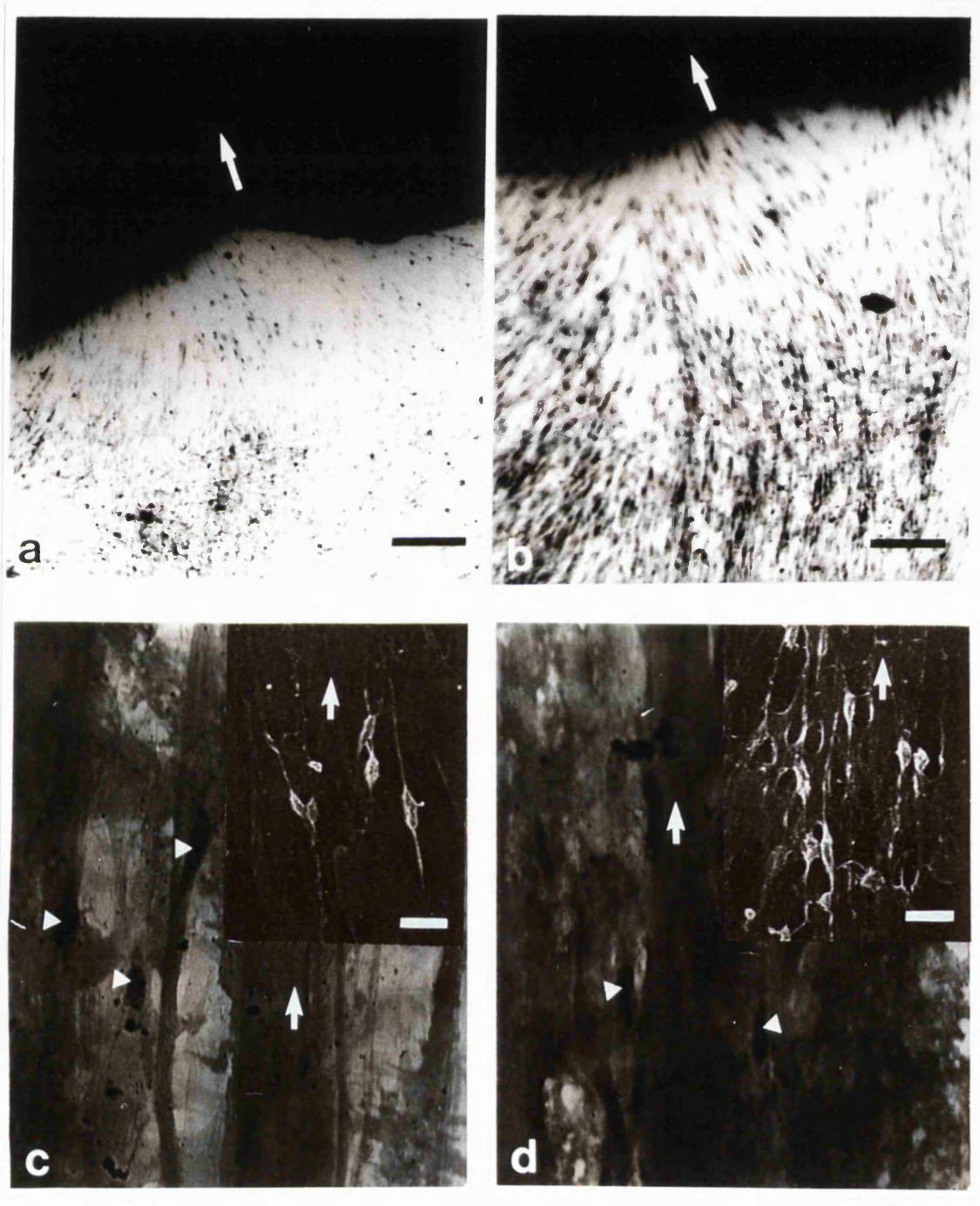
a
b
c
d

The results from this experiment showed that cables can be made that are between 0.2-1.5 cm in diameter and 1-14 cm long. These cables have fibrillar orientation and pore sizes to allow for infiltration of cells. Cables were extremely hygroscopic in nature which would be beneficial to adsorb greater amounts of neurotrophins which may support greater amounts of cell survival and regeneration. Cells may be grown within these cables which align parallel to the fibre axis and represents a suitable material to transplant between long nerve gaps and may be used to make other tubular grafts.

4.4. Copper stabilisation of large cables of fibronectin: cell substrate properties

4.4.1. Copper stabilisation of LFn-cables

Cables may be susceptible to rapid degradation once in vivo and in vitro, similarly to Fn-mats. Here the aim was to use copper (and zinc) ions to stabilise these cables for longer survival. Stability of cables was measured over a period of time and scanning electron and light microscopy was used to analyse cross-linking of fibres. Additionally, the increase in cell proliferation seen with Fn-mats may be beneficial in terms of transplanting cultured Schwann cells to the site of injury. For this reason, cell counts were performed to establish if a similar response to that seen with Fn-mats could be repeated.

Copper and zinc treated LFn-cables were more stable at 37°C than untreated fibres in PBS over a period of 15 days. 1 μM copper treated LFn-cables were stabilised by 1-1.5× control mats (Figure 4.22). Increasing concentrations of copper stabilised these fibres further in a dose dependent manner such that using 200 μM copper, the cables were stable with no dissolution of protein upto day 7. At day 8 only 3% of the total

protein dissolved at this concentration of copper. Incorporation of zinc resulted in a very similar profile of stabilisation as copper (Figure 4.22). However, copper and zinc together lead to a more stabilised structure causing less dissolution of protein when compared to copper and zinc ions alone (Figure 4.22).

4.4.2. Scanning electron microscopy

Once cables were stabilised with copper, cross-linking occurred between adjacent fibres, in cross-sectional surfaces of cables, such that the whole structure became more compact with low concentrations of copper. The pores in 1μM copper treated cables were reduced in size when compared to control cables treated in distilled water (Figure 4.23a). Further cross linking occurred in a dose dependent manner such that cables treated with 10, 100 and 200μM copper cross-linked adjacent fibres and left larger and larger pores in the centre of the cable while the outer regions became more densely packed (Figure 4.23b, c and d). No differences in cable structure in its longitudinal surface could be seen from that of control cables due to the density of fibre packing (Figure 4.24a and b).

Addition of zinc and Copper/Zinc to LFn-cables results in a very similar appearance (not shown).

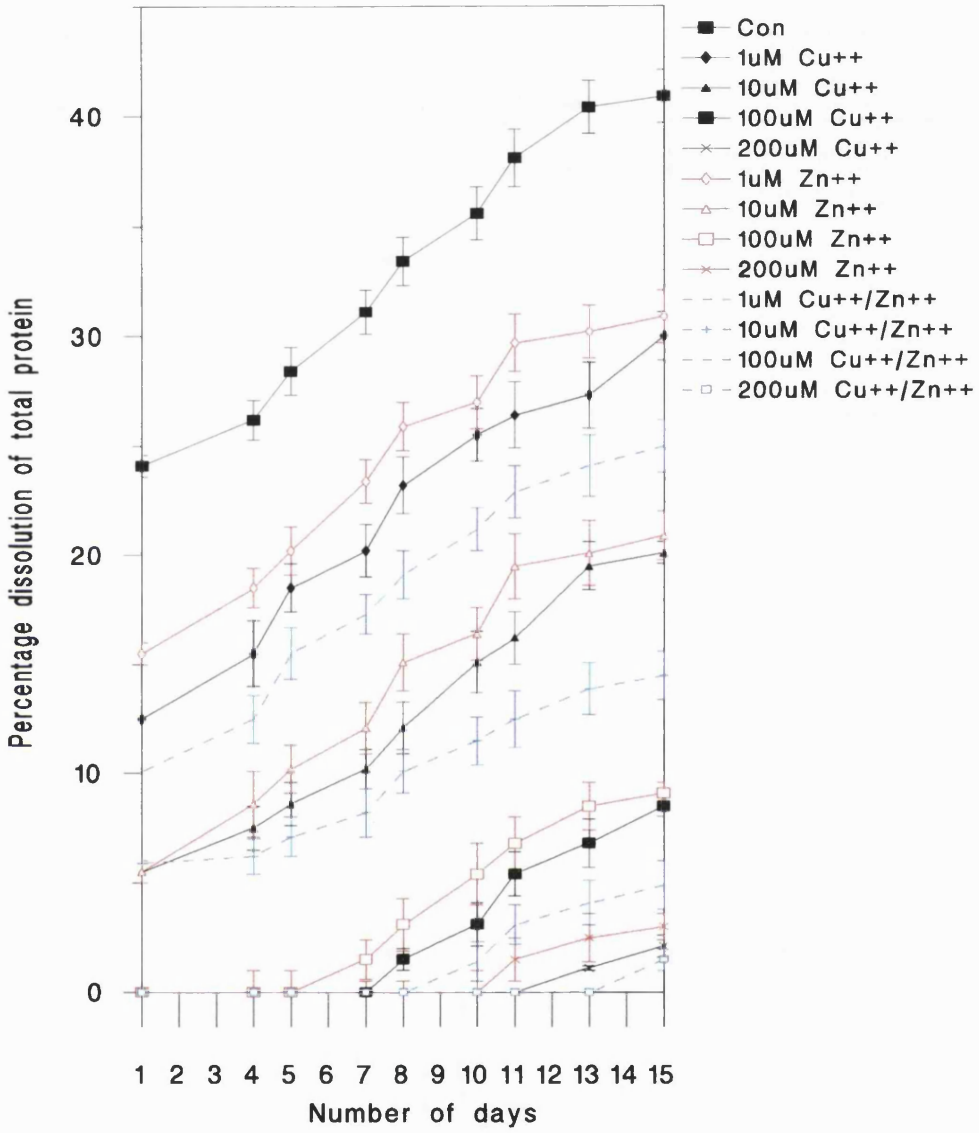

Figure 4.22. *Dissolution of Fn protein from copper and zinc treated LFn-cables at 37°C. LFn-cables were approximately 1 to 1.5 × more stable when treated with copper or zinc, however, LFn-cables treated with equimolar concentrations of copper and zinc were approximately twice that of control cables.*

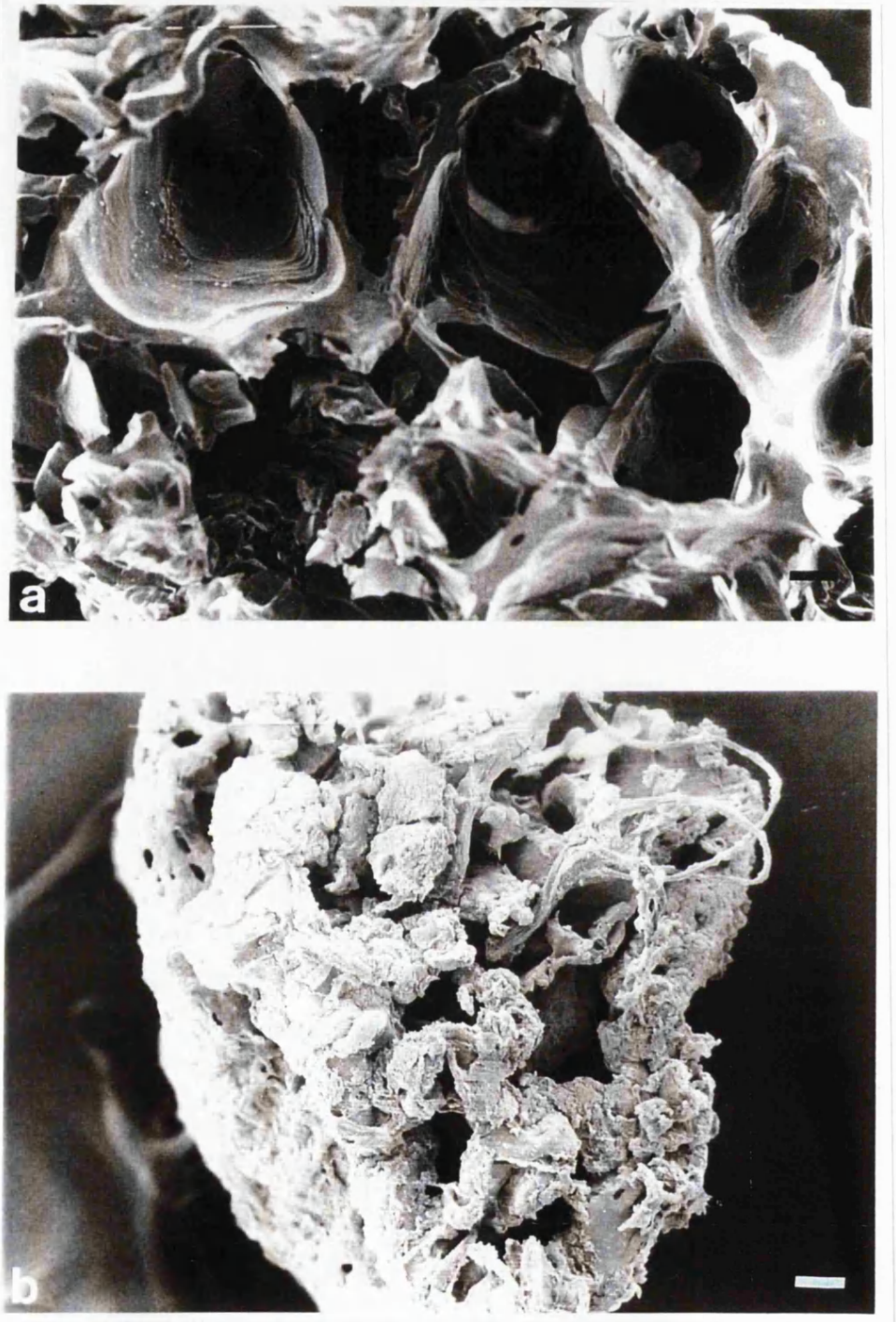

Figure 4.23. *Scanning electron micrographs of copper treated cables. SEM of the cross-section of (a) untreated and (b) 1μM Cu treated LFn-cables. After treatment with copper (similar structure with zinc), the fibres are cross-linked producing a reduction in pore size. Scale bar = 100μm.*

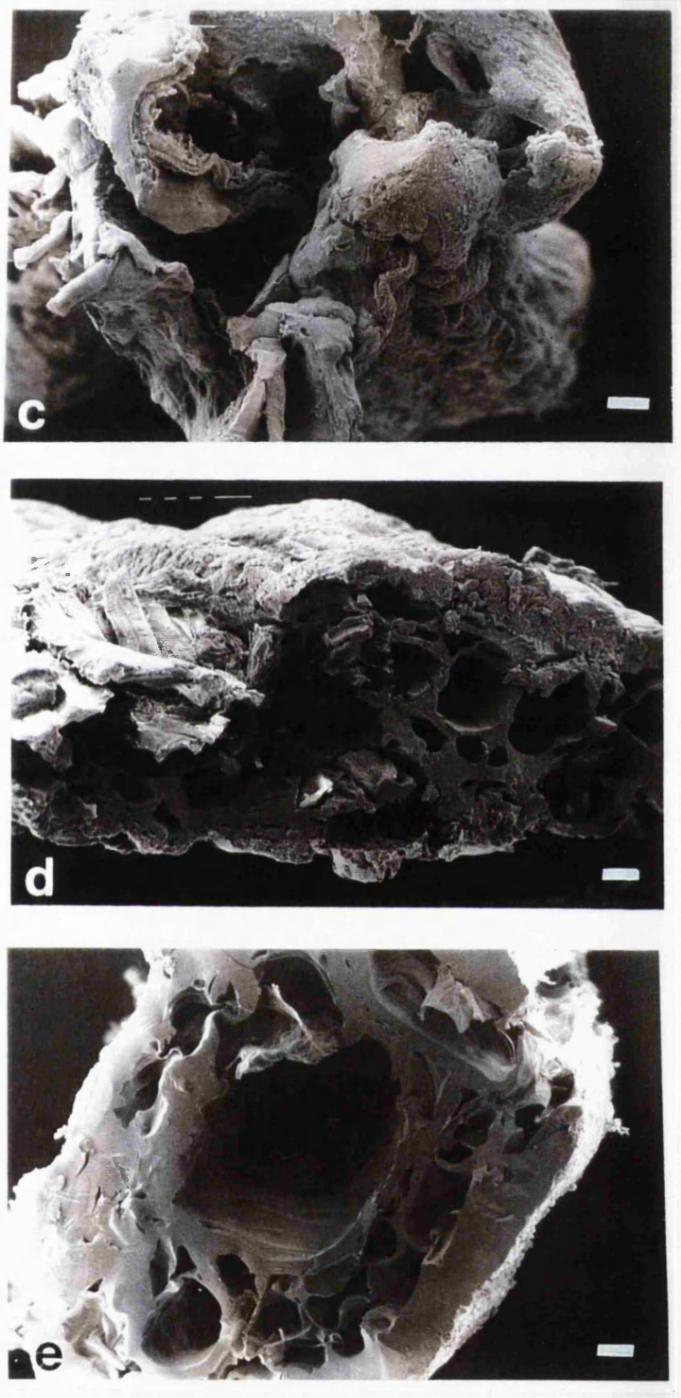

Figure 4.23. *Scanning electron micrographs of the cross-sectional surface of (c) 10 (d) 100 and (e) 200 μM treated LFn-cable. There was increased aggregation and collapse of the cable structure in a dose dependent manner such that cables treated with 200μM copper have a dense structure around the outer surface with large pores in the centre of the cable. Scale bar =100 μm.*

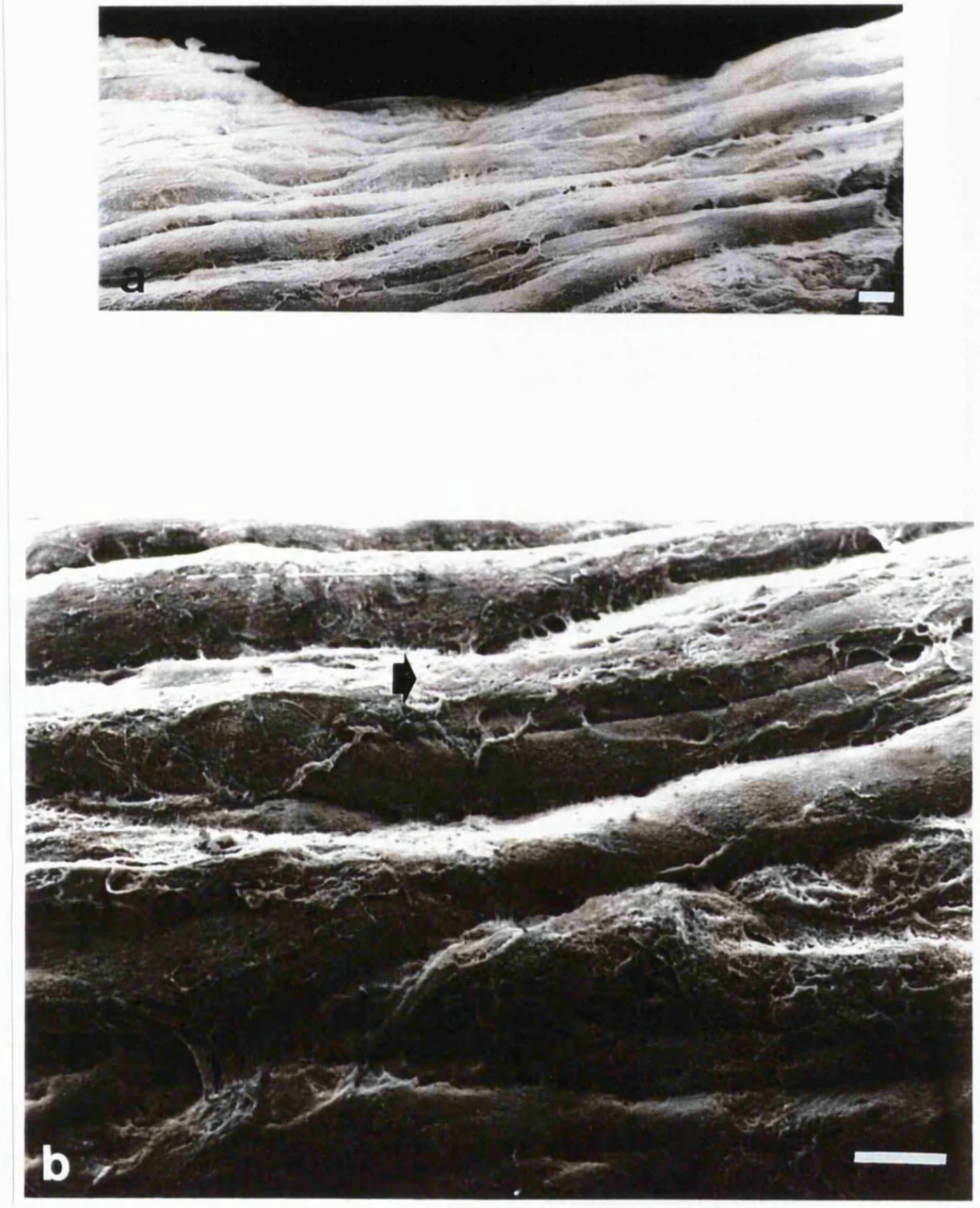

Figure 4.24. *Scanning electron microscopy of the longitudinal surface of copper stabilised LFn-cables. This shows very little difference in the structure from that of control cables. (a) low and (b) high power of freeze dried cables. Scale bar =100μm. Arrow shows longitudinal fibre orientation.*

4.4.3. Histology of treated LFn-cables

LFn-cables which were treated with 1-200μM copper, sectioned and stained toluidine blue showed a very similar appearance of cable structure as compared to the scanning electron micrographs (SEM's). The pore sizes reduced in size in a dose dependent manner with fibres densely packed around the edges (Figure 4.25a, b, c , d and e) as was observed by SEM.

4.4.4. Copper assay

The amount of copper and zinc that became incorporated into LFn-cables is shown in Table 4.3. Copper (also for zinc and copper/zinc) levels were undetectable by atomic absorption spectroscopy for 1 and 10 μM treatments. A more sensitive method is required to detect such low concentrations of copper ions which time did not permit for this thesis. Upon treatment of the cable with 100 and 200 μM copper, the mean amount bound to the cable was 17 and 30 nmole of Cu^{2+}/mg of Fn, respectively, while there was 20 and 34 nmoles in respective treatments of zinc. The amount of copper and zinc bound to cables with equimolar concentrations of copper and zinc at the 100 and 200μM treatment levels were, 15 nmoles of Cu/10 nmoles of zinc and 20 nmoles of Cu /and 19 nmoles of zinc, respectively.

4.4.5. Cell culture on LFn-cables

The mean total number of human dermal, rat tail and rat tendon fibroblasts recovered from copper, zinc and copper/zinc treated cables after 3 weeks in culture was not significantly different in all these cell populations (Figure 4.26a, b and c). However, the mean total number of Schwann cells recovered from 1μM treated cables was

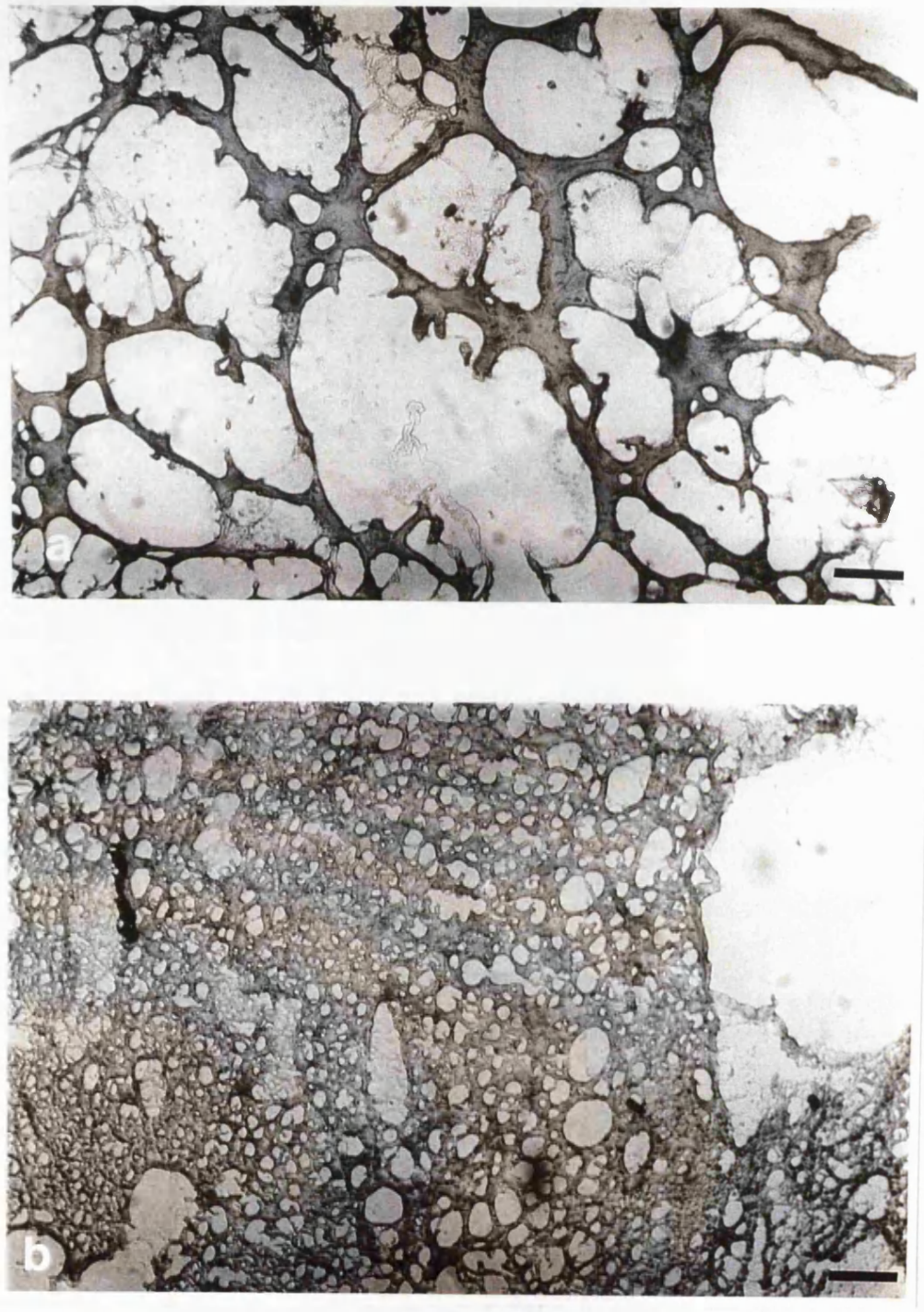

Figure 4.25. *Histology of copper treated cables stained with toluidine blue. (a) untreated; (b) 1μM copper treated cables. Increased aggregation of fibres can be seen with the copper treated cable.*

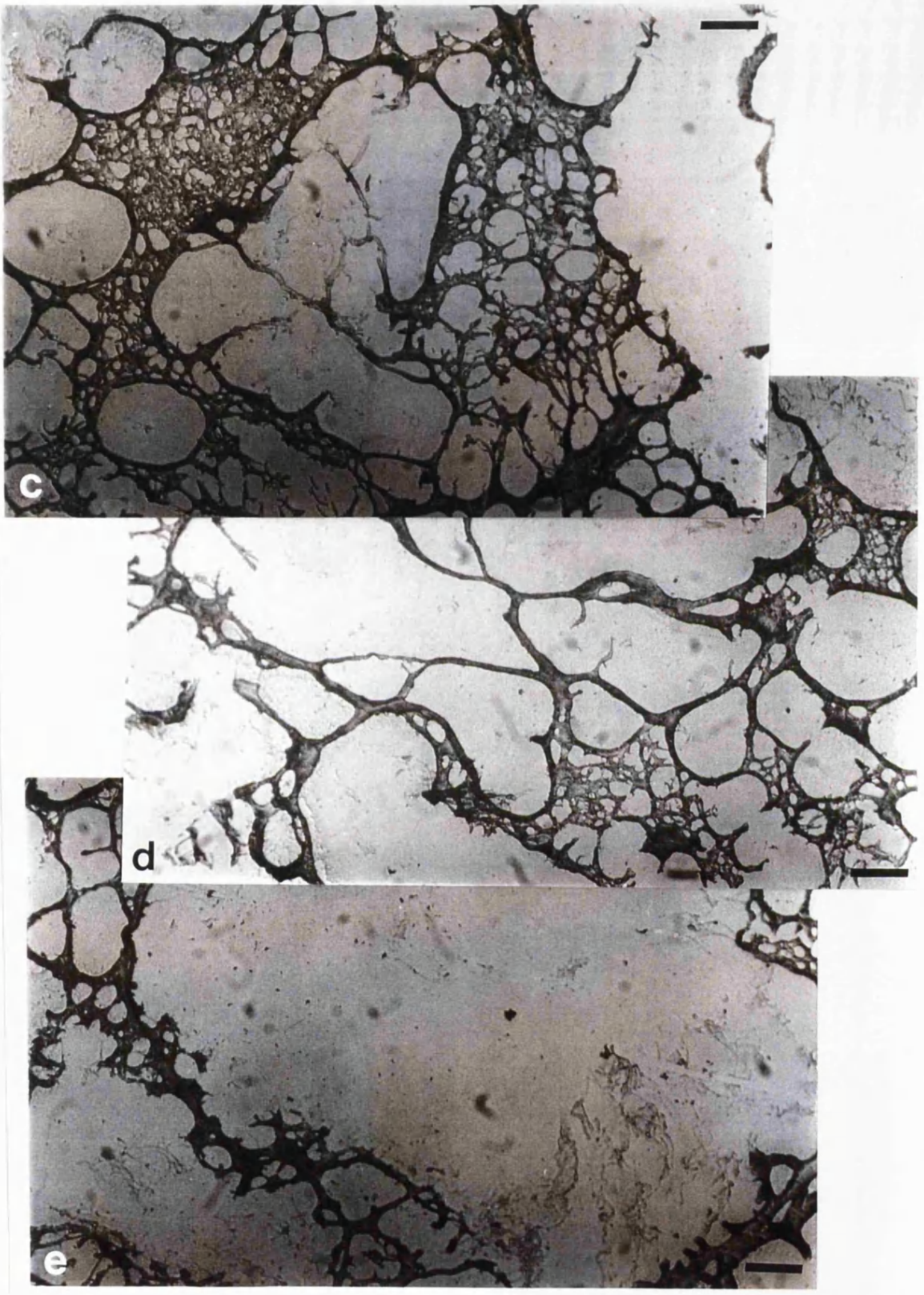

Figure 4.25. *(c) 10; (d) 100 and (e) 200 μM copper treated cables. Increased aggregation caused fibre condensations within the cable leaving large pores in the centre of the cable while the edges became densely packed. Scale bars in a-e =50μm.*

Treatment ions	Number of nano moles of ions in cable (nM/mgFn)			
Concentration of treatment solution(μM)	**1**	**10**	**100**	**200**
Cu	ND	ND	17	30
Zn	ND	ND	20	34
Cu / Zn	ND	ND	15 / 10	20 / 19

Table 4.3. *The mean amount of copper and zinc incorporated into cables.*

significantly greater ($p<0.0001$) than that of cells alone and those cultured on plain LFn-cables (Figure 4.26d). With copper alone, Schwann cells were only able to grow on 1μM treated LFn-cables but with zinc and copper/zinc, Schwann cells were able to grow on 10μM treated LFn-cable. Increase in cell numbers over non treated mats was 58%. 100 and 200μM treated LFn-cables in all the treatment forms was toxic to Schwann cells but not human dermal, rat tail and rat tendon fibroblasts. The number of cells in each population increased slightly (not significant) in a dose dependent manner in all the different treatments of cables.

The mean number of fibroblasts recovered from within the cable also increased (not significant) in a dose dependent manner in all the treatments of LFn-cables (Figure 4.27a, b,c and d). However, there was a three-fold increase in the number of Schwann cells recovered from 1μM treated LFn-cables ($p<0.00001$ plain LFn-cable vs 1μM treated cable) (Figure 4.27d). The greatest increase was observed for equimolar concentration of copper and zinc together. There was a further increase in the number of Schwann cells within 10μM treated Zn and Cu/ZnLFn-cables with a significant increase in the number of cells within 10μM treated Cu/ZnLFn-cable ($p<0.00001$) for

Figure 4.26. *Mean total number of cells recovered after 3 weeks in culture on copper and zinc treated LFn-cables. Graphs show the number of cells using (a) human dermal, (b) rat skin, (c) rat tendon fibroblasts and (d) Schwann cells recovered from copper and zinc treated cables after 3 weeks in culture. Schwann cells were only able to grow at 1μM Cu and 10 μM Zn and Cu/Zn. There were very similar numbers recovered for fibroblasts, however Schwann cell numbers were greatest after 3 weeks in treated cables.*

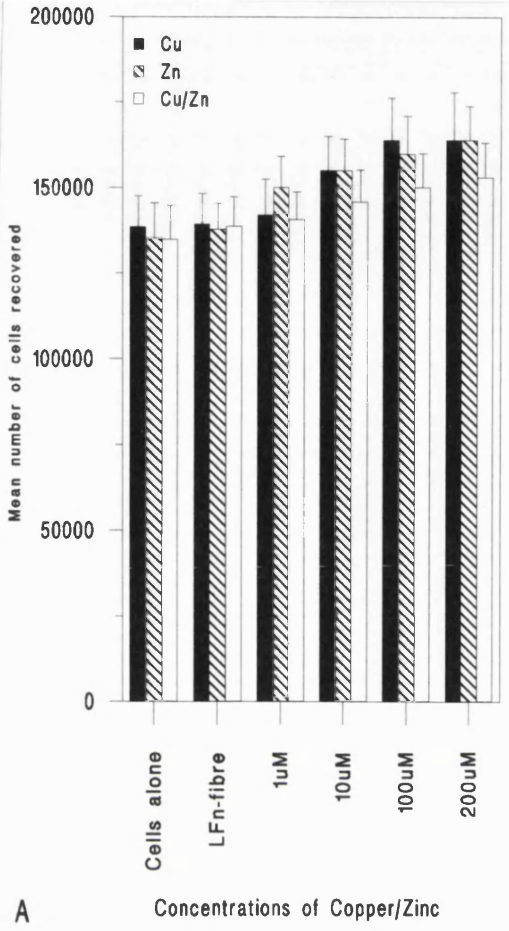
200000
150000
100000
50000
0
Mean number of cells recovered
Cu
Zn
Cu/Zn
Cells alone
LFn-fibre
1uM
10uM
100uM
200uM
Concentrations of Copper/Zinc

A

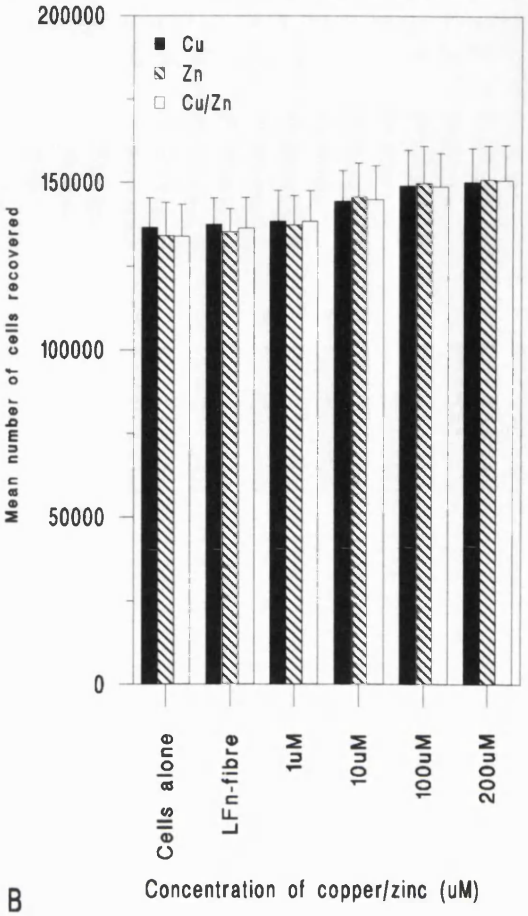
200000
150000
100000
50000
0
Mean number of cells recovered
Cu
Zn
Cu/Zn
Cells alone
LFn-fibre
1uM
10uM
100uM
200uM
Concentration of copper/zinc (uM)

B

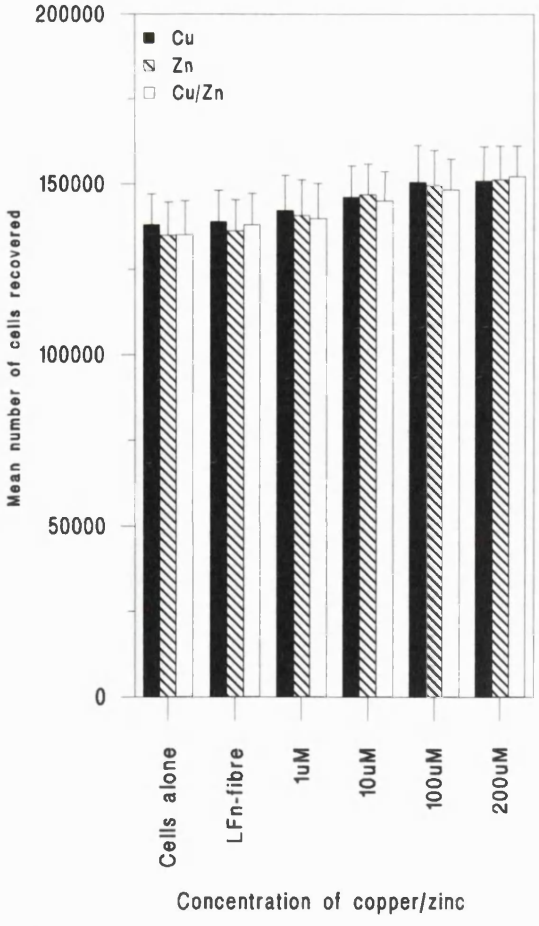
200000
150000
100000
50000
0
Mean number of cells recovered
Cu
Zn
Cu/Zn
Cells alone
LFn-fibre
1uM
10uM
100uM
200uM
Concentration of copper/zinc

C

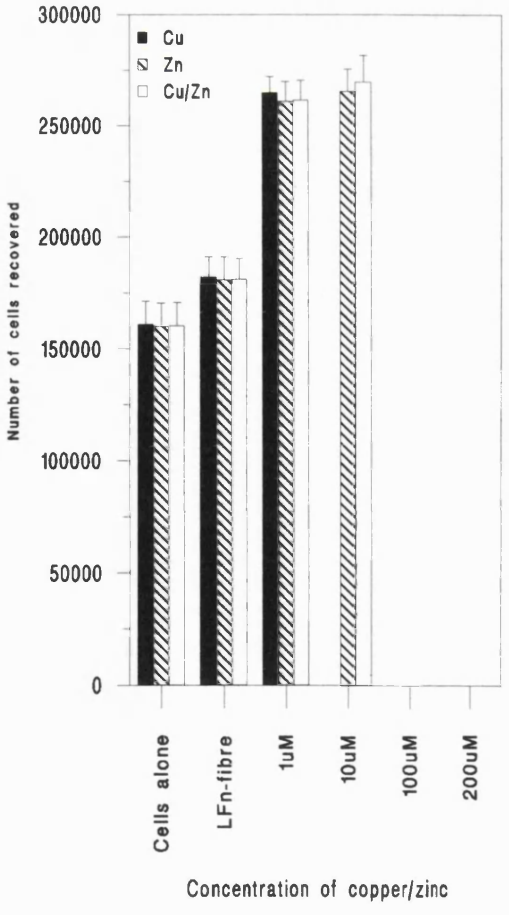
300000
250000
200000
150000
100000
50000
0
Number of cells recovered
Cu
Zn
Cu/Zn
Cells alone
LFn-fibre
1uM
10uM
100uM
200uM
Concentration of copper/zinc

D

Figure 4.27. *Mean number of cells recovered from within copper and zinc treated cables after 3 weeks in culture. Graphs show number of cells using (a) human dermal, (b) rat skin and (c) rat tendon fibroblasts and (d) Schwann cells recovered from within copper and zinc treated cables after 3 weeks in culture. Schwann cells were only able to grow at 1μM Cu and 10 μM Zn and Cu/Zn. There were very similar numbers recovered for fibroblasts, however Schwann cell numbers were greatest after 3 weeks within treated cables compared to untreated cables.*

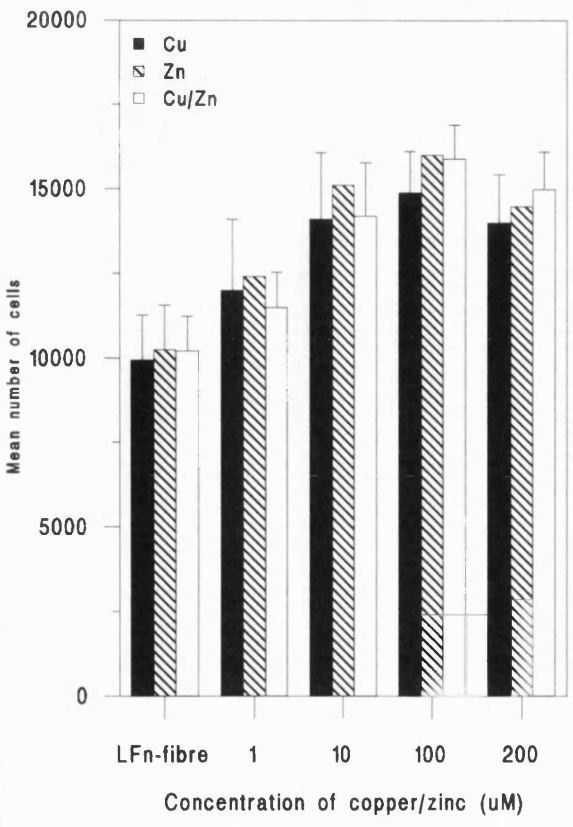
20000
15000
10000
5000
0
Cu
Zn
Cu/Zn
Mean number of cells
LFn-fibre
1
10
100
200
Concentration of copper/zinc (uM)

A

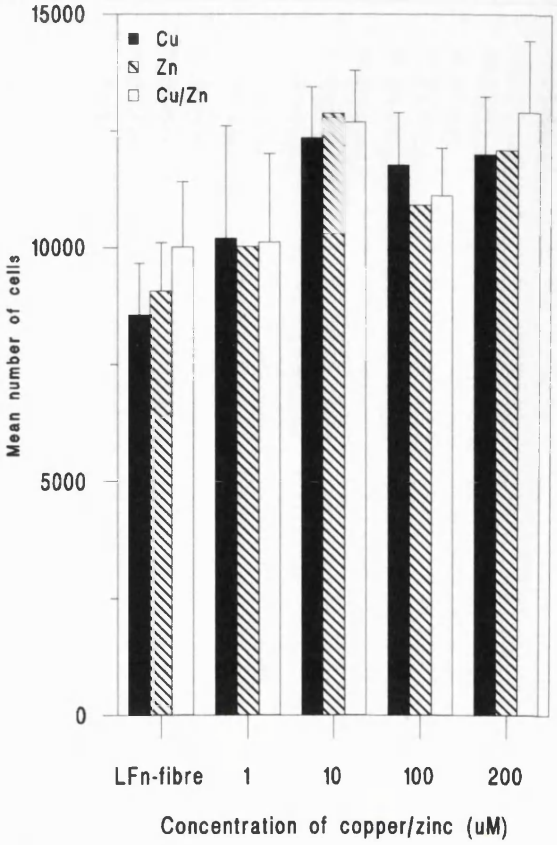
15000
10000
5000
0
Cu
Zn
Cu/Zn
Mean number of cells
LFn-fibre
1
10
100
200
Concentration of copper/zinc (uM)

B

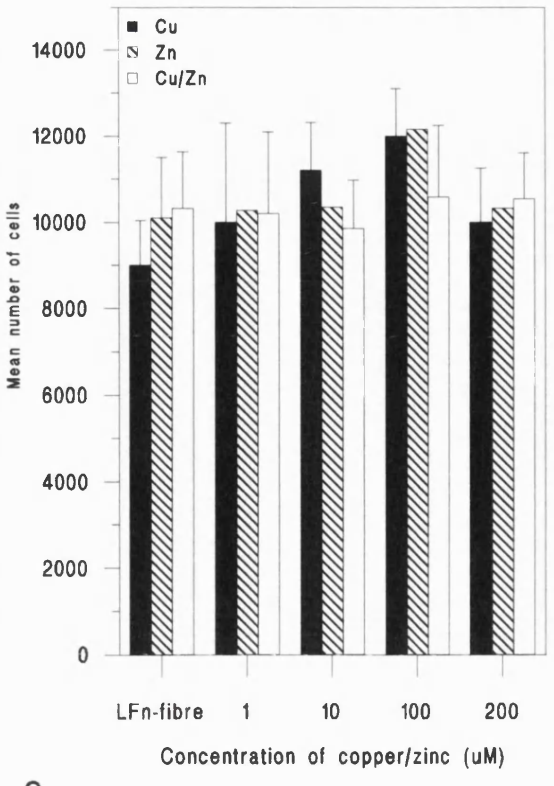
14000
12000
10000
8000
6000
4000
2000
0
Cu
Zn
Cu/Zn
Mean number of cells
LFn-fibre
1
10
100
200
Concentration of copper/zinc (uM)

C

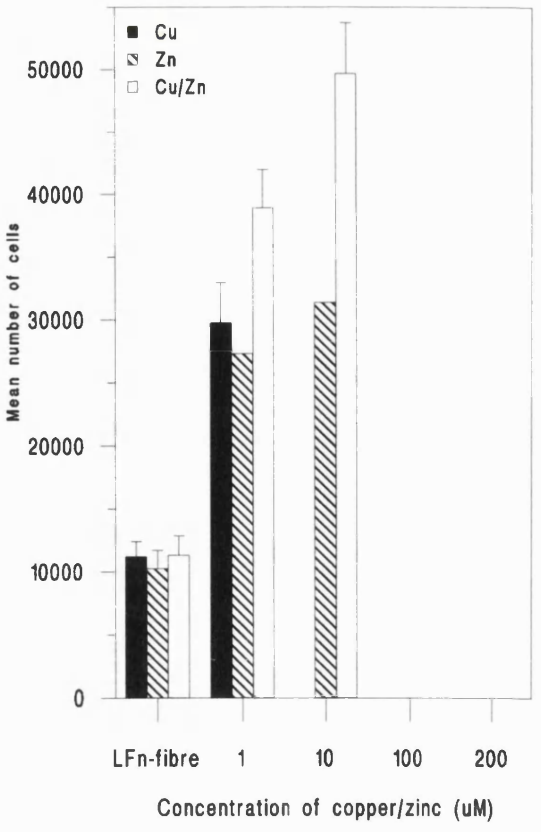
50000
40000
30000
20000
10000
0
Cu
Zn
Cu/Zn
Mean number of cells
LFn-fibre
1
10
100
200
Concentration of copper/zinc (uM)

D

10μM treated Cu/ZnLFn-cable vs 1μM treated Cu/ZnLFn-cable.

4.4.6. Histology of cultured Schwann cells with CuLFn-cables

When Schwann cells were cultured with CuLFn-cables, cells which were attached to the plastic culture dish were orientated parallel to the axis of the cable at each cut end in a very similar way to that in Figure 4.21b. Longitudinal sections immunostained, showed that almost all cells (apart from a few contaminating fibroblasts) stained for S-100 protein showing that cells were infact Schwann cells. Confocal microscopy revealed cells aligned along the axis of cable adopting a migratory bipolar phenotype (Figure 4.28). Cells were present along the whole length of the cable in a similar aligned manner.

Figure 4.28. *Immunostaining of Schwann cells (arrowheads) within LFn-cables stained with anti S-100 protein showing orientated cells along the direction of the fibres (direction of fibres shown by arrow) within the cable. Scale bar = 10μm.*

The results from this experiment showed that copper and zinc ions stabilised LFn-cables by twice that of control cables. Fibrillar orientation within cables was retained while Schwann cell proliferation was increased by three times that seen in control cables. Schwann cells were able to grow well at low concentrations of copper and assumed parallel alignment to the direction of fibre axis. This showed that LFn-cables are a suitable alternative to Fn-mats and that copper and zinc stabilisation confers an additional benefit.

4.5. Large Cables and Mats from Fibronectin: Effect of Freeze Drying on Fibrillar Structure

Initially, LFn-cables once produced were washed in PBS followed by several rinses in distilled water before being freeze dried. Once rehydrated the pH was still acidic which prevented cell survival. A 24 hours wash in DMEM was sufficient to remove the acidity. However, the fibrillar structure collapsed and a solid conduit with very few pores were seen. A similar loss of fibrillar structure was seen with Fn-mats following rehydration and dehydration. The aim of this experiment was to remove the acidity without disrupting fibrillar structure. This was done by soaking freshly made cables in Tris-HCl buffer at different concentrations followed by freeze-fracture to look at the internal structure by scanning electron microscopy.

4.5.1. pH and structure of LFn-cables after removal of acidity

LFn-cables were made with fibrillar structure as described previously in Chapter 2.17. The cables were acidic in nature due to their production process and before use in vivo or in vitro, this acidity must be removed. Acidity tests after initial production showed

that the freshly made material, washed in distilled water for 10 minutes, has a pH of <1. However, washing the cables in PBS for 2 hours in a large volume on a mechanical roller, reduced the acidity making cables around pH 4. Treatment in 50 mM, 100 mM and 200 mM Tris-HCl buffer (pH 7.6) reduced the acidity further in a dose dependent manner to pH 5.5, 6.5 and 7, respectively (20mg cable: 200mL of buffer). This is summarised in table 4.4. Cables which were washed in the above buffers and cut in half to test the acidity of the inner surface, showed similar pH values as the whole cable.

Treatment (20mg LFn-cable: 200mL)	**pH**
10 mins in distilled water	<1
PBS for 2 hrs	4
50mM Tris buffer for 2 hrs	5.5
100 mM Tris Buffer for 2 hrs	6.5
200 mM Tris buffer for 2 hrs	7

Table 4.4. *Summary of pH for LFn-cables following various acidity removing treatments.*

Freeze-fracture of cables followed by SEM showed that untreated freeze dried cables (pH <1) had an orientated fibrillar structure (Figure 4.29a). Upon treatment with PBS (pH 4) the cables retained their fibrillar structure similar to that seen for freshly made cables (Figure 4.29b). However, as the acidity was reduced with increasing concentrations of Tris-HCl buffer, the cables lost fibrillar structure and formed aggregates with no directional element (Figure 4.29c-e) such that cables treated in 200

mM Tris buffer formed a solid cable with no pores or fibres at all (Figure 4.29e). In contrast, un-fixed and un-processed cryo-sections of cables treated in buffers to remove acidity showed that fibrillar structure was retained without causing any aggregation of fibres within cables (Figure 4.30-typical examples). This clearly shows that fibres within cables are only able to aggregate with each other if the water molecules are removed thereby bringing together adhesive sites on the Fn molecule. This was very almost identical to that already shown in Figure 4.16.a.

4.5.2. Structure of Fn-mats following rehydration

Fn-mats which were unprocessed (i.e. freeze dried directly after formation followed by sputter coating) revealed a fibrillar structure throughout the mat as reported previously (Ejim et al., 1993) (Figure 4.31a). Upon processing which involves fixing in 2.5% gluteraldehyde in phosphate buffer followed by dehydration in a graded series of alcohols, critical point drying and then sputter coating mats for SEM, there is some aggregation of fibres within the mat causing some loss of overall fibrillar structure (Figure 4.31b). Upon rehydrating the mats for increasing times, there was a loss of fibrillar structure such that eventually a non porous, non-fibrillar material was seen (Figure 4.31c-e).

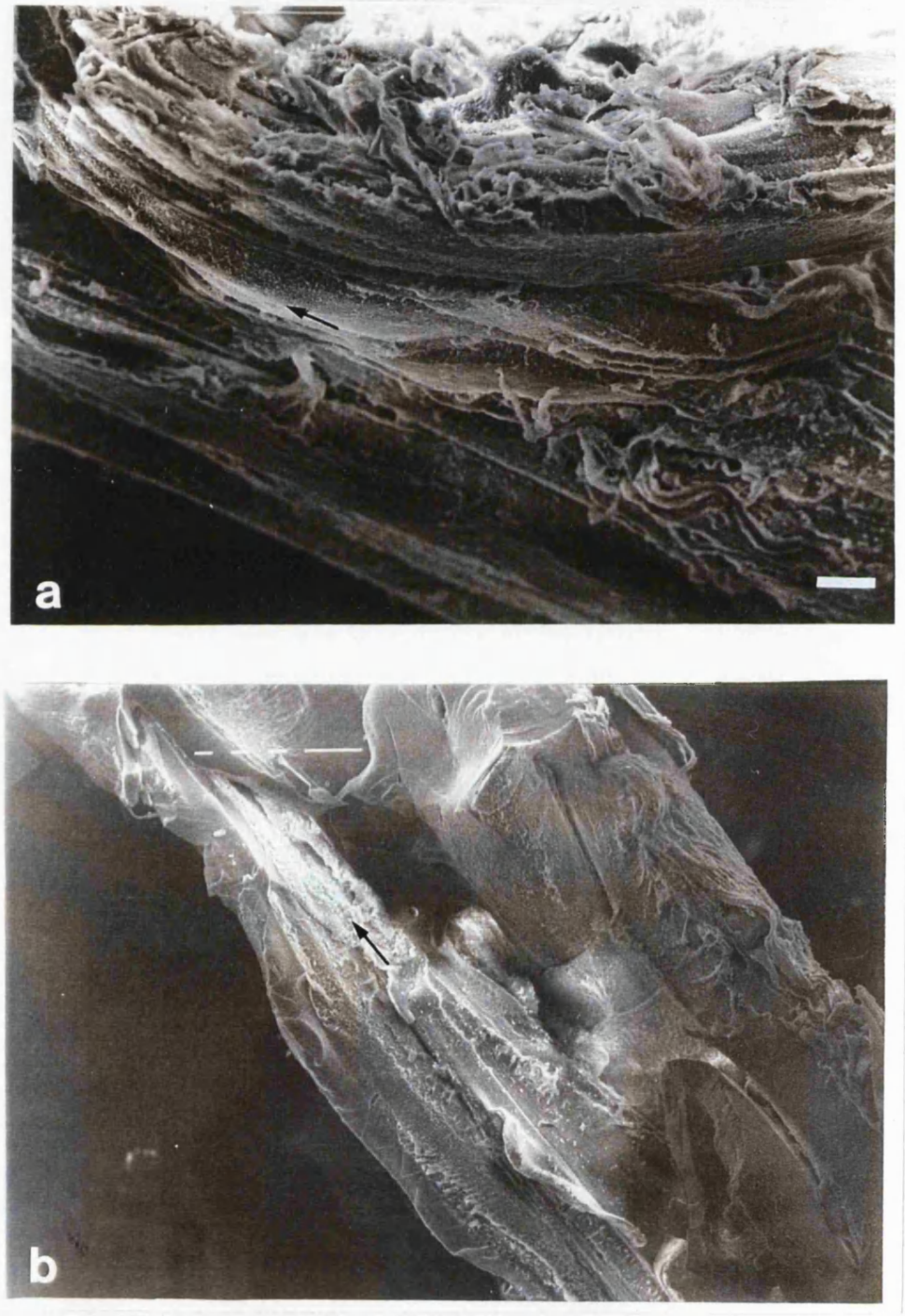

Figure 4.29. *Freeze-fractured, scanning electron micrograph of the effect of removal of pH followed by dehydration from LFn-cables. SEM's after treatment with (a)PBS (untreated was exactly the same in structure), (b) 50mM Tris-HCL buffer,.*

Figure 4.29. *(c)100 mM and (d) 200 mM Tris buffer. Increased loss of fibrillar structure as more acidity is removed. Scale bar in a-d = 100 μm.*

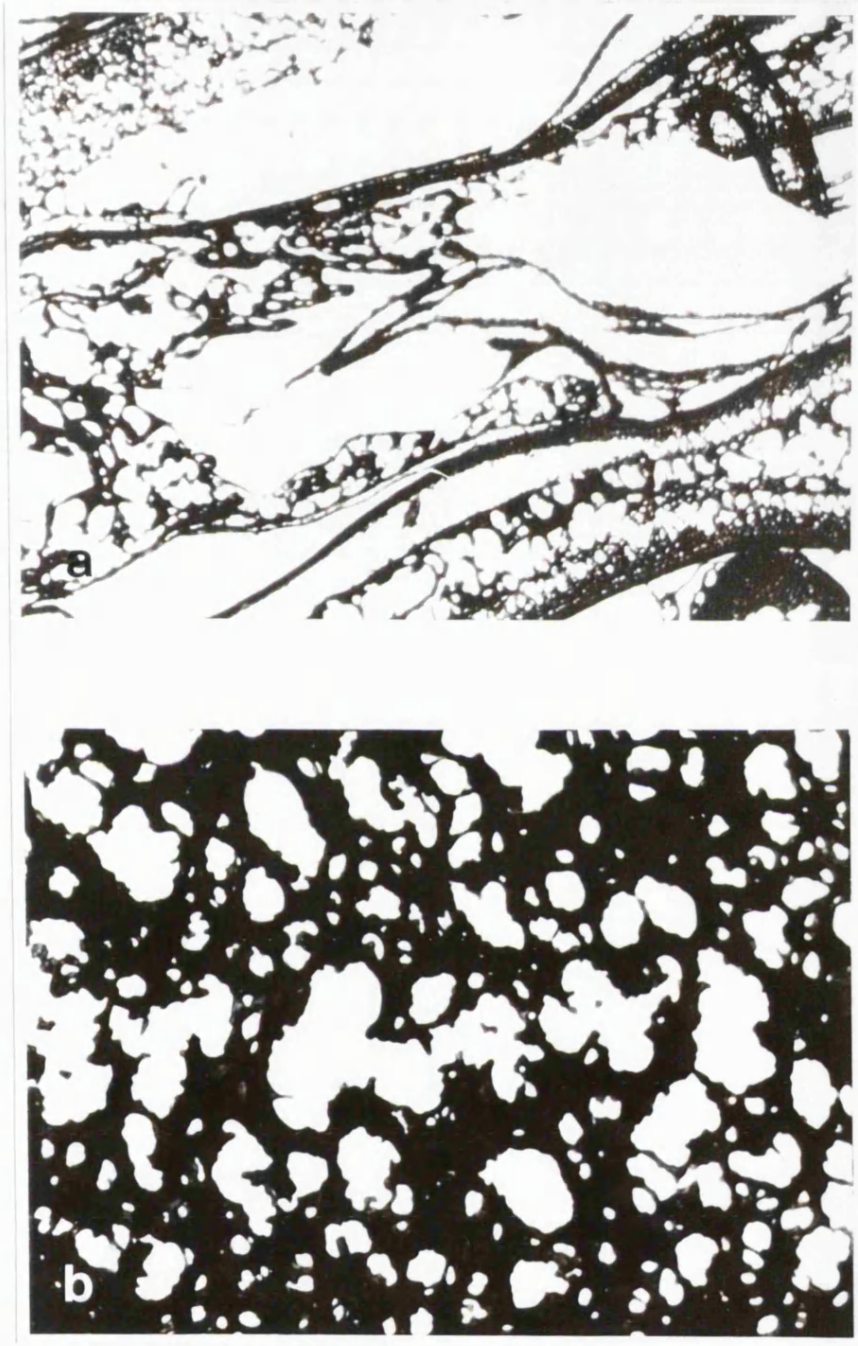

Figure 4.30. *Unfixed cryo-sections of LFn-cables to show that fibrillar structure is maintained in cables that have not been fixed, processed or freeze-dried. Typical example shows cable treated in 200mM Tris-HCL buffer. (a) shows longitudinal and (b) cross-sectional structure. These showed a very similar structure to those shown in Figure 4.16b and 4.17c. Scale bars in a and b= 50 μM.*

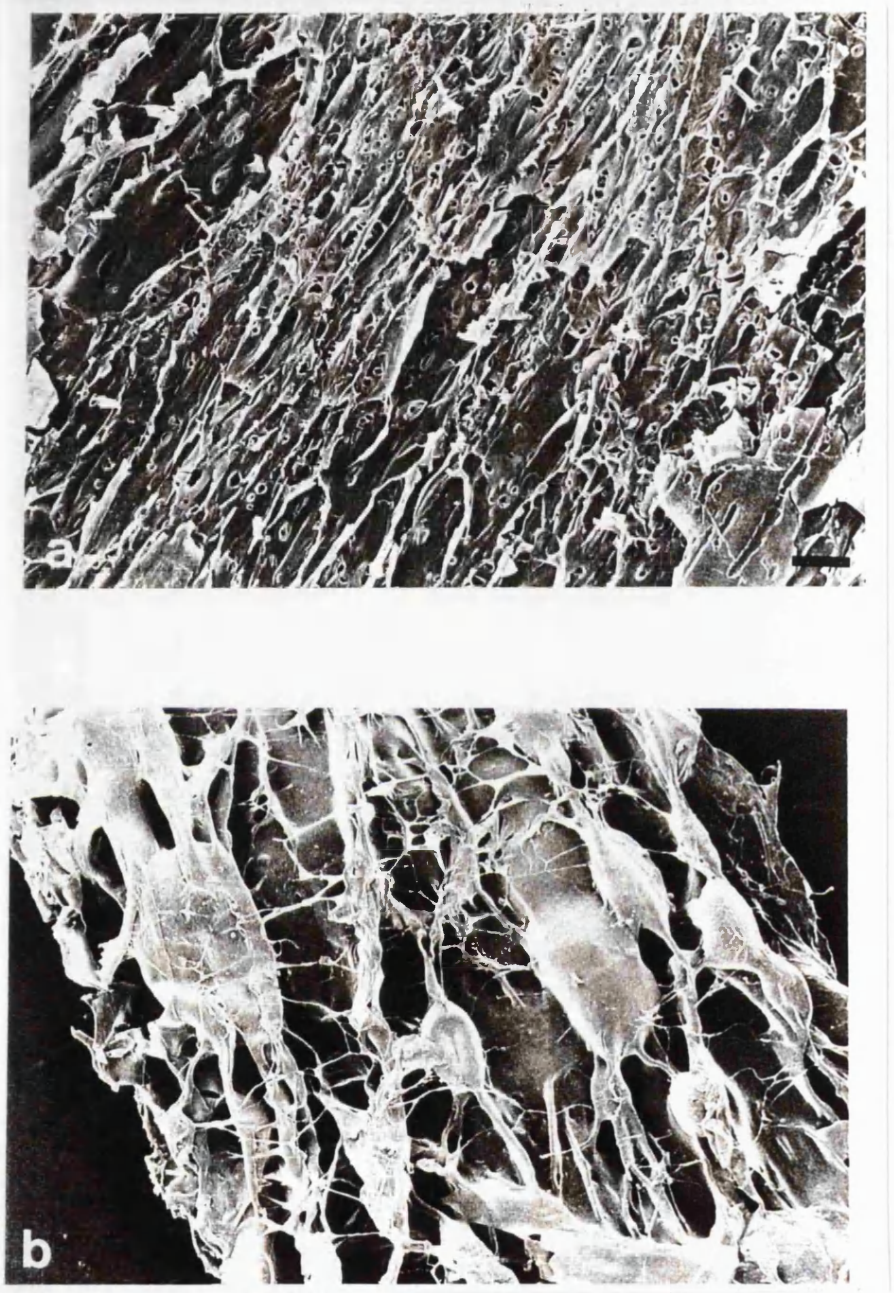

Figure 4.31. *Scanning electron micrographs to demonstrate the effect of rehydration of Fn-mats. Micrographs represent (a) control, unprocessed, (b) processed.*

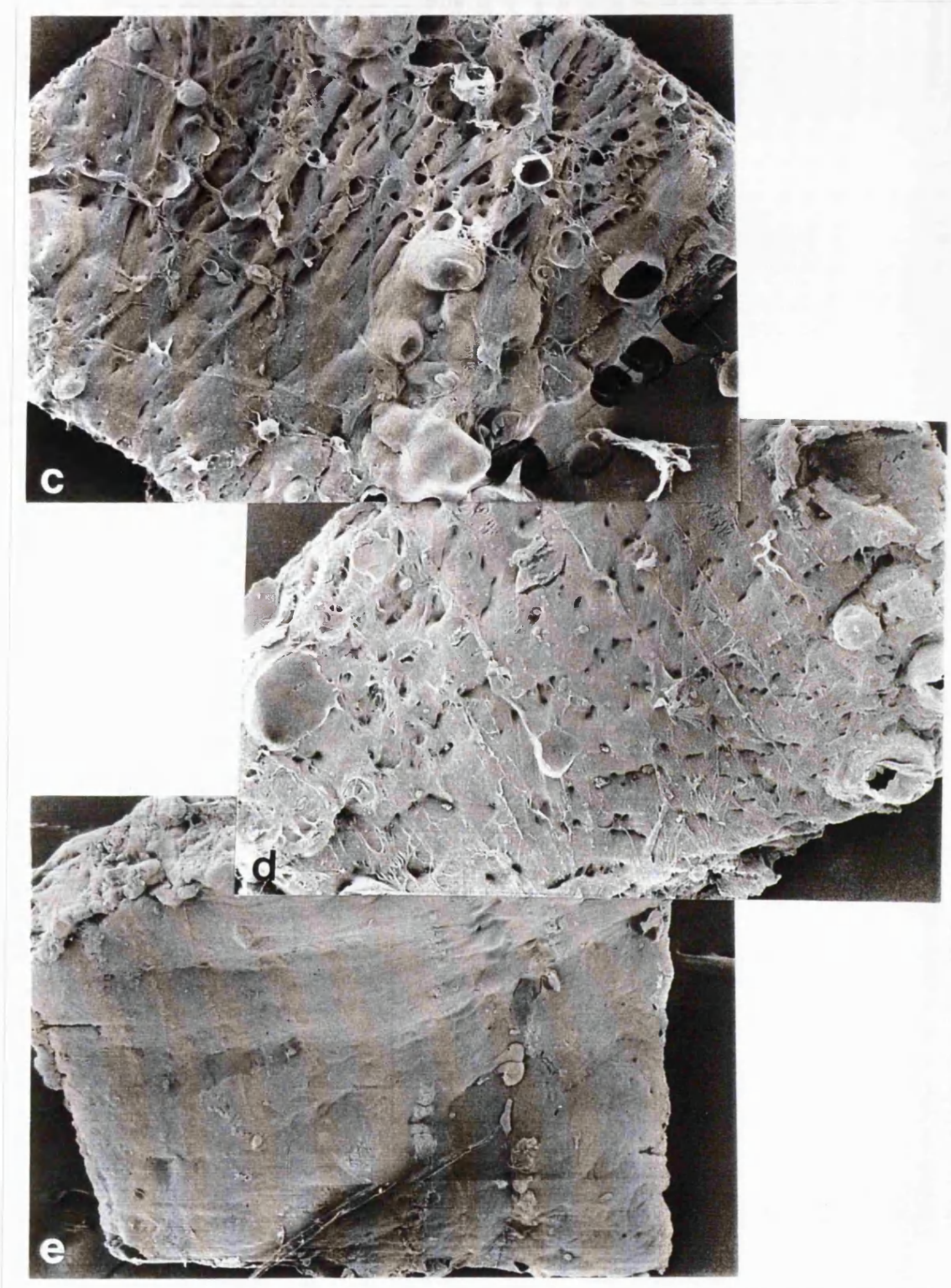

Figure 4.31. *Rehydrated for (c) 30 minutes, (d) 4 hours and (e) overnight, before processing for SEM. Note the increased loss of fibrillar arrangement upon increasing hydration times. Bar = 100 μm.* (Scanning electron micrographs courtesy of Miss. Kirsty Smith).

The results showed that the acidity from LFn-cables could be removed effectively by 15 minutes treatment in Tris-HCl buffer. Freeze-fracture of the cable showed that as more and more acidity was removed followed by dehydration, the structure became more solid in appearance. A similar loss of structure was seen with Fn-mats upon hydration and dehydration. In the case of LFn-cables, hydrogen ions maintain the spatial arrangement of Fn fibrils and prevents the structure becoming solid. Fn-mats however, lose fibrillar structure due to protein unfolding and refolding as a result of dehydration/rehydration.

4.6. A Study of Adhesion, Alignment and Migration of Cultured Schwann Cells on Ultrathin Fibronectin Fibres.

The aim of this experiment was to assess the effects of single fibres of Fn which represents a simple surface on which parameters of topography, cell adhesion, migration and contact guidance can be investigated. These reactions of cells to these single fibres could then be adapted to appraise why Fn-mats enhance peripheral nerve regeneration. Individual strands of Fn were made and the reaction of Schwann cells, human dermal fibroblasts, rat tendon and rat skin fibroblasts were assessed. In particular, cell alignment, migration speed and F-actin organisation was investigated by scanning electron microscopy, time-lapse video and confocal laser microscopy followed by image analysis.

4.6.1. Schwann cells in culture with Fn-fibres

Ultrathin Fn-fibres were used as a model for contact guidance on Fn substrata, mimicking the Fn-mat, but forming a measurable system. Schwann cells attached to Fn-fibres rapidly and spread on the culture vessel over a period of 4 hours by which

time they were bipolar in nature with long potruding filopodia. Cells from the periphery apparently migrated towards the fibre and became aligned with the axis of the fibre before moving alongside it. Figure 4.32a shows Schwann cells after 10 hours in culture on a Fn-fibre measuring 3 μm in diameter stained with haemotoxylin and eosin for greater clarity. Figure 4.32b shows a scanning electron micrograph (SEM) of Schwann cells already attached and/ or becoming attached to the fibre at 10 hours. Schwann cells that were docking with the fibre were seen to send out long filopodia at the leading edge which formed attachment points onto the fibre as they migrated along the fibre with the rest of the cell also forming attachment sites as contact was made with the fibre. This is in contrast to control experiments in figure 4.32c and d (Schwann cells cultured on plastic dishes coated in poly-L-lysine + Fn (monolayer film)) and figure 4.32e and f (Schwann cells cultured on poly-L-lysine alone), where cells assumed a random orientation and appeared less well spread. (Cells cultured on poly-L-lysine + LN were similar to those on poly-L-lysine + Fn (monolayer film) in all aspects throughout this study and therefore micrographs are not shown for cells plated on this substrata). By 24 hours there were many cell layers had docked with the Fn-fibre and aligned with the axis of the fibre forming an "alignment band" (Figure 4.33a: H&E stained and b: SEM). This alignment band of cells extended from the surface of the Fn-fibre to a zone at least 50μm, perpendicular to the fibre (Figure 4.33g: H&E stained and h: SEM). However, cells grown on other substrata (Figure 4.33c, d on poly-L-lysine + Fn (monolayer film) substrata, figure 4.33e and f on poly-L-lysine alone were randomly organised with most cells less well orientated than the cells which were in contact with Fn-fibres.

Figure 4.32. *The effects of different substrata on the behaviour of Schwann cells in culture at 10 hours after plating. Schwann cells cultured on poly-L-lysine + LN + Fn-fibre coated coverslips* ***(a)*** *stained with H&E and* ***(b)*** *scanning electron micrograph. Cells that docked alongside the fibre became orientated along the fibre axis (f: arrow) with long filopodial extensions and docking Schwann cells formed attachments to the fibres as indicated by the arrowheads.* ***(c)*** *and* ***(d)*** *Show Schwann cells on poly-L-lysine + Fn coated coverslips stained with H&E and by scanning electron microscopy, respectively. Cells were randomly orientated but once they touched one another they became orientated along their own axis.* ***(e)*** *and* ***(f)*** *Show Schwann cells on coverslips coated with poly-L-lysine alone stained with H&E and by scanning electron microscopy, respectively. Schwann cells were randomly orientated throughout and were less extended along their para-axial length. Scale bar in a= 15 μm (same scale for c and e) and scale bar in b = 10 μm (same scale bar in d and f).*

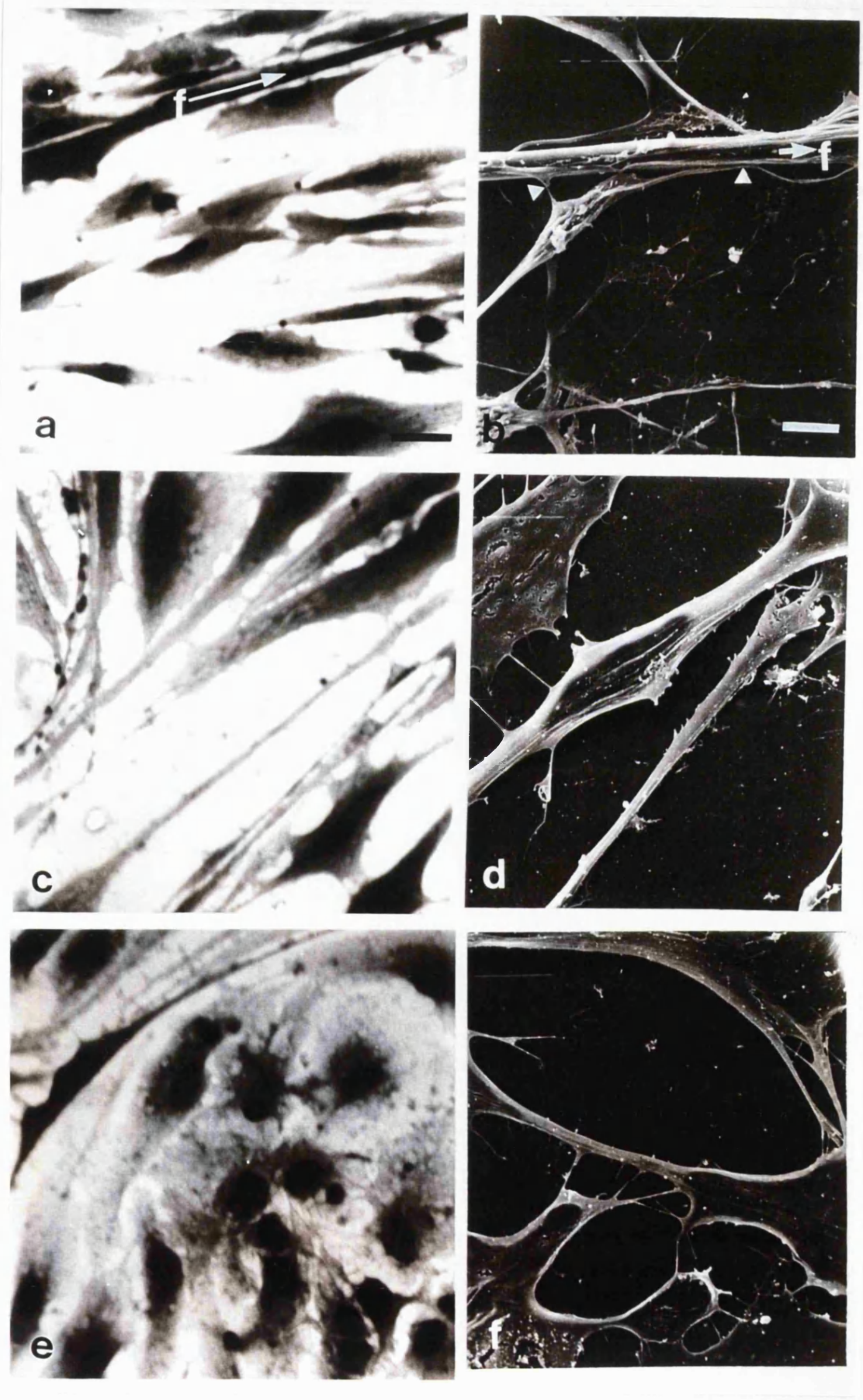
f
a
f
b
c
d
e
f

Figure 4.33. *Schwann cells grown in culture on different substrata at 24 hours after plating. Schwann cells aligned along the axis of Fn-fibres in* ***(a)*** *stained with H&E and* ***(b)*** *scanning electron micrograph. A greater number of cells were aligned along Fn-fibres (arrow: f shows fibre orientation) than that observed at 10 hours with the band of aligned cells reaching 50μm away from the fibre.* ***(c)*** *H&E stained and* ***(d)*** *scanning electron microscopy, respectively, of Schwann cells plated on poly-L-lysine + Fn coated coverslips showing no predominant orientation however, cells are bipolar in nature.* ***(e)*** *H&E stained and* ***(f)*** *scanning electron microscopy of Schwann cells plated on poly-L-lysine coated coverslips showing random orientation of cells. Scanning electron microscopy shows extensive microspikes from cells attached to the coverslips.* ***(g)*** *H&E stained and* ***(h)*** *scanning electron micrograph of Schwann cells 50μm away from the fibre at the edge of the alignment band showing cells orientated along the same axis as the Fn-fibre (original Fn-fibre orientation indicated by arrows). Scale bar in a = 15 μm (same scale bar for c, e and g) and scale bar in b = 10 μm (same scale bar for d, f and h).*

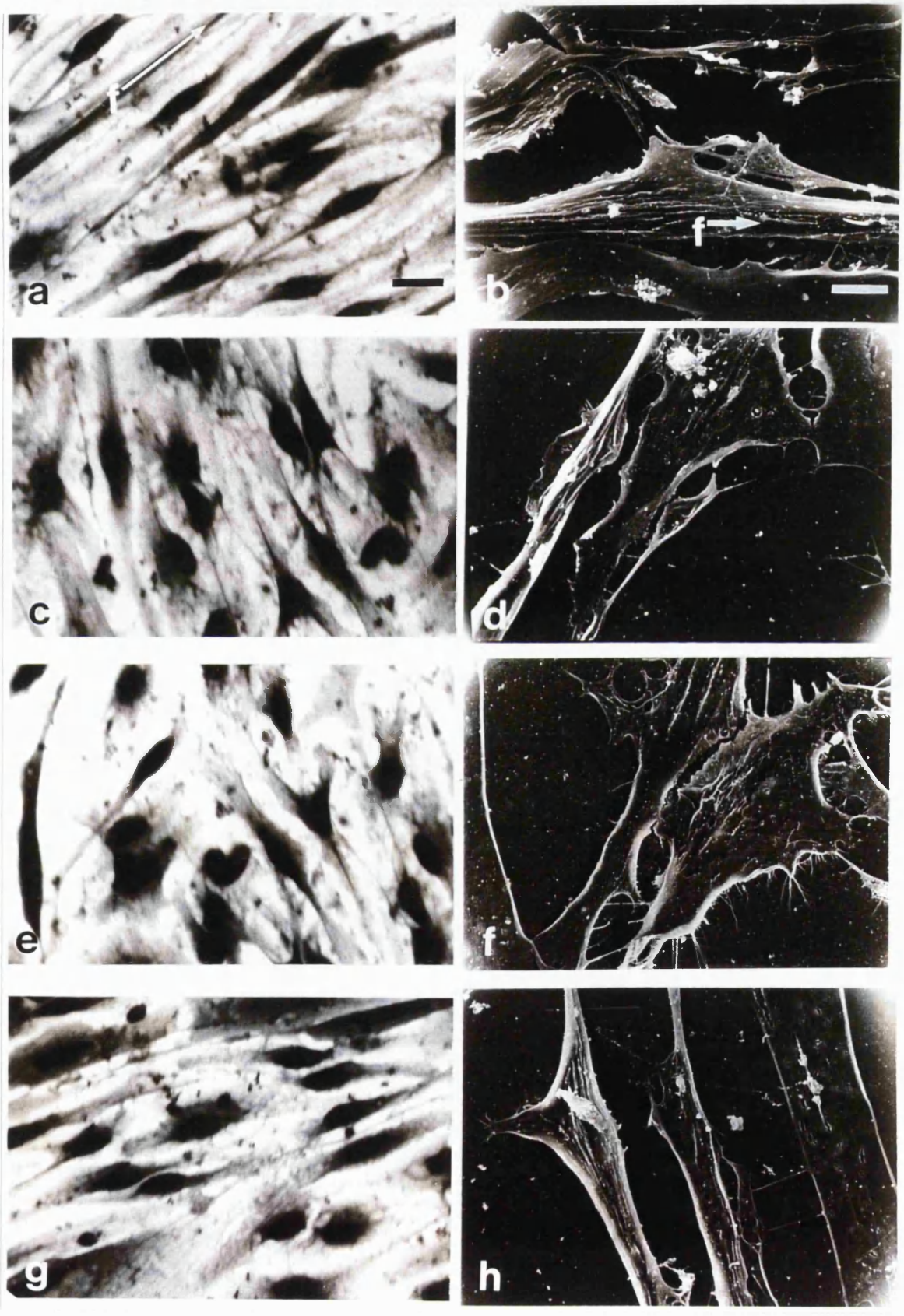
f
a
f
b
c
d
e
f
g
h

4.6.2. Speed of Schwann cell movement on Fn-fibres

The speed of cell movement over a 10 hour time period on the test substrata is shown in Table 4.5. Schwann cells moved significantly faster on Fn-fibres with a mean velocity of 35 ± 2.7μm/hr compared to cell speeds on poly-L-lysine + Fn (monolayer film); mean velocity of 30.2 ± 3.5μm/hr ($p<0.01$) and on poly-L-lysine + LN; mean velocity of 29.7 ± 4μm ($p<0.01$). The slowest movement of Schwann cells was seen on poly-L-lysine coated substrata with a mean velocity of 21.7 ± 3.7μm/hr. The total cell path and total cell translocation (T) moved by Schwann cells were significantly greater on poly-L-lysine + LN + Fn-fibre substrata compared to that moved by cells on poly-L-lysine + LN + Fn ($p<0.0001$). Cells in contact with the fibre tended to have a higher persistence value than cells on the coated plastic substrata showing a continuous movement pattern once in contact with the fibre.

4.6.3. Cell orientation measurements

The mean orientation of cells were measured using the image analysis software and shown in Table 4.6. As time progressed Schwann cells became more orientated and a greater number of cells docked with the fibre to become aligned along the axis of the fibre and previously attached cells. By 10 hours cells had begun to form layer upon layer of aligned cells (Figure 4.33a and b). Schwann cells plated in culture with poly-L-lysine + LN + Fn-fibres (S value = 0.97) in contact with the strand at 10 hours after plating were significantly more aligned than those cultured on poly-L-lysine + Fn (monolayer film) (S value = 0.42) ($p<0.0002$) or on poly-L-lysine + LN (S value = 0.42) ($p<0.0002$) or on poly-L-lysine alone (S value = 0.27) ($p<0.0001$). Schwann cells became further aligned such that at 24 hours the mean orientation of cells plated

Substrata	V_{real} (μm/hr)	$V_{effective}$ (μm/hr)	Cell Path (μm)	T (μm)	Pr	N
Poly-L-Lysine	21.7 ± 3.7	21.7 ± 3.7	217 ± 37	108 ± 21	0.50	0
Poly-L-Lysine + Fn	29.7 ± 4.0	29.7 ± 4.0	297 ± 40	197 ± 30	0.66	0
Poly-L-Lysine + LN + Fn-fibre	35.0 ± 2.7*	35.0 ± 2.7	350 ± 27	350 ± 27	1	0

Table 4.5. *Measurement of the speed of cell movement (mean ± s.d.)on different substrata for a period of 10 hours. *Poly-L-Lysine + LN + Fn-fibre; $p<0.0012$ for Poly-L-Lysine + Fn vs Poly-L-Lysine + LN + Fn-fibre, students t-test. T= total cell translocation; Pr = persistence; N = number of 1 hour intervals (stops). Schwann cells showed a continuous movement, so N = 0 and $V_{real} = V_{effective}$.*

Substrata	Orientation (degrees)		S value	
	10 hours	**24 hours**	**10 hours**	**24 hours**
Poly-L-Lysine	37.2 ± 23	29 ± 12	0.82	0.83
Poly-L-Lysine + LN	34.2 ± 20	25 ± 11	0.86	0.88
Poly-L-Lysine + LN + Fn-fibre	7 ± 2*	4 ± 2**	0.97***	0.98****

Table 4.6. *Orientation values (mean ± s.d.) at 10 and 24 hours after culture. *$p<0.0055$ for Poly-L-Lysine + LN vs Poly-L-Lysine + Fn-fibre; ** $p<0.0094$ for Poly-L-Lysine + LN vs Poly-L-Lysine + Fn-fibre; *** $p<0.0082$ for Poly-L-Lysine + LN vs Poly-L-Lysine + LN + Fn-fibre; **** $p<0.0002$ for Poly-L-Lysine + LN vs Poly-L-Lysine + LN + FN, students t-test. S-value is an Orientation index (Herman), a value of 1 denotes perfect alignment; 0 would denote totally random orientation. Schwann cells plated on Fn-fibres were significantly more orientated to the axis of the fibre than cells on other substrata.*

onto poly-L-lysine + LN + Fn-fibre (S value = 0.98) was significantly greater than that of poly-L-lysine + Fn (monolayer film) (S value = 0.69) ($p<0.0001$) or poly-L-lysine + LN (S value = 0.64) ($p<0.0002$) and poly-L-lysine alone (S value = 0.52) ($P<0.0001$).

4.6.4. Measurement of cell area and extension

Cell area (Figure 4.34a) and extension (Figure 4.34b) parameters were measured from density sliced binary images of cells using the Openlab Image analysis software package. Schwann cells on all test substrata increased their area and extension. However, cells in contact with Fn-fibres exhibited significantly higher cell spread area and extension (along its long axis) than cells cultured on poly-L-lysine/LN ($p<0.005$). Cells cultured on poly-L-lysine alone exhibited the least cell spread area and cell extension. After 24 hours in culture Schwann cells had extended significantly more on substrata containing Fn-fibres than on poly-L-lysine/LN ($p<0.0025$). Once again cells cultured on poly-L-lysine alone exhibited the least amount of spread area and extension.

4.6.5. Regression analysis

Regression analyses of the width of the cell alignment band and paraxial elongation in relation to the fibre width, Figure 4.35a and b, respectively, showed that there was no effect of increasing or decreasing the fibre diameter on the subsequent width of this aligned band of cells.

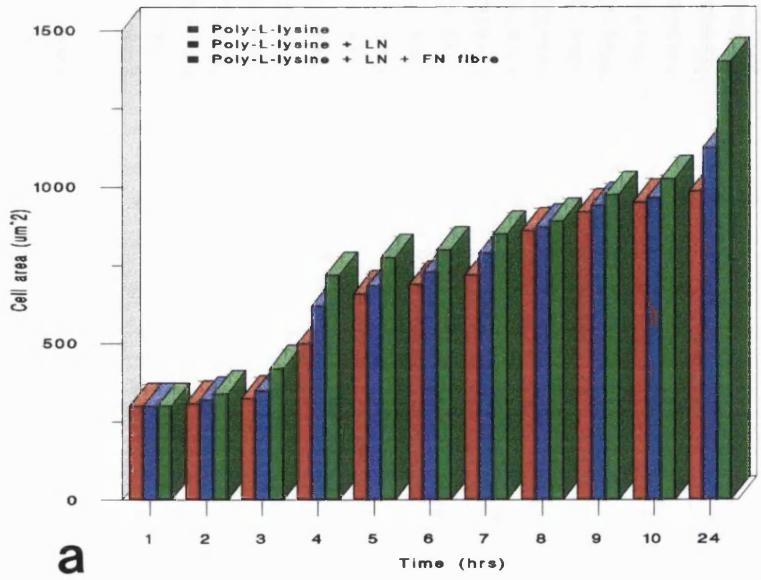

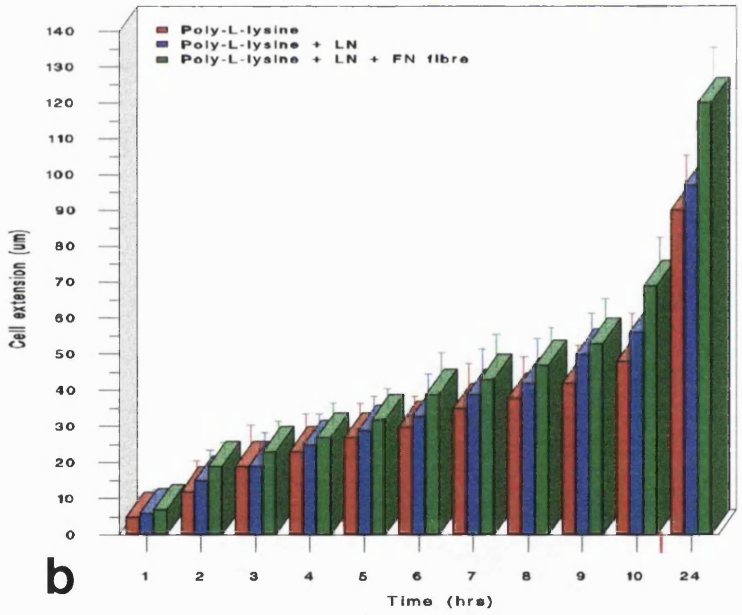

Figure 4.34. Cell spreading and extension on different substrata. (a) Time course of cell spreading area on the test substrata. The cell spread area was significantly greater for Schwann cells plated on Fn-fibre substrates than other substrata. (b). Time course of cell extension on the test substrata. Cellular extension was greater in Schwann cells of Fn-fibre substrates.

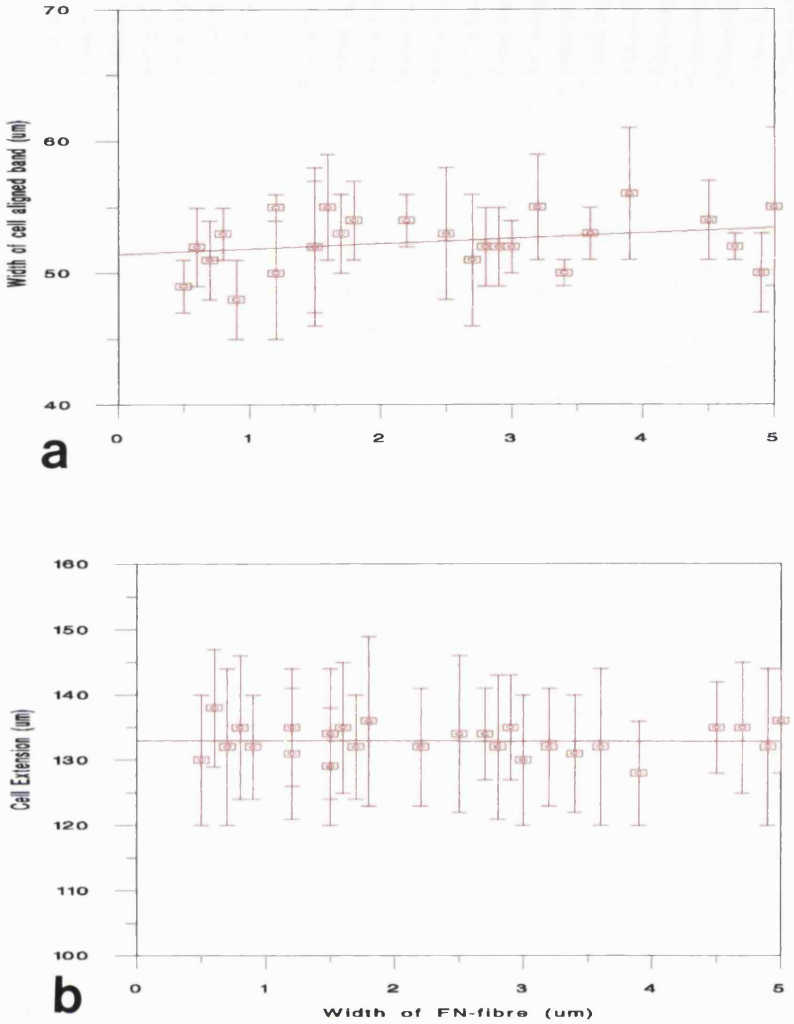

Figure 4.35. Regression analysis. (a) Regression analysis of the width of cell aligned band in relation to fibre width (r^2 = 0.07838). (b) Regression analysis of paraxial elongation in relation to fibre width (r^2 = 0.00022). There was no significant correlation between the width of the cell aligned band or cellular extension in relation to the fibre diameter.

4.6.6. Localisation of F-actin and vinculin

Figure 4.36 shows the distribution of F-actin and vinculin in Schwann cells on different substrata after 10 hours. Schwann cells which were migrating along poly-L-lysine + LN + Fn-fibres were well spread and bundles of F-actin were orientated within the direction of the fibres and concentrated at the leading edge of the cell and in areas of

cell attachment to the Fn-fibre (Figure 4.36a). The cells in contact with the fibre formed condensations of vinculin at attachment sites, as they migrated along the fibre (Figure 4.36b). Schwann cells which were spread on poly-L-lysine alone, poly-L-lysine + LN and poly-L-lysine + LN + Fn coated substrata had F-actin fibres distributed mainly around the cell margins and along the numerous actin-rich microspikes (Figure 4.36c). Vinculin distribution in cells on these substrata tended to be diffused around the bottom surface of cell, in contact with the glass culture surface (Figure 4.36d).

There was a very similar distribution of F-actin and vinculin in Schwann cells after 24 hours in culture on poly-L-lysine alone, poly-L-lysine + LN and poly-L-lysine + LN + Fn substrata, to that seen at 10 hours (not shown: cf Figure 4.36c and d). However, Schwann cells which attached directly to Fn-fibres or docked with other prealigned cells in the alignment band, showed F-actin elongated along in the same plane as the Fn-fibre (Figure 4.37a). Greater numbers of Schwann cells were attached with the Fn-fibre forming condensations of vinculin attachment sites to the Fn-fibre (Figure 4.37b). Cells cultured with Fn-fibres which were within the alignment band (upto 50 μm away from the Fn-fibre) had aligned F-actin fibres throughout this area (Figure 4.37c) and cells were attached to other cells and to the culture surface via vinculin containing adhesion plaques (Figure 4.37d). Outside the 50 μm alignment zone, cells were seen to assume a random orientation (Figure 4.37d). There was no correlation between reorganisation of the cytoskeleton across the 50μm band with the filopodial length of Schwann cells.

Figure 4.36. *Immunostaining of F-actin and vinculin at 10 hours.* ***(a)*** *F-actin and* ***(b)*** *vinculin distribution in Schwann cells plated on Fn-fibres. F-actin and vinculin distribution in Schwann cells on poly-L-lysine + LN + Fn-fibre showed F-actin (open arrow: docked cell) along the axis of the Fn-fibre (=f: arrow) and concentrated at the leading edge of cells together with some condensations of vinculin forming-rich attachment plaques to the Fn-fibres. Cells which were docking (arrow heads) showed that the F-actin fibres were bending to the direction of the fibres as the cell moved along.*

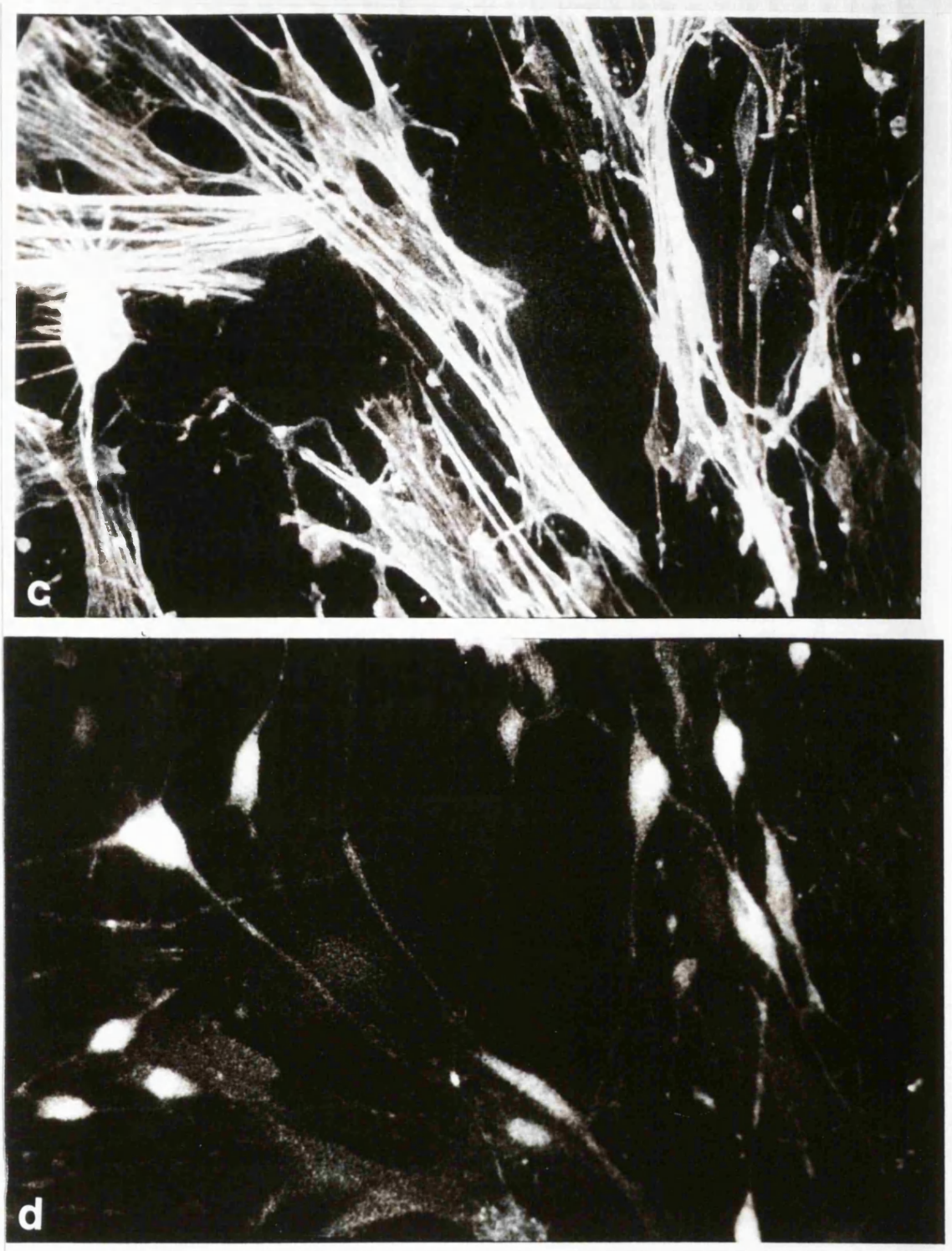

Figure 4.36. *(c) F-actin and* ***(d)*** *vinculin distribution in Schwann cells plated on poly-L-lysine alone or poly-L-lysine + Fn (monolayer film). F-actin and vinculin distributions in cells on poly-L-lysine alone and poly-L-lysine + LN + Fn substrata, respectively, showed no predominant orientation of F-actin fibres and vinculin in all cells. b, c and d use same scale bar as a.*

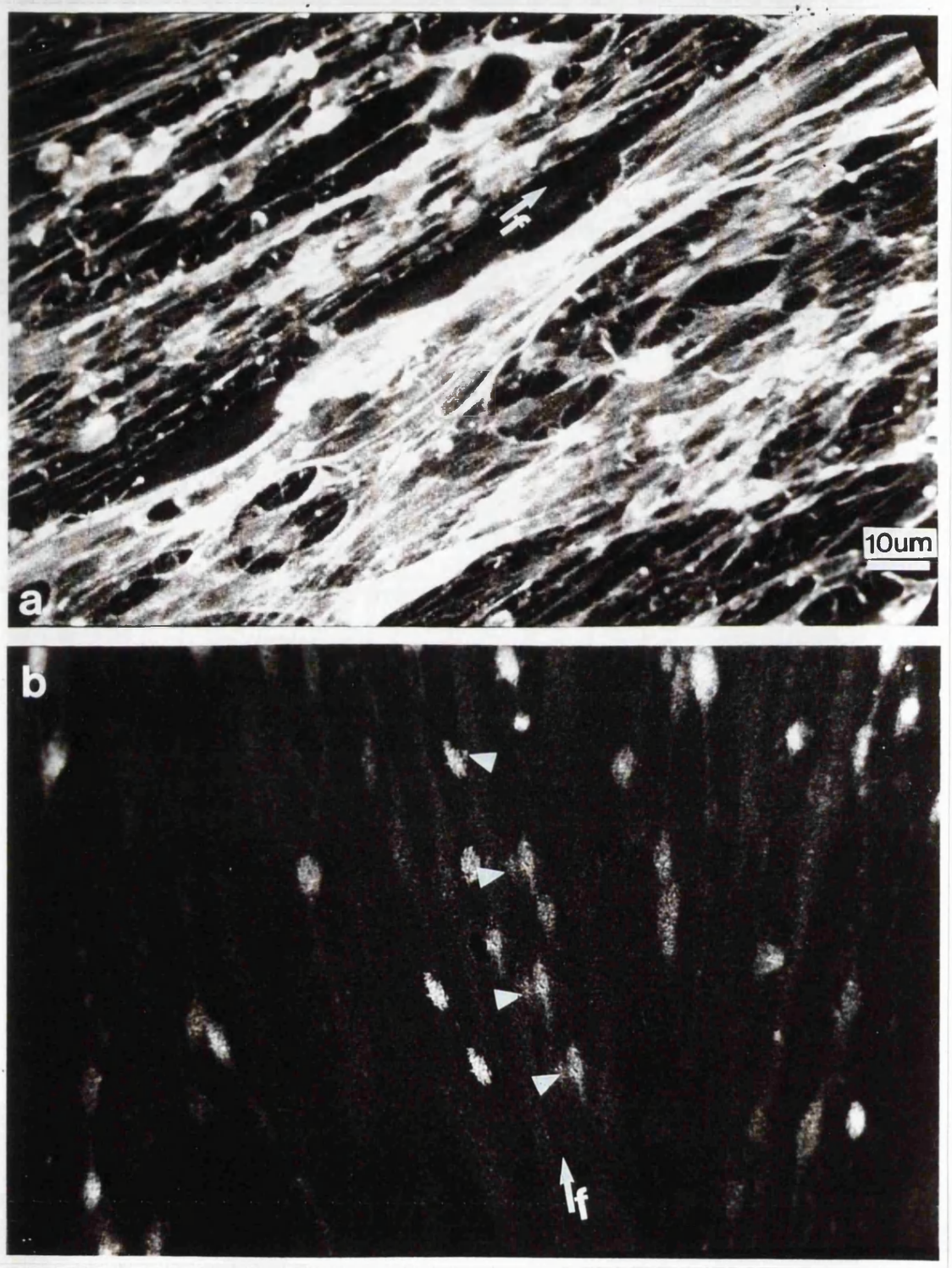

Figure 4.37. *Immunostaining of F-actin and vinculin after 24 hours.* ***(a)*** *F-actin and* ***(b)*** *vinculin distribution in Schwann cells cultured with Fn-fibres. F-actin was aligned to the direction of the Fn-fibre (f: arrow) with cells showing an aligned band upto 50 μm from the Fn-fibre. There were greater number of cells attached to the Fn-fibre forming vinculin-rich condensations along the fibre (Figure 4.37b: arrowheads).*

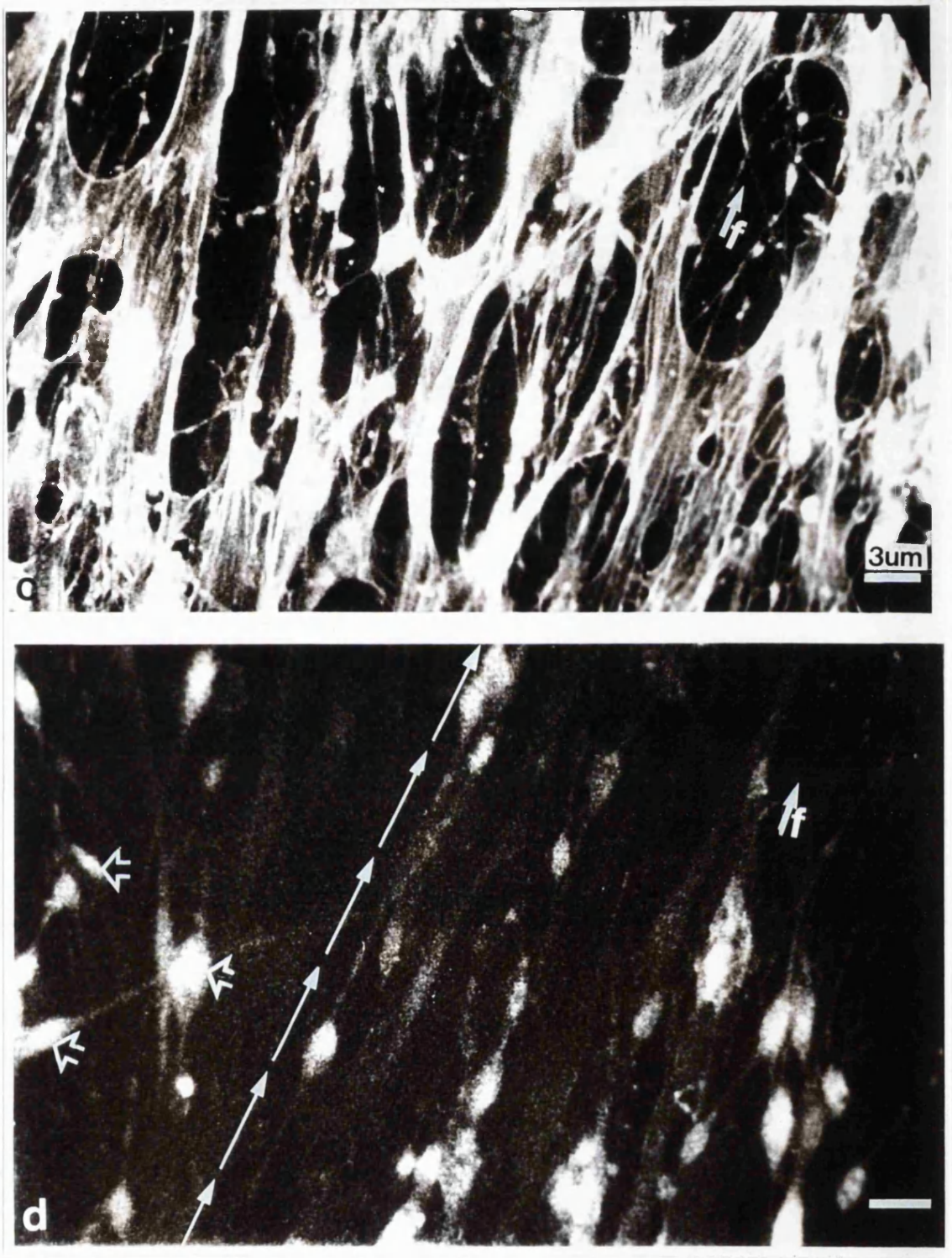

Figure 4.37. ***(c)*** *F-actin and* ***(d)*** *vinculin distribution in cells on Fn-fibres in the aligned cell band. F-actin was aligned in the whole region of the 50 μm cell band to the direction of the fibre (f: arrow). After the cut off line (Figure 4.37d: filled arrows) cells became disorganised (Figure 4.37d: open arrows). b and d use same scale bar as a.*

These results showed that Schwann cells migrated significantly faster on Fn-fibres than on plain substrata with the formation of an aligned band of cells upto 50μM away from the original fibre. F-actin was aligned parallel to the fibre axis of those Schwann cells in contact with the Fn-fibre and also in the region of the alignment band.

4.7. Low Concentrations of Fibrinogen Increase Cell Migration Speed on Fibronectin/Fibrinogen Composite Cables

In this experiment a starting material different to Fn-fibres was used. This comprises Fg as well as Fn. Here, the aim was to modulate cell migration speed by varying the content of Fg within these cables and to work out the optimal concentration of Fg to cause maximum migration speeds. The content of Fg was manipulated and migration speeds were recorded for Schwann cells, human dermal, rat tendon and rat skin fibroblasts. This was correlated to integrated density of fluorescence for vinculin.

4.7.1. Cells in culture on Fn/Fg-cables

Pure Fn-strands were smaller in diameter, typically 50-100 μm, compared to cables which contained Fg which typically measured 200-250 μm, made by the same extrusion method. Schwann cells attached to Fn-strands and Fn/Fg-cables and spread on the culture surface over a period of 4 hours by which time they were bipolar with long protruding filopodia. Cells migrated towards the strands/cables and became aligned with the axis of the strands/cables. By 10 hours many cells were seen to migrate along the same axis as the pure Fn-strand (not shown - similar to Figure 4.32a and b in section 4.6.). Whereas Schwann cells cultured on larger Fn/Fg-cables populated the top of the cable and migrated along the same axis as the cable (Figure

4.38b and c). In contrast Schwann cells plated on plain glass migrated in a haphazard way (Figure 4.38a). (Other ratios of Fn:Fg-cables were similar in appearance to b and c and therefore not shown). Human dermal, rat tendon and rat tail fibroblasts behaved in an almost identical way (not shown).

4.7.2. Speed of cell migration on Fn/Fg-cables

The speed of Schwann cell, human dermal, rat tendon and rat skin fibroblast movement over a 10 hour time period on Fn/Fg-cables is shown Figure 4.39. As the concentration of Fg is increased Schwann cells migrated faster compared to pure Fn-strand, with the peak velocity of 49 ± 0.8 μm/hour at 50% Fg/50% Fn concentration in the composite cable ($p<0.0061$). Higher concentrations of Fg in the composite cable hindered cell migration from that which cause maximal cell migration speed, such that in the 75% Fg composite, the mean velocity fell significantly to 35.1 ± 1.1 μm/hr ($p<0.0001$).

Human dermal, rat tendon and rat skin fibroblasts migrated in a very similar fashion although Schwann cells migrate significantly faster than these cell types on such Fn/Fg-cables. The increase in velocity (0-50% Fg) was 1.44 fold for Schwann cells and 1.45 fold for human dermal fibroblasts. The increases in velocity were statistically significant ($p<0.00001$ for Schwann cell on 50% Fg vs 0% Fg; $p<0.00001$ for human dermal fibroblasts on 50% Fg vs 0% Fg) and also peak velocity (50% Fg) was significantly greater for Schwann cells than fibroblasts ($p<0.0001$ for Schwann cell vs human dermal fibroblasts at 50% Fg ratio). However, by 73% Fg ratio, all cell types migrated at around the same velocity.

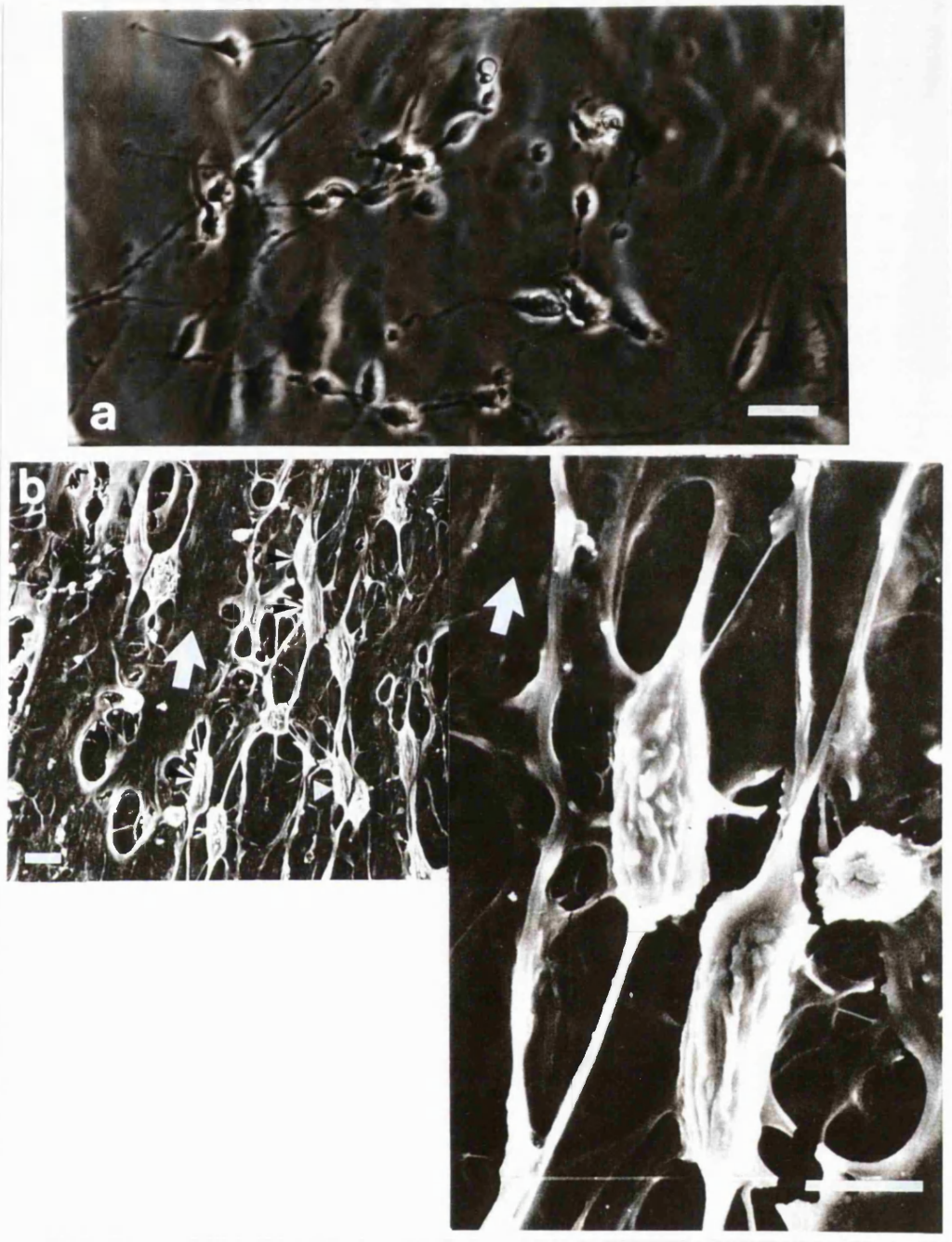

Figure 4.38. *Schwann cells cultured on different concentrations of Fg. (a) shows phase contrast micrograph of Schwann cells cultured plain glass substrata (coated with 1% BSA as control), showing that Schwann cells did not have any predominant orientation. (b) SEM to show low and inset: high magnification of Schwann cells cultured on 50% Fn:Fg-cable. These showed that Schwann cells (arrowheads) populated the top surface of the cable which assumed a parallel orientation to the cable (cable orientation indicated by thick arrow) Scale bar in a = 20μm, b = and c = 10μm.*

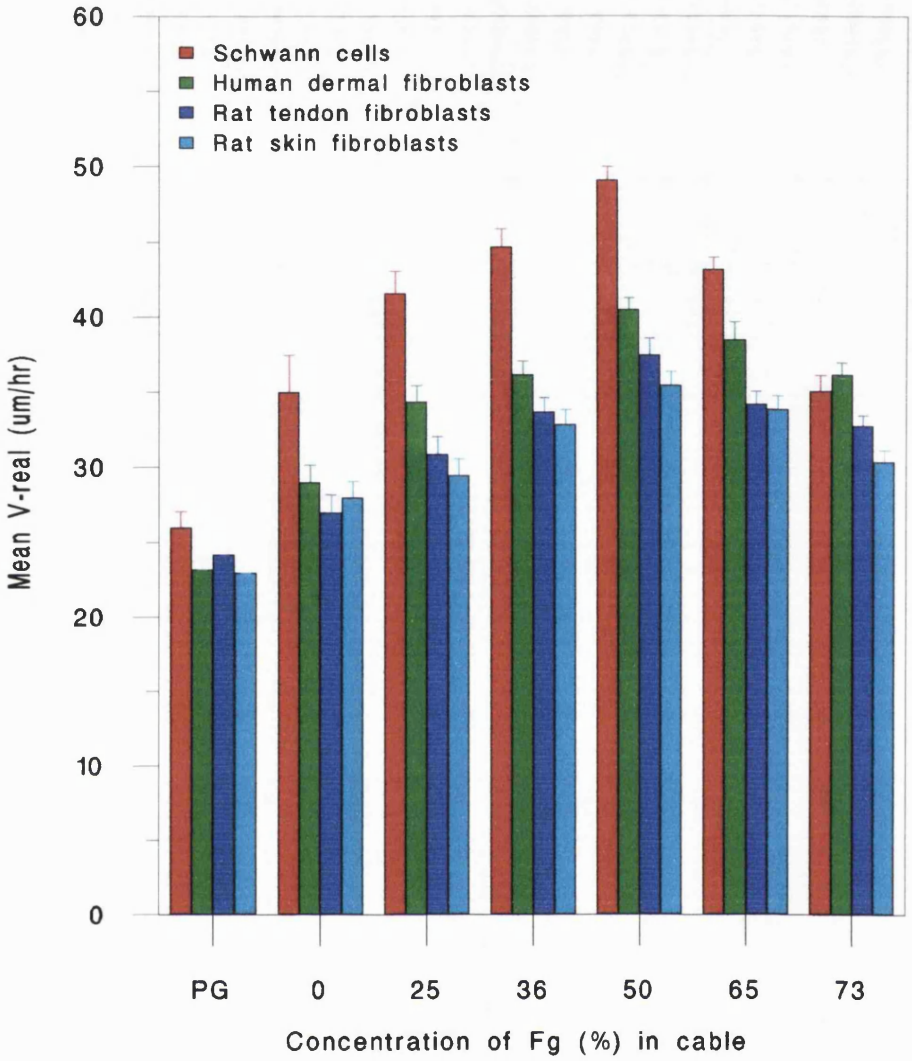

Figure 4.39. The mean speed of cell migration on Fn/Fg-cables. As the proportion of fibrinogen (Fg) increased, the mean cell velocity also increased upto a maximum where the substrate concentration ratio was 1:1 (50:50 Fn:Fg). After this point the cell velocity reduced. (Number of determination/ratio = 8). PG= plain glass but coated with 1% BSA as control.

4.7.3. Cell spreading

At maximum migration speed (49 μm/hr on 50% Fn/Fg-strand) Schwann cells were moderately well spread and extended on Fn/Fg-cables and moved by extending

filipodia in the direction of migration (Figure 4.40 and 4.41). At lower Fg concentrations cells were more spread although they still exhibited a bipolar morphology. Above the Fn/Fg ratio required for maximum cell migration, Schwann cells were less well spread than those at maximum cell migration Fn/Fg ratio. Human dermal, rat tail and skin fibroblasts behaved in a similar way (Figure 4.40 and 4.41).

4.7.4. Cell adhesion to Fn/Fg-strands

Cell adhesion to coated glass substrata with the varying concentration of Fg and Fn showed that all types of cells were able to attach to the substrata with low concentrations of Fg coating. However, significantly fewer numbers of cells were attached to the 64% Fg coated substrata with even fewer numbers attached at the 75% Fg coating concentration (Table 4.7). A similar effect was seen with cells cultured on different Fn/Fg-ratios of cables but much fewer cells were attached to the strands due to their relative surface area (not shown).

4.7.5. Imunolocalisation of vinculin

Fluorescence of vinculin attachment sites were integrated using a computer software package attached to the confocal microscope. For cells attached to Fn/Fg-cables, only fluorescence derived from the attachment plaques were measured (immunostaining of vinculin similar to that in Section 4.6.). These results showed that mean integrated fluorescence per cell of any of the populations studied, was greatest for cells in contact with pure Fn-fibres (Figure 4.42), with the lowest fluorescence seen for cells on plain glass substrata. As the concentration of fibrinogen was increased, a dose dependent decrease in mean integrated fluorescence/cell was observed for each of the different

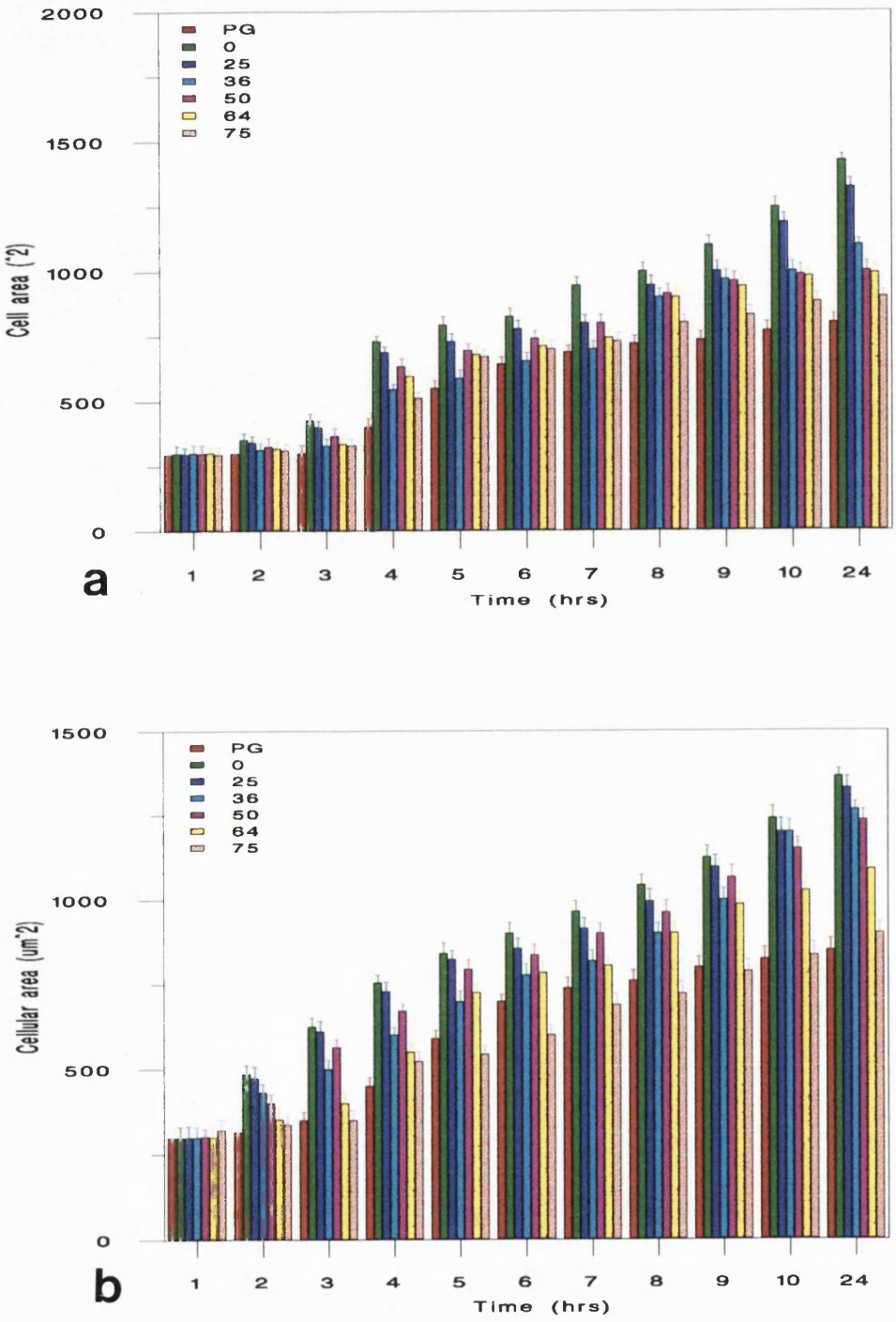

Figure 4.40. *Changes in cell spread area over time on increasing the concentration of Fg in Fn/Fg-cables. The cells were able spread more with increasing concentrations of Fg in a dose dependent manner. However, above 50:50 Fn:Fg, there is a reduction in cell spread area. (a) Schwann cells and (b) human dermal fibroblasts.*

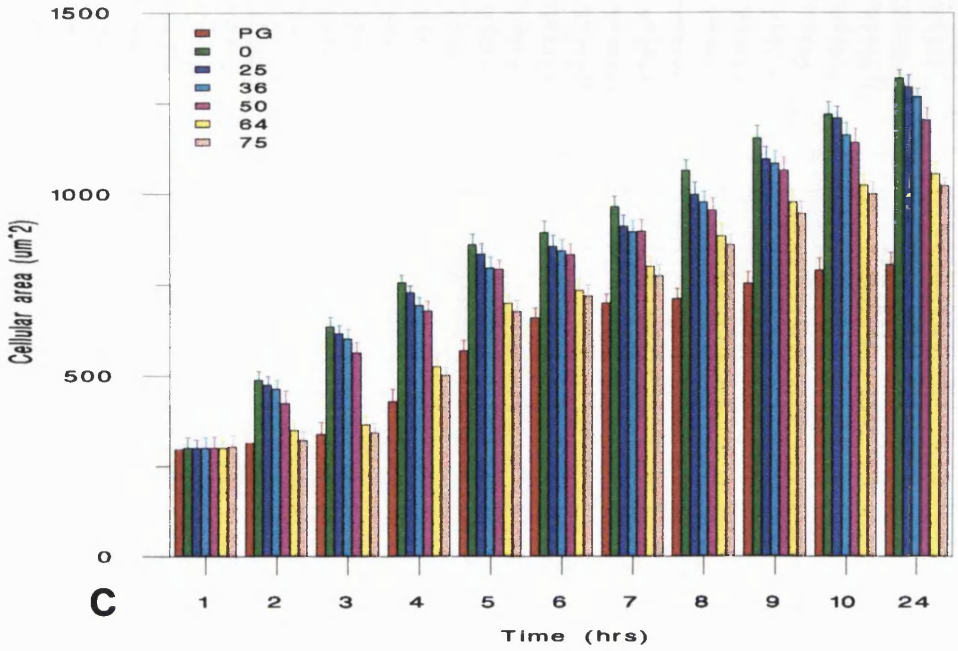

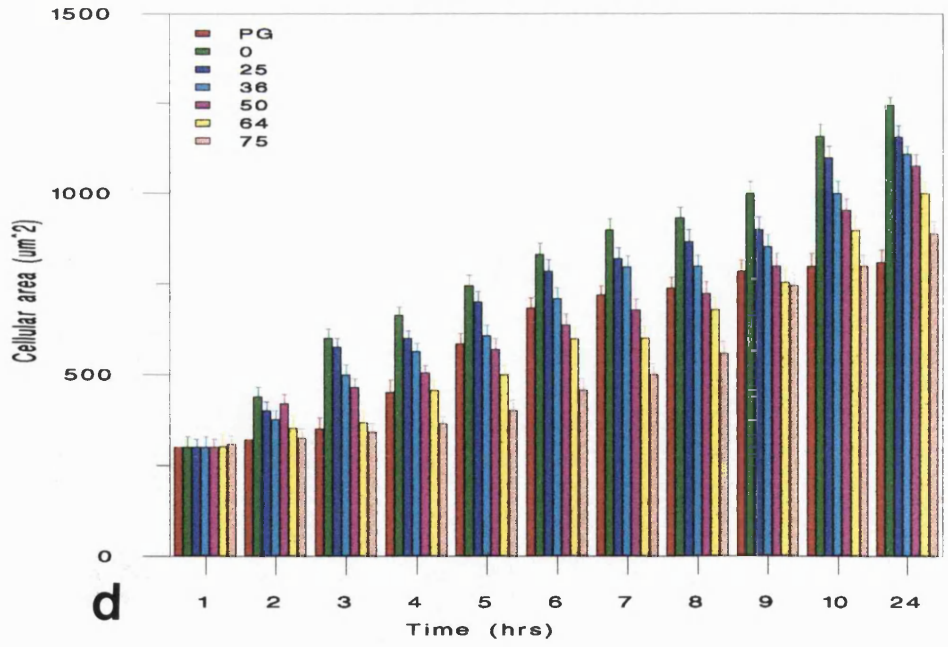

Figure 4.40. *(c) rat skin and (d) rat tendon fibroblasts.*

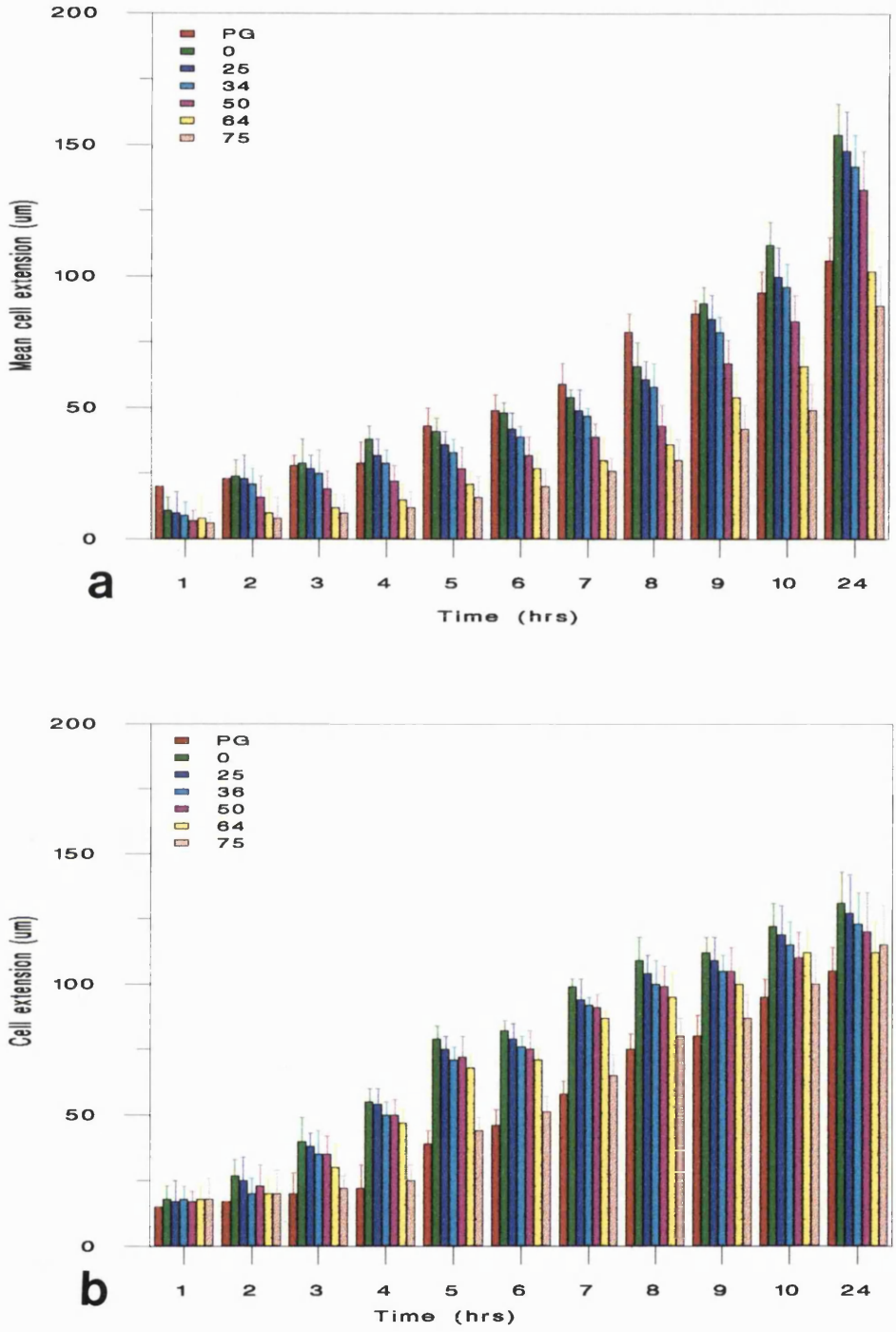

Figure 4.41. *Changes in cell extension over time on increasing the concentration of Fg in Fn/Fg-cables. The cells were able extend more with increasing concentrations of Fg in a dose dependent manner. However, above 50:50 Fn:Fg, there is a reduction in cellular extension. Cell extension for (a) Schwann cells (b) human dermal fibroblasts.*

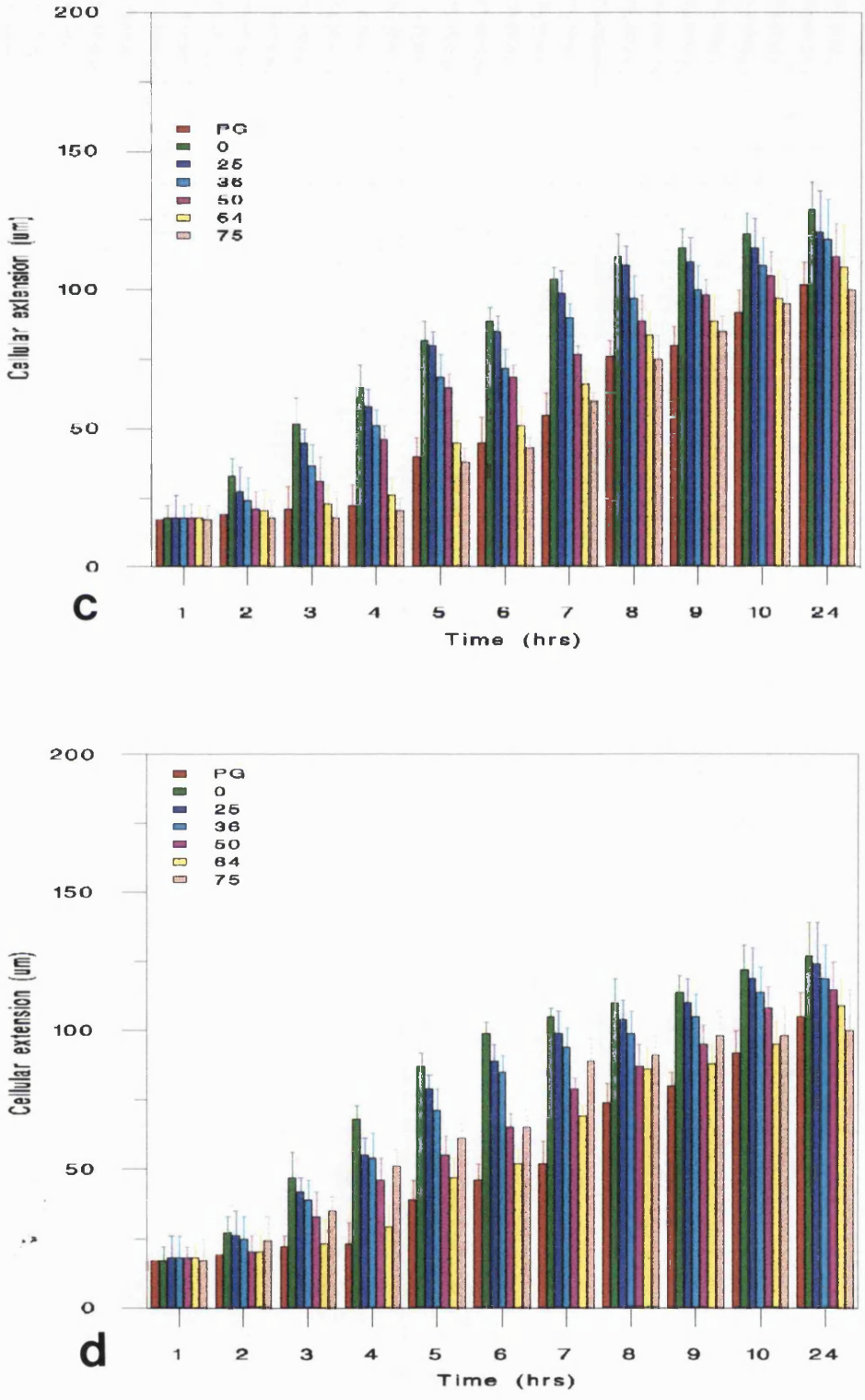

Figure 4.41. *(c) Rat skin fibroblasts and (d) rat tendon fibroblasts.*

Conc. of Fg (%)	Sc's	HDF's	RTF's	RSF's
PG	197,000 ± 2,309	199,800 ± 2,394	198,903 ± 2,109	198,345 ± 2,030
0	198,000 ± 1,209	199,765 ± 1,098	199,843 ± 1,190	199,000 ± 1,892
25	199,245 ± 1,309	199,354 ± 1,390	198,453 ± 1,290	198,002 ± 2,100
36	198,876 ± 1,200	198,980 ± 1,456	198,800 ± 2,987	197,900 ± 2,109
50	199,363 ± 1,105	198,900 ± 1,328	198,878 ± 1,354	199,045 ± 2,3054
64	*159,034 ± 1,293	*178,908 ± 1,100	*168,901 ± 1,986	*174,092 ± 1,789
75	**1,090 ± 900	**2,348 ± 756	**1,987 ± 876	**1,876 ± 926

Table 4.7. *The mean (± s.d., n=10) number of cells attached to different coating concentrations of Fg over a period of 10 hours. PG = plain glass but coated with 1% BSA, Sc = Schwann cells, HDF = human dermal fibroblasts, RTF = rat tendon fibroblasts and RSF = rat skin fibroblasts. As few as 0.5% of control cell attachment was supported on glass coverslips coated with 75% Fg. *p<0.00 for all cells grown on 64% Fg vs those grown on PG and 0-50% Fg; **p<0.00001 for all cells grown on 75% Fg vs those grown on PG and 0-50% Fg.*

types of cells. Schwann cells seemed to utilise fewer vinculin attachment sites than human dermal, rat tendon and rat skin fibroblasts but this is due to the relative differences in size, Schwann cells being smaller.

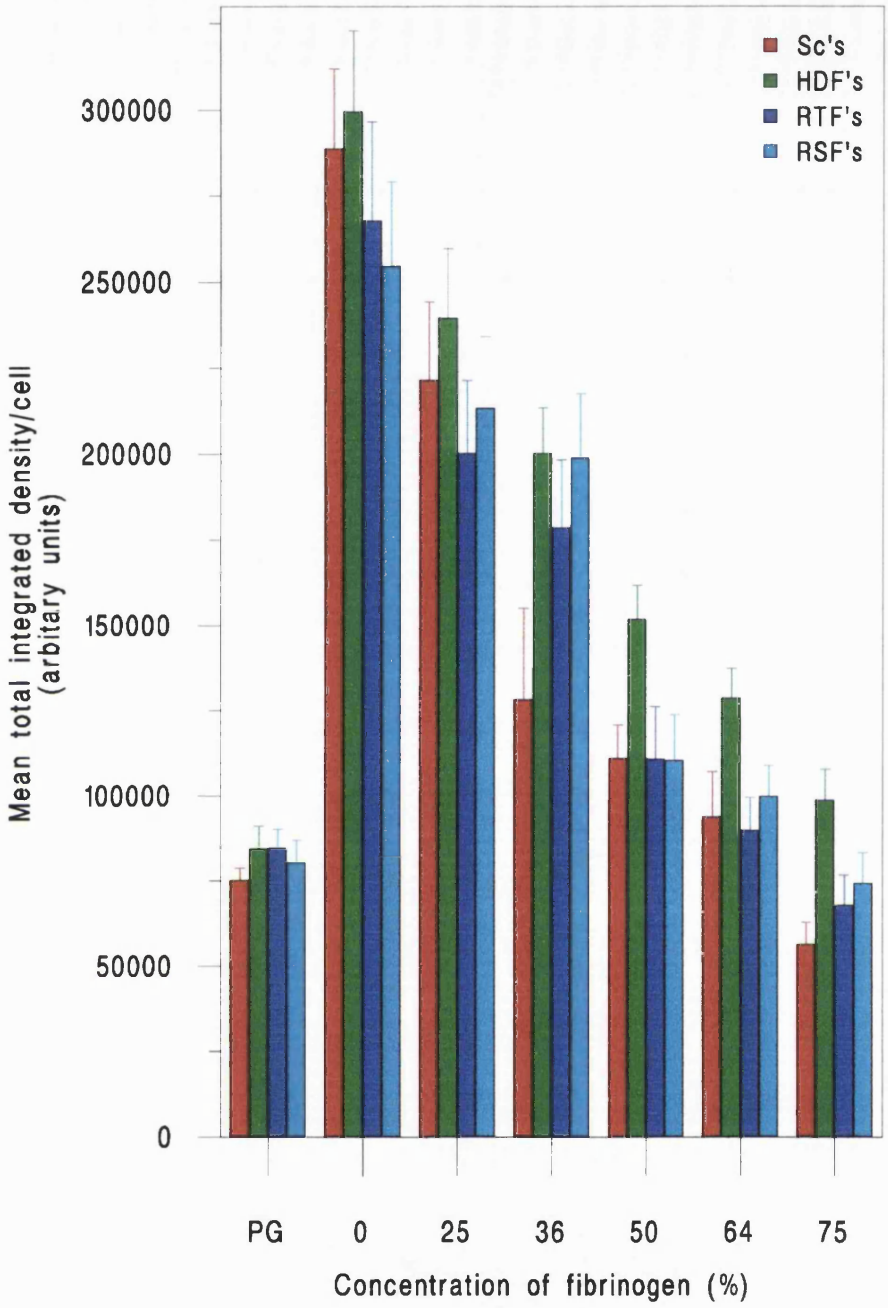

Figure 4.42. Mean integrated fluorescence per cell to represent the intensity of vinculin immunostaining with increasing concentrations of Fg in Fn/Fg-cables. Integrated fluorescence is directly proportional to the number of focal adhesions. As the concentration of Fg increases the number of vinculin attachment points increases for each cell type in a similar way upto a maximum on 50:50 Fn:Fg but thereafter vinculin intensity reduces.

The results in this section show that the speed of cell migration can be manipulated by varying the content of Fg in Fn/Fg-cables. Maximum cell migration occurred at a 1:1 ratio of Fn:Fg. This may represent an intermediate ligand concentration where cells do not stick too heavily that they are unable to break off attachments at the rear and attach enough to be able to exert tractional forces inorder to migrate. The integrated density of fluorescence of vinculin immunostaining could be correlated with the speed of cell migration. Where high amounts of vinculin immunostaining was detected (i.e. pure Fn-strands), cells migrated slowest upto an optimal migration level. Where a very low amount of vinculin immunostaining was detected, cell migration was hindered. This is due to cells being unable to form enough stable attachments to the substrata (i.e. 'slippery surface').

4.8. Increased Cell Migration and Alignment on Fibronectin Strands and Cables After Stabilisation with Micromolar Concentrations of Copper

The aim of this experiment was two-fold. In the first instance, Fn-strands and cables need to be stabilised for longer survival in vitro or in vivo. Secondly, the aim was to speed up cell migration by blocking off some of the highly adhesive sites with copper ions. Fn-strands and cables were treated with micromolar concentrations of copper and protein dissolution assessed as before. Cell migration speed was correlated with vinculin immunostatining by image analysis of time-lapse video micrographs and vinculin immunostaining.

4.8.1. Copper stabilisation of Fn-strands and Fn-cables

Fn-strands and Fn-cables, chelate copper almost immediately from a copper sulphate solution (CuFn-fibres), chelate copper almost immediately and became visibly blue, when viewed under a dissecting microscope (10 minute treatment in 200μM copper sulphate (Chapter 4.1.). As shown previously Fn-strands were approximately twice as stable to dissolution than untreated Fn-strands (Figure 4.43a and b). However, overall loss of protein (dissolution) from Fn-cables treated with 200μM Cu^{2+} was less than that observed with the same concentration of copper treated Fn-strands (Figure 4.43b). Parallel assessment of stability at 37°C indicated a similar response to treatment with copper (Figure 4.44a and b). The greatest protein dissolution occurred after 24 hours and by day 7 protein loss from Fn-strands ranged from 26 to 24% (treatments with 1-200μM Cu^{2+}) in contrast to control Fn-fibres with 42% protein dissolution. Protein dissolution from Fn-cables ranged from 31 to 22% (treatments with 1-200μM Cu^{2+}) in contrast to control Fn-cables with 55% protein dissolution.

4.8.2. Measurement of the speed of cell movement on glass, Fn and CuFn-strands/cables.

The appearance of cells in culture on Fn-strands and cables do not differ to that already shown in this thesis. The speed of cell movement, persistence parameter (Pr), cell path, total cell translocation (T) and number of stoppages (N) over a period of 10 hours in culture with Fn-strands and Fn-cables are shown in Table 4.8, Table 4.9 and graphically in Figure 4.45 and 4.46, respectively. Schwann cells, human dermal, rat tendon and rat skin fibroblasts moved significantly faster on Fn-strands compared to plain glass substrata ($p<0.0001$). The speed of cell movement was significantly greater

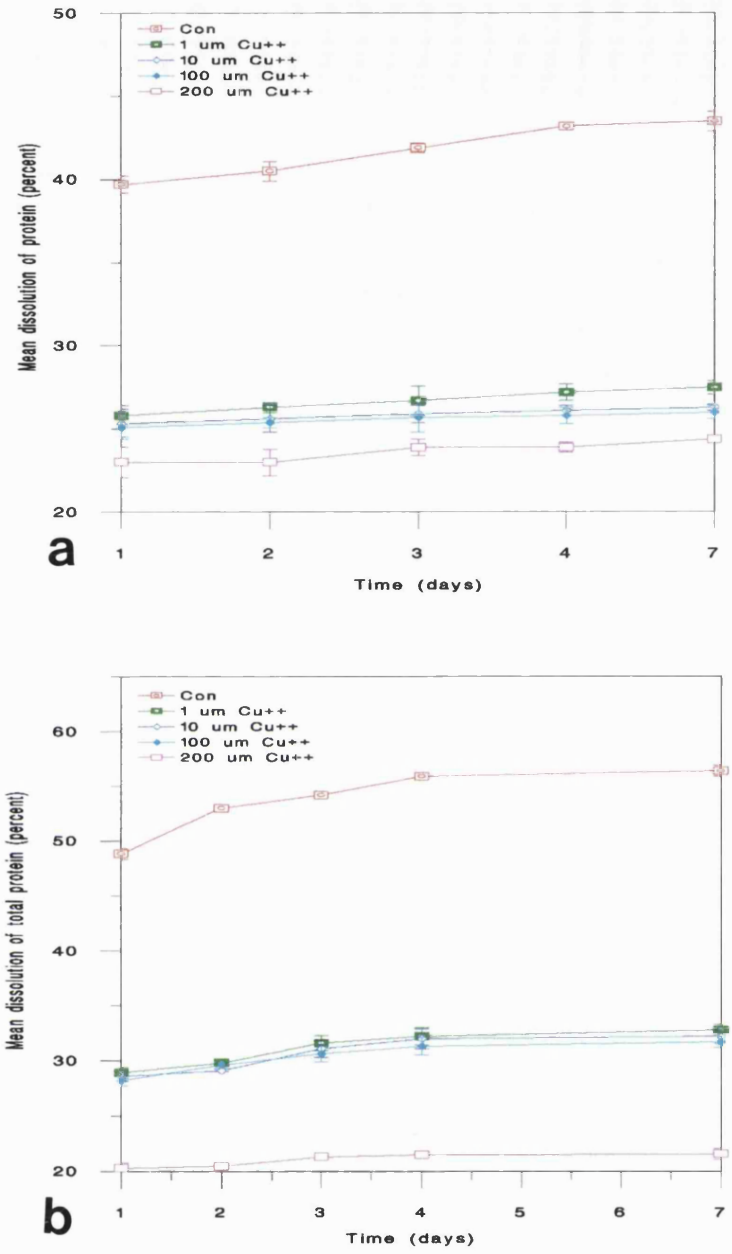

Figure 4.43. *Dissolution of Fn-protein from (a) Fn-strands and (b) Fn-cables at room temperature upon treatment with copper ions (n=10 / treatment). The lowest treatment of copper produced strands which were twice as stable as control untreated strands. Increasing concentrations of copper caused a dose dependent increase in stability of Fn-strands. However, increasing the concentration of copper treatment on Fn-cables caused a minimal amount of stability upto 100μM copper treatment. 200μM copper treatment however, caused a significant increase in stability.*

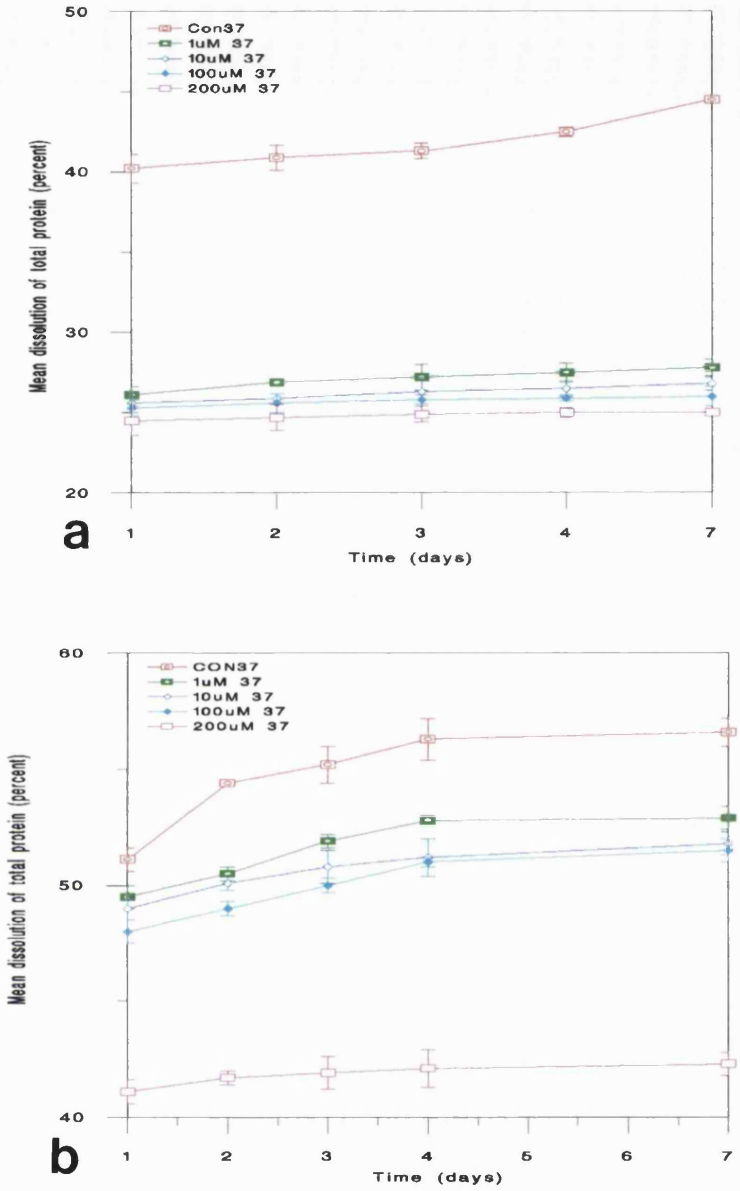

Figure 4.44. *Dissolution of Fn-protein from (a) Fn-strands and (b)Fn-cables at 37°C upon treatment with copper ions (n= 10 / treatment). The lowest treatment of copper produced strands which were twice as stable as control untreated strands. Increasing concentrations of copper caused a dose dependent increase in stability for Fn-strands. There was a minimal increase in stability of Fn-cables with treatments of copper upto 100μM, however, treatment of the cables with 200μM copper caused a significant increase in stability, similar to that observed at room temperature .*

on Fn-strands + 1μM copper compared to plain Fn-strands ($p<0.001$) while reducing the number of times cells remain stationery, denoted by N in Table 4.8 and 4.9. Increasing concentrations of copper further increased the speed of cell movement on Fn-strands however, these failed to reach statistical significance.

Cell migration on Fn-cables followed a similar pattern to that observed for migration on Fn-strands. However, migration speeds for all cell types were generally faster on Fn-cables compared to that on Fn-strands. Schwann cells migrated significantly faster on Fn-cables than Fn-strands reaching a peak migration speed of 46μm/hr ($p<0.0025$). Peak migration speed for Schwann cells on both Fn-strands and cables was reached with 10μM treatment of copper. Total cell translocation represented by T in table 4.8 and 4.9 was greatest for cells plated on copper treated Fn-cables than on Fn-strands. Movement of cells, denoted by cell path in Table 4.8 and 4.9, was greatest for cells at treatment concentrations of Fn-strands and cables which caused maximal cell migration speeds.

Schwann cells were only able to survive upto 50μM copper treatment as higher concentrations were toxic. In contrast human dermal, rat tendon and rat skin fibroblasts were able to survive with the highest treatment of copper and reach a peak cell speed on Fn-strands with 100 μM copper treatment on Fn-strands. Beyond this point there was a loss in cell speeds. Maximal cell speed on Fn-cables was reached after treatment of the cables with 10 μM copper. Again after this point there was a reduction in cell migration speeds.

Substrata	V_{real} (μm/hr)	$V_{effective}$ (μm/hr)	Cell Path (μm)	T (μm)	Pr	N
Schwann cells						
Control (plain glass)	19 ± 5	12 ± 3	90 ± 17	69 ± 25	0.75	4 ± 3
BPL Fn-strand	35 ± 2.7	35 ± 2.7	350 ± 27	350 ± 27	1	0
Fn-strand + 1μM Cu^{2+}	41 ± 1.5	41 ± 1.5	412 ± 15	412 ±15	1	0
Fn-strand + 10μM Cu^{2+}	42 ± 1.1	42 ± 1.1	421± 12	421 ± 12	1	0
Fn-strand + 50μM Cu^{2+}	42 ± 1.1	42 ± 1.1	421± 12	421 ± 12	1	0
Human dermal fibroblasts						
Control (plain glass)	15 ± 5	9 ± 3	80 ± 20	59 ± 22	0.65	4 ± 3
Fn-strand	29 ± 7	29 ± 5	205 ± 50	205 ± 50	0.89	2 ± 1
Fn-strand + 1μM Cu^{2+}	33 ± 10	33 ± 8	332 ± 29	332 ± 35	0.92	3 ± 2
Fn-strand + 10μM Cu^{2+}	36 ± 9	36 ± 8	360 ± 39	365 ± 25	0.93	3 ± 1
Fn-strand + 50μM Cu^{2+}	38 ± 5	38 ± 6	382 ± 26	385 ± 22	0.93	3 ± 1
Fn-strand + 100μM Cu^{2+}	40 ± 6	39 ± 6	402 ± 26	400 ± 22	0.95	2 ± 1
Fn-strand + 150μM Cu^{2+}	39 ± 5	39 ± 6	392 ± 21	395 ± 23	0.94	2 ± 1
Fn-strand + 200μM Cu^{2+}	36 ± 5	36 ± 8	362 ± 39	361 ± 25	0.91	4 ± 2
Rat tendon fibroblasts						
Control (plain glass)	13 ± 5	10 ± 3	75 ± 10	55 ± 12	0.67	4 ± 3
Fn-strand	27 ± 10	16 ± 10	160 ± 25	150 ± 50	0.90	3 ± 2
Fn-strand + 1μM Cu^{2+}	28 ± 14	18 ± 12	190± 25	180 ± 32	0.92	3 ± 1
Fn-strand + 10μM Cu^{2+}	30 ± 10	25 ± 8	300 ± 39	295 ± 25	0.93	2 ± 1
Fn-strand + 50μM Cu^{2+}	31 ± 5	28 ± 6	315 ± 22	305 ± 32	0.94	2 ± 1
Fn-strand + 100μM Cu^{2+}	33 ± 16	29 ± 10	335 ± 22	309 ± 12	0.95	2 ± 1
Fn-strand + 150μM Cu^{2+}	30 ± 6	25 ± 6	301 ± 32	293 ± 20	0.94	2 ± 1
Fn-strand + 200μM Cu^{2+}	28 ± 5	22 ± 8	282 ± 39	261 ± 25	0.91	4 ± 2
Rat skin fibroblasts						
Control (plain glass)	12 ± 8	12 ± 3	78 ± 10	58 ± 12	0.66	4 ± 3
BPL Fn-strand	26 ± 10	18 ± 6	180 ± 40	97 ± 27	0.48	4 ± 2
Fn-strand + 1μM Cu^{2+}	32 ± 5	20 ± 9	200 ± 20	200 ± 24	0.65	2 ± 1
Fn-strand + 10μM Cu^{2+}	33 ± 9	28 ± 8	333 ± 29	295 ± 15	0.93	2 ± 1
Fn-strand + 50μM Cu^{2+}	34 ± 8	30 ± 4	345 ± 22	305 ± 22	0.94	2 ± 1
Fn-strand + 100μM Cu^{2+}	35 ± 6	33 ± 10	350 ± 12	331 ± 22	0.95	2 ± 1
Fn-strand + 150μM Cu^{2+}	32 ± 6	28 ± 9	320 ± 22	293 ± 10	0.94	2 ± 1
Fn-strand + 200μM Cu^{2+}	29 ± 6	25 ± 8	290 ± 29	245 ± 21	0.91	3 ± 2

Table 4.8. Movement of Schwann cells, human dermal fibroblasts, rat tendon fibroblasts and rat skin fibroblasts on plain glass, Fn-strands and Fn-strands stabilised with different concentrations of copper ions, over a period of 10 hours. ($V_{real} = V_{effective}$ when $N = 0$ and $Pr = 1$).

Substrata	V_{real} (μm/hr)	$V_{effective}$ (μm/hr)	Cell Path (μm)	T (μm)	Pr	N
Schwann cells						
Control (plain glass)	17 ± 5	13 ± 5	90 ± 12	65 ± 15	0.77	3 ± 2
Fn-cable	39 ± 2.5	39 ± 2.2	391 ± 12	391 ± 12	1	0
Fn-cable + 1μM Cu^{2+}	45 ± 2.9	45 ± 2.7	452 ± 25	452 ± 25	1	0
Fn-cable + 10μM Cu^{2+}	46 ± 2	46 ± 2	460 ± 23	460 ± 23	1	0
Fn-cable + 50μM Cu^{2+}	40 ± 2	40 ± 2	400 ± 23	400 ± 23	1	0
Human dermal fibroblasts						
Control (plain glass)	15 ± 8	12 ± 3	78 ± 10	58 ± 12	0.64	4 ± 3
Fn-cable	33 ± 5	32 ± 5	330 ± 20	327 ± 20	0.75	2 ± 1
Fn-cable + 1μM Cu^{2+}	37 ± 10	37 ± 9	370 ± 20	359 ± 10	0.93	2 ± 1
Fn-cable + 10μM Cu^{2+}	42 ± 5	39 ± 8	382 ± 39	400 ± 25	0.94	3 ± 1
Fn-cable + 50μM Cu^{2+}	40 ± 5	39 ± 8	402 ± 22	395 ± 22	0.95	2 ± 1
Fn-cable +100μM Cu^{2+}	39 ± 8	39 ± 6	425 ± 20	369 ± 12	0.96	2 ± 1
Fn-cable +150μM Cu^{2+}	37 ± 5	39 ± 6	392 ± 21	359 ± 23	0.94	2 ± 1
Fn-cable +200μM Cu^{2+}	35 ± 10	35 ± 9	372 ± 20	355 ± 10	0.93	2 ± 1
Rat Tendon fibroblasts						
Control (plain glass)	16 ± 5	13 ± 3	79 ± 10	62 ± 10	0.64	4 ± 3
Fn-cable	30 ± 6	19 ± 5	293 ± 10	203 ± 10	0.81	2 ± 1
Fn-cable + 1μM Cu^{2+}	36 ± 5	36 ± 7	358 ± 20	350 ± 12	0.93	2 ± 1
Fn-cable + 10μM Cu^{2+}	40 ± 5	33 ± 5	368 ± 29	362 ± 15	0.94	3 ± 1
Fn-cable + 50μM Cu^{2+}	38 ± 5	34 ± 8	391 ± 12	355 ± 12	0.95	2 ± 1
Fn-cable +100μM Cu^{2+}	37 ± 5	36 ± 6	405 ± 10	342 ± 22	0.96	2 ± 1
Fn-cable +150μM Cu^{2+}	35 ± 4	35 ± 6	392 ± 21	335 ± 13	0.94	2 ± 1
Fn-cable +200μM Cu^{2+}	34 ± 9	34 ± 5	371 ± 20	335 ± 10	0.93	2 ± 1
Rat skin fibroblasts						
Control (plain glass)	15 ± 8	12 ± 3	80 ± 9	65 ± 10	0.65	4 ± 3
Fn-cable	29 ± 12	25 ± 5	293 ± 20	212 ± 15	0.83	2 ± 1
Fn-cable + 1μM Cu^{2+}	36 ± 5	36 ± 7	358 ± 20	350 ± 12	0.93	2 ± 1
Fn-cable + 10μM Cu^{2+}	39 ± 5	33 ± 5	368 ± 29	355 ± 15	0.94	3 ± 1
Fn-cable + 50μM Cu^{2+}	38 ± 5	34 ± 5	378 ± 22	347 ± 25	0.94	3 ± 1
Fn-cable +100μM Cu^{2+}	37 ± 5	34 ± 8	391 ± 12	340 ± 12	0.95	2 ± 1
Fn-cable +150μM Cu^{2+}	36 ± 4	35 ± 6	391 ± 11	335 ± 15	0.94	2 ± 1
Fn-cable +200μM Cu^{2+}	35 ± 9	35 ± 5	375 ± 10	325 ± 10	0.93	2 ± 1

Table 4.9. Movement of Schwann cells, human dermal fibroblasts, rat tendon fibroblasts and rat skin fibroblasts on plain glass, Fn-cables and Fn-cables stabilised with different concentrations of copper ion. ($V_{real} = V_{effective}$ when N= 0 and Pr=1).

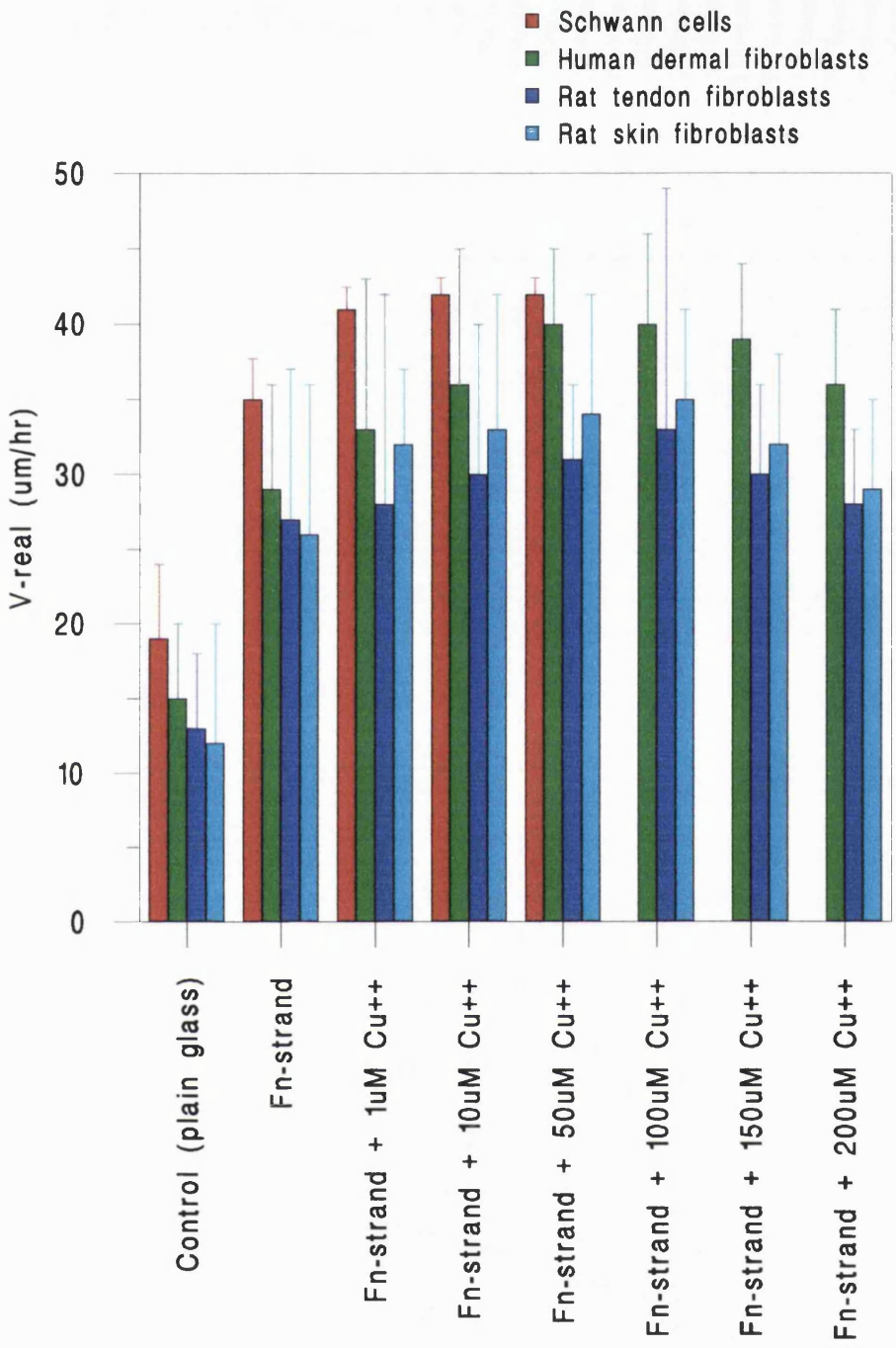

Figure 4.45. *The mean speed of cell migration after stabilisation of Fn-strands by copper ions. Peak cell migration for fibroblasts is reached at 100 μM copper concentration. Concentrations above 50 μM copper are is toxic to Schwann cells.*

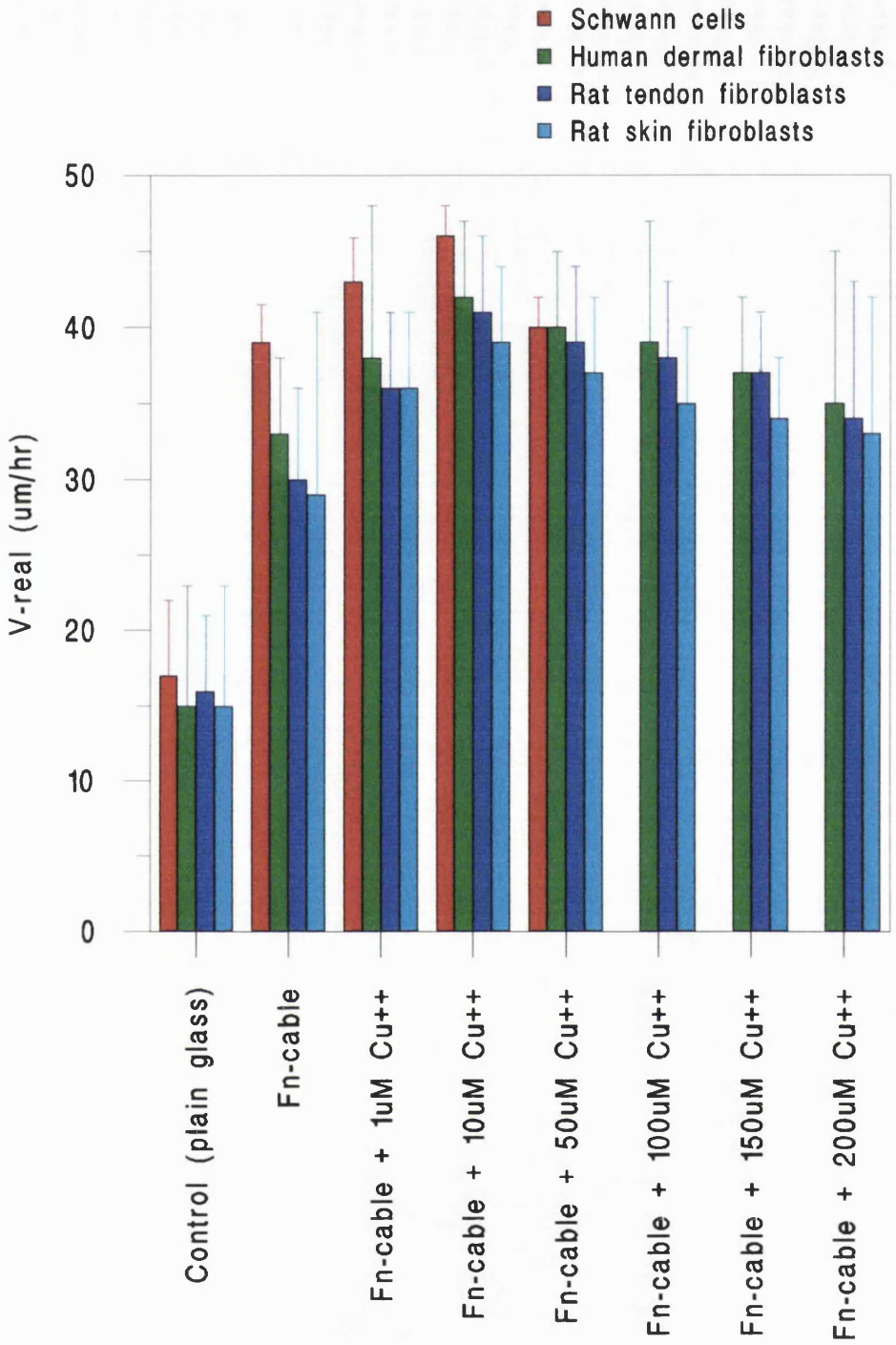

Figure 4.46. *The mean speed of cell migration after stabilisation of Fn-cables by copper ions. Peak cell migration for fibroblasts is reached at 100 μM copper concentration. Concentrations above 50 μM copper are is toxic to Schwann cells.*

Persistence (Pr), a measure of cell movement increased significantly when cells were grown with Fn-fibres compared to plain glass ($p<0.0001$). Pr further increased when cells were plated with copper incorporated Fn-fibres compared to plain Fn-fibres ($p<0.0001$). Cells migrating on Fn-cables generally made fewer stops during migration compared to those on Fn-strands.

4.8.3. Cell spreading on glass, Fn-strands/cables and CuFn-strands/cables

Cells cultured on Fn-strands and Fn-cables adhered to the strands/cables and spread rapidly. Once cells were migrating along and on Fn-strands and cables, cellular extension (Figure 4.47: Fn-strands and 4.48: Fn-cables) and cellular area (Figure 4.49: Fn-strands and 4.50: Fn-cables) increased when compared to plain glass substrata. As the concentration of copper ions increased, cellular extension and area both decreased with time in a dose dependent manner. Maximal cellular area and cellular extension was seen for cells grown on plain Fn-strands and cables compared to copper treated fibres. Cells generally spread less on untreated and copper treated Fn-cables when compared with equally untreated or treated Fn-strands.

4.8.4. Integrated density measurements for vinculin immunostaining

Integrated density measurements, to represent the relative number of vinculin-mediated attachments to the substratum showed that upon increased concentration of copper, vinculin density decreased (Figure 4.51 and 4.52). The greatest integrated density was observed for cells on plain Fn-strands with the lowest value for cells migrating on 200μM copper treated Fn-strands. Integrated fluorescence was less for cells migrating

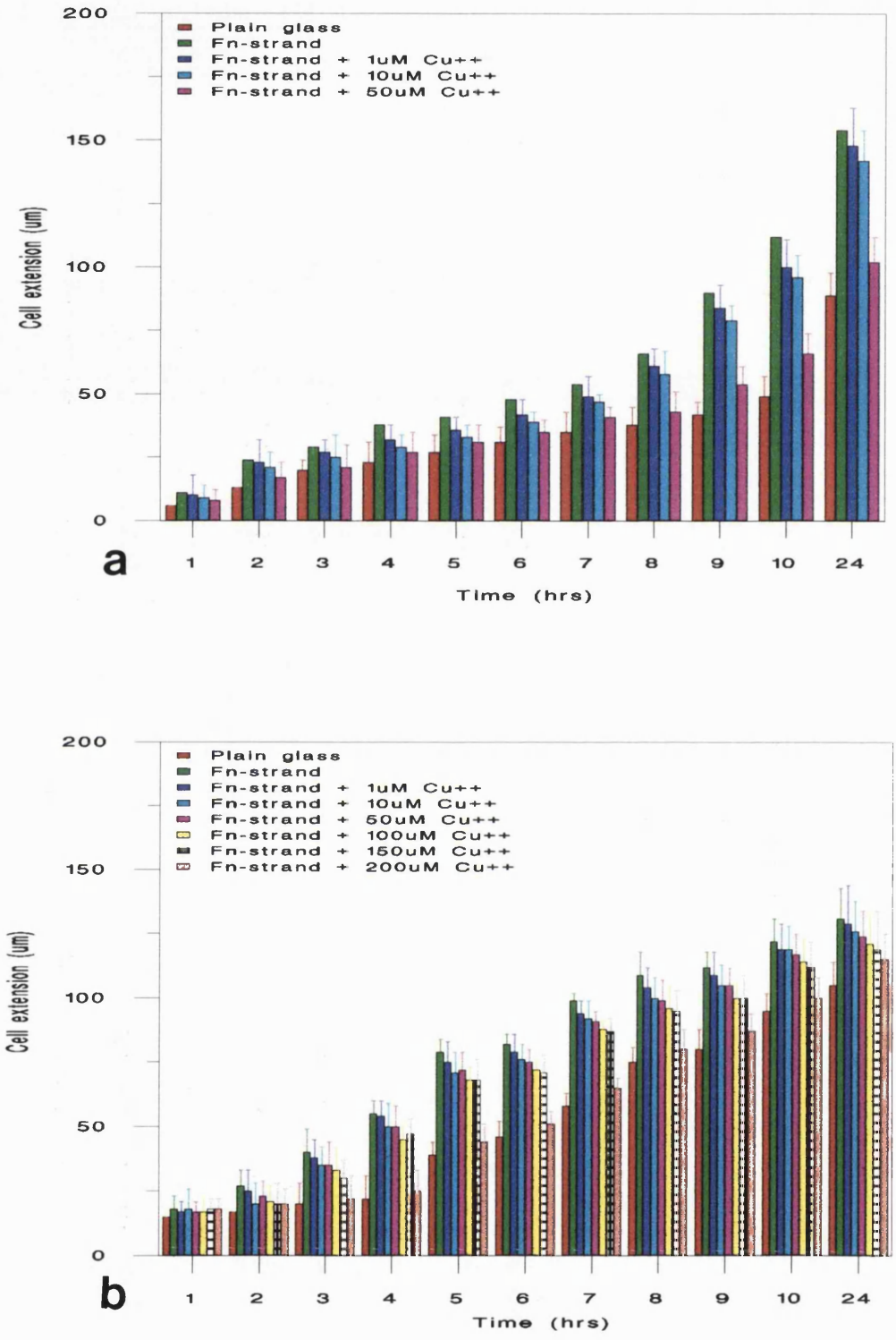

Figure 4.47. *Changes in cellular extension over time on CuFn-strands. Mean cellular extensions for (a) Schwann cells (b) human dermal fibroblasts.*

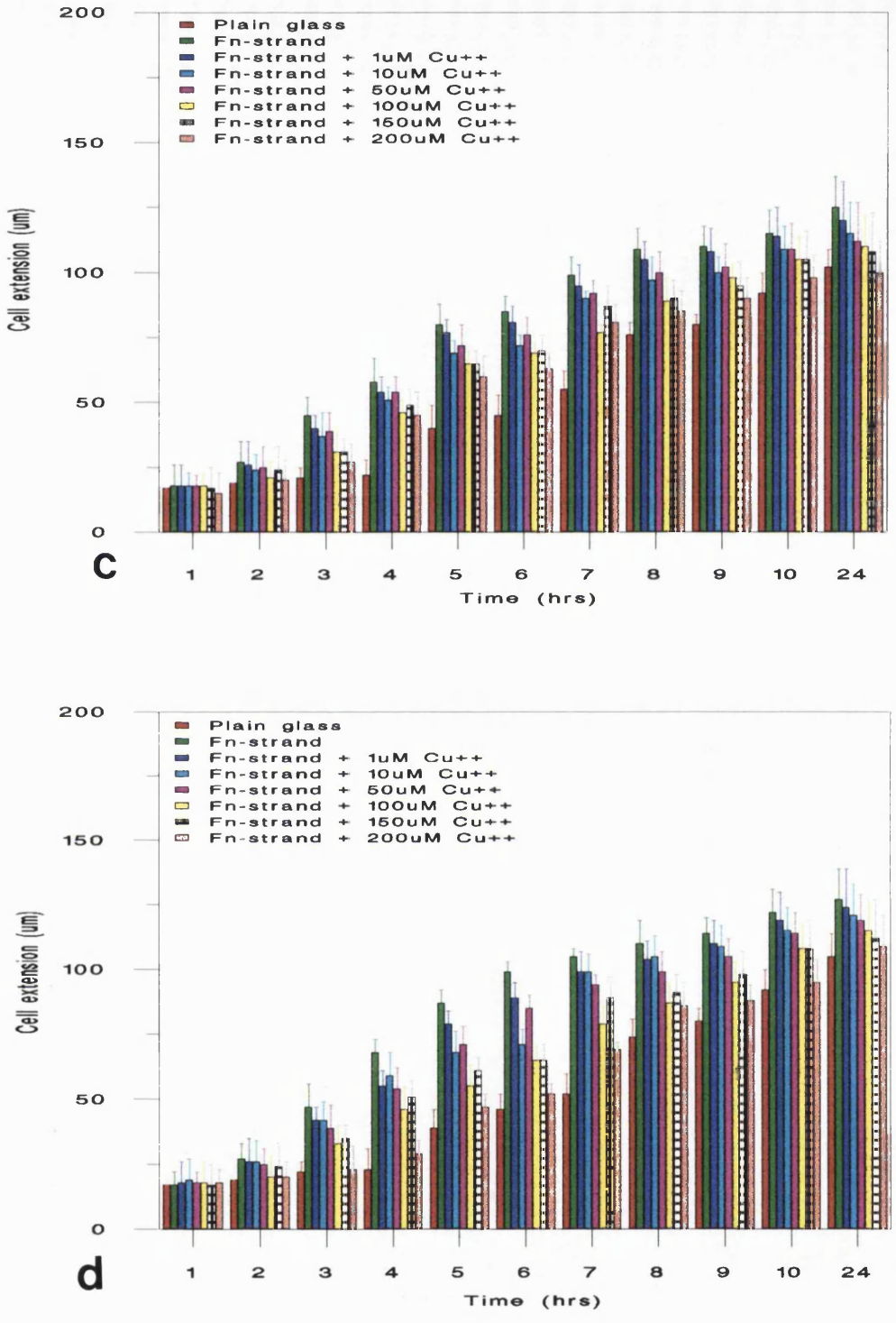

Figure 4.47. *Cellular extensions for (c) rat tail and (d) rat skin fibroblasts.*

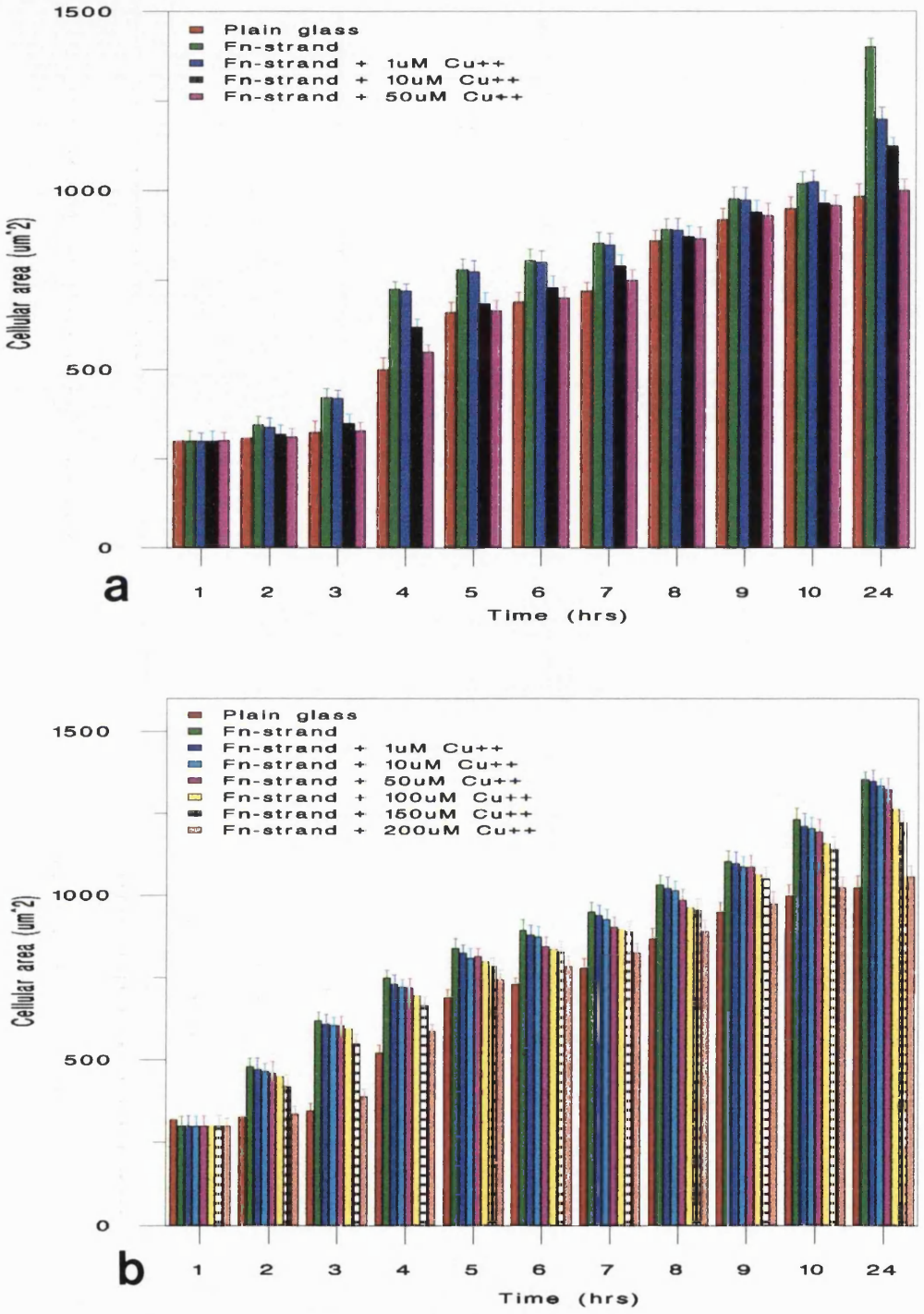

Figure 4.48. *Changes in cellular area over time for cells cultured on CuFn-strands. Mean cellular areas for (a) Schwann cells (b) human dermal fibroblasts.*

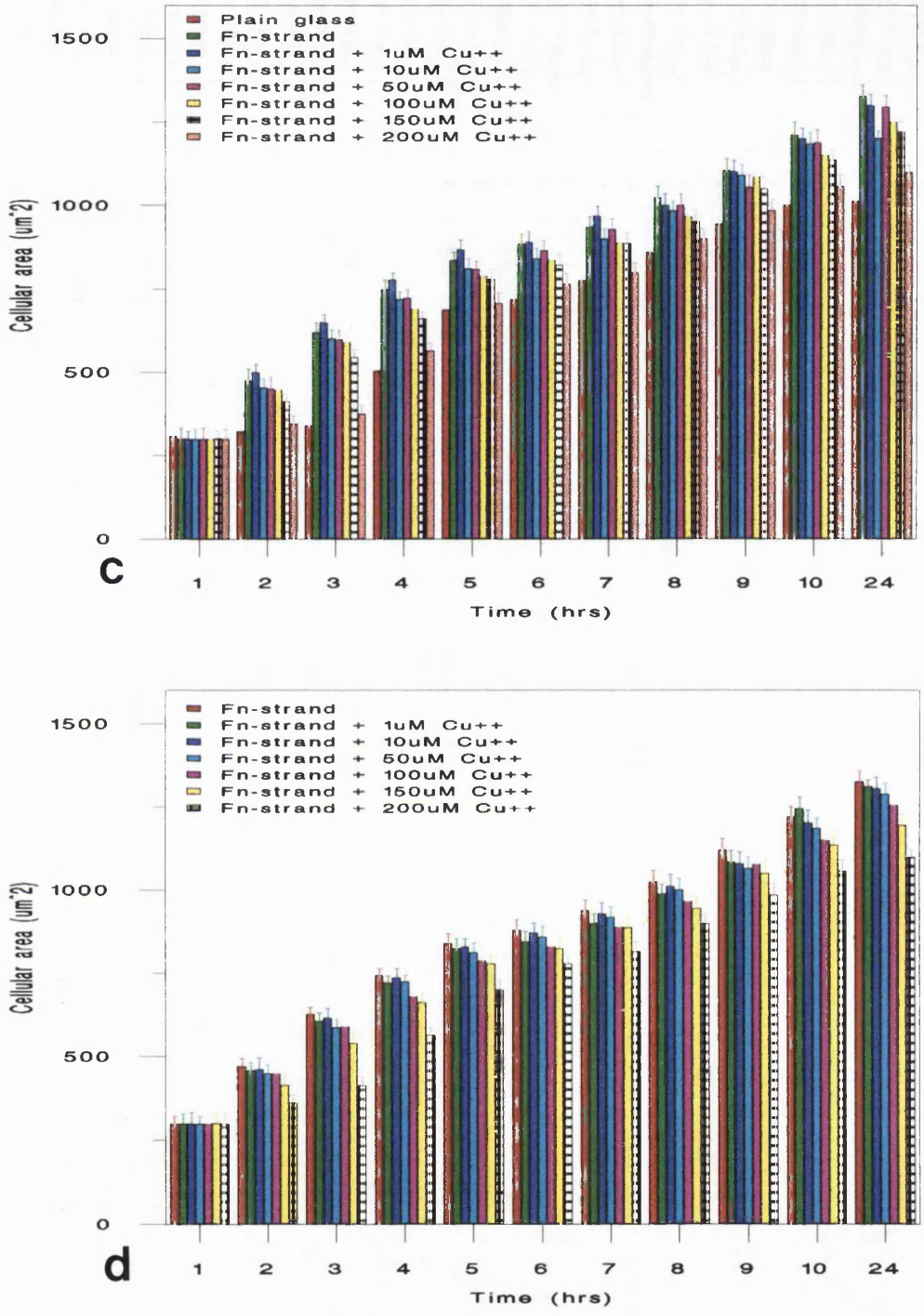

Figure 4.48. *Cellular areas for (c) rat tail and (d) rat skin fibroblasts.*

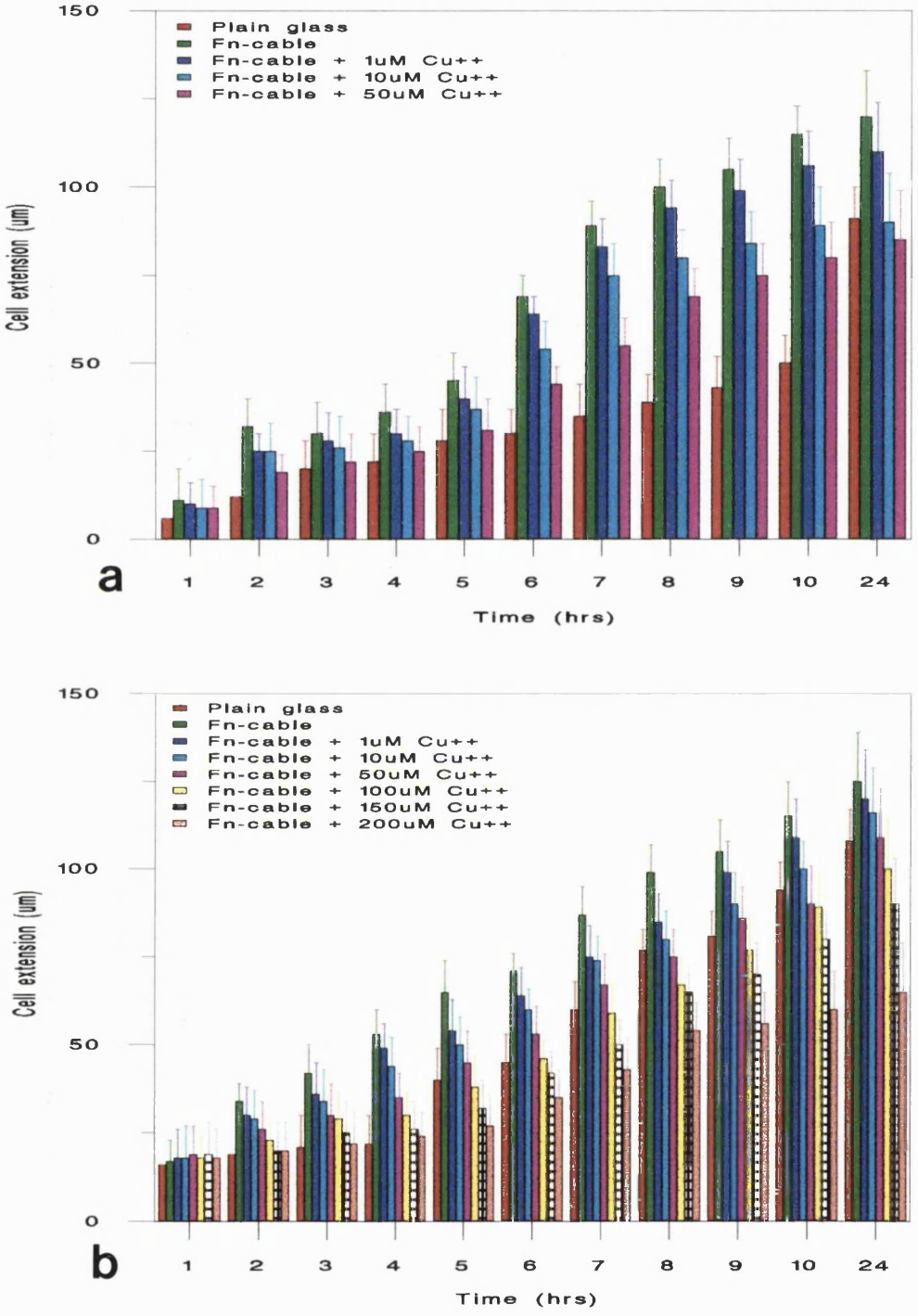

Figure 4.49. *Changes in cellular extension over time for cells cultured on CuFn-cables. Mean cellular extensions for (a) Schwann cells (b) human dermal fibroblasts.*

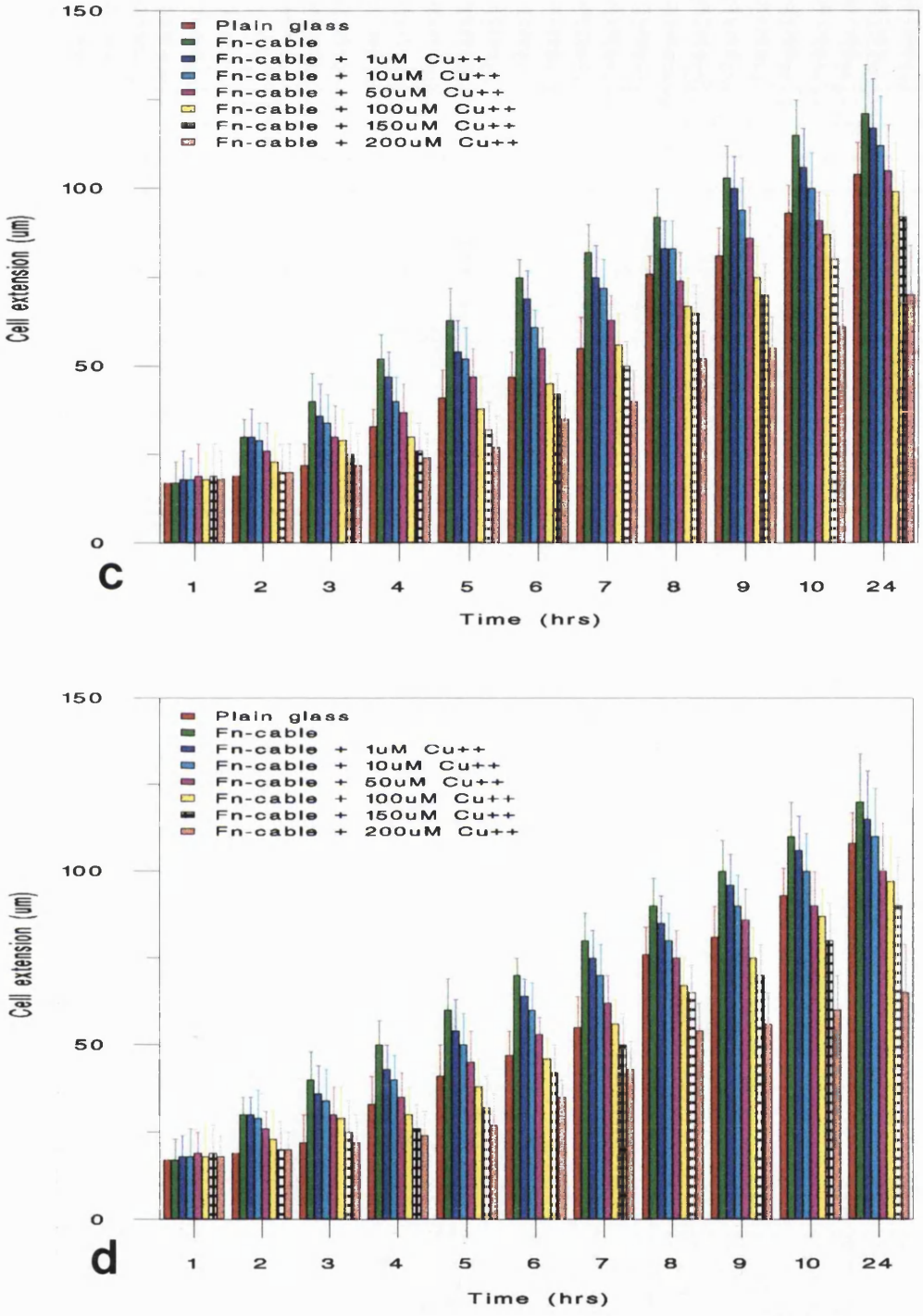

Figure 4.49. Changes in cellular extension for (c) rat tail and (d) rat skin fibroblasts.

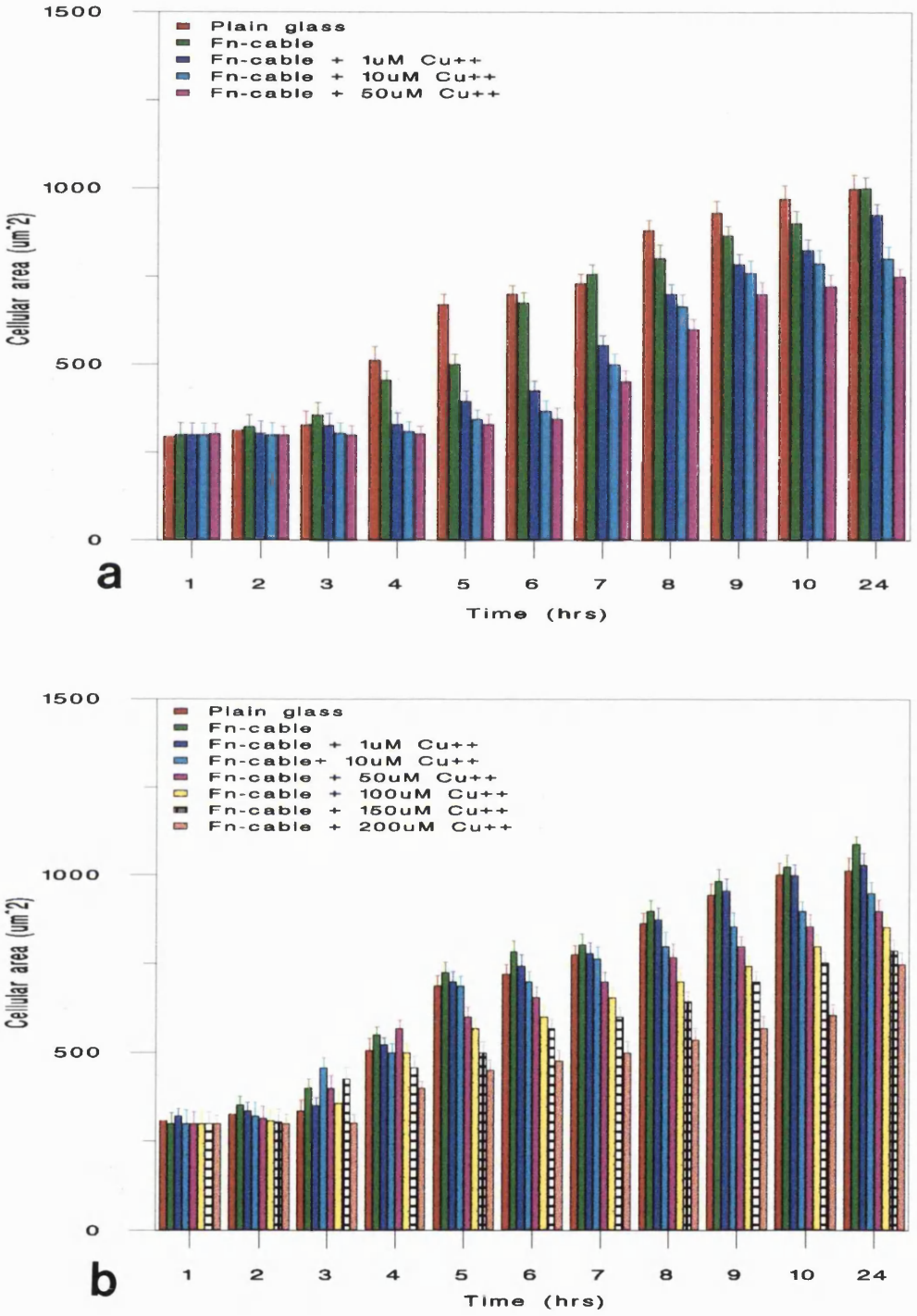

Figure 4.50. *Changes in cellular area over time for cells cultured on CuFn-cables. Cellular areas for (a) Schwann cells (b) human dermal fibroblasts.*

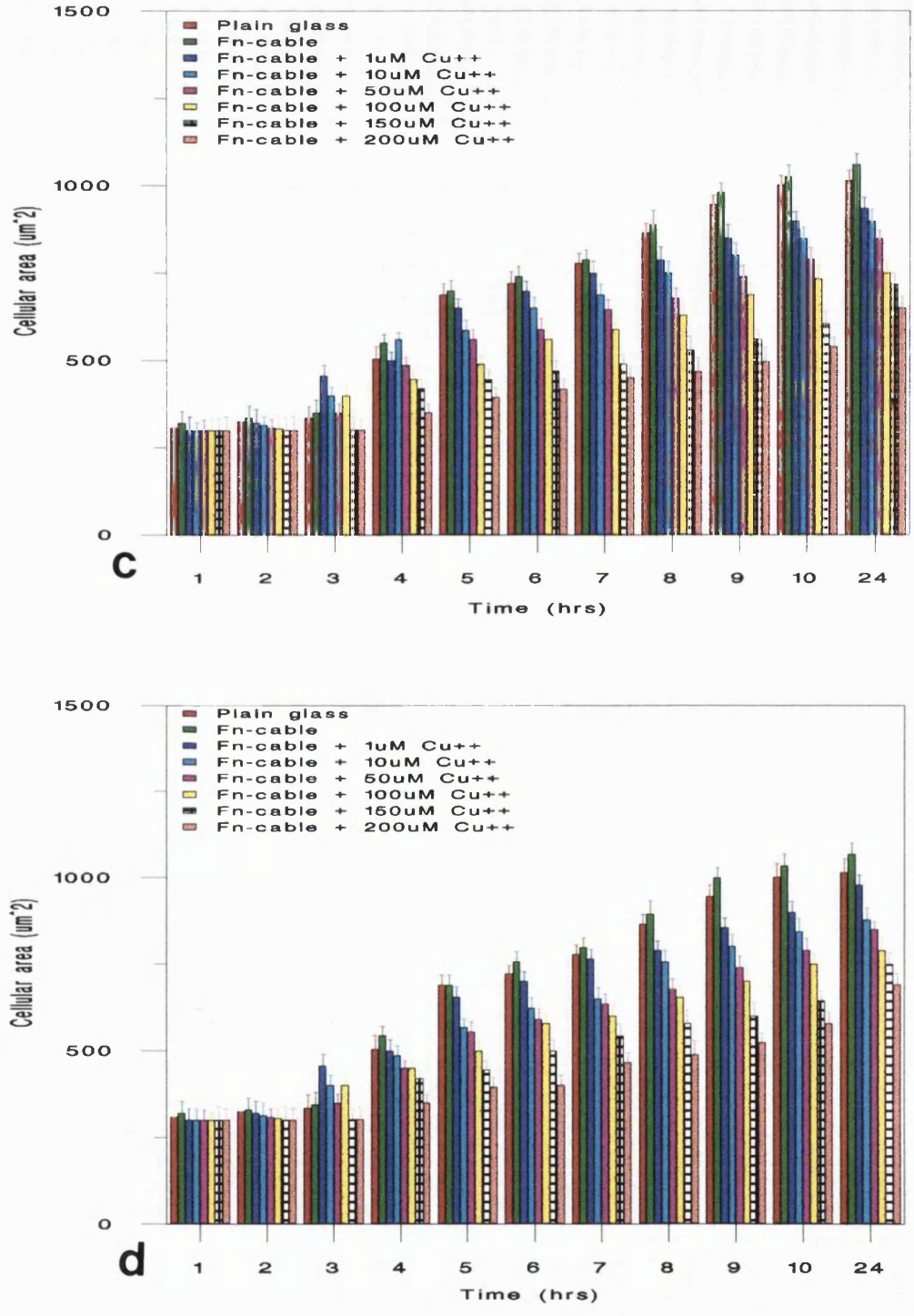

Figure 4.50. Changes in cellular area for (c) rat tail and (d) rat skin fibroblasts.

on Fn-cables than on Fn-strands at all concentrations of copper and on untreated Fn-cables.

At the maximal migration speed for cells plated on both copper treated Fn-strands (maximum speed reached when Fn-fibres were treated with 100μM copper) and Fn-cables (maximum speed reached when Fn-fibres were treated with 10μM copper), the integrated density measurements were very similar for each cell type on these substrata.

The results from this section showed that Fn-strands and cables can be stabilised by 2-3 three times that of controls. The results also showed that cell migration speed increased with increasing concentrations of copper upto a maximum level which can be correlated with vinculin immunostaining. This represents a useful tool for modulating the speed of cell migration on Fn-strands and cables.

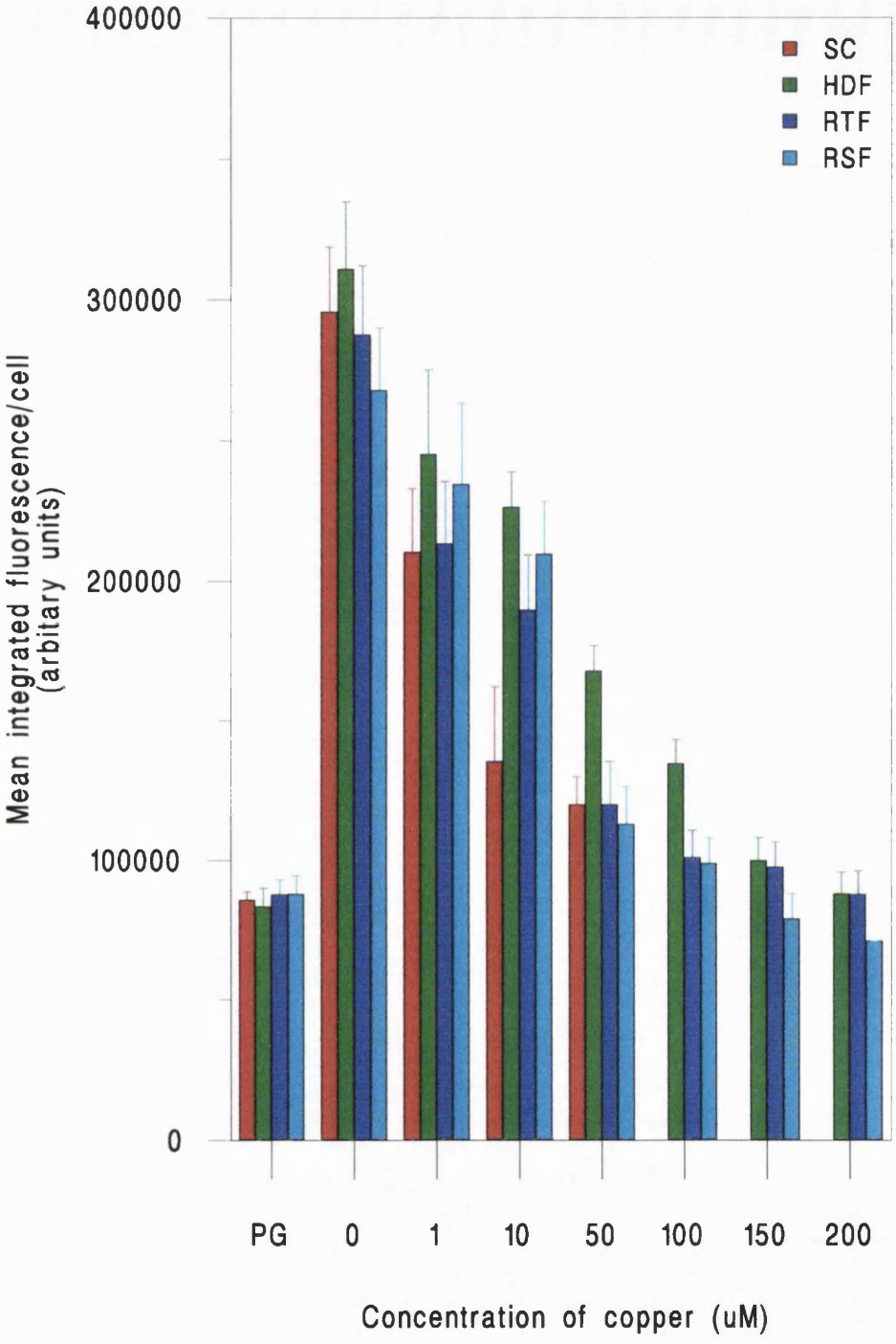

Figure 4.51. *Integrated density measurements for cells on Fn-strands with increasing concentration of copper. As the concentration of copper increased, integrated fluorescence decreased. SC = Schwann cells, HDF = human dermal fibroblasts, RTF = rat tail fibroblasts and RSF = rat skin fibroblasts.*

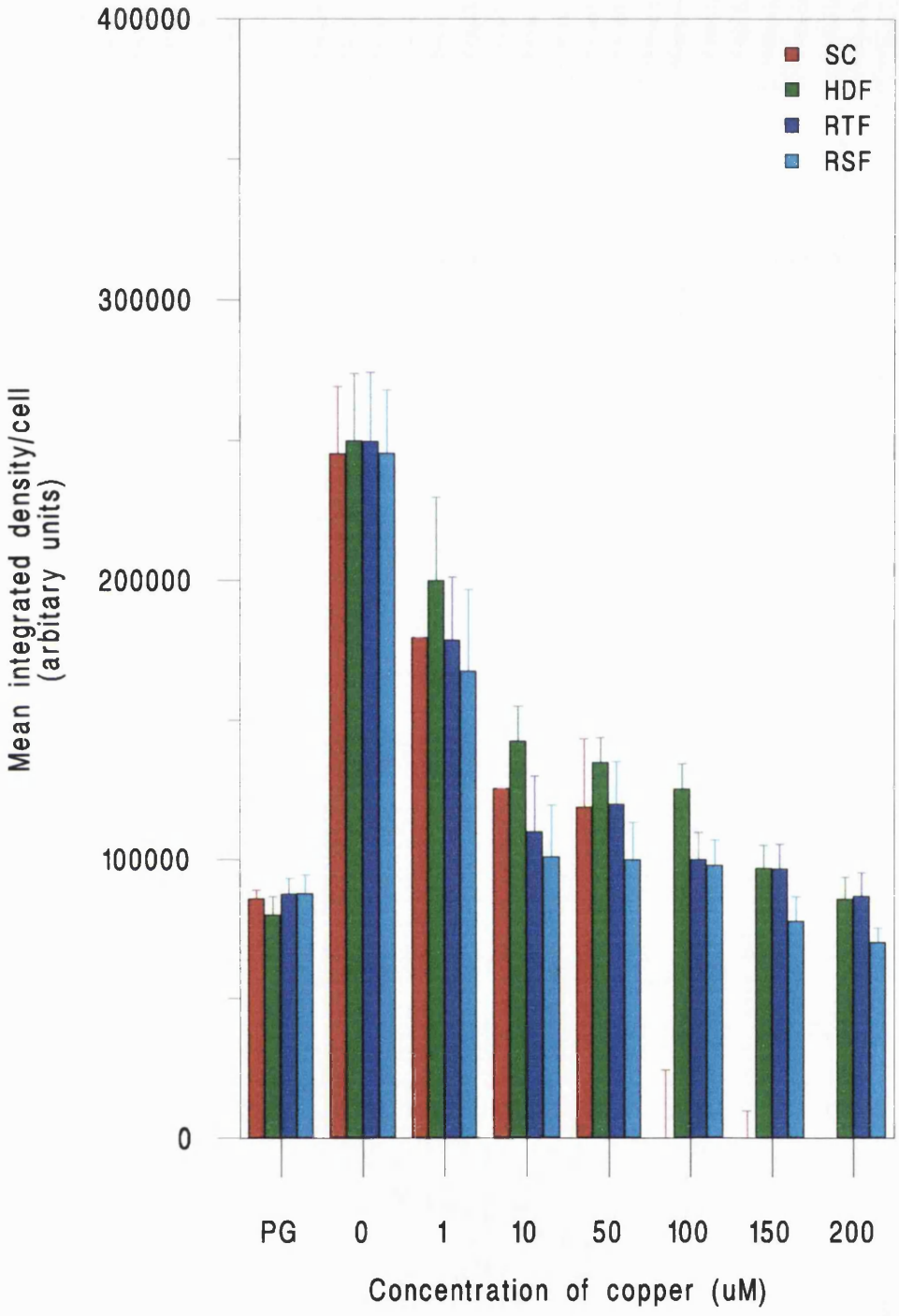

Figure 4.52. *Integrated density measurements for cells on Fn-cables with increasing concentration of copper. As the concentration of copper increased, integrated fluorescence decreased. SC = Schwann cells, HDF = human dermal fibroblasts, RTF = rat tail fibroblasts and RSF = rat skin fibroblasts.*

5.0. DISCUSSION

In the UK, injuries to peripheral nerves requiring surgical repair are relatively common with 4-5000 operations per year. Major areas that are affected include hands, shoulders, face and legs. From the clinical point of view, complete severance of the nerve trunk represents the most serious situation. Commonly, a nerve autograft, which is taken from a donor site is required to bridge the created gap. However, the limitations of the length and diameter together with the problems of donor site morbidity results make this an increasing less favourable option.

The proficiency of microsurgical techniques have contributed to improved clinical output in selected situations, however, the results still remain unsatisfactory. Recently however, attention has switched to the manipulation of the local microenvironment at the zone of injury and/or at the axonal and target cell area to improve nerve repair. Normally axons are able to traverse a 10 mm gap in silicone chambers, however, when the gap length was increased to 15 mm in rats, axons were unable to reach the distal segment (Lundborg et al., 1982; Danielson et al., 1983). Pre-filling these chambers with dialysed homologous plasma, rapidly providing a fibrin matrix speeded up the process of regeneration (Williams et al., 1987). Silicone tubes packed with a degradable collagen-glycosaminoglycan polysaccharide matrix was shown to support regeneration across a 15 mm gap in the rat sciatic nerve (Yannas, 1985; Yannas et al., 1985). DaSilva et al., 1985 and Madison et al., 1985, induced sciatic nerve regeneration across a 20 mm gap through tubes lined with either a laminin-containing gel or a collagen matrix.

Addition of cultured Schwann cells to the lumen of the tubes also supported nerve regeneration (Lundborg et al., 1982; Shine et al., 1986, Ikeda et al., 1991). It has been shown that these Schwann cells produce a variety of growth factors including NGF, which stimulate the regeneration of peripheral nerves and then remyelinate regenerated axons (Bunge, 1981; Assouline et al., 1987; Fawcett and Keynes, 1990; Ikeda et al., 1991; Raivich and Kreutzberg, 1993). This represents a useful tissue engineering approach to improving peripheral nerve repair.

In this thesis, the problems mentioned above have been tackled in four ways:

1. stabilisation of conduit materials for longer survival in vivo.

2. modification of Fn-mats by growth factor incorporation.

3. formation and modification of new materials suitable to promote contact guided repair of peripheral nerves.

and

4. Behaviour of Schwann cells on normal and modified Fn-strands and cables as a 'simple model' for the Fn-mat/cable materials.

5.1. Stabilisation of Fibronectin Mats

Fn-mats have been found to be useful materials for the organisation of repair in certain tissues which require directional and migratory cues. Fn-mats are totally biodegradable with variable fibre diameter and a predominant orientation. When modified by incorporation of heparin (HepFn-mat), these mats swell rapidly when rehydrated in PBS or tissue culture medium and dissolve within 24 hours unless chemically cross-linked (Ejim et al., 1993). However, plain Fn-mats are stable for at least 4 weeks in

culture experiments and approximately 15 days when implanted in vivo (Porter et al., submitted). Stability is clearly critical to their function and it is important to be able to modify how long they survive in different applications and implant sites.

Fn-mats have been used to enhance regeneration of lesions in a rat sciatic nerve injury model (Whitworth et al., 1995a), providing an aligned substrate for regenerating axons and Schwann cell migration (Whitworth et al., 1995a; Porter et al., submitted). Nerve growth factor has been delivered locally via Fn-mats to the repair site to further enhance peripheral nerve regeneration in the rat sciatic nerve model in control and diabetic rats (Whitworth et al., 1995b; 1996). However, Fn-mats were almost completely degraded by 15 days post-implantation and stabilisation could be helpful in the repair of longer nerve gaps. The hypothesis here is that micromolar concentrations of copper will stabilise Fn-mats for longer survival in vivo and therefore support outgrowth of a greater volume of regenerating axons. Additionally, local delivery of Cu^{2+} would assist some aspects of tissue repair as it is an essential component of the enzymes lysosome oxidases and SOD and in ascorbate transport into the cell. These are central to collagen production and inflammatory mediation.

In this study micromolar concentrations of copper were used to stabilise Fn-mats inorder to use them *in vitro* or *in vivo* for longer time periods and looked at the effects of stabilisation on the structure of the mat and cell-substrate properties. It was apparent that copper incorporation significantly improved stability. This seems to be entirely dependent on the interaction of Cu^{2+} ions with the Fn-fibres since the nature of the counterion had no effect on stability. In addition, in all tests, stability was dose

dependent. Scanning electron micrographs of Fn-mats revealed increased cross-linking with high levels of copper resulting in a loss of orientation, however, lower levels were able to stabilise Fn-mats significantly without disrupting the overall orientation which is a key feature to be maintained in order to guide cells to repair in a particular orientation. Higher doses of copper may cause increased cross-linking of Fn-fibres as a result of an increased number of copper ions forming interactions between fibres which in turn pull the fibres closer together eventually forming sheet like structures. Cross-linking of fibres occurred even in control Fn-mats due to rehydration in (Cu free) solution to act as a precise control for the copper treatment. We have already shown that rehydration leads to some fusion of fibres (Ejim et al., 1993; also discussed later in this thesis) but the appearance of this ultrastructure is quite different to copper treated Fn-mats. It seems likely that stabilisation involves ionic interaction between negatively charged residues on the fibronectin molecule and the divalent copper ion. Copper has been shown to bind extremely tightly to various protein ligands (e.g. hemocyanin, tyrosinase and type III copper oxidases) with an equilibrium constant of 10^{18} (Solomon, 1981). Copper atoms have been shown to link to pairs of neighbouring peptide nitrogen atoms along the entire length of the chain in fibres of silk fibroin dispersed in cupriethylenediamine (reviewed by Lundgren, 1949). It is also possible that in our system copper binding is via the same mechanism causing cross-linking of Fn-fibres in the Fn-mats (Figure 5.1). In addition, interactions of Cu with proteins in general is widely used in histological stains and protein assays such as the Folin Lowry assay (Brown, 1992).

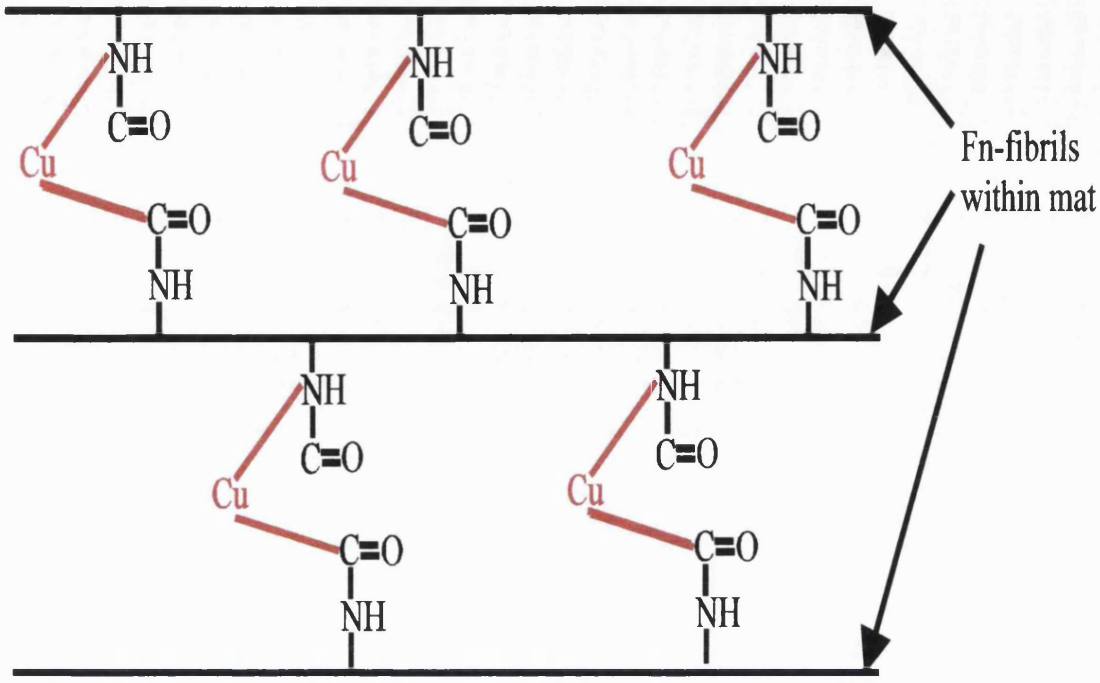

Figure 5.1. *Possible mechanism for copper stabilisation of Fn-mats. Copper ions form cross-links between neighbouring Fn-fibrils throughout the structure of the Fn-mat. Cross-linking occurs via neighbouring peptide nitrogen atoms leading to Fn-mat stabilisation.*

The increase in stability of Fn-mats may be due to copper ion poisoning of trypsin, which is known to be susceptible to copper treatment. Experiments have shown that an increase in copper ions caused a decreased activity of trypsin in the hydrolysis of casein and soybean protein and in some cases trypsin inhibition (Steinhart et al., 1981). Low concentrations of copper (4.5 × 10-7 mol Cu2+/l), however, was shown to cause a stimulation of trypsin activity on a substrate of sodium-benzoyl-l-arginine-p-nitroanilid (L-BAPA) while higher concentrations reduced trypsin activity (Wieninger-Rustemeyer et al., 1981; Kirchgessner et al., 1980a; Kirchgessner et al., 1980b). In our experiments, treatment of Fn-mats with high (>10μM) concentrations of copper may have inhibited trypsin activity thus leading to higher stabilisation seen with these

treatment concentrations. However, cross-link formation observed in scanning electron micrographs would have an additive effect to Fn-mat stability. Copper treated Fn-mats may have an adverse effects on other enzymes by inhibiting their activity and thus may cause adverse cellular responses. This remains to be investigated.

The effect of copper ions on cells in vitro was an unexpected finding in that at low copper levels Schwann cell proliferation was significantly increased. This may reflect a cell culture deficiency and will be tested in vivo. Schwann cells are known to respond to a limited number of mitogens in culture (Davis and Stroobant, 1990; Rutkowski et al., 1995). Early attempts to propagate Schwann cells showed that crude extracts from bovine pituitary were strongly mitogenic (Raff et al., 1978) while later studies showed that pituitary extracts in conjunction with cyclic adenosine monophosphate (cAMP) raising agents were more potent (Brockes et al., 1980; Raff et al., 1978). In all our experiments we also used pituitary extracts and a cAMP raising agent (forskolin) in accordance to these reports. The additive effect of soluble Fn, as a result of Fn-mat dissolution into the culture medium cannot be ruled out, as soluble Fn is known to be an effective mitogen for Schwann cells (Evercooren et al., 1982). Indeed in experiments with untreated Fn-mats, Schwann cell proliferation was greater than that observed for cells plated on plain glass substrata. However, taking into consideration the additive effects of all of these agents on Schwann cell proliferation, our results show that copper ions are also a significantly potent mitogenic agent.

The increase in the number of Schwann cells found resident within copper incorporated mats was also surprising. This has a two-fold implication in that there is increased

Schwann cell recruitment into the mat or that copper mats stimulate Schwann cell proliferation. The chemotactic activity of fibronectin is well documented in literature (Evercooren et al., 1982; reviewed by Grinell, 1984,). Although the rate of proliferation was not measured in these experiments with a cell proliferation marker such as Bromodeoxyuridine (BrdU- a marker of cell proliferation which is incorporated into the DNA during the S-phase of the cell cycle which is then detected by an immunofluorescent method), there indirect evidence to suggest that the increased number of cells within the Fn-mats treated with copper is primarily due to cell proliferation rather than recruitment from the surrounding area. This is inferred from experiments with copper treated Fn-cables (discussed later) where the number of BrdU positive cells were significantly greater when compared to untreated Fn-cables (Personal communication Professor Susan Hall; Z. Ahmed et al., in prep). If this is true, then this suggests that Schwann cells proliferate faster in the presence of substratum bound Cu^{2+} (i.e. when on solid phase Cu).

The effect of copper ions did not have a marked effect on fibroblast populations, however, a differential response was observed when compared to Schwann cells. Fibroblasts were able to survive at the highest treatment concentrations of copper (200μM) used in these experiments while 10μM concentrations were toxic to Schwann cells. This suggests Schwann cells may utilise copper ions to increase their metabolic activity or that an enzyme may be switched on which causes increased cell proliferation. The differential response of fibroblasts to somewhat higher copper levels where Schwann cells do not grow well or die suggests that multi-layered Fn-constructs could be produced, capable of cell segregation by differential exclusion. In terms of

nerve regeneration materials, one example would be to use a low copper cone to direct Schwann cell / neurite growth with higher levels in the outer sheet, suitable for fibroblastic regeneration of a epineurial sheath (Figure 5.2). The incorporation of zinc into Fn-mats would prove to be an added benefit as zinc is present in filamentous structures in connective tissues as a component of all MMP's (Williams, 1989) and may prevent peripheral neuropathies.

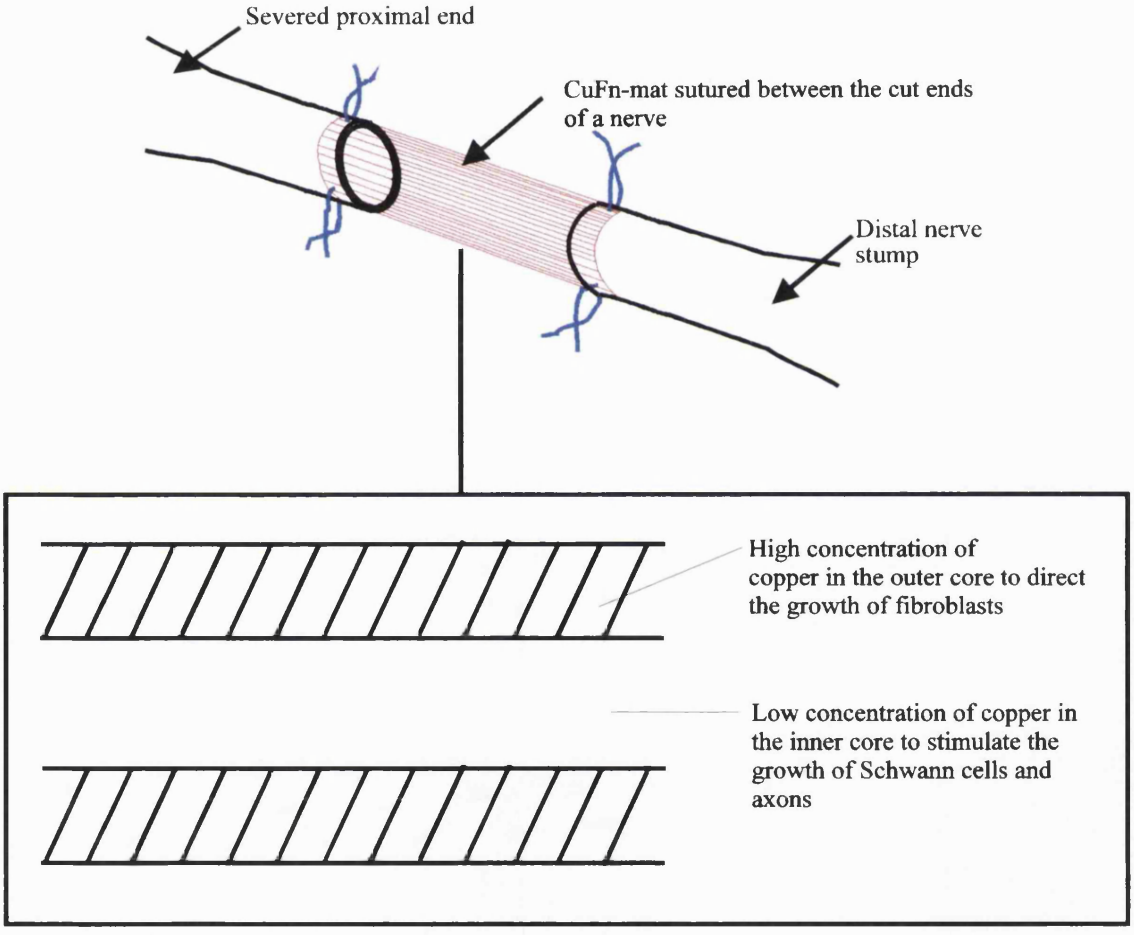

Figure 5.2. A possible method for use of copper stabilised Fn-mats in peripheral nerve regeneration. Diagram shows a CuFn-mat in place between a nerve gap. Exploded diagram shows a longitudinal cross-section of the design of the Fn-mat with a core suitable to promote the growth of Schwann cells and axons while the outer core stimulates fibroblast growth and formation of the epineurium.

These results could be used to design a tissue engineering approach to the construction of conduits which would support regeneration of peripheral nerves over long distances (>15mm). Schwann cells have been shown to promote neurite growth in vitro (Engele et al., 1991; Schwab and Thoenen, 1985) and in vivo (David and Aguayo, 1981; Kromer and Cornbrooks, 1985; Collier and Springer, 1994). Schwann cell engrafting has also been shown to promote nervous system regeneration in experimental models including trauma to central and peripheral neurones, central neurodegeneration and genetic demyelination (Levi et al., 1994; Zager and Black, 1988; Bunge et al., 1988; Fisher and Gage, 1993). Fn-mats modified by copper ions may be seeded with pre-aligned cultured Schwann cells and implanted between nerve gaps. This strategy is expected to increase the number of grafted Schwann cells as well as those that migrate out form the distal stump thereby facilitating the outgrowth of axons and improving peripheral nerve regeneration. It is envisaged that macrophages which initially invade the Fn-mat in vivo will not be effected in any way while using low doses of copper. Indeed copper has been shown to have an anti-inflammatory effect (Sorenson, 1987) and this may also be beneficial to growing axons as the Fn-mat scaffold may disintegrate slower thereby providing support to outgrowing axons for longer time periods.

In addition Fn-mats treated with copper concentrations suitable for fibroblasts may be used to deliver a copper directly to the site of wound repair where a beneficial effect may be produced as copper is an important cofactor in collagen production. Copper from these mats would be released as the Fn-mat dissolves and by the action of inflammatory cells over a period of time. In severe burn trauma patients the response

of ceruloplasmin, the principal copper-containing component of blood (Sorenson, 1987), as an acute-phase reactive protein was absent (Cunningham et al., 1993) and that burn severity was correlated to a reduction in ceruloplsamin. Therefore, supplying copper to these areas may prove to be beneficial as copper may be provided in a slow but continued release to the surrounding area.

In conclusion, CuFn-mats are significantly more stable than plain Fn-mats and it is expected that these mats would be useful for repair of longer nerve gaps. It is also possible that use of different levels of copper incorporation could be used to segregate cell growth where layered devices are used in tissue engineering applications.

5.2. Nerve Growth Factor Delivered Locally via Fibronectin Mats Enhances Peripheral Nerve Regeneration in The Non-Human Primate

The regeneration of peripheral nerves have been attempted in many types of experimental animals and tubular guide materials have been used to enhance regeneration, in some cases augmented with neurotrophic or other stimulatory factors. A suitable conduit material would be readily available; support and direct neurite outgrowth; immunologically compatible whilst minimising tension at the suture lines following implantation (Fawcett and Keynes, 1986). Fn-mats appear to meet many of these criteria (Whitworth et al., 1996).

The effect of growth factors on peripheral nerve regeneration has been studied extensively as they have the ability to promote neuronal survival and enhance regeneration of cultured neurones (Lindsay, 1988; Fernyhough et al., 1993). It is

thought that successful enhancement of peripheral nerve repair will be dependent on targeted delivery of growth factors in a continuous manner (Whitworth et al., 1995a: 1995b; 1996). Whitworth et al, 1996 have shown that Fn-mats soaked in NGF solution will release the growth factor slowly over a period of 7 days in vitro, whilst remaining biologically active (Whitworth et al., 1996). Such NGF soaked mats were shown to enhance regeneration across of 1cm peripheral nerve defects in the rat sciatic nerve model (Whitworth et al., 1996). Previous reports have shown that levels of NGF protein and mRNA are thought to increase within the injured nerve (Heumann et al., 1987; Richardson and Ebendal, 1982) with a marked increase in low affinity NGF receptors on the surface of Schwann cells (Anton et al., 1994; Taniuchi et al., 1986) which exhibit an interdependent relationship with advancing axons.

The purpose of this study was to assess the effect of NGF delivered locally via fibronectin mats on the regeneration of peripheral nerves in monkeys. It has already been shown that Fn-mats incorporated with NGF were effective in increasing axonal regeneration and that Fn-mats are effective in guiding the repair process (Whitworth et al., 1995a, 1996; Porter et al., submitted). Here, a long term post-operative primate model was chosen as primates serve as a better model for the response than rodents or other laboratory animals and the length of time would also allow a degree of regeneration to reach the target organ. Furthermore, Fn-mats which are produced from human plasma fibronectin, when implanted into a rat model elicited a mild immune response (Porter et al., submitted) whereas primates, being closely related to humans may respond differently. Morphological studies were carried out to establish the degree of regeneration and the effectiveness of Fn-mats to direct the repair. The results

of this study might give useful information whether Fn-mats together with neurotrophic factors may be of clinical use to enhance regeneration of peripheral nerves in humans.

Fn-mats alone and with NGF were grafted in primate nerve gaps and left for 4 months before assessing the effectiveness of the graft material to regenerate peripheral nerves. A pure sensory nerve was to avoid the problem of sensory-motor mismatch. Larger gaps were not feasible in this model due to the constraints of animal welfare deciding which nerve was possible to use and the anatomical site. All experimental animal groups produced a successful bridge of regenerating axons which were parallel to the axis of the original mat with the total disappearance of the Fn-mat. However, the regenerates were qualitatively different. Plain Fn-mats appeared to have been least effective, having a greater deposition of connective tissue and significantly less number of myelinated axons (~50% less) within the graft area than any other group. However, Fn-mats+NGF stimulated an increased number of regenerating axons compared to plain Fn-mat, which exhibited similar number, clear parallel orientation, thick myelination, fasciculation and structural similarity to those formed after nerve grafts. In previous work on the rat sciatic nerve model, the number of myelinated axons was also found to be significantly greater in animals grafted with Fn-mat+NGF compared to Fn-mats alone (Whitworth et al., 1996).

Regenerating axons are thought to be unable to regain their original normal calibre after injury and the thickness of myelin is known to be directly proportional to the diameter of axons (Fields et al., 1989). However, in our experiment we were able to

show a significant increase in the median axonal diameter, median myelin thickness and G-ratio in animals grafted with Fn-mats+NGF compared to all other experimental groups. NGF is known to be required for the survival of sensory and sympathetic neurons (Levi-Montalcini, 1987) and is known to be trophic for unmyelinated and small myelinated fibres. In our experiment the exogenous NGF appeared to act on larger axons and this increased their size and thickness of myelin by ~50%, while G-ratio increased by 87% compared to those grafted with Fn-mats alone. These results suggest that NGF improves myelination probably by accelerating early events such as organisation of nonneuronal elements in the initial interstump bridge, as suggested earlier (Derby et al., 1993). Fn-mats on the other hand have been shown to act as a framework to support and direct cellular components of axonal regeneration in an amount similar to that supported by autologous nerve grafts (Whitworth et al., 1995a). Fn adsorbed to tissue culture plastic, glass or collagen has been shown to enhance neurite outgrowth (Akers et al., 1981) and lead to a four-fold increase in the number of aggregates extending neurites when compared to untreated tissue culture vessels. Fn has also been shown to promote Schwann cell growth and motility (Evercooren et al., 1982). It is likely that the combined effects of both Fn and NGF lead to the outcome seen in animals grafted with Fn-mats+NGF.

Neurofilaments (NF) have been shown to be important in regulating axonal diameter (calibre) which increases at the same time as with myelination and is important since axonal calibre is a principal determinant of the conduction velocity at which nerve impulses are propagated along the axon (Arbuthnott et al., 1980; Cleveland et al., 1991; Hoffman et al., 1987; Lee and Cleveland, 1994; Marzalek et al., 1996;

Sakaguchi et al., 1993). Although NFs are implicated in specifying axonal size a mechanism for this interaction is currently unsettled. However, determination of axonal diameter is specified by other factors as well as simple NF content. The NF-H subunit has been shown to modulate axonal diameter in transgenic mice by selectively slowing neurofilament transport (Marzalek et al., 1996). Parhad et al, 1995 have shown that levels of neurofilament mRNA decrease in the dorsal root ganglia of Fischer rats with age and that this is concomitant with decreases in the levels of expression of transcripts for the NGF receptors trkA and p75 suggesting that a decrease in the availability of NGF may affect NF expression. Lee et al, 1982 and Kim, 1992 showed that NGF induced the production of neurofilaments in a tumor-derived cell line (PC12W) suggesting a direct modulatory effect on NF expression by NGF. NGF is known to act on small axons but by supplying exogenous NGF to the regenerating nerve as in our experiment, it may have stimulated NF mRNA accumulation in both the large and small calibre axons causing them to increase their size, thus leading to the increased numbers of larger myelinated axons observed in our Fn-mat+NGF group. The increased calibre of axons may be beneficial as large myelinated fibres have a faster conduction velocity due to less resistance and better insulation provided by thick myelin (Arbuthnott et al., 1980), therefore sensation (as is the case in our model) by the target organ would occur quicker. Conversely, larger axons might be associated with abnormal effects by allowing greater magnitudes of impulses to flow through which would cause increased pain sensation by the target organ in the case of sensory axons and greater magnitudes of response in the case of motor axons.

Fn-mats also directed the growth of the epineurium and collagen fibrils within the nerve, as reported earlier in a rat sciatic nerve model (Porter et al., in prep). However, animals grafted with Fn-mats showed thin epinurial regeneration compared to the other experimental groups. Ultrastructurally, the epineurium and perineurium in the Fn-mat+NGF and nerve graft groups were very similar and showed both parallel and perpendicular arrangements of collagen fibrils to the nerve fibre axis, together with fibroblasts neatly organised encircling the axons and providing structural integrity to the regenerating nerve. There was reduced regeneration of connective tissues in the Fn-mat alone group. However, the presence of exogenous NGF was able to correct this deficiency and enhance growth of different subtypes of tissues within the regenerating nerve.

The degree of regeneration is clearly important to prevent degeneration and atrophy of the target organ and it is also a good indication of functional recovery (Gutman and Young, 1994). Dr. Giorgio Terenghi (Blond McIndoe Centre, England) and Dr. Mikael Wiberg (University of Umea, Sweden) also examined whether NGF stimulates target organ re-innervation, in this case the skin from the dorso-radial aspect of the hand (Z. Ahmed et al., submitted). The study revealed that the Fn-mat+NGF group suffered significantly less dennervation 1 month post-operatively compared to the Fn-mat alone and nerve graft groups (Ahmed et al., submitted). This is in agreement with previous reports that NGF promotes the survival and maintenance of sensory nerves (Levi-Montalcini, 1987) and protects adult sensory neurons from cell death and atrophy following nerve damage (Ljungberg et al., 1997; Rich et al., 1987). At 4 months post-operatively, the extent of reinnervation was greatest for the Fn-mat+NGF

group (~7% and ~30% greater when compared to nerve grafts and Fn-mats alone, respectively) with the least amount of reinnervation shown by the Fn-mat alone group indicating that local delivery of NGF via Fn-mats stimulates both survival of sensory neurons and reinnervation of their target tissue (Ahmed et al., submitted). It cannot be excluded that some of the nerve terminals present in the skin biopsies were from collateral sprouting from neighbouring areas. However, it seems unlikely that this process alone would contribute to the substantial reinnervation of such large areas of skin normally innervated by the radial nerve.

In conclusion, this study has demonstrated that Fn-mats support successful, organised regeneration of axons and collagen in peripheral nerves in the primate. The use of NGF impregnated Fn-mats augments the size and number of myelinated axons and the quality of the regenerate such that the outcome of these implants is comparable to that of nerve autografts. The clinical implications of these results are promising, as in future it may be possible to repair defects in peripheral nerves using Fn-mats impregnated with trophic factors. This would be an advantage on the use of conventional autologous nerve grafts as it would eliminate the problems of donor site morbidity without compromising the regeneration outcome.

5.3. Large Cables of Fibronectin

To overcome the current limitations of Fn-mats, such as the time taken for processing, difficulties with scale up and reproducibility of the materials a production technique has been developed for making large fibronectin cables (LFn-cables). In the nerve repair application, LFn-cables would not only provide trophic support and directional cues

for regenerating components of peripheral nerves whilst being simple to produce reproducibly in large amounts. Fn-mats can only be used for nerve lesions upto 2 cm long. Modification of these cables with copper (and zinc) may be useful in stabilising the structure of the LFn-cables and may provide a surface for favourable cell-matrix interactions as has been observed with Fn-mats, described earlier in section 5.1. This is especially important in designing long nerve conduits where a slower rate of degradation is required otherwise axons and Schwann cells will lose their support material and hinder nerve regeneration. The aim here was to develop and test the idea that LFn-cables could be used to repair long nerve lesions and potentially as support materials in other comparable tissue engineering applications such as formation of new blood vessels. The predicted hypothetical requirements for such applications are: fibrillar orientated structure, porosity, support cell seeding and cell adhesion/migration and must resist rapid degradation inorder to support cells for as long as possible. This leads us to develop and design a substrate requirement profile composed of fibronectin, fibrinogen and micromolar concentrations of copper ions. The experiments in this section were designed to test how clearly the LFn-cables and modification came to satisfying that prediction.

Peripheral nerve injuries commonly result in large gaps which the surgeon is unable to repair by simple suturing. Such defects must be repaired immediately to prevent atrophy of de-innervated target tissues. Currently, autografting is the benchmark procedure for repairing peripheral nerve lesions despite the major problems associated with donor site morbidity. Bioartificial conduits have been used to bridge such defects with varying degrees of success. Such materials need to be non-immunogenic and

provide directional and attachment cues to orientate the regenerating components of the nerve. Fn-mats fit this criteria and have previously been assessed in vivo. These have been reported to successfully produce rat peripheral nerve regeneration (Whitworth et al., 1995a; Porter at al., in prep).

In this study the method of Underwood et al. submitted, was adapted to produce large diameter cables (LFn-cables) by extruding a concentrated solution, principally of fibronectin through a suitable diameter orifice. LFn-cables were then modified by copper incorporation in a comparable way to that used previously for Fn-mats (Ahmed et al., 1998, Section 5.1). Physical parameters of the production process could be changed to manipulate the size of the cable obtained by increasing the force applied to pull the fibres out of solution (i.e. drawing the fibres down to the required diameter) leading to expulsion of more liquid to make thinner and denser LFn-cables. The diameter of the resultant cable was also manipulated by increasing the size of the extrusion orifice, an effective method to prepare LFn-cable implants in a range of sizes.

LFn-cables once hydrated, have a parallel fibril alignment with a range of pore sizes from 50-100μm in diameter. These pores would be large enough to support regenerating axons and Schwann cells providing an aligned surface for contact guidance. It has been shown previously that Fn-mats are an attractive substrate for macrophages, which are required in the peripheral nerve to clear debris for the advancing axons (Brown et al., 1991). The proteolytic enzyme activities released by such macrophages would rapidly break down the material enhancing its porosity and facilitating access for regenerating axons. Matrices of fibronectin are known to

enhance neurite outgrowth (Wojciak-Stothard et al., 1997; Akers et al., 1981; Greenberg et al., 1981). Matrices of fibrinogen are effective in inducing adhesion, spreading and microfilament organisation in endothelial cells (Dejane et al., 1987) and mouse NIH 3T3 fibroblasts (Corbett et al., 1996).

Modification of these cables with micromolar concentrations of copper caused a dose dependent effect of copper on the stability of LFn-cables, such that even at the lowest concentration of copper used, CuLFn-cables were one and a half times more stable than untreated cables. Cross-linking between adjacent fibres of fibronectin within the cable also increased in a dose dependent manner without loss of overall fibrillar orientation, however, the relative homogeneity of the pores within the cable was lost. The pores in the centre of the cable became larger with increasing doses of copper with denser regions of protein aggregates forming around the outer edges of the cable. Zinc treated LFn-cables gave a very similar result as copper alone. Interestingly however, cables treated with equimolar concentrations of copper and zinc together (i.e. twice the number of divalent metal ions) resulted in the cables being nearly twice more stable than untreated cables. The mole to mole ratio between copper : protein and zinc : protein, which bound to LFn-cables at 100 and 200 μM treatment concentrations were similar. However, at the 100 μM treatment of the cable with equimolar concentrations of copper and zinc, the approximate molar ratios were 13:9:1 (Cu:Zn:protein). At the 200 μM treatment concentration, an equal number of Cu:Zn ions were interacting with the protein (ie. 15:15:1, Cu:Zn:protein). These would therefore contribute to the cross-linking density of fibres within cables at these treatment concentrations.

The exact mechanism of copper stabilisation of these cables is unknown, however, as we postulated in our earlier paper (Ahmed et al., 1998 and in Section 5.1), it is likely that the mechanism involves ionic interaction between negatively charged residues on the Fn molecule and the divalent cation. In Fn-mats there would primarily be intermolecular cross-linking between Fn-Cu-Fn while in Fn-cables we would also see Fn-Cu-Fg bonding due to the presence of Fg in cables. Copper has been shown to have an extremely high binding equilibrium constant of 10^{18} M to various protein ligands including hemocyanin, tyrosinase and type III copper oxidases (Solomon, 1981). Additionally, its interaction with proteins in general is widely used in protein tests such as the Folin Lowry assay (Brown, 1992), the exact mechanism of which is similarly uncertain.

The effectiveness of porous LFn-cables as a substrate for infiltration by Schwann cells is clearly important since these are the supporting cells for axons in the PNS (reviewed by Ikeda, 1996; Ikeda et al., 1991; Collier and Springer, 1994) and shown to promote the regeneration of peripheral nerves (Lundborg et al., 1982; Shine et al., 1986; Ikeda et al., 1993) and then remyelinate regenerated axons (Fawcette and Keynes, 1990; Raivich and Kreutzberg, 1993). Previous reports have also shown that transplanted cultured Schwann cells within various scaffold materials were effective in enhancing peripheral nerve repair (Ikeda et al., 1991; Shine et al., 1985; Gulati, 1995; Gulati et al., 1995; Harvey et al., 1995; Plant et al., 1995; Brown et al., 1996; Paino et al., 1994; Li and Raisman, 1994). This is primarily due to their trophic influences to regenerating axons by the production of various neurotrophic factors including NGF (Bunge, 1981;

Heumann et al., 1987; Rush, 1984; Assouline et al., 1987) and BDNF (Acheson et al., 1991).

In this system, treatment of the cable with 1μM copper or zinc alone caused ~65% increase in the number of Schwann cells within the cable compared to those which were untreated, while treatment with equimolar concentrations at 1μM caused an increase of ~70%. Treatment with copper alone were toxic to Schwann cells at 10μM but with 10μM zinc and equimolar copper and zinc the increase in cell numbers were ~68% and ~80%, respectively. There was a similar increase in the number of Schwann cells after copper treatment of Fn-mats which has already been discussed. We have also discussed possible ways of copper action on Schwann cell proliferation in Section 5.1. The increased number of Schwann cells would be useful in that the greater the number the greater the amount of neurotrophic growth factors produced. If it is true that Schwann cells are the rate limiting factor in peripheral nerve lesions and neuropathies (Williams et al., 1993; Guenard et al., 1992; Franklin and Blakemore, 1993), then copper modified LFn-cable would provide an ideal system for the delivery of these cells to the regenerating nerve.

Ikeda et al., 1991, used a transplanted Schwann cell density of 32 cells/mm^2 in silicone tubes and found a promotion of peripheral nerve regeneration. They suggested that nerve regeneration could be improved further if they were to transplant Schwann cells at a density close to 1055 cells/mm^2, which is the density of cells in normal nerve (Ikeda et al., 1991). In our experiments, treatment with 10 μM equimolar concentrations of copper and zinc gave a final cell density after 3 weeks of ~806

cells/mm^2 while treatment with 1μM copper alone gave a final density of 439 cells/mm^2. Clearly then, a conduit comprised of an equimolar concentration of copper and zinc would be expected to give a better outcome than LFn-cables alone since it may also promote increased cell proliferation of Schwann cells that infiltrate the conduit from the distal end thereby bringing the number of Schwann cells within the conduit near to levels found in normal nerve. The added advantage of incorporating zinc together with copper may be beneficial to nerve cells. It has been shown that overexpressing Cu/Zn superoxide dismutase (Cu/Zn-SOD) enhanced the survival of dopaminergic neurons in a rat model of Parkinson's disease (Nakao et al., 1995). This was attributed to the antioxidant property of Cu/Zn-SOD reducing the formation of free radicals (Nakao et al., 1995). It is known that the pathogenesis of neuronal injury in neurodegenerative disorders involve a series of reactions of oxygen free radicals which lead to oxidative stress (Olanow, 1994; Coyle and Puttfarcken, 1993).

In terms of tissue engineering, cultured Schwann cells may be seeded within copper modified LFn-cables and grown in vitro prior to grafting them between nerve gaps. This would ensure a neurotrophin rich environment suitable to promote the regeneration of peripheral nerves. The ability of cell to orientate parallel to the fibres within cables will further promote the regeneration process by allowing a surface for axons to migrate (reviewed by Ide, 1996). Fn has been shown to enhance directed migration of Schwann cells and stimulate Schwann cell proliferation (Evercooren et al., 1982). Additionally, Fn and its receptor, α5β1, have been shown to be transiently present at the sites of nerve lesions and suggested to be involved in Schwann cell and regenerating axon extension from the proximal stump (Lefcort et al., 1992; Ide, 1996).

If this is true, then LFn-cables will provide a suitable surface for the migration of these components of the regenerating nerve. In long nerve conduits (>15 mm), the limited ability of Schwann cells to traverse the gap may be overcome by seeding cultured Schwann cells within the conduit thereby guiding axons to reach their target site.

If an LFn-cable is hydrated in a solution of neurotrophic growth factor, upon hydration the growth factor is impregnated into the cable and thus may be used to deliver such factors to a local site of injury. This technique has already been used to deliver NGF (Whitworth et al., 1995, 1996) and NT-3 (Sterne et al., 1997a, 1997b) via Fn-mats to a local site in the rat sciatic nerve model. It was found that NGF and NT-3 were released from the mat over a period of 7 days in a bioactive form capable of promoting neurite outgrowth from dorsal root ganglia (DRG) from 10- day-old chick embryos. Using this system a beneficial effect of NGF and NT-3 on peripheral nerve regeneration was observed in normal (Whitworth et al., 1996; Sterne et al., 1997a, 1997b and diabetic rats (Whitworth et al., 1995b). From this study it seems likely that LFn-cables may impregnate a greater amount of growth factor due to the increased hydration property of LFn-cables compared to Fn-mats. This will provide a greater amount of the growth factor to the site where the cable is implanted and cause increased nerve regeneration.

Before using LFn-cables in vivo however, the acidity needs to be removed. Acidity of the cable is an inherent property due to its production method which relies on a concentrated solution of Fn being extruded through an orifice into a highly acidic solution (pH<1). When the cables were washed briefly in PBS, little difference was

seen in the pH of cables. Before use in culture, cables were washed for 4 hours in PBS and tissue culture medium (DMEM) due to the acidity. However, the longer the cables were soaked to remove the acidity, increasing loss of fibrillar structure was noted. A more effective way of removing acidity was devised and is described later.

These points suggest that LFn-cables are a suitable material to provide directional cues to cells. They can be produced with large fibre diameter and upto 14 cm in length, modified successfully by copper and zinc ions and potentially used as a delivery system for increased numbers of pre-aligned Schwann cells to the site of regeneration. LFn-cables may be used to deliver growth factors to the site of nerve injury. LFn-cables may also be used in complex nerve injuries where multiple nerve lesions occur. This will limit the amount of donor nerve used and alleviate some of the problems associated with nerve grafting. Furthermore, modified LFn-cables may also be used to guide the ingrowth of new blood vessels into the repair site as has been done with Fn-mats (Hobson et al., 1997). LFn-cables and CuLFn-cables were not tested in vivo as they were produced at a late stage in this thesis.

5.4 Large Cables and Mats from Fibronectin: Effect of Freeze Drying on Fibrillar Structure

Oreinted fibrillar structures are important in tissue engineering and other applications where alignment of cells and structures are critical to their success. This includes applications such as peripheral nerve regeneration and formation of capillary vessels. To obtain a usable, stable form of LFn-cables and Fn-mats, we routinely freeze-dry our samples.

LFn-cables once produced are highly acidic (<pH1) and this must be removed before cables can be used in vivo. However, in attempting to remove the acidity by soaking cables in washes of PBS and DMEM for long periods until acidity is at acceptable levels, the cables were observed to lose their fibrillar structure and lead to extensive cross-linking of fibre. This is clearly not desirable as a major characteristic in any biological scaffold is to be porous. Our intended use for LFn-cable is in peripheral nerves where porosity must be maintained to allow infiltration by Schwann cells and regenerating axons as well as the topography of the cable to allow for cell migration by contact guidance. Here, experiments were designed to neutralise the acidity of the cables as quickly as possible to prevent damage to the fibrillar nature of cables while trying to understand the mechanism why cables aggregate.

LFn-cables once formed were treated in a variety of neutralising buffers and found that treatment in 200 mM Tris buffer (pH 7.6) neutralised the acidity within 15 minutes, while those treated in PBS remained acidic (pH4) even after 2 hours. The cables treated in 200 mM Tris buffer were neutral throughout the structure suggesting that there were no diffusion barriers. This quick neutralisation step is clearly advantageous as it will limit the amount of fibre aggregation.

The internal structure of the cables were then elucidated by freeze-fracture which does not require any fixatives as these will promote the aggregation of fibres. We found that cables which were freshly made and rinsed in distilled water for 10 minutes (i.e. <pH1) retained a fibrillar structure while those treated with increasing concentrations of Tris buffer, formed aggregated with no fibrillar structure. However, there was an

intermediate stage at pH4 (i.e. treatment in PBS for 2 hours) where fibrillar structure was still maintained. We hypothesise that upon extrusion of the Fn solution into the precipitating bath, protonation of the molecules within the cable takes place. These hydrogen ions cause the fibrils within the cable to remain by repelling other protonated fibres thereby maintaining a spatial arrangement which subsequently gives the cable its fibrillar structure. This hypothesis is supported by observations that upon removing a substantial amount of the acidity (i.e. pH 5.5 upwards) followed by dehydration, there is aggregation of Fn-fibres within the cable with an eventual loss in overall fibrillar structure. Removal of the hydrogen ions expose the 'self-association' centres of Fn-fibres and upon dehydration these adhere together, resulting in the loss of structure.

Self-association could occur via the Fn-Fn and Fn-Fg sites which become exposed. However, there is an intermediate stage where (pH 4) fibrillar structure of the cable is retained suggesting that there may be enough of these protonated molecules causing a repulsive force on neighbouring molecules thereby retaining an overall fibrillar nature (Figure 5.3). In addition cables which were freshly made, treated in 200 mM Tris buffer and freeze-dried followed freeze-fracture and SEM did not retain any fibrillar at all showing that the above hypothesis may hold true. In contrast cables that were not freeze-dried, unprocessed and unfixed retained fibrillar structure at all treatment concentration showing that dehydration causes these self-association sites to aggregate.

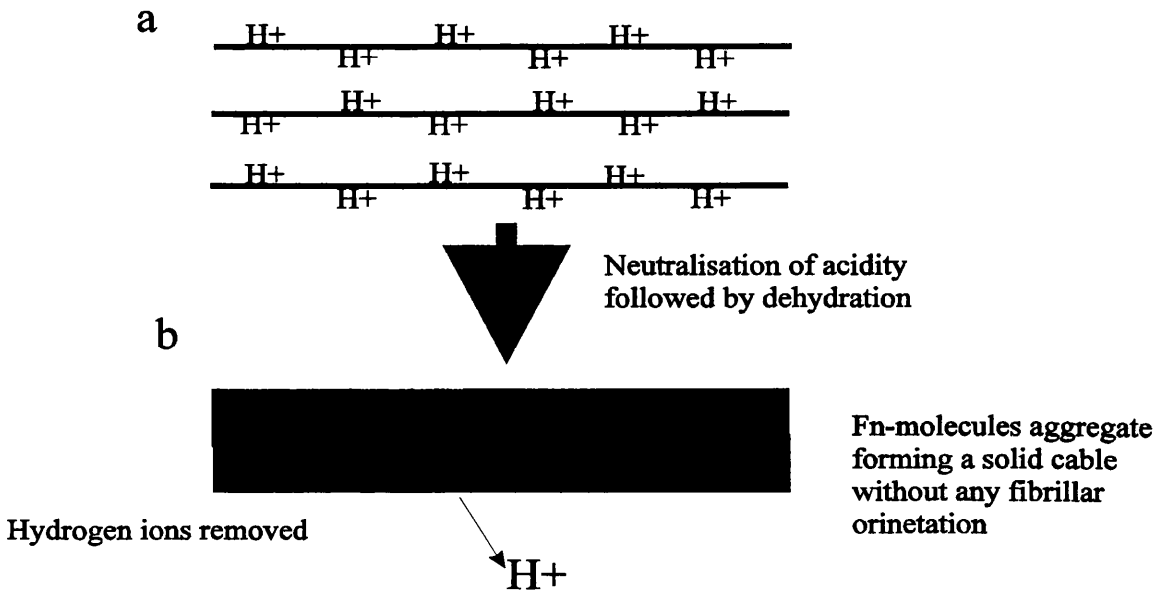

Figure 5.3. *Diagrammatic representation of the proposed cable structure once precipitated in the acid bath and when dehydrated. (a) shows that the fibres within the cable are protonated which repel each other to maintain a fibrillar arrangement of fibres but once the acidity is removed (b) and the cable is dehydrated the fibres no longer have this protonated layer to keep them apart and thus aggregate to for a solid structure.*

A similar effect of fibre aggregation upon rehydration and repeated dehydration was also observed in Fn-mats. Rehydrating the Fn-mats for increasing time periods caused increased aggregation eventually forming a non-porous, non-fibrillar structure. This is in contrast to Fn-mats which are normally freeze dried directly after formation which retain clear fibrillar arrangement as reported earlier (Ejim et al., 1993). Indeed these Fn-mats have been used successfully in vivo to guide the regeneration of peripheral nerves in rats and monkeys (Whitworth et al., 1995a; 1995b; Sterne et al., 1997a; 1997b; Ahmed et al., submitted). Fn-mats have been shown by us to have a fibrillar

ultrastructure, once it is in place within the nerve lesion in rats which is suitable to promote cell entry and migration (Porter et al., submitted).

The mechanisms for loss of structure may be different between the LFn-cable and Fn-mats may be different due to the mats being produced at neutral pH, however, the effect of rehydration and dehydration is the same. It is known that numerous proteins undergo unfolding as a response to freeze-drying (Allison et al., 1996). Some proteins that are unfolded in the dry solid state aggregate during dehydration while others refold. With proteins that normally aggregate after rehydration, minimising unfolding during freeze-drying with stabilisers has been shown to favour the recovery of native protein molecules after rehydration (Allison et al., 1996). In LFn-cables, the fibres generally aggregate as the H^+ ions are removed but as suggested above unfolding and refolding of the protein molecules may add to the aggregation process. However, it is likely that Fn molecules in Fn-mats are folded in the dry state and upon subsequent rehydration/dehydration the protein molecules unfold and expose the Fn-Fn self-association sites which aggregate leading to the disappearance of the fibrillar structure of the Fn-mat.

In conclusion our results show that hydration followed by dehydration together with SEM processing cause protein fibres in Fn-materials to aggregate. The more dehydration/rehydration takes place the worse the structure becomes. This may have important implications to others in the field working with artificial materials and proteins who rely on drying to stabilise the structure or for easier storage purposes to consider.

5.5. Behaviour of Schwann cells on normal and modified Fn-strands and cables as a 'simple model' for the Fn-mat/cable materials

Individual strands and cables of fibronectin are important in understanding the mechanism of contact guidance along such fibres as a step towards understanding their interactions in vivo. Furthermore, these guidance fibres will help us to understand how Fn-mats and cables work. Following peripheral nerve injury, the quicker the axons regenerate and reach their target, the less the damage caused to the target organ. Individual fibres of Fn allowed this component to be investigated. The stability of a particular guidance material is important and may be critical to its function especially if this material is to provide a continued guidance cue without premature resorption. This is important in tissue engineering applications where a bioresorbable material is required to provide the maximum amount of cellular infiltration and support while at the same time a controlled resorption takes place. Fibronectin also has the added advantages of being a promoter of cell adhesion which may be used to provide cells with directional attachments as well as topographical cues.

The aim of these experiments are: (1) to test the idea that Fn-fibres promote Schwann cell migration by the combine effect of topography (i.e. contact guidance) and by allowing a substrata favourable for cell adhesion (and subsequent migration), (2) that incorporation of Fg (which is assumed to be less adhesive for cells) will increase the speed of cell migration on Fn-cables by blocking-off highly adhesive sites on the Fn-molecule and finally (3) incorporation of micromolar concentrations of copper will increase the stability of Fn-strands and cables and cause an increase in cell migration by blocking off adhesive sites on Fn-strands/cables. The experiments in this section were

used to test how closely the methodologies used came to satisfying our predictions of the optimum cell migration substrata. These experiments will help us to understand how Fn-mats and cables work in vivo and allow us to be able to design new approaches and materials to tackle problems with target organ atrophy and new tissue engineering approaches to producing materials where guidance of cells by contact guidance is essential.

The movement of cells exhibiting contact guidance is said to be 'bi-directional' in which the cell has an ability of migrating in opposite directions. These directional cues are provided by chemical, structural and/or mechanical ansitropies of the substratum (Dunn, 1982). It is generally believed that contact guidance is an important morphogenetic mechanism, where traction force exerted by cells might even create the fibre orientation that then serves to guide their migration (Stopak and Harris, 1982). The process of contact guidance has also been implicated as an important component of several homeostatic processes (Katz and Lasek, 1980), such as wound healing, where retraction of the fibrin clot by platelets and contraction of the wound site by fibroblasts could cause radial orientation of extracellular matrix fibres and thereby guide cells to the wound site (Lackie, 1986).

Cell behaviour on glass or silica fibres has been extensively investigated by several authors (Curtis and Varde, 1964; Rovensky and Samiolov, 1994). Such artificial fibres can be thought of as models of natural fibres of the extracellular matrix. In this study we have used aggregated Fn-fibres derived from plasma Fn which in size and composition resemble natural fibres found in vivo. The subsequent cell guidance

exhibited on these fibres is likely to be as a result of the combined effects of the topography and the chemistry of the fibre (Wojciak-Stothard et al., 1997). Thin, cylindrical substrata have been previously reported to cause elongation and subsequent directional movement of cells (Curtis and Varde, 1964). Similar cell behaviour was also observed on oriented patterns of adhesive proteins (Britland et al., 1992) and grooves made on chromium-plated quartz by electron beam lithography (Dunn and Brown, 1986). Our experiments showed that Schwann cells are contact guided by Fn-fibres. Focal contacts and actin microfilaments were oriented in the direction of the fibre. This is consistent with the observations of Wojciak-Stothard et al., 1997 and the theory of Ohara and Buck (1979) that formation of focal adhesions within certain directions predetermines the orientation and guidance of the whole cell.

Fibronectin fibres (Fn-fibres) and fibronectin-coated, planar substrata promoted the adhesion and spreading of cells, though Fn-fibres had a greater, statistically significant effect. Schwann cells adhered rapidly but were only able to migrate after 4 hours along Fn-fibres, possibly due to the need for cells to overcome the effect of the curvature of the fibre (Curtis and Clark, 1990). After this period cells migrated significantly faster on Fn-fibres than on other substrata. Fn-fibres also significantly increased cell path length and persistence of cell movement, which resulted in cells exhibiting a greater unidirectional movement. It seems reasonable to suggest that this is a result of the properties of Fn to promote cellular migration together with a result of the topography of the Fn-fibres. Orientated arrays of topographical cues, such as grooves and ridges have been reported to increase the persistence and speed of fibroblast movement (Curtis et al., 1995). The increased persistence and the total length of cell path

observed with Schwann cells are in agreement with results of Wojciak-Stothard et al., 1997, using macrophages, fibroblasts and neurites cultured on similar Fn-fibres.

It is unclear, however, how cells dock onto and align with each other, many cell diameters away form the primary orientating cue (ie. the Fn-fibre). It may be that parallel cytoskeletal elements in one cell tend to align adjacent cells by polarisation of cell-cell interaction points. However, a similar explanation is that this is sterically the most favourable form of packing at higher cell densities, around a single line of cells. This phenomenon may be utilised to advantage in tissue engineering where orientation is critical, such as blood vessels, capillaries and tendons. Scanning micrographs in this study have shown that microspikes or filopodia link between adjacent cells and it is possible that these filopodia can act to signal between cells, co-ordinating alignment of cells resulting in the band of aligned cells. However, it is unclear in this case why the alignment band suddenly ends beyond 50 μm from the original contact surface on the Fn-fibre. Regression analysis of the width of the cell aligned band and paraxial elongation showed no significant effect on increasing Fn-fibre width. This is dissimilar to that effected by microfabricated ridges reported by Dunn and Brown, 1986 who showed that cell alignment and paraxial elongation was inversely proportional to the ridge width. This indicates a different mechanism of cell behaviour between the two systems which may reflect the different capacities for adhesion of cells to such surfaces, with Fn-fibres promoting cell adhesion and subsequent alignment.

We did not look at whether Schwann cells attempted to myelinate Fn-fibres. It is unlikely that Schwann cells would myelinate these fibres as they are because Schwann

cells need to wrap themselves around the fibre before they start to lay down a myelin sheath. In the regenerating nerve, axon to Schwann cell attachment is mediated via various adhesion molecules including the immunoglobulin superfamily, such as neural cell adhesion molecule (NCAM) and L1, and the cadherin superfamiliy, e.g. N-cadherin and E-cadherin (Bixby and Harrris, 1991; Letourneau et al., 1994). However, these are thought not to be present at the time of myelination. It is therefore possible that myelination may be induced in vitro around these fibres if a 3-dimensional system were used i.e. Fn-fibres placed in collagen gels and seeded with Schwann cells. This remains to be investigated.

Cells spread on Fn-fibres were frequently elongate and polarised, apparently taking on a migratory phenotype. These changes were accompanied by alignment of F-actin microfilaments to the direction of the fibre, which was again more prominent in cells on Fn-fibres than on poly-L-lysine/Fn solution, poly-L-lysine/laminin or poly-L-lysine alone, consistent with the theories that topographical and surface properties of the fibres promote cell migration. Vinculin staining, showed that focal contacts had formed between Fn-fibres and Schwann cells which were aligned with the direction of the fibres again consistent with a primarily migratory phenotype. The presence of Fn-fibres significantly promoted the persistence, speed of migration, orientation and spreading of Schwann cells, consistent with the idea that 3-D mats of Fn will be effective guides to promote regenerating components of the peripheral nerves.

These experiments indicate the potential importance of directional cues for promoting nerve regeneration for which Schwann cells are required to migrate and provide myelin

to regenerating axons and their early growth into any implant and alignment are important for effective repair. The use of materials derived from Fn-fibres in peripheral nerve regeneration would not only have a dual positive effect in guidance as well as in stimulating cellular migration, since soluble Fn promotes neurite outgrowth (Akers et al., 1981). The results of this study taken together with that of Wojciak-Stothard et al., 1997, support and explain the effectiveness of 3-dimensional Fn-mats to promote regeneration of peripheral nerves (Whitworth et al., 1995a; Whitworth et al., 1995b; Whitworth et al., 1996; Porter et al., submitted; Sterne et al., 1997a; Ahmed et al., submitted). Since axonal regeneration follows behind Schwann cell infiltration, increased migration on Fn-materials is likely to reduce a major problem in peripheral nerve regeneration namely, atrophy of the target organ (Sterne et al., 1997b).

Cell adhesion and migration is involved in numerous physiological processes and is important in biotechnological applications, including tissue engineering and development of artificial organs (Garcia et al., 1997). Fn, besides collagen, is a major extracellular protein of the extracellular matrix (ECM) and plays a role in cell adhesion, spreading, cytoskeletal organisation, cell differentiation, morphogenesis in early vertebrate development and tissue remodelling (Darribere et al., 1992; Grinnell, 1978). Migration of cells in higher organisms is mediated by adhesion receptors, such as integrins which link cells to the extracellular matrix and transmit the forces necessary to undergo locomotion. Cell adhesion has been shown to linearly increase with increasing density of adsorbed Fn (Garcia et al., 1997). This increase in strength was effectively blocked by a monoclonal antibody directed against the RGD cell binding domain in rat osteosarcoma cells (ROS 17/2.8) (Garcia et al., 1997).

In most experiments a single layer of a specific substratum such as Fn adsorbed onto glass, plastic or other artificial material has been used to quantify cell adhesion strength and migration. This however, is different from the situation in vivo where ECM proteins such as collagen and Fn appear in the form of fibres assembled into a three-dimensional mesh. Our system with single strands of Fn adherent glass coverslips represents, a two-dimensional surface which is a closer approximation of the effect of such fibres in vivo. Here a different strategy involving the incorporation of Fg, was used to speed up cell migration on Fn/Fg-cables where a different starting material to that described above was used in which the normal percentage ratio was Fn:Fg = 75:25. During manufacture of Fn-cables, the percentage composition of Fg was varied and these Fn/Fg-cables were then used to test the behaviour of Schwann cells on the speed of cell migration, measurement of cell area and extension and subsequently correlated with integrated vinculin immunostaining density.

Our study showed that Fn/Fg-cables significantly increased cell migration on these fibres compared to cells grown on plain glass substrata. Schwann cells, human dermal, rat tendon and rat skin fibroblasts migrated faster on increasing concentrations of Fg within the cable upto a peak on 50% Fn/50% Fg. Schwann cells migrated 40% faster on 50:50 Fn:Fg-cables than Fn-cables with no Fg. Increasing the Fg concentration beyond this point resulted in a loss of cell velocity such that on 25% Fn/75% Fg-cable, cell speed was reduced by at least 11-29% compared to migration on 50% Fn/Fg-cables. The greatest reduction in cell velocity was observed for Schwann cells which seem to move faster than other populations of cells in the first instance. This suggests that Scwhann cell attachment and subsequent migration is more sensitive to Fg than

other cell populations. However, Fg has previously been shown to induce adhesion and spreading of human endothelial cells in vitro (Dejane et al., 1987) and human dermal fibroblasts (Gailit et al., 1997). Grinnell et al, 1980, however, reported that baby hamster kidney cells did not attach to substrata composed of Fg, but that adhesion was supported when plasma Fn was covalently cross-linked to Fg.

Maximum cell migration velocity is mathematically predicted to occur at an intermediate ratio of cell-substratum adhesiveness to intracellular contractile elements, at which the cell can form new attachments at the cell front but is able to break attachments at the rear (DiMilla et al., 1991; 1993; Palacek et al., 1997). The ability of cells to migrate on a particular substratum depends on many variables related to integrin-ligand interactions including ligand levels (DiMilla et al., 1991; Goodman et al., 1989), integrin levels (Bauer et al., 1992; Keely et al., 1995) and integrin-ligand binding affinities (Duband et al., 1991; Huttenlocher et al., 1996). Other variables such as lamellipodal extensions, intracellular force generation, integrin clustering and avidity effects, and integrin signalling are important to the process of cell adhesion and migration (Lauffenburger and Horwitz, 1996; Huttenlocher et al., 1996).

At the maximum cell migration speed in our study, the ligand concentration was enough to cause the cells to attach and migrate on Fn/Fg-cables with a phenotype resembling a moderately spread cell. However, high concentrations of Fn cause the cell to increase the number of vinculin attachment plaques, seen from relative integrated fluorescence, and therefore the cells will be attached more tightly while occupying a greater spread area. This causes the cells to increase the number of ligand-receptor

interactions and subsequently makes the cell less mobile and unable to break attachments at the rear of the cell as it moves (Abercrombie et al., 1970; Marks et al., 1991; Jay et al., 1995), hindering cell migration. Reduced migration on Fn/Fg-strands may be due to the inability of cells to form stable attachments to the Fn/Fg-strand surface (Wessels et al., 1994). This may be as a result of Fg blocking off cell binding sites within the Fn molecule either due to steric hinderence or direct coupling of Fg to Fn or that Fg is less adhesive than Fn (Figure 5.4). Cell adhesion was severely hindered on 75% Fg coated substrata which may be attributed to the fact that the cells used in our system were unable to form, stable attachments to this less adhesive substrata. This suggests that the predominant integrins expressed have little or no affinity for Fg. The concentration of Fn and Fg required to cause maximal cell migration in our system was much higher than that reported earlier where these proteins were adhered onto glass substrata alone (Palacek et al., 1997). This is distinctly different from our system where cables not only offer cell binding sites but also topography and both of these parameters as well as all others mentioned above will contribute to the overall cell adhesion and migration process. Clearly, this indicates important differences between coated tissue culture surfaces and single fibres or strands when studying cell behaviour.

In conclusion, these results confirm that maximal cell migration occurs at an intermediate ratio of cell-substratum adhesiveness and additionally, that different cell populations are effected differently with increasing adhesiveness. Cell migration on Fn/Fg-cables was faster than on coated glass substrata due to the effects of topography speeding up apparent cell velocities. Further, cell adhesion and subsequent migration

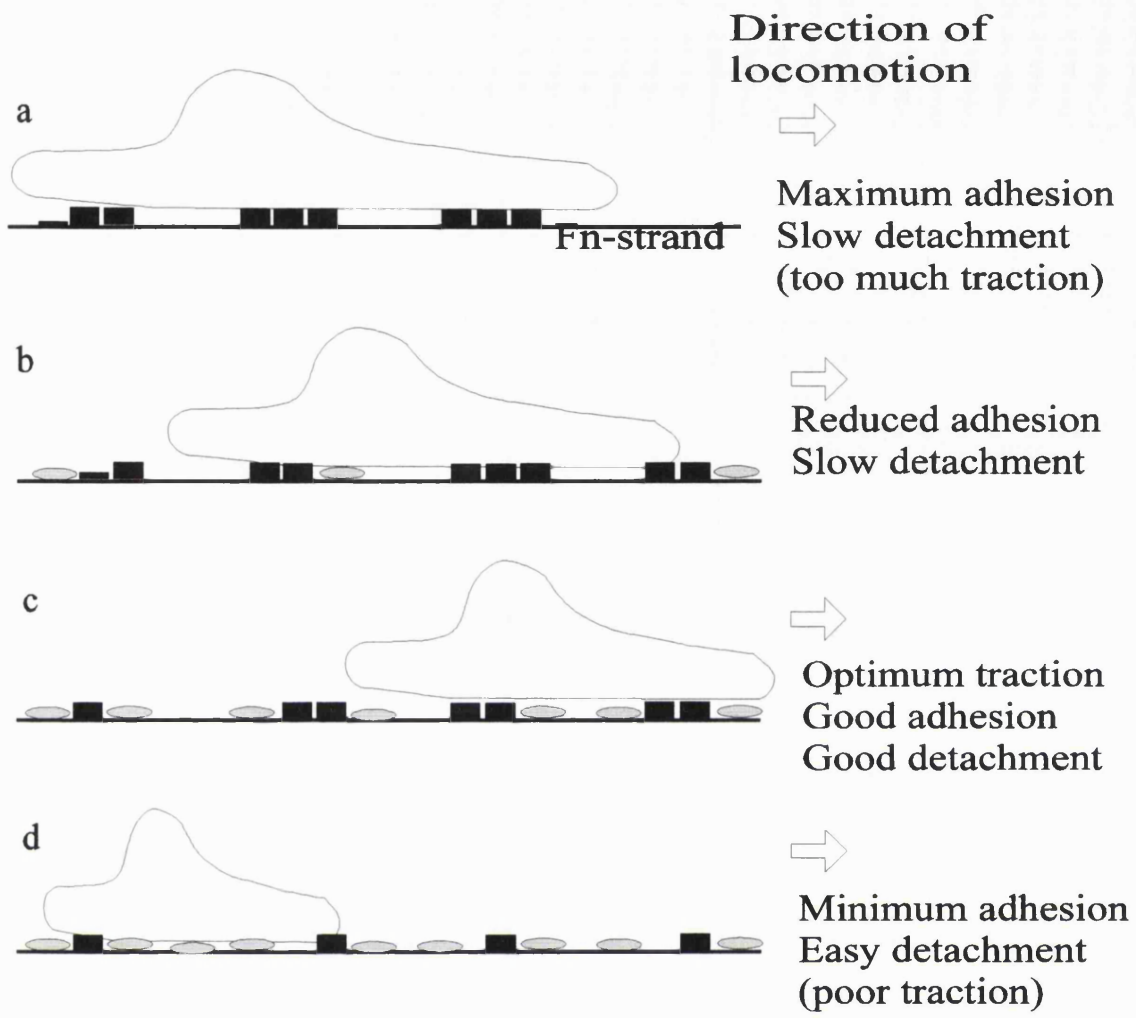

Figure 5.4. *Proposed mechanism for increased cell migration with increasing concentrations of Fg. (a) represents pure Fn-strand where cells attach to Fn via the most of the available plaques (dark squares) and therefore are unable to break off attachments at the rear due to the number of stable attachments formed. (b) represents Fn-strand composed of 25% Fg (represented by hatched ovoid) where cells cannot attach to all available sites and therefore break off contacts at the rear easier than on pure Fn-strands (i.e. (a)). (c) represents Fn-strand with 50% Fg (i.e. intermediate ligand level) where cells form fewer attachments than in (b) and therefore break off easily when they migrate. In contrast, (d) represents Fn-strands with 75% Fg where the cell is unable to form enough stable attachments and therefore cell migration is hindered.*

could be significantly reduced using high concentrations of Fg within Fn/Fg-cables which seems to reduce the adhesiveness of Fn. In addition, important differences exist between coated tissue culture surfaces and fibres or strands/cables which need further investigation.

In the next experiment, we postulated that treatment of Fn-strands and cables with copper ions will cause material stabilisation and also increased cell migration speed by blocking off adhesive sites on the Fn molecule and providing the optimal surface for migration of cells. Both Fn-strands and Fn-cables were used and it was postulated that less copper ions will be needed to cause optimum cell migration on Fn-cables than on Fn-strands. This is because Fn-cables already contain 25% Fg which cause some blocking off of adhesive sites while Fn-strands are entirely composed of Fn.

The results from this experiment showed that Fn-strands and Fn-cables could be stabilised with copper ions, increasing the stability by 2-3 fold. This is similar to other reports in this thesis with Fn-mats and cables showing that the mechanism is consistent. Cells cultured on these treated strands/cables were able to align parallel to the fibres, as we have described earlier. Schwann cells however, show more sensitivity to copper treatment and were able to grow on Fn-strands treated with a maximum of 50μM copper while all fibroblast types were able to survive upto the maximum concentration used in our study. This is different to Fn-mats and LFn-cables where Schwann cells were only able to survive at the 1μM treated level. The difference may be attributed to the fact that Fn-mats and LFn-cables represent many of these single fibres thereby chelating more copper ions and it is this which is presented to the cell surface causing

toxicity to cells above 1μM treatment levels in these materials. With Fn-strands and cables, treatment concentrations above 50 μM were toxic suggesting that these strands/cables chelated toxic levels of copper ions with increased treatment concentrations.

Interestingly, treatment of the strands with increasing concentrations of copper caused a dose dependent increase in migration speed with a maximum for fibroblasts reached at 100μM copper on Fn-strands while maximum migration speed was reached at 10 μM copper on Fn-cables. After these points the migration speed decreased. In the case of Schwann cells there was a significant increase in migration speed with the lowest concentration of copper upto a maximum with 50μM copper treatment with Fn-strands. This difference in cell migration may be attributed to a difference in substrate composition of these two fibres. Indeed, Fn-cables contain Fg which we have already shown to be less adhesive. Although the concentration of copper needed to cause maximum cell migration were significantly different, the maximal attainable speed of cells was not significantly different. This suggests that integrin coupling with intracellular motors remains unaltered as the ligand concentration is varied, as suggested by Palacek et al., 1997.

Cellular extension and area for all cell types followed a similar dose dependent pattern over the period of 24 hours studied. Interestingly, cells spread less on untreated or treated Fn-cables compared to Fn-strands. Cells cultured on untreated Fn-strands were well spread while those cells at treatment level of copper causing maximal migration speed, were moderately well spread. Cells which were cultured on high copper treated

Fn-strands were not as well spread as those at the maximal migration speed. Similar results with other test systems have been shown by others (Palacek et al., 1997).

Integrated density for vinculin in all cell types showed a reduction from untreated strands/cables to the maximum copper treatment level suggesting that fewer attachments were formed as the dose of copper increased. Integrated density measurements were less for cells on Fn-cables suggesting that fewer stable attachments were forming to this substratum when compared to those on Fn-strands. This is due to the 25% Fg in Fn-cables making the strand less adhesive, possibly by blocking off some of the highly adhesive sites on the Fn molecule, as we have suggested earlier, and not allowing cells to form as many stable attachments as Fn-strands which are made from pure Fn (i.e. highly adhesive). However, as the concentration of copper ions increased, more cell binding sites on the Fn molecule were blocked off. This allowed cells to form enough stable attachments while allowing attachments at the rear to be broken off easily, hence increasing apparent cell migration speed. The same diagram as Figure 5.4. may be adapted as a possible mechanism for this increased migration, where the hatched ovals now represent copper ions rather than Fg. Copper ions may cause this increased migration speed through direct coupling to a reactive group on the Fn molecule thereby blocking off adhesive sites in both cases. However, when high levels of copper were present many of these adhesive sites were blocked off which leads to cells no longer being able to form enough stable attachments and therefore migration speed is hindered. It may be that high levels of copper caused a decrease in cell energy (ATP) thereby causing cells to lose their ability to spread and move. Copper may also poison an important enzyme needed for cell spreading and migration

and may also cause a decrease in matrix protease activity therefore the cells have a decreased ability to cause plaque lysis inorder for them to migrate.

In conclusion, copper treatment of Fn-strands/cables causes an increase in cell migration speed by potentially blocking off adhesive sites on the Fn molecule so that the cell does not bind too tightly for it to break attachments at the rear when migration is required. The optimum treatment concentration to cause this in fibroblasts was 10-100μM copper while Schwann cells were much more sensitive to copper treatment and reached their maximum migration speed when strands/cables were treated with 50μM copper.

Taking the results from this section together, we can develop new strategies to increase the stability of Fn-materials and modification of these to cause increased Schwann cell migration speed and therefore may be able to reduce atrophy of the target organ, a common failure in peripheral nerve injuries. These approaches may also be useful in designing new materials for tissue engineering applications where enhanced cell spreading and more specifically, enhanced cell migration may be desired. The ability of Fn-fibres to align cells 50μm away from the original contact guidance cue shows that we can make parallel arrays of these single fibre 50 μm away on a suitable backing material such as collagen sponges (already available in a clinical grade). This may be used as one approach to a possible scale of the Fn-mat system. In addition, incorporation of copper giving material stabilisation will allow a more controlled resorption of the material while allowing increased cell migration. Similarly, Fg may also be incorporated into the cable to give enhanced cell migration.

Conversely, high concentrations of Fg or copper ions may be used to control cell spreading and migration and may be useful is in approaches to clinically treat cancer, where a reduction in cell migration represents a potential strategy to limit the spread of cancer to distal parts of the body i.e. metastasis.

6.0 CONCLUSIONS

Conclusions which may be drawn from this thesis are:

1. Low concentrations of copper significantly stabilises Fn-mats and LFn-cables without loss of fibrillar structure while increasing the rate of proliferation of cultured Schwann cells within such materials.

2. NGF impregnated mats promote the regeneration of peripheral nerve fibres while improving the quality of the regenerate and reinnervation of sensory targets. From our work and those by Whitworth et al. and Sterne et al., it can be seen that for improved regeneration of peripheral nerves a 'cocktail' of growth factors is needed.

3. Large cables of fibronectin may be manufactured with fibrillar orientation, different dimensions and may be seeded with aligned Schwann cells.

4. Cellular migration is encouraged by individual fibres of Fn with the formation of an 'aligned band' of cells which also align cytoskeletal elements within cells. These fibres with cells grown in vitro forms a good model of the Fn-mat system in vivo.

5. The speed of cell migration, in particular for Schwann cells, may be manipulated either using high concentrations of Fg or copper ions. This would be useful as the time taken for Schwann cells to migrate from the proximal to the distal end would be quicker and thus limit end organ atrophy, a major drawback of peripheral nerve injuries.

6. When choosing bio-materials which require freeze-drying or any form of drying as a method for easier storage or to stabilise such structures, careful attention must be paid because drying may "damage" the structure.

Taken together, all these results suggest a first design for an ideal conduit material for peripheral nerve repair. This would be (a) the dimensions (fibrous), (b) fibre orientation (c) composed of 50:50 Fn: Fg, (d) treated with micromolar concentrations of copper/zinc (e) seeded with cultured Schwann cells and (f) soaked with a 'cocktail' of neurotrophic growth factors including NGF and NT-3.

7.0 CLINICAL IMPLICATIONS

1. Copper impregnated Fn-mats may be used to deliver copper to the site of injury, especially in burn injuries where copper levels are thought to be reduced and is essential for collagen production.

2. The favourable outcome of the primate study with Fn-mats + NGF and work done by Whitworth et al. suggests that clinical trials could go ahead as soon as permission can be granted. It is anticipated that in such a situation Fn-mats + NGF grafts will be successful in promoting the repair of peripheral nerve lesions of upto 1 cm long and also cause less dennervation of end organ targets and improved reinnervation leading to good functional recovery.

Fn-mats may also be used in longer defects where a short segment of nerve autograft may be interposed between two segments of Fn-mats (Figure 7.1). This would limit the amount of donor nerve used and reduce donor site morbidity. These mats may then be impregnated with neurotrophic factors.

3. Large cables of Fn, once proved successful in animal models may be used to repair long peripheral nerve lesions and other complex procedures where multiple branches need to be grafted. The ease of production and dimensions of LFn-cables may make this material a good alternative to using nerve grafts for short or long nerve lesions.

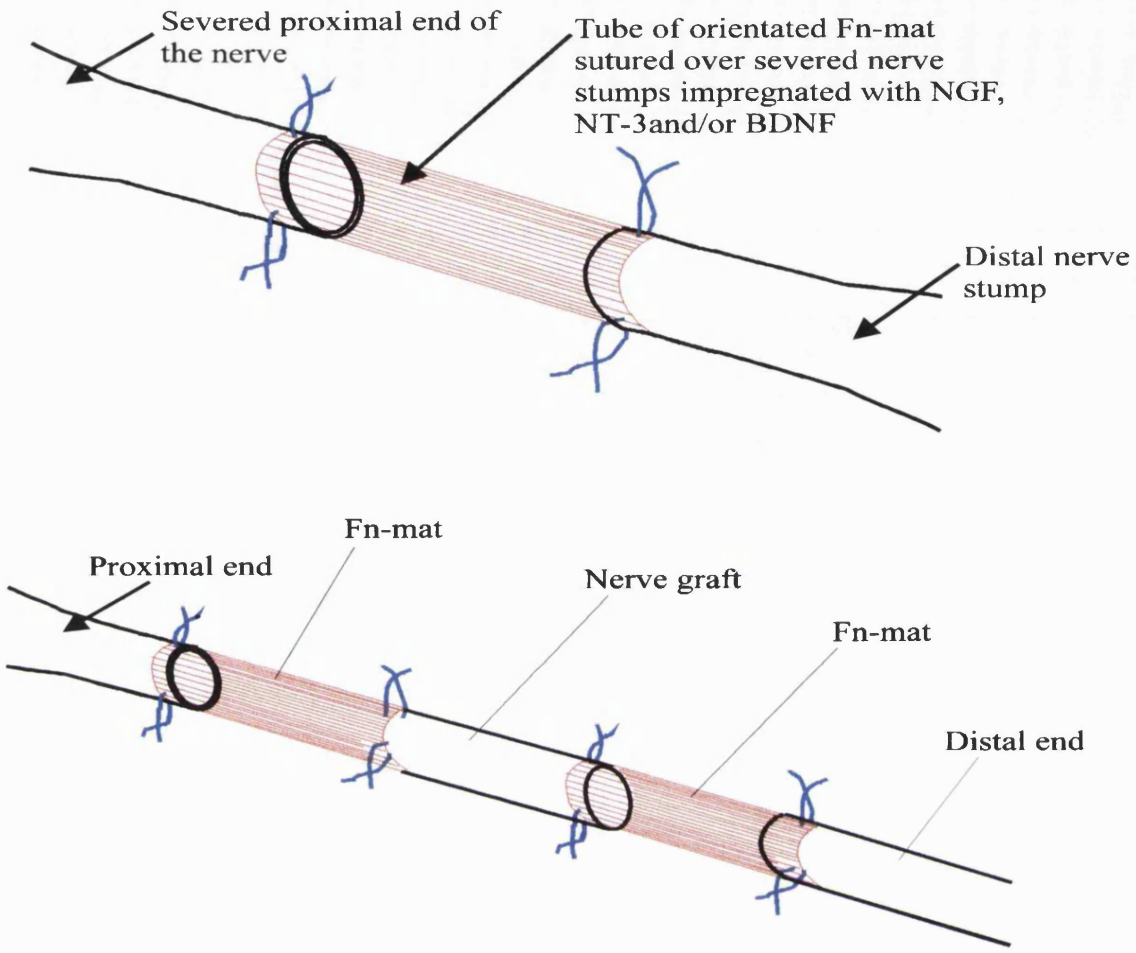

Figure 7.1. *Diagrammatic representation of possible use of Fn-mats in long peripheral nerve lesions. A nerve graft is interposed between two Fn-mats and sutured between the created gap. The nerve graft will have Schwann cells which will help to promote the repair process.*

8.0 FURTHER WORK

1. LFn-cables need to be tested in vivo using the same model as Whitworth et al. and also longer gap lengths need to be tested to work out the maximal possible distance that can be regenerated with these materials.

2. Copper impregnated Fn-mats and LFn-cables must be tested to work out how long the mats survive in vivo and also the speed of axonal regeneration through these mats. This will entail setting up the same animal model as used by Whitworth et al. where a 1 cm gap is created in the sciatic nerve. This would be used to test Fn-mats vs CuFn-mats. Early as well as late time points need to be studied i.e. 3, 5, 7, 14, 21, 30 and 60 days by both immunohistochemistry and transmission electron microscopy.

3. It is clear from previous work and work in this thesis that the right concentration of a 'cocktail' of neurotrophic growth factors (including NGF, NT-3, NT-4/5 and BDNF) impregnated into Fn-mats need to be tested in an animal model for speed and quality of the regenerate and also end organs.

4. A limitation of using Fn-mats impregnated with neurotrophic factors is that these factors are released from the mat within 7 days. However, a continued supply of such growth factors will be beneficial in promoting further cell survival and thus improve the outcome of the repair. A new approach using modern genetic engineering techniques may also be employed to provide continued release of growth factors locally to facilitate improved peripheral nerve repair. The gene sequence for human recombinant NGF is already available in a 'clinical grade' quality. This may be used to

transfect the NGF gene into fibroblasts, which are easy to culture and obtained by a simple punch biopsy of the patient (therefore no problem of rejection). The transfected fibroblasts can then be grown in culture into Fn-mats or LFn-cables and grafted between the nerve lesion. This approach has already been used in animal model and have been shown to be effective in promoting the repair process (Tuszinski et al., 1994; Kawaja et al., 1992).

5. The ideal conduit design outlined in Chapter 6.0 need to be tested in vivo.

9.0 PUBLICATIONS AS A RESULT OF THIS STUDY

1. Stabilisation of fibronectin mats with micromolar concentration of copper. In Press (Biomaterials). **Ahmed Z.**, Idowu B.D., Brown R.A.

2. Regeneration of peripheral nerves through orientated fibronectin mats: An ultrastructural study. Submitted to Tissue Engineering.
   Porter R.A., **Ahmed Z.**, Brown R.A., Whitworth I.H., Terenghi G.

3. Nerve growth factor delivered locally via fibronectin mats enhances peripheral nerve regeneration in the non-human primate. Submitted to Neuropathology Applied Neuropathology. **Ahmed Z.**, Brown R.A., Wiberg M., Ljungberg C., Meru N., Terenghi G.

4. Adhesion, alignment and migration of cultured Schwann cells on ultrathin fibronectin fibres. In Press (Cell Motility and the Cytoskeleton).
   Ahmed Z and Brown R.A.

5. Production of large fibres of fibronectin as a potential conduit for repair of long peripheral nerve lesions. In prep. **Ahmed Z.**, Underwood S., Brown R.A.

6. Copper stabilisation of large fibronectin cables: cell substrate properties. In prep.
   Ahmed Z., Briden A., Brown R.A., Hall S.M.

7. Mats and Cables from fibronectin: effect of freeze-drying on fibrillar structure. In Prep. **Ahmed Z.**, Smith K., Brown R.A.

8. High concentrations of fibrinogen inhibit cell adhesion and migration on fibronectin/fibrinogen composite strands. In prep.
   Ahmed Z ., and Brown R.A.

Published Abstracts

1. Stability and cell-substrate properties of fibronectin mats using copper ions. Wound Repair and Regeneration 1997, 5:A266.

   Ahmed Z., Idowu B.D., Brown R.A.

2. Nerve growth factor enhances peripheral nerve regeneration in primates. Wound Repair and Regeneration 1997, 5:A266.

   Ahmed Z., Brown R.A., Wiberg M., Ljungberg C., Whitworth I.H., Terenghi G.

3. A study of adhesion and alignment of cultured Schwann cells on ultrathin fibronectin fibres. Wound Repair and Regeneration 1997, 5:A266.

   Ahmed Z., and Brown R.A.

4. Production of large cables of fibronectin with potential as a conduit for the repair of long peripheral nerve lesions. Wound Repair and Regeneration 1997, 5:A266.

   Ahmed Z., Underwood S., Brown R.A.

Oral Presentations

1. Production of large cables of fibronectin with potential as a conduit for the repair of long peripheral nerve lesions. ETRS meeting, 23-26 August 1997, Koln, Germany. **Ahmed Z.**, Underwood S., Brown R.A.

Poster presentations

1. Micromolar concentrations of copper stabilises fibronectin mats.

Smith & Nephew Advance in Tissue Engineering and Biomaterials, University of York, 20-23 July 1997. **Ahmed Z.**, Idowu B.D., Brown R.A.

2. Enhancement of peripheral nerve regeneration in primates using nerve growth factor. Smith & Nephew Advance in Tissue Engineering and Biomaterials, University of York, 20-23 July 1997. **Ahmed Z.**, Brown R.A., Wiberg M., Ljungberg C., Whitworth I.H., Terenghi G.

3. Stability and cell-substrate properties of fibronectin mats using copper ions. ETRS 23-26 August 1997, Koln, Germany. **Ahmed Z.**, Idowu B.D., Brown R.A.

4. Nerve growth factor enhances peripheral nerve regeneration in primates. ETRS meeting, 23-26 August 1997, Koln, Germany. **Ahmed Z.**, Brown R.A., Wiberg M., Ljungberg C., Whitworth I.H., Terenghi G.

5. A study of adhesion and alignment of cultured Schwann cells on ultrathin fibronectin fibres. ETRS meeting, 23-26 August 1997, Koln, Germany. **Ahmed Z.**, Brown R.A.

REFERENCES

Abercrombie M., Heaysman J.E.M., and Pegrun S.M. (1970). The locomotion of fibroblasts in culture. I. Movements of the leading edge. Exp. Cell Res. 59: 393-398.

Acheson A., Barker P.A., Alderson R.F., Miller F.D., and Murphy R.A. (1991). Detection of brain-derived neurotrophic factor-like activity in fibroblasts and Schwann cells: inhibition by antibodies to NGF. Neuron 7: 265-275.

Aebischer P., Guenard V, Winn S.R. et al (1988). Blind-ended semipermeable guidance channels support peripheral nerve regeneration in the absence of a distal nerve stump. Brain Research 454: 179-187.

Aebischer P., Valentini R.F., Dario P., Domenici C., and Gaillett P.M. (1987). Piezoelectric guidance channels enhance regeneration in the mouse sciatic nerve after axotomy. Brain Research 436: 165-168.

Ahmed Z., Idowu B.D., and Brown R.A. Stabilisation of fibronectin mats with micromolar concentrations of copper. Biomaterials 20: 201-209.

Akers R.M., Mosher D.F., and Lilien J.E. (1981). Promotion of retinal neurite outgrowth by substratum-bound fibronectin. Developmental Biology 86: 179-188.

Akiyama S.K., Yamada S., Chen W.T., and Yamada K.M. (1991) Analysis of fibronectin receptor function with monoclonal antibodies: role in cell adhesion, migration, matrix assembly, and cytoskeletal organization. J. Cell. Biol. 109: 863-875.

Albelda S.M., and Buck C.A. (1990). Integrins and other cell adhesion molecules. FASEB (Fed. Am. Soc. Exp. Biol.) J. 4: 2868-2880.

Ali I.U., Hynes R.O. (1987). From the cell in contact. Cell 14:439-446.

Ali I.U., and Hynes R.O. (1978). Role of disulfide bonds in the attachment and function of large, external, transformation-sensitive glycoprotein at the cell surface. Biochim. Biophys. Acta 510: 140-150.

Allison S.D., Dong A., and Carpenter J.F. (1996). Counteracting the effects of thiocynate and sucrose on chymotrypsinogen secondary structure and aggregation during freezing, drying, and rehydration. Biophysics J. 71: 2022-2032

Aloe L., Cozzari C., and Levi-Montalcini R. (1985). Cyclotidine-induced release of nerve growth factor from mouse submadibular glands enhances regeneration in sympathetic fibres in adult mice. Brain Res. 332: 259-265.

Angeletti R.H., and Bradshaw R.A. (1971). Nerve growth factor from mouse submaxillary gland: amino acid sequence. Proc. Natl. Acad. Sci. USA. 68: 2417-2420.

Anton E.S., Weskamp G., Reichardt L.F., and Matthew W.D. (1994). Nerve growth factor and its low affinity receptor promote Schwann cell migration. Proc. Natl. Acad. Sci. USA 91: 2795-2799.

Anton E S., Hadjiargyrou M., Patterson P.H., and Matthews W.D. (1995). CD9 plays a role in Schwann cell migration in vitro. J. Neurosci. 15: 584-595.

Arbuthnott E.R., Boyd I.A., and Kalu K.U. (1980). Ultrastructural dimensions of myelinated peripheral nerve fibres in the cat and their relation to conduction velocity. J. Physiol. 308: 125-137.

Archibald S J., Krarup C., Shefner J., et al (1989) Semi-permeable collagen based nerve guide tubes are as effective as standard nerve grafts to repair transected peripheral nerves: An electrophysiological study in the non-human primate Society of Neuroscience Abstracts 15: 125.18.

Archibald S.J., Krarup C., Shefner J., et al (1991) A collagen based nerve guide conduit for peripheral nerve repair An electrophysiological study of nerve regeneration in rodents and non-human primates Journal of Comparative Neurology 306:685-696.

Archibald S.J., and Madison R (1988). Functional recovery following rat sciatic nerve regeneration through collagen nerve guides: Comparison of direct anastomosis, nerve graft and entubulation repair Society of Neuroscience Abstracts 14:204.7.

Assouline J.G., Bosch P., Lim R., Kim I.S., Jensen R., and Pantazis N.J. (1987). Rat astrocytes and Schwann cells in culture synthesize nerve growth factor-like promoting factors. Dev Brain Res 31: 103-118.

Bandtlow C.E., Heumann R., Schwab M.E., and Thoenen H. (1987). Cellular localisaton of nerve growth factor by in situ hybridisation. EMBO J 6: 891-899.

Barbacid M. (1995). Neurotrophic receptors and their receptors. Curr. Opin. Cell Biol. 7: 148-155.

Barde Y-A. (1989). Trophic factors and neuronal survival. Neuron 2: 1386-1403.

Barnhart M.I., and Anderson G.F. (1962). Intracellular localisation of fibrinogen. Proc. Soc. Exp. Biol. Med. 110: 734-737.

Baudet C., Naveilhan P., Jehan F., Brachet P., and Wion D. (1995). Expression of nerve growth factor is controlled by the microtubule network Journal of Neuroscience 41 :462-470.

Bauer J.S., Schreiner C.L., Giancotti F.G., Ruoslahti E., and Juliano R.L. (1992). Motility of fibronectin receptor-deficient cells on fibronectin and vitronectin: collaborative interactions among integrins. J. Cell Bio. 116: 477-487.

Bell M.A., and Weddell A.G.M. (1984a). A morphometric study of intrafascicular vessels of mammalian sciatic nerve. Muscle Nerve 7: 524-534.

Bell M.A., and Weddell A.G.M. (1984b). A descriptive study of the blood vessels of the sciatic nerve in the rat, man and other mammals. Brain 107: 871-898.

Berkemeier L.R., Winslow J.W., Kaplan D.R., Nikolics K., Goeddel D.V., and Rosenthal A. (1991). Neurotrophin-5: a novel neurotrophic factor that activates trk and trkB. Neuron 7: 857-866.

Beuche W., and Friede R.L. (1984). The role of non-resident cells in Wallerian degeneration. Journal of Neurocytology 13: 767-96.

Beveridge J A., and Politis M.J. (1988). Use of exogenous electric current in the treatment of delayed lesions in the peripheral nerves. Plastic and Reconstructive Surgery 82: 573-579.

Bickle T.A., Hershey J.W., and Traut R.R. (1972). Spatial arrangement of ribosomal proteins: reaction of the Escetichia coli 30S subunit with bisimidoesters. Poc. Natl.Acad. Sci. USA. 69: 1327-1331.

Bixby J.L., and Harris W.A. (1991). Molecular mechanisms of axon growth and guidance. Ann Rev Cell Biol 7: 117-159.

Bixby J.L., Lilien J., and Reichardt L.F. (1995). Identification of the major proteins that promote neuronal process outgrowth on Schwann cell in vitro 107: 353-361.

Bothwell M. (1996). p75 NTR: a receptor after all. Science 272: 506-507.

den Braber E.T., de Ruijter J.E., Smits H.T., Ginsel L.A., von Recum A.F., and Jansen J.A. (1995) The effect of parallel surface microgrooves and surface energy on cell growth. J Biomed Meter Res. 29: 511-518.

Bradford M.M. (1976). A rapid and sensitive method for the quantitation of microgram quantities of protein utilizing the principle of protein-dye binding. Anal Biochem 72: 248-254.

Braun R.M. (1964). Experimental peripheral nerve repair tubulation. Surgical Forum l 5:452-454.

Brewster W.J., Fernyhough P., Diemel L.T., Mohiuddin L. and Tomlinson D.R. (1994). Diabetic neuropathy, nerve growth factor and other neurotrophic factors. Trends. Neurosci. 17: 321-325.

Britland S., Clark P., Connoly P., and Moores G. (1992). Micropatterned substratum adhesiveness: a model for morphogenetic cues contolling cell behaviour. Exp. Cell Res. 198: 124-129.

Brockes J.P., Fields K.L., and Raff M.C. (1979). Studies on cultured rat Schwann cells. I. Establishment of purified populations from cultures of peripheral nerve. Brain Research 165: 105-118.

Brockes J.P., Lemke G.E., and Balzer Jr D.R. (1980). Purification and preliminary characterisation of a glial growth factor from the bovine pituitary. J Biol Chem 255: 8374-8377.

Brown R.A. (1992). An appreciation of the Folin-Lowry protein assay. J Pharm Pharmacol 44: 369.

Brown R.A., Blunn G.W. and Ejim O.S. (1994). Preparation of orientated fibrous mats from fibronectin: composition and stability. Biomaterials 15: 457-464.

Brown R.E., Erdmann D., Lyons S.F., and Suchy H. (1996). The use of cultured Schwann cells in a rabbit hind-limb model. J Reconstr Microsurg 12: 149-152.

Brown M.C. Perry V.H., Lunn E.R., Gordon S., and Heumann R. (1991). Macrophage dependance of peripheral sensory nerve regeneration: possible involvement of nerve growth factor. Neuron 6:359-70.

Bunge M.B., Williams A.K., and Wood P.M. (1982). Neuron-Schwann cell interaction in basal lamina formation. Developmental Biology 90:449-460.

Bunge R.P. (1981). Contributions of tissue culture studies to our understanding of basic processes in peripheral nerve regeneration. In: Posttraumatic peripheral nerve regeneration. Gorio A. Millesi, H. Millesi and Mingrino S (eds). 1st ed. Raven Press, New York, pp105-113.

Bunge R.P. (1993). Expanding roles for the Schwann cell: ensheathment, myelination, trophism and regeneration. Curr. Opin. Neurobiol. 3: 805-809.

Bunge R.P., Kleitman N., Ard M.D., and Duncan I.D. (1988). Culture preparations of neuroglial cells useful for studies of myelin repair and axonal regeneration in the central nervous system. Prog Brain Res 78: 312-316.

Burt A.M., and McGrouther D.A. (1992). Production and use of skin cell cultures in therapeutic situation. In: Animal Cell Biotechnol. Academic Press, New York, pp 150-168.

Carsons S.E. (1989). Fibronectin in Health and Disease. CRC Press, USA.

Chao M.V., Bothwell M.A., Ross A.H., Koprowski H., Lanahan A.A., Buck C.R., and Sehgal A. (1986). Gene transfer and molecular cloning of the human NGF receptor. Science 232: 518-521.

Chang H.W., Takei K., Sydor A.M., Born T., Rusnak F., and Jay D.G. (1995). Asymmetric retraction of growth cone filopodia following focal inactivation of calcineurin. Nature 376:686-690.

Chernousov M.A., Fogerty F.J., Koteliansky V.E. and Mosher D.F. (1991). Role of the I-9 and III-1 modules of fibronectin in formation of an extracellular matrix. Journal of Biological Chemistry 266:10851-10858.

Cherouhdi B., Gould T.R., and Brunette D.M. (1991). A light and electron microscopic study of the the effects of surface topography on the behaviour of cells attached to titanium-coated percutaneous implants. J Biomed Mater Res. 25: 387-405.

Chisoe W.F., Vezey E.L., and Skvarla J.J. (1994). Hexamethyldisilazane as a drying agent for pollen scanning electron microscopy. Biotechnic and Histochemistry 69: 192-198.

Chongliang H.E., Zhongwei C., and Zhengrong C. (1992). Enhancement of motor regeneration by growth factor. Microsurgery 13: 151-154.

Clark P., Connolly P., Curtis A.S.G., Dow J.A.T and Wilkinson C.D. (1990). Topographical control of cell behaviour: II. multiple grooved substrata. Development 108: 635-644.

Clark R.A., Lanigan J.M., DellaPelle P., Manseau E., Dvorak H.F., and Colvin R.A. (1982). Fibronectin and fibrin provide a provisional matrix for epidermal cell migration during wound reepithelialization. J. Invest. Dermatol. 79: 264.

Clark P., Connolly P., Curtis A.S., Dow J.A., and Wilkinson C.D. (1991). J Cell Sci. 99: 73-77.

Clegg C., and Hayes D. (1974). Identification of neighbouring proteins in the ribosomes of Escherichia coli. A topographical study with cross-linking reagent dimethylsuberimidate. Eur. J. Biochem. 42: 21-28.

Cleveland D.W., Monteiro M.J., Wong P.C., Gill S.R., Gearhart J.D., and Hoffman P.N. (1991). Involvement of neurofilaments in the radial growth of axons. J. Cell Sci. Suppl. 15: 85-95.

Cillier T.J. and Springer J.E. (1994). Neural graft augmentation through cografting: implantation of cells as sources of survival and growth factors. Prog Neurobiol 44: 309-331.

Corbett S.A., Wilson C.L., and Schwarzbauer J.E. (1996). Changes in cell spreading and cytoskeletal organization are induced by adhesion to a fibronectin-fibrin matrix. Blood 88:158-166.

Coyle J.T., and Puttfarcken P. (1993). Oxidative stress, glutamate, and neurodegenerative disorders. Science 262: 689-694.

Crang A.J., and Blakemore W.F. (1986). Observations on Wallerian degeneration in explant cultures of cat sciatic nerve. Journal of Neurocytology 15:471-82.

Cunningham J.J., Leffell M., and Harmatz P. (1993). Burn severity, copper dose, and plasma ceruloplasmin in burned children during total parenteral nutrition. Nutrition 9:329-32.

Curtis A.S.G., and Varde M. (1964). Control of cell behaviour: topographical factors. J Natl Can Inst 33: 15-26.

Curtis A.S.G., and Clark P. (1990). The effects of topographic and mechanical properties of materials on cell behaviour. Critical Reviews in Biocompatibility 5: 343-362.

Curtis A.S.G., Wilkinson C.D., and Wojciak-Stothard B. (1995). Cellular guidance, movement and growth: accelerating cell movement. J Cell Engin. 1: 35-38.

Cuthbert J.A. (1995). Wilson's disease: a new gene and an animal model for an old disease. J Investig Med 43: 323-36.

Daniel R.K., and Terzis J.K. (1977). Reconstructive Microsurgery. Little Brown, Boston.

Danielsen N., Kerns J.M., Holmquist B., Zhao Q., Lundborg G., and Kanje M. (1994). Pre-degenerated nerve grafts enhance nerve regeneration by shortening the initial delay period. Brain Research 666:2659-2673.

Darribere T., Koteliansky V.E., Chernousov M.A., et al. (1992). Distinct regions of human fibronectin are essential for fibril assembly in an in vivo developing system. Dev. Dynam. 194: 63-70.

DaSilva C., Madison R., Dikke S.E., Chiu T-H., and Sidman R. (1985). An in vivo model to quantify motor and sensory peripheral nerve regeneration using bioresorbable nerve guide tubes. Brain Research 342: 307-315.

David S. and Aguayo A.J. (1981). Axonal elongation into peripheral nervous system 'bridges' after central nervous system injury in adult animals. Science 214: 931-933.

Davies A.M. (1994). Role of neurotrophins in successive stages of sensory neuron development. Prog. Growth Factor Res. 5: 263-289.

Davies G.E., and Stark G.R. (1970). Use of dimethyl suberimidate, a cross-linking reagent, in studying the subunit structure of oligomeric proteins. Proc. Natl. Acad. Sci. USA. 66: 651-656.

Davies A.M., and Wright E.M. (1995). Neurotrophin autocrine loops. Current Biology 5: 723-726.

Davis J.B., and Stroobant P. (1990). Platelet-derived growth factors and fibroblast growth factors are mitogens for rat Schwann cells. J Cell Biol 110: 1353-1360.

Dechant G., Rodriguez-Tebar A., and Barde Y-A. (1994). Neurotrophin receptors. Prog. Neurobiol. 42: 347-352.

Dejane E., Colella S., Languino L.R., Balconi G., Corbascio G.C., and Marchisio P.C. (1987). Fibrinogen induces adhesion, spreading and microfilament organisation of human endothelial cells in vitro. J. Cell Biol. 104: 1403-1411.

Dellon A.L., and MacKinnon S.E. (1988). Alternative to the classical nerve graft with a bioresorbable polyglycolic acid tube. Plastic and Reconstructive Surgery 82:849-856.

Denny-Brown D. (1946). Importance of neural fibroblasts in the regeneration of nerve. Arch. Neuro. Psychiat. Chicago 55: 171-215.

Derby A., Engleman G.E. Friedrich G, Neises S.R., Rapp., and Roufa D.G. (1993). Nerve growth factor facilitates regeneration across nerve gaps: Morphological and behavioral studies in rat sciatic nerve. Experimental Neurology 119:176-191.

DeSimone D.W. (1994). Adhesion and matrix in vertebrate development. Curr. Opin. Cell Biol. 6: 747.

Diemel L., Brewester W.J., Fernyhough P., and Tomlinson D.R. (1994). Expression of neurtopeptides in experimental diabetes: effects of treatment with nerve growth factor or brain-derived neurotrophic factor. Mol. Brain Res. 21: 171-175.

DiMilla P.A., Stone J.A. Quinn J.A., Albelda S.M., and Lauffenburger D.A. (1991). Maximal migration of human smooth muscle cells on fibronectin and type IV collagen occurs at an intrmediate attachment strength. J. Cell Biol. 122: 729-737.

DiMilla P.A., Barbee K., and Lauffenburger D.A. (1993). Mathematical model for the effects of adhesion and mechanics on cell migration speed. Biophysics J. 60: 15-37.

Dong A., Prestrelski S.J., Allison S.D., and Carpenter J.F. (1995). Infrared spectroscopic studies of lyophilization and temperature induced protein aggregation. J. Pharm Sci. 84: 415-424.

Duband J-L., Dufour S., Yamada S.S., Yamada K.M., and Thiery J.P. (1991). Neural crest cell locomotion induced by antibodies to β1 integrin. A tool for studying the roles of substratum molecular avidity and density in migration. J. Cell Sci. 98: 517-538.

Dunn G.A. (1982). Contact guidance of cultured tissue cells: a survey of potentially relevant properties of the substratum. In *Cell Behaviour* (eds. R. Bellairs, A. Curtis and G.A. Dunn), Cambridge University Press, UK, pp247-280

Dunn G.A., and Brown A.F. (1986). Alignment of fibroblasts on grooved surfaces described by a simple geomettric transformation. J. Cell Sci. 83: 313-340.

Dunn G.A., and Heath J.P.(1976). A new hypothesis of contact guidance in tissue cells. Exp Cell Res. 101: 1-14.

Ebendal T. (1976). The relative roles of contact inhibition and contact guidance in orientation of axons extending on aligned collagen fibrils in vitro. Experimental Cell Research 98: 159-169.

Ejim O.S., Blunn G.W., and Brown R.A. (l993). Production of artificial orientated mats and strands from plasma fibronectin: a morphological study. Biomaterials 14:734-748.

Elsdale T., and Bard J. (1972). Collagen substrata for studies on cell behaviour. Journal of Cell Biology 54: 626-637.

Engele J., Schubert D., and Bohn M.C. (1991). Conditional media derived from glial cell lines promote survival and differentiation of dopaminergic neurons in vitro. Role of mesencephalic glia. J Neurosci Res 30: 359-371.

Ernfors P., Wetmore L., Olson L., and Persson H. (1990). Identification of cells in rat brain and peripheral tissue expressing mRNA for members of the nerve growth factor family. Neuron 5: 511-526.

Evercooren B-V.A., Kleinman K., Seppa E.J., Rentier B., and Dubois-Dalcq M. (1982). Fibronectin promotes rat Schwann cell growth and motility. Journal of Cell Biology 93:211-216.

Fawcett J.W. and Keynes R.J. (1986). Muscle basal lamina: a new graft material for peripheral nerve repair. J. Neurosurg. 65: 354-363.

Fawcett J.W. and Keynes R.J. (1990). Peripheral nerve regeneration. Rev Neurosci 13: 43-60.

Fernyhough P., Willars G.B., Lindsay R.M., and Tomlinson D.R. (1993). Insulin and insulin like growth factor-1 enhances regeneration in cultured adult rat sensory neurones. Brain Res. 607: 117-124.

Fernyhough P., Diemel L., Hardy J., Brewester W.J., Mohiuddin L., and Tomlinson D.R. (1995). Human recombinant nerve growth factor replaces deficient neurotrophic support in the diabetic rat. Eur. J. Neurosci. 7: 1107-1110.

Fields R.D., Le Beau J.M., Longo F.M., and Ellisman M.H. (1989). Nerve regeneration through artificial tubular implants. Progress in Neurobiology 33: 87-134.

Fine E.G., Valentini R.F., Bellamkonda R., and Aebischer P. (1991). Improved nerve regeneration through piezoelectric vinylidenefluoridetrifluoroethylene copolymer guidance channels. Biomaterials 12:775-780.

Fisher L.J., and Gage F.H. (1993). Grafting in the mammalian central nervous system. Physiol Rev 73: 583-616.

Franklin R.J.M., and BlakemoreW.F. (1993). Requirement for Schwann cell migration within CNS environments: a viewpoint. Int J Dev Neurosci 11: 641-649.

Furie B., and Furie B.C. (1988). The molecular basis of blood coagulation. Cell 53: 505.

Gailit J., Clark R.A.F. (1994). Wound repair in the context of the extracellular matrix. Curr. Opin. Cell Biol. 6: 717.

Gailit J., Clarke C., Newman D., Tonnesen M.G., Mosesson M.W., and Clark R.A.F. (1997). Human fibroblasts bind directly to the fibrinogen at RGD sites through integrin αvβ3. Exp. Cell Res. 232: 118-126.

Gamble H.J., and Eames R.A. (1965). An electron microscope study of the connective tissue of human peripheral nerves. J. Anat. 99: 655-663.

Garcia A.J., Ducheyne P., and Boettiger D. (1997). Cell adhesion strength increases linearly with adsorbed fibronectin surface density. Tissue Engineering 3: 197-206.

Glazer A.N. (1976). The chemical modification of proteins by group-specific and site-specific reagents. In *The Proteins* (eds H. Neurath and R.L. Hill). Academic Press, New York, pp2-88.

Green A.M., Jansen J.A., van der Waerden J.P., and von Recum A.F.(1994). Fibroblast response to microtextured silicone surfaces: texture orientation into or out of the surface. J Biomed Mater Res. 28: 647-653.

Grob P.M., Ross A.H., Koprowski H., and Bothwell M. (1985). Characterization of the human melanoma nerve growth factor receptor. J. Biol. Chem. 260: 8044-8049.

Griebanow K., and Klibanov A.M. (1995). Lyophilization-induced reversible changes in the secondary structure of proteins. Proc. Natl. Acad. Sci. USA. 92: 10969-10976.

Griffin J.W., George R., and Ho T. (1993). Macrophage systems in peripheral nerves. A. review. Journal of Neuropathology and Experimental Neurology 52:553-60.

Grinnel F. (1978). Cellular adhesiveness and extracellular substrata. Int. Rev. Cytol. 53: 65-144.

Grinnel F., Field M., and Mitner D. (1980). Fibroblast adhesion to fibrinogen and fibrin substrata: requirement for cold-insoluble globulin (plasma fibronectin). Cell 19: 517-525.

Grinnel F. (1984). Fibronectins and wound healing. J. Cell Biochem. 26: 107-116.

Guenard V., Kleitman N., Morrisey T.K., Bunge R.P., and Aebischer P. (1992). Syngenic Schwann cells derived from adult nerves seeded in semi-permeable guidance channels enhance peripheral nerve regeneration. J Neurosci 12: 3310-3320.

Guido S., and Tranquilo R.T. (1993). A methodology for the systematic and quantitative study of cell contact guidance in oriented collagen gels. J. Cell Sci. 105: 317-331.

Gulati A.K. (1995). Immunological fate of Schwann cell-populated acellular basal lamina nerve allografts. Transplantation 59:1618-1622.

Gulati A.K., Rai D.R., and Ali M. (1995). The influence of cultured Schwann cells on regeneration through acellular basal lamina grafts. Brain Research 705:118-124.

Gutman S.L., Risse G., and von der Mark K. (1989). The E8 subfragment of laminin promotes locomotion of myoblasts over extracellular matrix. J. Cell Bio. 109: 799-809.

Gutman E. and Young J.G. (1944). The reinnervation of muscle after various periods of atrophy. Journal of anatomy 78: 15.

Hadjiargyrou M., and Patterson P.H. (1995). An anti-CD9 monoclonal antibody promotes adhesion and induces proliferation of Schwann cells in vitro. Journal of Neuroscience 15: 574-583.

Hallbrook F., Ibanez C.F., and Persson H. (1991). Evolutionary studies of the nerve growth factor family reveal a novel member abundantly expressed in *Xenopus* ovary. Nature 6:845-858.

Harding S., Underwood S., Brown R.A., and Dunnill P. Contact guidance cable prepared from fibronectin suitable for large scale processing: assessment of cell alignment function. (In prep).

Harrison R.G. (1914). The reaction of embryonic cells to solid structures. Journal of Experimental Zoology 17: 521-544.

Harvey A.R., Plant G.W., and Tan M.M. (1995). Schwann cells and the regrowth of axons in the mammalian CNS: a review of transplantation studies in the rat visual system. Clin Exp Pharmacol Physiol 22: 569-579.

Hemler M.E. (1990). VLA proteins in the integrin family: structures, functions, and their roles on leukocytes. Ann. Rev. Immunol. 8: 365-400.

Henry E.W., Chiu T.H., Nyilas E., et al. (1985). Nerve regeneration through biodegradable polyester tubes. Experimental Neurology 90:652-656.

Heumann R., Korsching S., Bandtlow C., and Thoenen H. (1987). Changes of nerve growth factor synthesis in non-neuronal cells in response to sciatic nerve transection. Journal of Cell Biology 104: 1623-1632.

Hirono T., Torimitsu K., Kawana A., and Fukada J. (1988). Recognition of artificial microstructures by sensory nerve fibres in culture. Brain Research 446: 189-194.

Hobson M.I. Brown R.A., Green C.J. and Terenghi G. (1997). Interrelationship between angiogenesis and nerve regeneration: a histochemical study. British Journal of Hand Surgery 50: 125-131.

Hoffman P.N., Cleveland D.W., Griffin J.W., Landes P.W., Cowan N.J., and Price D.L. (1987). Neurofilament gene expression: a major determinant of axonal calibre. Proc. Natl. Acad. Sci. 84:3472-3476.

Hohn A.M., Leibrock J., Bailey K., and Barder Y.A. (1990). Identification and characterization of a novel member of the nerve growth factor/brain-derived neurotrophic factor family. Nature 344:339-341.

Hurtado H., Knoops B., and DeAgilar R P. (1987). Rat sciatic nerve regeneration in semipermeable artificial tubes. Experimental Neurology 97:751 -757.

Huttenlocher A.J., Ginsberg M.H., and Horwitz A.F. (1996). Modulation of cell migration by integrin mediated cytoskeletal linkages and ligand-binding affinity. J. Cell Biol. 134: 1551-1562.

Hynes R.O. (1987). Integrins: a family cell surface receptors. Cell 48: 549-554.

Hynes R.O. (1990). Fibronectins. Springer-Verlag. New York.

Hynes R.O. (1992). Integrins: Versatility, modulation and signaling in cell adhesion. Cell 69: 11.

Hynes R.O. and Destree A. (1977). Extensive disulfide bonding at the mammalian cell surface. Proc. Natl. Acad. Sci. USA. 74: 2855-2859.

Ide C. (1996). Peripheral nerve regeneration. Neurosci. Res. 25: 101-121.

Ikeda K., Oda Y., Nakanishi I., Tomita K., and Nomura S. (1991). Cultured Schwann cells transplanted between nerve gaps promote nerve regeneration. Neuro-Orthopaedics 11:7-16.

Ip N.Y., Ibanez C.F., Nye S.H., McCain J., Jones P.F., Gies D.R., Belluscia L., LeBeau M.M., Espinora R III., Squinto S.P. et al., (1992). Mammalian neurotrophin-4: structure, chromosomal localization, tissue distribution and receptor specificity. Proceedings of the National Academy of Science 89:3060-3064.

Jackson M.J. (1989). Physiology of zinc: general aspects. In *Zinc in Human Biology.* Edited by C.F. Mills. Springer-Verlag, London. pp 1-14.

Jay P.Y., Pham P.A., Wong S.A., and Elson E.L. (1995). A mechanical function of myosin. II. in cell motility. J. Cell Sci. 108: 387-393.

Johnson D., Lanahan A., Buck C.R., Sehgal A., Morgan C., Mercer E., Bothwell M., and Chao M.V. (1986). Expression and structure of the human NGF receptor. Cell 47: 545-554.

Juliano R.L., and Varner J.A. (1993). Adhesion molecules in cancer: The role of integrins. Curr. Opin. Cell Biol. 5: 812.

Kaplan D.R., Hempstead B.L., Martin-Zanca D., Chao M.V., and Parhad., L.F. (1991). The trk proto-oncogene product: a signal transducing receptor for nerve growth factor. Science 252: 554-557.

Kaplan D.R., and Stephens R.M. (1994). Neurotrophin signal transduction by the trk receptor. J. Neurobiol. 25: 1404-1417.

Katz M.J., and Lasek R.J. (1980). Guidance cue patterns and cell migration in multicellular organisms. Cell Motility 1: 141-157.

Kawaja M., Rosenberg M., Yoshida K., and Gage F.H. (1992). Somatic gene transfer o NGF promotes survival of axotomised septal neurons and the regeneration of their axons in adult rats. J. Neurosci. 12: 2849-2864.

Keely P.J., Fong A.M., Zutter M.M., and Santoro S.A. (1995). Alteration of collagen-dependent adhesion, motility, and morphogenesis by the expression of antisense α2 integrin mRNA in mammary cells. J. Cell Sci. 108: 595-607.

Keski-Oja J., Mosher D.F. and Vaheri A. (1977). Dimeric character of fibronectin, a major cell surface-associated glycoprotein. Biochem. biophys. Res. Commun 74: 699-706.

Keynes R.E.J. (1987). Schwann cells during neural development and regeneration: leaders or followers? Trends in Neuroscience 10: 137- 139

Kies C. (1987). Copper Bioavailabilty and Metabolism. In Advances in Experimental Medicine and Biolgy. Plenum Press, New York. Volume 258: 1-20.

Kim K.H. (1992). A role of retinoic acid in the regulation of the morphology and levels of intermediate filament proteins and mRNAs in PC12 cells. Exp. Cell. Res. 203: 374-82.

Kirchgessner M., Steinhart H., and Wieninger-Rustemyer R. (1980a). Influence of copper in combination with other trace elements on the activity of trypsin. Int J. Vitam. Nutr. Res. 50: 179-184.

Kirchgessner M., Wieninger-Rustemyer R., and Steinhart H. (1980b). Effects of copper ions on trypsin activity.

Klein D.G., and Hayes G.J. (1964). The use of a resorbable wrapper for peripheral nerve repair. Journal of Neurosurgery 21 :737-750.

Kobyashi H., Ishii M., Chanoki M., Yashiro N., Fushida K., Kono T., Hamada T., Wasaki H., and Ooshima A. (1994). Immunohistochemical localisation of lysyl oxidase in normal human skin. British Journal of Dermatology 131:325-30.

Korn A.H., Feairheller S.H., and Filachione E.M. (1971). Gluteraldehyde: nature of the reagent. J. Mol. Biol. 65: 525-529.

Kromer L.F and Cornbrooks C.J. (1985). Transplants of Schwann cell cultures promote axonal regeneration in the adult mammalian brain. Proc Natl Acad Sci USA 82: 6330-6334.

Kutsky R.J. (1987). Handbook of Vitamins, Minerals and Hormones. 2nd ed. Van Nostrand Reinhold Co. New York, pp 101-112.

Lackie J.M. (1986). *Cell movement and cell behaviour*. Allen & Unwin, London, England.

Lauffenburger D.A., and Horwitz A.F. (1996). Cell migration: a physically integrated molecular process. Cell 84: 359-369.

Lee M.K., and Cleveland D.W. (1994). Neurofilament function and dysfunction: involvement in axonal growth and neuronal disease. Curr. Opin. Cell Biol. 6: 34-40.

Lee V., Trojanowski J.Q., and Schlaepfer W.W. (1982). Induction of neurofilament triplet proteins in PC12 cells by nerve growth factor. Brain-Res. 238: 169-80.

Lefcort F., Venstrom K., McDonald J.A., and Reichardt L.F. (1992). Regulation and expression of fibronectin and its receptor, $\alpha 5\beta 1$, during development and regeneration of peripheral nerve. Development 116: 767-782.

Leibrock J., Lottspeich F., Hohn A., Hofer M., Hengerer B., Masiakowski P., Thoenen H., and Barde Y.A. (1989). Molecular cloning and expression of brain-derived neurotrophic factor. Nature 341:149-151.

Letourneau P.C., Condic M.L., and Snow D.M. (1994). Interactions of developing neurons with the extracellular matrix. J Neurosci 14: 915-928.

Levi-Montalcini R. (1987). The nerve growth factor 35 years later. Science 237:1154-1162.

Levi A.D.O., Guenard V., Aebischer P., and Bunge R.P. (1994). The functional characteristics of Schwann cells cultured from human peripheral nerve after transplantation into a gap within the rat sciatic nerve. J Neurosci 14: 1309-1319.

Lewin G.R., and Barde Y.A. (1996). Physiology of the neurotrophins. Annu. Rev. Neurosci. 19: 289-317.

Li Y., and Raisman G. (1994). Schwann cells induce sprouting in motor and sensory axons in the adult rat spinal cord. Journal of Neurocytology 14: 4050-4063.

Lindholm D., Heumann R., Meyer M., and Thoenen H. (1987). Interleukin-1 regulates synthesis of nerve. Nature 330:658-9.

Lindsay R.M. (1996). Role of neurotrophins and trk receptors in the development and maintenence of sensory neurons: An overview. Philos. Trans. R. Soc. Lond. Biol. Sci. 351: 365-73.

Lindsay R.M., Rodriguez-Tebar A., and Barde Y. (1988). Nerve growth factors (NGF, BDNF) enhances axonal regeneration but are not required for survival of adult sensory neurones. J. Neurosci. 8: 3337-3342.

Lindsay R.M., and Harmar J.J. (1989). Nerve growth factor regulates expression of neuropeptide genes in adult sensory neurons. Nature 337: 362-364.

Lindsay R.M., Wiegand S.J., Altar C.A. and DiStefano P.S. (1994). Neurotrophic factors: from molecule to man. Trends Neurosci 17: 182-190.

Liu H.M., Lei H.Y., and Kao Ko-P. (1995). Correlation between NGF levels in wound chamber fluid and cytological localization of NGF and NGF receptor in axotomized rat sciatic nerve. Exp. Neurol. 132: 24-32.

Ljungberg C., Novikov L, Kellerth J-O., and Wiberg M. (1997). Neurotrophins and their effect on survival of lesioned sensory neurons: an anatomical study in the rat. Submitted.

Longo F.M., Skaper S.D., Manthorpe M. et al. (1983). Temporal changes of neurotrophic activities accumulating in vivo within nerve regeneration chambers. Experimental Neurology 81:756-769.

Low R.N. (1976). The perineurium and connective tissue of peripheral nerve. In *The peripheral nerve* (ed. D.N. Landon). Chapman and Hall, London, pp 159-187.

Lundborg G. (1975). Structure and function of the intraneurial microvessels as related to trauma, edema formation and nerve function. J. Bone Joint Surg. 57A: 938-948.

Lundborg G. (1979). The intrinsic vascularization of human peripheral nerve: structural and functional aspects. J. Hand Surg. 4: 34-41.

Lundborg G. (1988). Nerve regeneration (chapter 5) in 'Nerve Injury and Repair'. Churchill Livingstone. UK.

Lundborg G. et al. (1987). Peripheral Nerve. In Injury and repair of the musculoskeletal soft tissues. AAOS.pp 294-352.

Lundborg G., Dahlin L.B., and Danielson N.P., et al. (1981). Reorganisation and orientation of regenerating nerve fibres, perineurium, and epineurium in preformed mesothelial tubes: an experimental study on the sciatic nerves of rat. Journal of Neuroscience Research 6:265-281.

Lundborg G., Dahlin L.B., Danielsen N., Gelberman R.H., Longo F.M., Powell H.C., and Varon S. (1982). Nerve regeneration in silicone chambers: influence of gap length and distal stump components. Exp. Neurol. 76: 361-375.

Lundborg G., Longo F.M., and Varon S. (1982). Nerve regeneration model and trophic factors in vivo. Brain Research 232:157-161.

MacKinnon S.E., Dellon A.L., Hudson A., et al. (1984). Nerve regeneration through a pseudosynovial sheath in a primate model. Plastic and Reconstructive Surgery 75:833-839.

MacKinnon S.E., and Dellon A.L. (1988). Surgery of the peripheral nerve. Thieme Medical Publishers, New York.

Madison R., DaSilva C.F., Dikkes P., Chiu T., and Sidman R.L. (1985). Increased rate of peripheral nerve regeneration through using bioresorbable nerve guides and a laminin containing gel. Experimental Neurology 88: 767-772.

Madison R., Disman R.L., Nyilas E., et al. (1984). Non-toxic nerve guide tubes support neovascular growth in transected rat optic nerve. Experimental Neurology 86:448-461.

Madison R.D., Archibald S.J., and Krarup C. (1989). Peripheral nerve injury. In *Wound healing-biochemical and chemical aspects* (eds. I.K. Cohen, R.F. Diegelmann and W.J. Lindblad), W.B. Saunders, New York. pp 450-487.

Maisonpierre P.C., Belluscio L., Squinto S., Ip N.Y., Furth M.E., Lindsay R.M., and Yancopoulos G.D. (1990). Nuerotrophin-3: a new neurotrophic factor related to NGF and BDNF. Science 247:1446-1451.

Maness L.M., Kastin A.J., Weber J.T., Bansks W.A., Beckman B.S. and Zadina J.E. (1994). The neurotrophins and their receptors: structure, function and neuropathology. Neurosci. Biobehav. Rev 18: 143-159.

Marks P.W., Hendey B., and Maxfield F.R. (1991). Attachment to fibronectin or vitronectin makes human neutrophil migration sensitive to alterations in cystolic free calcium concentration. J. Cell Biol. 112: 149-158.

Marano N., Dietzschold B., Earley J.J. Jr., Schatteman G., Thompson S., Grob P., Ross A.H., Bothwell M., Atkinson B.F., and Kaprowski H. (1987). Purification and amino terminal sequencing of human melanoma nerve growth factor receptor. J. Neurochem. 48: 225-232.

Marsh, N. (1981). Fibrinogen and fibrin degradation. In Fibrinolysis. John Wiley and Sons, Chichester, UK, pp 46-68.

Marzalek J.R., Williamson T.L., Lee M.K., Xu Z., Hoffman P.N., Becher M.W., Crawford T.W., and Cleveland D.W. (1996). Neurofilament subunit NF-H modulates axonal diameter by selectively slowing neurofilament transport. J. Cell Biol. 135: 711-724.

McDonald J.A. (1988). Extracellular matrix assmebly. Annual Review Cell Biology 4:183-207.

McMahon S.B., Armanini M.P., Ling L.H., and Phillips H.S. (1994). Expression and coexpression of Trk receptors in subpopulations of adult primary sensory neurons projecting to identified peripheral targets. Neuron 12: 1161-1171.

Molander H., Olsson Y., Engkvist O. et al. (1982). Regeneration of peripheral nerve through a polyglactin tube. Muscle and Nerve 5:54-57.

Morla A., and Ruoslahti E. (1992). A fibronectin self-assembly site involved in fibronectin matrix assembly: reconstruction in a synthetic peptide. J. Cell Biol. 118: 421-429.

Morla A., Zhang Z and Ruoslahti E. (1994). Superfibronectin is a functionally distinct form of fibronectin. Nature 367:193-196.

Morrison P.R., Edsall J.T., and Miller S.G. (1948). Preparation and properties of serum and plasma proteins. XVIII. The separation of purified fibrinogen from fractions of human plasma. Journal of American Chemical Society 70:3013-3108.

Mosher D.F. (1984). Physiology of Fibronectin. Annual Review of Medicine 35:561-575.

Mosher D.F. (1993). Assembly of fibronectin into a extracellular matrix. Current Opinions in Structural Biology 3:214-222.

Mosher D.F., Fogerty F.J., Chernousov M.A., and Barry E.L. (1991). Assembly of fibronectin into extracellular matrix. Ann. N.Y. Acad. Sci. 614: 167-180.

Mosher D.F., Sottile J., Wu C., and McDonald J.A. (1992). Assmebly of extracellular matrix. Current Opinion Cell Biology 4:810-818.

Myers J.S., and Hardman J.K. (1971). Formaldehyde-induced cross-linkages in the subunit of E. Coli tryptophan synthetase. J. Biol. Chem. 25: 3863-3869.

Nagai T., Yamakawa N., Aota S., Yamada S., Akiyama S.K., Olden K., and Yamada K.M. (1991). Monoclonal antibody characterization of two distant sites required for function of the central cell-binding domain of fibronectin in cell adhesion, migration and matrix assembly. J. Cell Biol. 114: 1295-1305.

Nakao N., Frodl E.M., Widner H., Carlson E., Eggerding F.A., Epstein C.J., and Brundin P. (1995). Overexpressing Cu/Zn superoxide dismutase enhances survival of transplanted neurons in a rat model of Parkinsons's disease. Nature Medicine 1:226-130.

Nathaniel E.J.H., and Pease D.C. (1963). Degenerative changes in rat dorsal roots during Wallerian degeneration. Journal of Ultrastructural Research 9:511-32.

Newgreen D.F. (1989). Physical influences on neural crest migration in avian embryos: contact guidance and spatial restriction. Developmental Biology 131: 136-148.

Noakes P.G., and Bennett M.R. (1987). Growth of axons into developing muscles of the chick forelimb is preceded by cells that stain with Schwann cell antibodies. J. Comp. Neurol. 259: 330-347.

Nyilas E., Chiu T.H., Sidman et al. (l983). Peripheral nerve repair with bioresorbable prosthesis. Transactions of the American Society of Artificial Internal Organs 29:307-313.

Oakley C., and Brunette D.M. (1993). The sequence of alignment of microtubules, focal contacts and actin filaments in fibroblasts spreading on smooth and titanium substrata. Journal of Cell Science 106: 343-354.

Ochiai E.L. (1983). Copper and the biological evolution. Biosystems 16:81-6.

Ochs S. (1980). History of peripheral nerve repair. In *Peripheral nerve regeneration: its experimental and clinical basis*. W B Saunders, England.

O'Dell B.L. (1993). Roles of zinc and copper in the nervous system. Prog. Cli. Biol. Res. 380:147-62.

Ohara P.T., and Buck R.C. (1979). Contact guidance in vitro. Exp. Cell Res. 121: 235-249.

Olanow C.W. (1994). A radical hypothesis for neurodegeneration. Trends Neurosci 16: 439-444.

Osawa T., and Ide C. (1986). Changes in thickness of collagen fibrils in the endo- and epineurium of the mouse sciatic nerve during development. Acta Anat. 125: 245-251.

Owens M.R., and Cimino C.D. (1982). Synthesis of fibronectin by isolated perfused rat liver. Blood 59:1305-1309.

Palacek S.P., Loftus J.C., Ginsberg M.H., Lauffenburger D.A., and Horwitz A.F. (1997). Integrin-ligand binding properties govern cell migration speed through cell-substratum adhesiveness. Nature 385: 537-540.

Paino C.L., Fernandez-Valle C., Bates M.L., and Bunge M.B. (1994). Regrowth of axons in the lesioned rat spinal cord: promotion by implants of cultured Schwann cells. J Neurocytol 23: 433-452.

Parhad I.M., Scott J.N., Cellars L.A., Bains J.S., Krekoski C.A., and Clark A.W. (1995). Axonal atrophy in aging is associated with a decline in neurofilament gene expression. J. Neurosci. Res. 15: 355-66.

Pasqualini R., Bourdoulous S., Koivunen E., Woods V.L. Jr. and Ruoslahti E. (1996). A polymeric form of fibronectin has antimetastatic effects against multiple tumor types. Nature Medicine 2: 1197-1203.

Perry V.H., Brown M.C., and Gordon S. (1987). The macrophage response to central and peripheral nerve injury. Journal of Experimental Medicine 165:1218-23.

Pincelli C., Sevignani C., Manfredini R., Grande A., Fantini F., Bracci-Laudiero L., Aloe L., Ferrari S., Cossarizza A., and Gianetti A. (1994). Expression and function of nerve growth factor and nerve growth factor receptor on cultured keratinocytes. J. Invest. Dermatol. 103: 13-18.

Plant G.W., Harvey A.R., Chirila T.V. (1995). Axonal growth within poly (2-hydroxyethyl methacrylate) sponges infiltrate with Schwann cells and implanted into the lesioned rat optic tract. Brain Research 671: 119-130.

Pollock J.M. (1995). Nerve regeneration. Curr. Opin. Neurol. 8: 354-358.

Radeke M.J., Misko T.P., Hsu C., Herzenberg L.A., and Shooter E.M. (1987). Gene transfer and molecular cloning of the rat nerve growth factor receptor. Nature 325: 593-597.

Raff M., Abney C., Brockes J.P., and Hornby-Smith A. (1978). Schwann cell growth factors. Cell 15: 813-822.

Raivich G and Kreutzberg G.W. (1993). Peripheral nerve regeneration: Role of growth factors and their receptors. Int J Dev Neurosci 11: 311-324.

Raivich G and Kreutzberg G.W. (1993). Nerve growth factor and regeneration of the peripheral nervous system. Clinical Neurology and Neurosurgery 95 (Suppl): 584-588.

Raivich G., Hellweg R., and Kreutzberg G.W. (1991). NGF receptor-mediated reduction in axonal NGF uptake and retrograde transport following sciatic nerve injury and during regeneration. Neuron 7: 151-164.

Rajnicek A.M., and McCaig C.D. (1997). Guidance of CNS growth cones by substratum grooves and ridges: effects of inhibitors of the cytoskeleton, calcium channels and signal transduction pathways. Journal of Cell Science 110: 2915-2924.

Rajnicek A.M., Britland S., and McCaig C.D. (1997). Contact guidance of CNS neurites on grooved quartz: influence of groove dimensions, neuronal age and cell type. Journal of Cell Science 110: 2905-2913.

Reid R.L., Cutright D.E., and Garrison J.S. (1978). Biodegradable cuff an adjunct to peripheral nerve repair: A study in dogs. Hand 10:259-266.

Rich K.M., Luszczynski J.R., Osborne P.A., and Johnson E.M. (1987). Nerve growth factor protects adult sensory neurones from cell death and atrophy caused by nerve injury. J. Neurocytol. 16: 261-268.

Richardson P.M., and Ebendal T. 1982. Nerve growth factor activities in rat peripheral nerves. Brain Res. 246: 57-64.

Rodriguez-Tebar A., Dechant G., and Barde Y-A. (1990) Binding of brain-derived neurotrophic factor to nerve growth factor receptor. Neuron 4: 767-773.

Rosenthal A., Goeddel D.V., Nguyen T., Lewis M., Shih S., Laramee G.R., Nikolics K., and Winslow J.W. (1990). Primary structure and biological activity of a novel human neurotrophic factor. Neuron 4:767-773.

Rosiek O., Wegrzynowicz Z., Sawicki Z., and Kopec M. (1969). Fibrinogen-synthese in blutplattchen. Folia Haematologica 92: 553-557.

Rovensky C.L., and Samoilov V.I. (1994). Morphogenetic response of cultured normal and transformed fibroblasts and epitheliocytes to a cylindrical substratum surface. J. Cell Sci. 107: 1255-1263.

Ruoslahti E., and Pierschbacher M.D. (1987). New perspectives in cell adhesion: RGD and integrins. Science 238: 491.

Rush R.A. (1984). Immunohistochemical localisation of endogenous growth nerve factor. Nature 312: 364-367.

Rusovan A., and Kanje M. (1991). Stimulation of regeneration of the rat sciatic nerve by 50 Hz sinusoidal magnetic fields. Experimental Neurology 112:312-316.

Rusovan A., and Kanje M. (1992). Magnetic fields stimulate peripheral nerve regeneration in hypophysectiomized rats. Neuro Report 3:1039-1041.

Rutkowski J.L., Kirk C.J., Lerner M.A., and Tennekoon G.I. (1995). Purification and expansion of human Schwann cells in vitro. Nature Medicine 1: 80-83.

Saba T. (1989). Kinetics of plasma fibronectin: relationship to phagocytic function and lung vascular integrity. In Fibronectin (Ed. D. Mosher, 1989). Academic Press Inc.

Sakaguchi T., Okada M., Kitamura T., and Kawasaki K. (1993). Reduced diameter and conduction velocity of myelinated fibres in the sciatic nerve of neurofilament-deficient mutant quail. Neurosci. Lett. 153: 65-68.

Seddon H.J. (1972). Surgical disorders of the peripheral nerve. Baltimore, Williams and Wilkins.

Schwab M.E., and Thoenen H. (1985). Dissociated neurones regenerate into sciatic but not optic nerve explants in culture irrespective of neurotrophic factors. J Neurosci 5: 2415-2423.

Schwartz M.A., and Ingber D.E. (1994). Integrating with integrins. Mol. Biol. Cell. 5: 389.

Schwarzbauer J.E. (1991). Identification of the fibronectin sequences required for assembly of a fibrillar matrix. J. Cell Biol. 113: 1463-1473.

Scott J.M., Selby M., Urdea M., Quiroga M., Bell G.I., and Rutter W.J. (1983). Isolation and nucleotide sequence of a cDNA encoding the precursor of mouse nerve growth factor. Nature 302: 538-540.

Selmanpakoglu A.N., Cetin C., Sayal A., Isimer A. (1994). Trace element (Al, Se, Zn, Cu) levels in serum, urine and tissues of burn patients. Burns 20:99-103.

Shine H.D., Harcourt P.G., and Sidman R.L. (1985). Cultured peripheral nervous system cells support peripheral nerve repair regeneration through tubes in the absence of distal nerve stump. J Neurosci Research 14:393-401.

Shantha T.R. (1968). The perineurial epithelium: a new concept. Bourne G. II (ed). The structure and function of nervous tissue. Vol I. Academic Press. New York. pp 379-459.

Shattil S.J., Ginsberg M.H., and Brugge J.S. (1994). Adhesive signalling in platelets. Curr. Opin. Cell Biol. 6: 695.

Sheetz M.P., Wayne D.B., and Pearlman A.L. (1992). Extension of filopodia by motor-dependent actin assembly. Cell Motil. Cytoskel. 22: 160-169.

Smith S.J. (1988). Neuronal cytomechanics: The actin-based motility of growth cones. Science 242: 708-715.

Solomon E.I. (1981). Binuclear copper actice site. In Copper Proteins. Ed. Spiro T.G. John-Wiley and Sons, New York. pp41-108.

Sorenson J.R.J. (1987). Biology of Copper Complexes. Humana Press, Clifton, New Jersey. pp3-9.

Stein W.D., and Bronner F. (1989). Cell Shape: Determinants, Regulation, and Rehulatory role. Academic Press, San Diego, CA.

Steinhart H., Wieninger-Rustemeyer R., and Kirchgessner M. (1981). Effect of Cu++ ions on the activity of trypsin on natural substances. Arch-Tierernahr. 31: 119-25.

Sterne G.D., Brown R.A., Green C.J., and Terenghi G. (1997a). Neurotrophin-3 delivered locally via fibronectin mats enhances peripheral nerve regeneration. European Journal of Neuroscience 9: 1388-1396.

Sterne G.D., Coulton G.R., Brown R.A., Green C.J., and Terenghi G. (1997b). Neurotrophin-3 enhanced nerve regeneration selectively improves recovery of muscle fibers expressing myosin heavy chains 2b. J. Cell Biol. 139: 709-715.

Stolinski C. (1995). Structure and composition of the outer connective tissue sheaths of peripheral nerve. J. Anat. 186: 123-130.

Stoll G., Griffin J.W., Li C.Y., and Trapp B.D. (1989). Wallerian degeneration in the peripheral nervous system: participation of both Schwann cells and macrophages in myelin degeneration. J. Neurocytol. 18: 671-683.

Stopak D., and Harris A.K. (1982). Connective tissue morphogenesis by fibroblast traction. I. Tissue culture observations. Developmental Biology 90: 383-398.

Sunderland S. (1965). The connective tissues of peripheral nerves. Brain 88: 841-854.

Sunderland S. (1978). Nerves and nerve injuries. New York, Churchill Livingstone.
Sunderland S., and Bradley K.C. (1952). The perineurium of peripheral nerves. Anat. Rec. 113: 125-141.

Taniuchi M., Clark H.B., and Johnson E.M. (1986). Induction of nerve growth factor receptor in Schwann cells after axotomy. Proc. Natl. Acad. Sci. USA 83:4094-4098.

Tanuichi M., Clark H.B., Schweitzer J.B., and Johnson E.M. (1988). Expression of nerve growth factor receptors by Schwann cells of axotomized peripheral nerves: ultrastructural location, suppression by axonal contact, and binding properties. J. Neurosci. 8: 664-681.

Terzis J.K. (1987). Microreconstruction of nerve injuries. W.B. Saunders, Philadelphia.

Thomas P.K. (1963). The connective tissue of peripheral nerve: an electron microscope study. J. Anat. 97: 35-44.

Thomas P.K. (1988). Clinical aspects of PNS regeneration. Advances in Neurology 47:9-29.

Thomas P.K., Berthold C.H., and Ochoa J. (1993). Microscopic anatomy of the peripheral nervous system. In *Peripheral Neuropathy*, vol I (ed P.J. Dyck and P.K. Thomas). W.B. Saunders, Philadelphia.

Thomas P.K., and Jones D.G. (1967). The cellular response to nerve injury. II. Regeneration of the perineurium after nerve injury. J. Anat. 101: 45-55.

Townsend R.R., Hilliker E., Li Y.T., Laine R.A., Bell W.R., and Lee Y.G. (1982). J. Biol. Chem. 257: 9704-9710.

Traut R.R., Bollen A., Sun T.T., Hershery J.W., Sundberg J.W., and Pierce L.R. (1973). Methyl 4-mercaptobutyrimidate as a cleavable cross-linking reagent and its application to the E. coli 30S ribosome. Biochemistry 12: 3266-3273.

Tuszinski M.H., Paterson D.A., Jasodhara R., Baird A., Nakahara Y., and Gage F.H. (1994). Fibroblasts genetically modified to produce nerve growth factor induce robust neuritic ingrowth after grafting to the spinal cord. Exp. Neurol. 126: 1-14.

Ulrich A., Gray A., Berman C., and Dull T.J. (1983). Human beta nerve growth factor gene sequence is highly homologous to that of mouse. Nature 303: 821-825.

Underwood S., Afoke A., Brown R.A., MacLeod A.J., and Dunnill P. The physical properties of a fibrillar fibronectin-fibrinogen material with potential use in tissue engineering. (In press).

Underwood S., McLeod A.J., Brown R.A., and Dunnill P. Wet spun fibronectin-enriched fibres- a method for the large scale production of cell guidance scaffolds. (submitted).

Ushiki T., and Ide C. (1990). Three-dimensional organization of the collagen fibrils in the rat sciatic nerve as revealed by transmission and scanning electron microscopy. Cell Tissue Res. 260: 175-184.

Uzman B.G., and Villegas G.M. (1983). Mouse sciatic nerve regeneration through semipermeable tubes: A quantitative model. Journal of Neuroscience Research 9:325-338.

Venezie R.D., Toews A.D., and Morell P. (1995). Macrophage recruitement in different models of nerve injury: Lysozyme as a marker for active phagocytosis. Journal of Neuroscience 40:99-107.

Weinberg H.J., and Spencer P.S. (1987). The fate of Schwann cells isolated from axonal contact. Journal of Neurocytology 7:555-69.

Weiss P. (1945). Experiments on cell and axon orientation in vitro: the role of colloidal exudates in tissue organisation. J Exp Zool 100: 358-386.

Weiss P., Davis H. (1943). Pressure block in nerves provided with arterial sleeves. Journal of Neurophysiology 6:269-286.

Weiss P., Taylor A.C. (1946). Guides for nerve regeneration across gaps. Journal of Neurosurgery 3:375-389.

Wessels D., Vawter-Hugart H., Murray J., and Soll D.R. (1994). Three dimensional dynamics of pseudopod formation and the regulation of turning during the motility cycle of *Dictyostelium*. Cell Mot. Cytoskeleleton 27: 1-12.

Whitworth I.H., Brown R.A., Dore C.J., Green C.J., and Terenghi G. (1995a). Orientated mats of fibronectin as a conduit material for use in peripheral nerve repair. J. Hand Surg. 20B: 429-436.

Whitworth I.H., Terenghi G., Green C.J., Brown R.A., Stevens E., and Tomlinson D.R. (1995b). Targeted delivery of nerve growth factor via fibronectin conduits assists nerve regeneration in control and diabetic rats. European Journal of Neuroscience 7:2220-2225.

Whitworth I.H., Brown R.A., Dore C.J., Anand P., Green C.J., and Terenghi G. (1996). Nerve growth factor enhances nerve regeneration through fibronectin grafts. Journal of Hand Surgery 21B:4:514-522.

Wieninger-Rustemeyer R., Kirchgessner M., and Steinhart H. (1981). Effects of various enzyme-substrate ratios on trypsin activity in the presence of trace elements. Arch-Tierernahr. 31: 589-96.

Williams L.R. Longo F.M., Powell H.C., Lundborg G., and Varon S. (1983). Spatial-temporal progress of peripheral nerves within a silicone chamber: parameters for bioassay. J Comp Neurol 218: 460-470.

Williams R.J.P. (1989). An introduction to the biochemistry of zinc. In *Zinc in Human Biology*. Edited by C.F. Mills. Springer-Verlag, London. pp 15-31.

Williams P.L., and Hall S.M. (1971). Chronic Wallerian degeneration. An in vivo and ultrastructural study. J. Anat. 109: 487-503.

Wojciak-Stothard B., Crossan J., Curtis A.S.G., and Wilkinson C.D. (1995). Grooved substrata facilitate in vitro healing of completely divided flexor tendons. J Mater Sci Mater Med. 6: 266-271.

Wojciak-Stothard B., Denyer M., Mishra M., and Brown R.A. (1997). A study of the adhesion, orientation and movement of cells cultured on ultrathin fibronectin fibers. In vitro Cell Dev. Biol. 33: 110-117.

Yamada K.M. (1983). Cell surface interactions with endothelial cell materials. Annual Review of Biochemistry. 52:761 -769.

Yamada K.M. (1989). Fibronectin domains and receptors. In *Fibronectin*. D.F. Mosher, editor. Academic Press. Inc., New York. pp47-121.

Yamada K.M., and Olden K. (1978). Fibronectins: Adhesive glycoproteins of cell surface and blood. Nature 275:179-184.

Yannas I.V. (1985). Skin and nerve regeneration phenomena induced by polymeric templates. In: Transactions of the 5th European Conference on Biomaterials, Paris, Sep 4-6, pp159-163.

Yannas I.V., Orgill D.P., Silver J., Norregaard T.V., Zervas N.T., and Schoene W.C. (1985). In: Transactions of the 5th European Conference on Biomaterials, Paris, Sep 4-6, pp163.

Young B.L., Begovac P., Stuart D.G., et al. (1984). An effective sleeving technique in nerve repair. Journal of Neuroscience Methods 10:51-58.

Zachery R.B. and Holmes W. (1946). Primary suture of nerves. Surgical Gynecological Obstetrics 82:632-651.

Zager E.L., and Black P.M. (1988). Neural transplantation. Surg Neurol 29: 350-366.